

KATHOLIEKE UNIVERSITEIT LEUVEN
FACULTEIT TOEGEPASTE WETENSCHAPPEN
DEPARTEMENT ELEKTROTECHNIEK
AFDELING ESAT
Kardinaal Mercierlaan 94 — B-3001 Heverlee, Belgium

MODELING AND OPTIMAL ADAPTIVE CONTROL OF BIOTECHNOLOGICAL PROCESSES

Jury :
Prof. J. Berlamont, vice-decaan, voorzitter
Prof. J. Vandewalle, promotor
Prof. B. De Moor, promotor
Prof. G. Bastin, Université Catholique de Louvain
Prof. J. De Baerdemaeker
Prof. J. De Schutter
Prof. V. Goedseels
Prof. M. Reuß, Universität Stuttgart

Proefschrift voorgedragen tot
het behalen van het doctoraat
in de toegepaste wetenschappen

door

Jan VAN IMPE

Preface

Het is een goede gewoonte om op de eerste bladzijden van een doctoraatsthesis een woord van dank te richten tot iedereen, die op één of andere manier heeft bijgedragen tot de voltooiing ervan. Graag wil ik mij hierbij aansluiten.

In de eerste plaats denk ik dan aan mijn beide promotoren, de professoren Joos Vandewalle en Bart De Moor. Tijdens mijn verblijf in het Departement Elektrotechniek mocht ik gedurende enige jaren onderzoek doen in een ploeg waarvan zij de enthousiaste bezielers zijn. De grote vrijheid die ik van hen kreeg, maar tevens hun nooit aflatende bezorgdheid om de kwaliteit van het geleverde werk, hebben steeds een stimulerende invloed gehad. Ik wil Joos en Bart daarvoor oprecht bedanken.

Wegens het sterk interdisciplinair karakter van het biotechnologisch onderzoeksdomein, was (en is) er een zeer nauwe interactie met de Faculteit Landbouwwetenschappen van deze universiteit. Om zeker niemand te vergeten, wil ik hier enkel Professor Vic Goedseels, decaan van de Landbouwfaculteit en tevens lid van de jury, met naam vermelden. Ik wil hem ook persoonlijk bedanken, omwille van zijn voortdurende interesse voor het onderzoeksproject waarbinnen dit doctoraal werk kaderde.

Laat mij toe de andere leden van de jury in alfabetische volgorde te vermelden.

Je garde un très bon souvenir de ma collaboration avec Georges Bastin, Professeur à l'Université Catholique de Louvain. Ses nombreuses suggestions et remarques pertinentes ont eu une influence décisive, tant au niveau du contenu que de la rédaction de cette thèse. Je ne voudrais pas oublier de remercier tous les autres membres de l'Unité Auto. Qu'il me soit permis de citer les noms de Denis Dochain, Vincent Van Breusegem, Libei Chen, et Véronique Chotteau.

Professor Jean Berlamont, voorzitter van de jury, wil ik bedanken voor zijn bereidwillige medewerking tijdens de laatste fase van dit doctoraat.

Professor Josse De Baerdemaeker, tevens lid van het leescomité, en zijn onderzoeksgroep wil ik hier zeer hartelijk bedanken. Via hen ontstond ook de samenwerking met Toon Martens, directeur van de Universiteitsrestaurants Alma. In deze tekst zullen zij ongetwijfeld de resultaten van onze talrijke discussies terugvinden.

Mijn dank gaat uit naar Professor Joris De Schutter, die de nodige tijd heeft willen vrijmaken om als lid van de jury dit werk mee te beoordelen.

Ich betrachte es als eine besondere Ehre, daß auch Professor Matthias Reuß, von der Universität Stuttgart, akzeptiert hat zur Prüfungskommission zu gehören. Ich danke ihm von ganzem Herzen für sein langjähriges, wohlgemeintes Interesse für meine Arbeit. Der Leser wird bald feststellen daß ich von ihm inspiriert wurde.

Ik wil hier geen ellenlange opsomming geven van al de leden van onze eigen onderzoeksgroep die ik heb weten komen en gaan. Niettemin wil ik hen toch allemaal persoonlijk bedanken voor de vriendschappelijke en stimulerende sfeer waarin dit werk is kunnen groeien. Laat mij toe enkel mijn bureaugenoten van het eerste en het laatste uur te vermelden : Bart Nicolaï, Peter Vanrolleghem, en met hem ook Professor Willy Verstraete van de Universiteit Gent, Marc Moonen, en Peter Van Overschee. Ook Ingrid Tokka en Ann Deforce, uit het hoofdkwartier van Sista, en de verschillende systeemmanagers wil ik niet onvermeld laten.

Verder bedank ik ook mijn verschillende pendelgenoten tussen Gent en Leuven, in het bijzonder Herman Ramon en Dirk Thierens. Met hen werd de trein altijd een beetje reizen, ...in de wereld der regeltechniek.

Ik ben ook veel dank verschuldigd aan Professor Hubert Verachtert, promotor van mijn huidig mandaat als aangesteld navorser. Daardoor immers is de continuïteit van dit onderzoek gewaarborgd.

Tenslotte wil ik zeker niet nalaten volgende instellingen oprecht te bedanken voor hun onmisbare financiële steun : de Diensten voor Programmatie van het Wetenschapsbeleid, in het kader van het Nationaal Stimuleringsprogramma voor fundamenteel onderzoek inzake Biowetenschappen, de Katholieke Universiteit Leuven zelf, en het Nationaal Fonds voor Wetenschappelijk Onderzoek.

De aandachtige lezer heeft wellicht opgemerkt dat mijn huisgenoten van vroeger en nu, in dit voorwoord nog onvermeld zijn gebleven. Mijn echtgenote Myriam noem ik echter reeds bij naam op de eerste bladzijde van deze tekst. Zij weet intussen wat een doctorale studie zoal met zich meebrengt. Ik wil daarom dit werk aan haar opdragen. Ik bedank ook van harte alle leden van het gezin waarin ik mocht opgroeien, en de hele familie. In het bijzonder mijn ouders verdienen alle dankbaarheid. Schrijven dat zonder hen dit werk niet mogelijk was geweest, is beslist géén flauwe woordspeling.

Leuven, januari 1993

Jan Van Impe

Abstract

In this thesis we investigate whether the application of mathematical modeling techniques and modern model based control methods can contribute to the optimization of bioprocesses. The main contributions can be summarized as follows.

First, we present a unifying frame for representing all kinds of metabolism for biomass survival and possibly product synthesis by introducing the new concept of endogenous fraction.

Second, as an illustrative case study of modeling the reaction kinetics, we develop a new dynamic model describing microbial growth in food products as a function of both time and temperature, over the whole range of growth and inactivation.

Third, we illustrate that the application of an optimal feed rate profile can contribute in solving both the model parameter estimation problem and the model structure characterization problem which often occur during biotechnological modeling : optimization for model discrimination. As an example, we construct a new unifying unstructured model for the penicillin G fermentation process based on the concept of endogenous fraction.

Fourth, we present a unifying methodology for optimization of biotechnological processes : optimal adaptive control. This methodology links together two approaches : first optimal control, which provides the theoretical realizable optimum on the (unrealistic) assumption of a perfect knowledge of the model, and second adaptive control, for which there is no need for a complete knowledge of the process model, but which can not guarantee at least suboptimality of the results obtained. The gap between them is bridged by the development of heuristic control strategies. These are based on biochemical knowledge concerning the process and on a careful mathematical analysis of the optimal control solution. An adaptive model–independent implementation combines then excellent robustness properties with nearly optimal performance. As an example, we study the optimization of fed–batch fermentation processes with respect to the volumetric substrate feeding rate.

Fifth, as a side–result, we present a new, simple, but powerful general method to determine optimal control profiles in the case of a continuous but non–differentiable state space model.

Contents

0 Motivation 1

0.1 A general overview . . . 3
0.2 Chapter by chapter overview . . . 5
0.3 Software environment . . . 14

1 Systems and control tools 15

1.1 Modeling biotechnological processes . . . 16
1.1.1 Unstructured models . . . 17
1.1.1.1 Simple microbial growth process . . . 17
1.1.1.2 Extensions to the basic dynamics . . . 20
1.1.1.3 Models for the specific reaction rates . . . 25
1.1.2 Structured models . . . 28
1.1.3 Physiological models . . . 29
1.1.4 General state space model . . . 31
1.1.5 Minimal modeling . . . 33
1.1.6 The singular perturbation technique . . . 35
1.2 Optimal control theory . . . 36
1.2.1 Statement of the problem . . . 36
1.2.2 Parametric optimization . . . 37
1.2.3 The Minimum Principle of Pontryagin . . . 38
1.2.3.1 Problem without constraints on the control . . . 38
1.2.3.2 Problem with constraints on the control . . . 40
1.2.3.3 Problem with path constraints . . . 42
1.2.4 Singular control problems . . . 43
1.2.5 Optimization of the initial state . . . 45
1.2.6 A conjecture . . . 48
1.3 Conclusions . . . 56

2 A dynamic mathematical model to predict microbial growth and inactivation during food processing 57
2.1 Explicit bacterial growth models 59
2.1.1 Modeling bacterial growth as a function of time 59
2.1.2 Modeling bacterial growth as a function of temperature 60
2.1.3 The model of Zwietering *et al.* 65
2.2 A dynamic mathematical model 65
2.2.1 Limitations of the current explicit model 65
2.2.2 Design requirements for a dynamic model 67
2.2.3 A dynamic model for growth 69
2.2.4 A dynamic model including inactivation 70
2.2.5 Simulation results and discussion 74
2.2.5.1 Verification of model design requirements . . . 74
2.2.5.2 Notes on parameter sensitivity 78
2.3 Conclusions 80

3 Optimal control of fed-batch fermentation processes 83
3.1 Fed-batch fermentations 85
3.1.1 Advantages of fed-batch fermentations 85
3.1.2 Review of the literature 86
3.2 General optimization problem 89
3.2.1 General unstructured model for fed-batch reactors . . 89
3.2.2 Statement of the problem 90
3.3 Necessary conditions for optimality 94
3.3.1 Statement of the two point boundary value problem . 94
3.3.2 Extremal controls 95
3.4 Example : microbial growth process 97
3.5 Optimal control sequence for fed-batch fermentation processes with growth/production decoupling 102
3.5.1 Fermentations with growth/production decoupling . . 103
3.5.2 Optimal control sequence for monotonic μ and non-monotonic π 105
3.5.2.1 Bounded input u and fixed initial state 107
3.5.2.2 Computational algorithm 111
3.5.2.3 Unbounded input u and free initial substrate concentration 114

3.5.3 Optimal control sequence with state inequality constraints 115
3.5.3.1 Substrate concentration constraint 115
3.5.3.2 Biomass concentration constraint 116
3.5.4 Verification of all necessary conditions for optimality . 119
3.6 Physical interpretation of singular control 121
3.6.1 The generic case : maintenance coefficient $m > 0$ . . . 121
3.6.2 Special case : maintenance coefficient $m = 0$ 127
3.7 Heuristic control strategies 131
3.8 Conclusions 134

4 Analysis of two unstructured models for the penicillin G fed-batch fermentation process 137
4.1 The penicillin G fermentation process 138
4.2 The model of Heijnen, Roels and Stouthamer 141
4.2.1 The original model equations 141
4.2.2 A simplified weight balance 143
4.2.3 Statement of the optimization problem 147
4.2.4 A modified model 149
4.2.5 Optimal control using the modified model 152
4.2.6 Physical interpretation of singular control 162
4.2.7 Heuristic control strategies 166
4.2.8 Conclusions 170
4.3 The model of Bajpai and Reuß 172
4.3.1 Mathematical description 172
4.3.2 A variant for the growth kinetics 176
4.3.3 Statement of the optimization problem 178
4.3.4 Polynomial Control 180
4.3.5 Optimal control 181
4.3.6 Physical interpretation of singular control 187
4.3.7 Heuristic control strategies 188
4.3.8 Conclusions 190
4.4 Concluding remarks 191

5 A unifying unstructured model for the penicillin G fed-batch fermentation process **193**

5.1 Biochemical evaluation of two unstructured models for the penicillin G fed-batch fermentation process 195
5.1.1 Model equations 195
5.1.2 Biochemistry of the penicillin synthesis 197
5.1.3 Biochemical validation of the two models 199
5.1.3.1 Specific production rate kinetics 200
5.1.3.2 Maintenance or endogenous metabolism 205
5.1.3.3 Specific substrate to biomass conversion rate . 208
5.1.3.4 The remaining model parameters 209
5.1.4 Effect of the model parameters on feeding strategy optimization 211
5.2 A unifying unstructured model 214
5.2.1 Deficiencies in the current models 214
5.2.2 A unifying model 215
5.2.2.1 Design requirements 215
5.2.2.2 Specific rates 216
5.2.2.3 Special cases 217
5.2.3 Simulation Results 219
5.2.4 Conclusions 225
5.3 Optimal control using the unifying model 225
5.3.1 Optimal control strategy 225
5.3.2 Heuristic control strategies 226
5.3.3 Simulation results 227
5.3.4 Conclusions 232
5.4 Conclusions 233

6 Optimal adaptive control Case study : fed-batch fermentation processes **237**

6.1 Optimal adaptive control : motivation 239
6.1.1 Problem statement 239
6.1.2 Optimal control strategy 240
6.1.3 Case study : the penicillin G fed-batch fermentation process 242
6.1.4 Heuristic control strategies 242
6.1.5 Linearizing control 244

6.2 Optimal adaptive control using on-line measurements of C_s and C_x 250
6.2.1 Mathematical description 250
6.2.2 Simulation results 255
6.3 Optimal adaptive control using on-line measurements of C_s . 257
6.3.1 Mathematical description 257
6.3.2 Simulation results 259
6.4 Optimal adaptive control using on-line measurements of CER 260
6.4.1 Mathematical description 260
6.4.2 Simulation results 264
6.5 Conclusions 266

7 Conclusions and open problems **267**

A References **271**

B Nomenclature **283**

C Nederlandse samenvatting **287**
C.1 Algemeen overzicht 289
C.2 Overzicht hoofdstuk per hoofdstuk 292

List of Figures

1.1 Stirred Tank Reactor STR 17
1.2 Monod, Tessier, Blackman and Haldane kinetics 26
1.3 A counter–example in the static case 50
1.4 Approximation of a piecewise–smooth function by a family of smooth functions 55

2.1 A microbial growth curve 59
2.2 Maximum specific growth rate as a function of temperature . 62
2.3 Asymptote as a function of temperature 64
2.4 Lag time as a function of temperature 64
2.5 Prediction of the explicit model of Zwietering *et al.* versus the dynamic model for a step in the temperature profile 66
2.6 Value of the transition function $f_{trans}(T)$ for some values of the parameter α and $T_{trans} = 50°C$ 71
2.7 T_{zero} as a function of $n = \ln(N)$ for some values of T_{trans} and α, and $T_{max} = 44.9°C$ 73
2.8 The overall specific growth rate as a function of temperature 76
2.9 Predicted response of a microbial population to a hypothetic time–temperature profile 76
2.10 Sensitivity of the predicted response of a microbial population to variations in D_{ref} and z 79

3.1 Fed–batch bioreactor 89
3.2 Process with monotonic μ_{substr} and non–monotonic π 104
3.3 Process with non–monotonic μ_{substr} and monotonic π 104
3.4 Process with non–monotonic μ_{substr} and non–monotonic π . . 105
3.5 General feed rate profile for low initial substrate concentration 108

4.1 The specific rates σ and μ as functions of C_s 144
4.2 The specific rate π as a function of C_s 144
4.3 Constant glucose feed rate and corresponding cell, glucose, product, μ and π profiles 146
4.4 Dabes–type kinetics $\pi(\mu)$ for some values of the parameter B 151
4.5 Extremal values for $P(t_f)$, t_2 and t_f as functions of S_0 for $B = 10^{-11}$ 156
4.6 Optimal glucose feed rate and corresponding cell, glucose, product, π and μ profiles for $B = 10^{-11}$ 157
4.7 Extremal values for $P(t_f)$, t_2 and t_f as functions of S_0 for $B = \mu_{crit}$ 159
4.8 Optimal glucose feed rate and corresponding cell, glucose, product, π and μ profiles for $B = \mu_{crit}$ 161
4.9 Optimal production $P(t_f)$ as a function of B 161
4.10 π/σ as a function of C_s for some values of B 165
4.11 Optimal switch values for μ and C_s as a function of B with $k_h = 0$ 165
4.12 Optimal and suboptimal glucose feed rate for $B = 10^{-11}$ . . 168
4.13 Suboptimal glucose feed rate and corresponding cell, glucose, product, π and μ profiles for $B = \mu_{crit}$ and $\mu_{switch} = \mu_{crit}$ . . 169
4.14 Suboptimal glucose feed rate and corresponding cell, glucose, product, π and μ profiles for $B = \mu_{crit}$ and μ_{switch} free 169
4.15 Optimal and suboptimal glucose feed rate for $B = \mu_{crit}$ . . . 170
4.16 Constant glucose feed rate and corresponding cell, glucose, product, μ and π profiles, for μ Contois and parameter Set 2 175
4.17 Constant glucose feed rate and corresponding cell, glucose, product, μ and π profiles, for μ Monod and parameter Set 2 . 175
4.18 Optimal glucose feed rate and corresponding cell, glucose, product, μ and π profiles, for μ Contois and parameter Set 2 183
4.19 Optimal glucose feed rate and corresponding cell, glucose, product, μ and π profiles, for μ Monod and parameter Set 2 . 183
4.20 Optimal glucose feed rate and corresponding cell, glucose, product, μ and π profiles, for μ Contois and parameter Set 2, with $u_{MAX} = 0.05$ L/h, $C_{s,MAX} = 4$ g/L, $C_{x,MAX} = 23$ g/L . 185
4.21 Extremal values for $P(t_f)/t_f$, $P(t_f)$, t_2 and t_f as functions of S_0 186
4.22 Optimal and suboptimal glucose feed rate profiles, for μ Contois and parameter Set 2 189

5.1 Pathway of the penicillin G biosynthesis 198
5.2 Substrate, biomass and penicillin profiles during constant feed rate fermentation for some (K_p,K_i,π_m) combinations of Table 5.4 – $S_0 = 0$ g 204
5.3 Specific production rate π for some (K_p,K_i,π_m) combinations of Table 5.4 204
5.4 Substrate, biomass and penicillin profiles during constant feed rate fermentation for some (K_x,π_m) combinations of Table 5.5 – $S_0 = 0$ g 210
5.5 Substrate, biomass and penicillin profiles during constant feed rate fermentation for some (K_x,π_m) combinations of Table 5.5 – $S_0 = 335$ g 213
5.6 $\exp(-C_s/E)$ as a function of C_s for different values of E . . . 217
5.7 Substrate, biomass and penicillin profiles during constant feed rate fermentation for some (K_x,π_m) combinations of Table 5.6 – $S_0 = 0$ g 221
5.8 Substrate, biomass and penicillin profiles during constant feed rate fermentation for some (K_x,π_m) combinations of Table 5.6 – $S_0 = 1376$ g 221
5.9 Estimation of π_m for different values of E 222
5.10 Relative error of final biomass amount $X(t_f)$ and final product amount $P(t_f)$ as functions of E 222
5.11 Substrate, biomass and penicillin profiles during constant feed rate fermentation for some (E,π_m) combinations of Table 5.7 – $S_0 = 0$ g 224
5.12 Substrate, biomass and penicillin profiles during constant feed rate fermentation for some (E,π_m) combinations of Table 5.7 – $S_0 = 400$ g 224
5.13 Substrate, biomass, product, μ, π and u profiles during optimal feed rate fermentation for the values of E of Table 5.8 . 230
5.14 Heuristic C_s–control : $S(0)$, $X(t_f)$, t_2, t_f, $P(t_f)$ and $\mathcal{G}$ as functions of E 231

6.1 Process with monotonic μ_{substr} and non–monotonic π 240
6.2 Optimal control sequence 241
6.3 Nonlinear linearizing controller 248
6.4 Estimation of σ and μ 256
6.5 Prediction of C_s and adaptive controller 256
6.6 Adaptive control using on–line C_s measurements for $E = 10^{-9}$ g/L 259
6.7 Influence of f and λ on $P(t_f)$ 260
6.8 Estimation of μ and σ 264
6.9 Adaptive control using *CER* measurements for $E = 10^{-9}$ g/L 264
6.10 *CER* profile during optimal feed rate fermentation for the values of E of Table 5.8 265

List of Tables

2.1 Parameters reported by Zwietering *et al.* 65
2.2 Dynamic model equations 75

4.1 Parameters and initial conditions used in simulations 143
4.2 Simulation results with the controls of Heijnen *et al.* 148
4.3 Extremal values for S_0 near α for $B = 10^{-11}$ 155
4.4 Optimal and heuristic control results for $B = 10^{-11}$ 156
4.5 Extremal values for S_0 near α for $B = \mu_{crit} = 10^{-2}$ 160
4.6 Optimal and heuristic control results for $B = \mu_{crit} = 10^{-2}$ . . 160
4.7 Parameters and initial conditions used in simulations 174
4.8 Numerical results for polynomial, heuristic and optimal control using the model of Bajpai and Reuß with Contois kinetics for growth 182

5.1 Specific rates and parameters ([g/L] unit system) used in the model of Heijnen *et al.* 196
5.2 Specific rates and parameters ([g/L] unit system) used in the model of Bajpai and Reuß 196
5.3 Initial and operational conditions used in simulations 202
5.4 Estimation of π_m for different values of K_p and K_i for the Bajpai and Reuß model with constant feeding strategy, and corresponding final product amount – optimal initial substrate level and optimal product amount 203
5.5 Estimation of π_m for different values of K_x for the Bajpai and Reuß model with constant feeding strategy, and corresponding final product amount – optimal initial substrate level and optimal product amount 209

5.6 Estimation of π_m for different values of K_x for the unifying model ($E = 1$ g/L) with constant feeding strategy, and corresponding final product amount – optimal initial substrate level and optimal product amount 220
5.7 Estimation of π_m for different values of E for the unifying model with constant feeding strategy, and corresponding final product amount – optimal initial substrate level and optimal product amount 222
5.8 Numerical results for optimal and heuristic control for some values of E 229

6.1 Numerical results for optimal control for two limiting cases . 242
6.2 Numerical results for heuristic C_s–control for two limiting cases – $C_s(t_2) = (K_p K_i)^{1/2}$ 244

Chapter 0

Motivation

During the last few decades, the science of biotechnology has undergone rapid development. The scope of the field includes biotechnological production processes or fermentation processes, in which a considerable diversity of products are produced, as well as biological wastewater treatment processes, the most important of which is the activated sludge process. The dynamics of these processes are determined in the first place by a living microbial population.

The principle of microbial growth processes can be simplified as follows [Holmberg and Ranta 1982] : the micro–organisms (bacteria, fungi, yeasts, ...) grow with the consumption of certain nutrients or substrates (carbon derivatives (such as glucose), nitrogen, oxygen, ...), assuming that the environmental conditions (temperature, pH, aeration, agitation, ...) are favorable.

The search for solutions to certain social or technical production problems with the aid of micro–organisms has several marked advantages. Micro–organisms constitute living 'raw material' which is in principle never depleted. A second advantage is that use can often be made of substances which have not yet been considered to be of value as the culture medium for such organisms; this is sometimes even the case with waste substances. In this way biotechnology does not place an additional burden on the world's supply of raw materials. This also ensures that the environment is less polluted. The field of biotechnology, which is evolving quickly, in the long run offers the prospect of some answers to a number of serious problems confronting the world, problems with respect to disease control and environmental protection as well as food, where agricultural shortages as well as surpluses are urgent matters that have to be dealt with.

The aim of biotechnological cultivation can be threefold.

1. *Biomass production, such as baker's yeast.*

2. *Synthesis product production. We can distinguish between (i) intracellular (proteins, endotoxins, ...) and (ii) extracellular products (antibiotics, alcohol, ...). Another classification is as follows : (i) processes in which the products are strictly growth associated, such as ethanol, and (ii) processes in which the desired product is not necessarily growth associated (metabolite product), such as enzyme and antibiotic production.*

3. *Biological depollution of waste water, i.e. the consumption of certain polluting matters by the micro–organisms.*

In the field of food processing however, microbial growth is an undesired process. The shelf life of e.g. chilled prepared food products, for which there is an increased consumer interest, is usually limited due to spoilage by common micro–organisms and the increased risk for food pathogens.

Biotechnological processes may be classified according to the mode chosen for bioreactor operation.

During batch operation, no substrate is added during the fermentation nor is product removed until the end of the process. Some pharmaceutical preparations are made in this way, but generally batch operation is not commercially attractive.

During continuous operation, substrate is continually added and product continually removed, the total culture volume remaining constant. Examples are the continuous fermentation of milk in the production of margarine and the biological purification of waste water.

In fed–batch operation (also referred to as the Zulauf process) the nutrients are fed either intermittently or continuously during the course of an otherwise batch operation. From the control engineer's viewpoint this operation mode presents the greatest challenge. It provides an excellent means of regulating the nutrient feed rate to optimize the productivity, while at the same time obviating over– and under–feeding of nutrients. Baker's yeast and antibiotics (such as penicillins) are produced in fed–batches commercially.

0.1 A general overview

One of the main purposes of this thesis is to investigate whether the application of mathematical modeling techniques and modern model based control methods can contribute to the optimization of bioprocesses.

This can be motivated for each of the processes mentioned as follows.

1. *Fermentation processes* utilize sometimes expensive raw materials, require very large capital–intensive plants and yield products that are low in concentrations. Every small improvement in any of these variables may result in considerable reduction in the production costs.

2. In the field of *biological wastewater treatment*, increasing energy costs and stricter environmental standards have stressed the need for reliable automatic control.

3. In the field of *food processing*, optimization of the thermal treatment aims at reaching a satisfactory *trade off* between inhibiting spoilage by growing micro–organisms and maintaining at the same time nutritional and sensory quality aspects.

Mathematical modeling, monitoring and real–time control of biotechnological processes represent a challenging area of endeavor for both biotechnologists and control engineers. We want to emphasize from the outset that optimization of a particular biotechnological process —e.g. the penicillin G fed–batch fermentation which will be studied in detail— is not the only purpose of this work. In fact, any example handled in this work is only used as a vehicle for presenting the basic ideas, methodology and results. This thesis wants to augment the knowledge about the power and limitations of mathematical modeling and control techniques applied to processes whose dynamics are in the first place determined by a population of living micro–organisms.

In many practical applications, accurate modeling (and thus also model based control) is hampered by the following major problems which call for adequate engineering solutions.

1. The process kinetics are most often poorly understood nonlinear functions, while the corresponding parameters are time varying.
2. Up till now there is a lack of reliable sensors suited to real time monitoring of process variables which are needed in advanced control algorithms.

Therefore, the earliest attempts at control of a biotechnological process used no model at all. Successful state trajectories from previous runs which had been stored in the process computer were tracked using open loop control. Many industrial fermentations are still operated using this method.
During the last two decades, two trends for the design of monitoring and control algorithms for biotechnological processes have emerged [Bastin 1991].

In a *first approach*, the difficulties in obtaining an accurate mathematical process model are ignored. In numerous papers classical methods (e.g. Kalman filtering, optimal control theory, ...) are applied under the assumption that the model is perfectly known. Due to this oversimplification, it is very unlikely that a real life implementation of such controllers —very often this implementation is already hampered by e.g. monitoring problems— would result in the predicted simulation results.

In a *second approach*, the aim is to design specific monitoring and control algorithms without the need for a complete knowledge of the process model, using concepts from e.g. adaptive control and nonlinear linearizing control. A comprehensive treatment of these ideas can be found in [Bastin and Dochain 1990] and the references therein.

In this thesis, we adopt a rather pragmatic viewpoint : we try to combine the best of both trends into one unifying methodology for optimization of biotechnological processes : *optimal adaptive control.* This is motivated as follows.

Model–based *optimal control* studies provide a theoretical realizable optimum. In addition, in this work optimal control is used also as a technique to discriminate between different model structures for a given process. However, the real life implementation will fail in the first place due to modeling uncertainties.

On the other hand robust model–independent *adaptive controllers* can be designed, but there is a priori no guarantee for at least suboptimality of the results obtained.

The gap between both approaches is bridged by the development of *heuristic control strategies* with nearly optimal performance under all conditions. These suboptimal controllers are based on biochemical knowledge concerning the process and on a careful mathematical analysis of the optimal control solution. An adaptive model–independent implementation of these profiles combines then excellent robustness properties with nearly optimal performance.

0.2 Chapter by chapter overview

The material presented in this text is rather extensive. It is mainly intended for control scientists. As already mentioned, the main objective is to set the problems of modeling, monitoring, and control of biotechnological processes, which are of great importance in the industrial practice, in a mathematical framework commonly used in the control engineering community.

However, the thesis is also directed towards bioengineers who have some background in control engineering and would like to better apprehend how mathematical modeling and control theory apply to biological processes.

Therefore, we have tried to write the text in a pedagogical spirit. The main emphasis is not on the derivation of theoretical results as such, but rather on their interpretation from the bioengineering point of view.

The contributions reported in this thesis can be summarized as follows.

Chapter 1

Systems and control tools

Most of the material presented in the first chapter is introductory. The first section is entirely devoted to *modeling of biotechnological processes.* We distinguish between physiological, unstructured and structured models. We also present a new unifying frame for representing all kinds of metabolism for biomass survival and possibly product synthesis by introducing the new concept of *endogenous fraction.* This is at the basis of the results presented in Chapter 5. For an illustrative case study of modeling the reaction kinetics we refer to Chapter 2 where we develop a new model of the overall specific growth rate in food products as a function of temperature. Furthermore, the transition to the general state space model as introduced by Bastin and Dochain [1990] is illustrated with a simple example. We briefly explain the minimal modeling concept and the singular perturbation technique, both aiming at reducing the model complexity. As for structured models we

limit ourselves to some general remarks. We prefer not to include our recent work on estimator and controller design for the activated sludge wastewater treatment process using a structured compartment model, in order not to overload this text too much. In the remaining chapters only unstructured models are considered.

The second part of the chapter gives an overview of *optimal control theory*, starting from parametric optimization methods up to the Minimum Principle of Pontryagin [1962]. We present the issue of singular optimal control problems explicitly for the class of systems studied in this work. Furthermore, we prove necessary conditions if some or all initial states are additional degrees of freedom in the optimization. Finally, we present a new, simple, but powerful general conjecture that allows to determine optimal control profiles in the case of a continuous but non–differentiable state space model (Conjecture 1.1).

The new concept of endogenous fraction and the corresponding unifying frame for representing all kinds of metabolism for biomass survival and possibly product synthesis have been reported in [Van Impe et al. 1991c, 1992d]. Conjecture 1.1 has been reported in [Van Impe et al. 1990].

Some results —which are not included in this text— on the design of estimation and control algorithms for an activated sludge wastewater treatment process using a structured compartment model for the biotransformation processes can be found in [Vanrolleghem et al. 1991] and [Van Impe et al. 1991e, 1991f, 1992f].

Chapter 2

A dynamic mathematical model to predict microbial growth and inactivation during food processing

In this chapter we consider the modeling of one of the basic ingredients of the general state space model for a biotechnological process, namely the reaction kinetics. As an example, the modeling of (undesired) microbial growth in food products is under study. In contrast to fermentation processes where the substrates and possibly products are in general more important influencing factors than the environmental conditions such as temperature and pH, the situation in food processing is completely opposite. We limit ourselves to food products for which *temperature is the only significant factor affecting the growth rate.*

The principal aim of this chapter is to apply advanced dynamic modeling concepts into the field of predictive microbiology. There are a lot of mathematical models reported in the literature describing bacterial growth as a function of time and temperature. However, as these are all static —i.e. explicit— models, their predictive value can only be guaranteed at a constant temperature within the range of microbial growth. In this chapter we develop a *new dynamic model* describing a bacterial population as a function of both time and temperature, over the whole biokinetic range of growth and inactivation. Besides the fact that it can deal with time varying temperatures in a consistent way, additional features are : (i) the previous history of the food product under consideration is taken into account in a natural way, (ii) the model can easily describe micro–organisms with different behavior at temperatures around the transition from growth to inactivation, (iii) in the case of a constant temperature within the range of growth, the model reduces to the experimentally validated explicit model as proposed by Zwietering *et al.* [1990,1991], and (iv) the complete model has suitable mathematical properties to make advanced nonlinear parameter estimation schemes and modern optimization techniques applicable.

The material presented in this chapter is taken from [Van Impe et al. 1991d] and [Van Impe et al. 1992a].

Chapter 3

Optimal control of fed-batch fermentation processes

In this chapter the optimization of fed–batch bioreactors is under study. All results presented are general in this way that they are written in terms of the specific reaction rates. In other words, an exact analytical expression for these rates is not required a priori. In addition, no assumptions are made concerning the metabolism involved for biomass survival and possibly product synthesis. Much attention is given to carefully motivating from a microbiological viewpoint both the methods used and the results obtained. As such, even results already partially reported in the literature are given additional interpretations.

After describing some marked advantages of fed–batch operation mode and a review of the literature about the application of (optimal) control techniques to fed–batch fermentation processes, we present a general unstructured model for a fed–batch bioreactor characterized by one limiting substrate, a single micro–organism, and possibly one prod-

uct of interest. A general optimization problem is then formulated, with the volumetric substrate feed rate considered as the control input. Herein, we consider performance indices of both the yield type and the productivity type. The optimization of the initial substrate concentration is included also. This general optimization problem is then reformulated in the framework of optimal control theory, leading to a two point boundary value problem. It is shown that the solution reduces to the determination of the optimal control sequence and the corresponding switching times.

As an introductory example, the microbial growth process is considered. Although the solution has been reported already elsewhere [Parulekar and Lim 1985], we include an analysis of this example for three reasons. First, the deduced control sequences are justified here based on biochemical insight in the process. Second, the extension to processes with growth associated product formation is straightforward. Third, a similar line of reasoning will be adopted for fed–batch fermentations characterized by a decoupling between growth and product formation.

According to Modak *et al.* [1986], fermentation processes with a decoupling between growth and production are classified following the qualitative behavior of the specific growth and production rates with respect to substrate concentration. As an example, we derive the optimal control sequence for processes with monotonic growth rate and non–monotonic production rate. We are able to prove that the deduced control sequence minimizes the performance index globally. In addition, we present for the first time a complete solution in the realistic case of substrate and biomass inequality constraints. The resulting straightforward computational algorithm has some advantages over the algorithm proposed by Lim *et al.* [1986].

The singular arc is analyzed very carefully. The results obtained — summarized in Theorems 3.1 and 3.2— are at the basis of a *heuristic optimization methodology* which plays a central role throughout this thesis. These heuristic controllers are also motivated from the biochemical viewpoint. In contrast to the optimal control solution they are the translation of a more realistic control objective, namely set–point control, for which adaptive model–independent control algorithms can be developed (see Chapter 6).

Theorems 3.1 and 3.2 are reported in [Van Impe et al. 1992b]. The optimization of a fermentation process involving substrate and biomass constraints is reported in [Van Impe et al. 1992g].

Chapter 4

Analysis of two unstructured models for the penicillin G fed-batch fermentation process

The tools and methods developed in Chapter 3 are applied to the optimization of the penicillin G fed–batch fermentation process. In a first section, we briefly review the literature on modeling of this fermentation process.

In a second section, we consider the unstructured model of Heijnen, Roels and Stouthamer [1979], characterized by a continuous but non–differentiable growth associated specific production kinetics and an endogenous metabolism viewpoint. Based on Conjecture 1.1, we derive for the first time the optimal substrate feed rate profile resulting in the maximum amount of product for a given amount of substrate. The simulation results illustrate the efficiency of the computational algorithm developed in Chapter 3, even for these more or less degenerate kinetics. Based on the same conjecture, we prove an additional theorem (Theorem 4.1) characterizing the singular arc, which is the analogon of the theorems of Chapter 3. The realizable gain due to feed profile optimization is in the region of some hundred percents. Furthermore, the model is very sensitive towards different feeding policies. These results, together with the fact that the commonly observed biphasic behavior of the penicillin fed–batch fermentation has disappeared after optimization, raise some questions concerning the validity of this model.

In a third section, we analyze the unstructured model proposed by Bajpai and Reuß [1980,1981], characterized by a monotonic specific growth rate and non–monotonic specific production rate within a maintenance metabolism viewpoint. In solving the same optimization problem as formulated for the Heijnen *et al.* model, we compare different suboptimal strategies with the optimal control solution. As an extension of the results of Bajpai and Reuß —they only investigated control strategies with predefined structure— we conclude that using any of these strategies, a performance similar to the optimal one can be obtained provided the associated degrees of freedom are at their optimal val-

ues. Using this model the realizable gain is in the region of only a few percents up to several hundred percents depending on the parameter set used. We also consider the optimization of the productivity. The yield–productivity conflict in fed–batch reactors is clearly illustrated. Again, the proposed computational algorithm proves very reliable and efficient for both performance measures considered. A comparison with the results obtained by Lim *et al.* [1986] is also given.

Apart from the derivation of optimal control profiles for both models —which are important on their own—, we believe that the most important results from this chapter are the following. First, although both models have a more or less similar behavior when using a constant feed rate profile and have been validated using experimental data reported in the literature, clearly they exhibit a quite different behavior after feed profile optimization. As a result, this optimal control study can prove very useful in model characterization as will be illustrated in Chapter 5 : *optimization for model discrimination.* Second, although the optimal profile and the resulting realizable gain strongly depend on the model used, the heuristic controllers introduced in Chapter 3 have an excellent performance in all cases. As such, they can serve indeed as a basis for the development of model–independent control algorithms. This will be elaborated in Chapter 6 : *optimal adaptive control.*

The model of Heijnen et al. has been analyzed in [Van Impe et al. 1990]. An analysis of the Bajpai and Reuß model is reported in [Van Impe et al. 1991a].

Chapter 5

A unifying unstructured model for the penicillin G fed-batch fermentation process

The contradictory results obtained in Chapter 4 ask for a more detailed comparison of the model of Heijnen, Roels and Stouthamer [1979] and the model of Bajpai and Reuß [1980,1981].

First, we analyze the differences between both models from a biochemical point of view. The penicillin biosynthesis pathway as known up to now is briefly summarized. Using this biosynthetic framework, the *structural* differences between the two models and the corresponding *parameter* sets are discussed. This careful analysis reveals some physical and biochemical shortcomings in both models. In addition, the

parameter estimation problem is clearly illustrated : although some model parameters can not be estimated accurately using experimental data of simple constant feed rate fermentations with low initial substrate amount —in other words, this particular feed rate strategy is *not persistently exciting*—, they may be key factors in concluding whether or not altering the substrate feeding strategy has an important influence upon the final amount of product. It is illustrated that feeding strategy optimization studies can be a tool in designing experiments for parameter estimation purposes.

To complete this analysis, we investigate how to determine the exact metabolism involved, i.e. the correct *model structure*, and the possible effects on feeding strategy optimization results. This motivates the construction of a *new unifying unstructured model.* This new model corrects the physical and biochemical deficiencies in the previous models. It is essentially based on the unifying concept of *endogenous fractions* of energy supply for biomass maintenance and product synthesis respectively, as introduced in Chapter 1. Its main features are the consistency for all values of the variables, and the ability to adequately describe different metabolic conditions of the mould. The model presented here can be considered as the translation of the latest advances in the biochemical knowledge of the penicillin biosynthesis. Simulation results obtained using a very simple parametric optimization technique indicate that, analogous to the parameter estimation problem, there also exists a *model structure characterization problem.* A proper choice of the input feeding strategy to this new model can give indications about the metabolic nature of the mould. Furthermore, the model structure characterization problem is in some sense *decoupled* from the parameter estimation problem.

Therefore, the model structure characterization problem is studied in more detail using the non–parametric optimal control technique. The results indicate that there exists a maximum realizable gain depending on the metabolism involved. However, the computational algorithm proposed in Chapter 3 can be used under all metabolic conditions. Similarly, the performance of the heuristic strategies we propose is excellent independent of the metabolism involved. The simulations illustrate that this new unifying model is an excellent tool to discriminate between different model structures —i.e. to determine the actual metabolism involved— when applying an optimal feed rate profile.

Finally, we give some further comments on our new paradigm : *optimization for model discrimination.*

The evaluation of the models of Heijnen et al. and Bajpai and Reuß is partially reported in [Nicolaï et al. 1992]. The unifying unstructured model has been presented in [Nicolaï et al. 1991], and analyzed in more detail in [Van Impe et al. 1991c]. The behavior of the unifying model towards product optimization with respect to substrate feeding is described in [Van Impe et al. 1992d].

Chapter 6

Optimal adaptive control
Case study : fed-batch fermentation processes

The main contribution of this chapter is to illustrate how the insight, obtained by preliminary optimal control studies, leads to the design of easy to implement adaptive controllers. The controllers derived in this way combine a nearly optimal performance with good robustness properties against modeling uncertainties and process disturbances. Since they can be considered model–independent, they may be very helpful also in solving the model discrimination problem as discussed in Chapter 5.

As a case study, we consider the design of a substrate feeding rate controller for a class of biotechnological processes in stirred tank reactors, characterized by a decoupling between biomass growth and product formation. More specifically, we analyze the most common case of a process with monotonic specific growth rate and non–monotonic specific production rate as functions of substrate concentration.

First, the concept of *optimal adaptive control* is motivated in detail. Starting from the optimal control solution, the heuristic substrate controllers presented at different places throughout this thesis are reconsidered with respect to a real life implementation. We illustrate that a straightforward implementation is not robust at all. However, as these controllers are the translation of a realistic control objective —namely set–point control—, they can serve as a basis for the development of more reliable model–independent *adaptive control* schemes. To do so, they are interpreted within the framework of *nonlinear linearizing control theory.* By doing so, we incorporate a mechanism that makes them both stable and robust against disturbances.

The next step is then to cope with the monitoring problem, i.e. how to determine on–line the variables needed in the controller. In other words, how to make the nonlinear linearizing controller adaptive. As an example, simulation results are given for the penicillin G fed–batch fermentation process using the new unifying model. We present three possible solutions depending on which variables are on–line available. The use of *software sensors* is clearly illustrated. We also point out the *trade off* between *on–line measurement requirements* (such as accessibility and accuracy) and *a priori information needs* (such as yield and maintenance coefficients). Both a *linear regression estimator* and a *state observer based estimator* can be used for on–line tracking of the specific rates, which we consider as time varying parameters (*minimal modeling concept*). Furthermore, we illustrate that it is possible to take a measurement delay into account.

A remarkable result is the following. If there are no state inequality constraints, we only have to specify a reference level for the production phase. However, the controllers we propose can be implemented without difficulty form the start of the fermentation on. The first growth phase is then mainly used to obtain estimator convergence. Furthermore, the extension to a problem with constraints is straightforward. In other words, we are able to design a substrate concentration reference profile for the complete process which guarantees suboptimal performance. As such, this chapter can be considered as an extension of the methods presented in Chapter 5 of [Bastin and Dochain 1990], where the reference substrate concentration is kept constant throughout the whole fermentation process.

The material presented in this chapter is taken from [Van Impe et al. 1991b] and [Van Impe et al. 1992c and 1992e].

Chapter 7

Conclusions and open problems

Besides the development of a *new dynamic model describing microbial growth* in food products as a function of both time and temperature (over the whole range of growth and inactivation), the main contributions of this thesis can be summarized in the following paradigms :

1. *Optimization for model discrimination*
2. *Optimal adaptive control*

Some suggestions for further research are given at the end of this text.

0.3 Software environment

All simulation results presented throughout this thesis have been obtained using self–written code in FORTRAN. It was never our intention to write a complete software package for optimization of biotechnological processes, although this may be interesting too.

Nevertheless, some of the routines to calculate optimal and heuristic feed rate profiles for the penicillin G fermentation process have been collected into a more or less user–friendly program [Van Impe 1989]. The models of Heijnen *et al.* [1979] and Bajpai and Reuß [1980,1981], together with our unifying model, have been brought in explicitly. Needless to say that in a more general software package for optimization of fed–batch fermentations, the calculation of first and second order derivatives of the right–hand side of the model equations (which are needed along singular arcs) could be done by using a symbolic language (such as REDUCE, MACSYMA, MATHEMATICA).

For numerical integration, we have made use of the routines D02 from the NAG FORTRAN LIBRARY. These routines integrate a stiff system of first order ordinary differential equations, using a variable–order, variable–step method implementing the Backward Differentiation Formulae. As compared with standard packages such as MATLAB or MATRIX$_X$ (which also contain routines for stiff system integration), the D02 routines have the advantage that they can stop not only if the final time (specified a priori) is reached, but also if a user–specified function of the state variables equals zero (e.g. a concentration reaching some critical value). The importance of using a stiff system solver for simulating fed–batch fermentation processes with growth/production decoupling is illustrated in Chapter 4.

For function minimization, we have made use of the routines E04 from the NAG FORTRAN LIBRARY, and of an algorithm proposed by Brent [1973]. These algorithms perform minimization without the need for derivatives. This is a very useful feature for parametric optimization of dynamic systems, where the goal is to minimize a performance index (which is the result of a numerical integration with respect to time) with respect to the value of the free parameters of the input function(s).

All plots in this text have been generated using MATLAB and the drawing package XFIG. The text itself has been typeset using LaTeX.

A brief description of our optimization program for the penicillin G fermentation process can be found in [Van Impe 1989].

Chapter 1

Systems and control tools

As an area for control applications the field of biotechnology is still comparatively new. Only in a few cases the control approach has already led to computer–controlled full–scale systems [Halme and Holmberg 1979]. Mathematical modeling and parameter estimation have become prerequisites for the development of model–based control strategies. Software sensors for non–measurable parameters and state variables are necessary for practical implementation of control and supervising systems. In this chapter we present the background material and mathematical tools used throughout this work for modeling and control of biotechnological processes. The aim is not to provide a comprehensive overview of these topics, but rather to establish the general framework for the design of estimation and control algorithms which will be discussed in subsequent chapters.

In section 1.1 we distinguish between physiological, unstructured and structured models. An important contribution of this section is the introduction of the new concept of endogenous fraction. This allows to describe all kinds of metabolism for biomass survival and product synthesis within one unifying frame. It is at the basis of the results presented in Chapter 5 and 6. Furthermore, we present a general state space model for a biotechnological process [Bastin and Dochain 1990]. The minimal modeling concept in modeling the reaction kinetics is explained. In reducing the complexity of a state space model, the singular perturbation technique is illustrated with a simple example.

Section 1.2 gives an overview of optimal control theory. We briefly introduce the issue of parametric optimization as a suboptimal dynamic optimization method. The Minimum Principle of Pontryagin is at the basis of all control strategies presented in this work. Singular control problems are briefly discussed. Furthermore, we derive necessary conditions if some components of the initial state are not given a priori but can be used as additional control parameters. Finally, we present a new, simple, but powerful conjecture that allows to determine optimal control profiles in the case of a continuous but non–differentiable state space model (Conjecture 1.1).

1.1 Modeling biotechnological processes

In many cases, the objective of development of a mathematical model is aimed in the first place at providing the basis for controlling the performance of a bioreactor. Moreover, mathematical models are absolutely indispensable in the calculation of optimal operating conditions.

The biological behavior of biotechnological processes occurring in a bioreactor has a complexity unparalleled in the chemical industry. As a consequence, its prediction from information about the environmental conditions is extremely difficult. The number of reactions and species that are involved in the system may be very large. An accurate description of such complex systems can therefore result in very involved models, which may not be very useful from a control engineering viewpoint.

In the following, only the most relevant reactions and components will be taken into account in order to minimize the model complexity. So the dynamic model is *never* an exhaustive description of the process. For instance, nonlimiting substrates and fast intermediate reactions are most often omitted. Similarly, products of a reaction which do not serve as substrates in other reactions and are of no interest to the user may also be omitted.

In general, a model for a biotechnological process describes two kinds of phenomena. Firstly, the biological, chemical and biochemical reactions that transform some reactants into some products. Secondly, mass transfer processes due to exchanges of both the liquid and gaseous phase of the reactor contents with the environment.

We may distinguish between three different types of models used for control : *unstructured, structured* and *physiological* models [Johnson 1987].

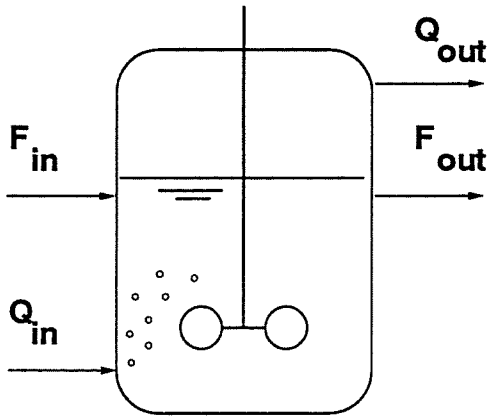

Figure 1.1: Stirred Tank Reactor STR

1.1.1 Unstructured models

An unstructured model involving only *lumped* variables may be used under the following assumptions. Firstly, we assume that the process is in a *completely mixed* condition, which implies that the composition of the medium is homogeneous in the reactor. Secondly, we assume that the activities of the compounds which are part of the functioning *biomass* can be specified by only one number, the total amount of biomass present in the culture.

The most widely used variables in an unstructured model are the concentrations (or the absolute amount) of *substrate*, *biomass* and *product*, and the culture *volume*.

Such models are useful in describing the overall observed microbial response. No provision is made for changes in the internal composition of the cells when the metabolism is shifted.

The dynamic model in general consists of a set of ordinary first order differential equations, derived from mass balances over the bioreactor.

Let us start with a basic example.

1.1.1.1 Simple microbial growth process

Consider the microbial growth of one population of micro–organisms (the *biomass*) on a single limiting *substrate* in the stirred tank reactor of Figure 1.1. We introduce the following notation.

S : absolute amount of substrate in the reactor
X : absolute amount of biomass in the reactor
V : reactor volume
C_s : $= S/V$ substrate concentration in the reactor and the effluent
$C_{s,in}$: substrate concentration in the influent
C_x : $= X/V$ biomass concentration in the reactor and the effluent
F_{in} : influent volumetric flow rate
F_{out} : effluent volumetric flow rate
μ : specific growth rate
$Y_{x/s}$: biomass on substrate yield coefficient

The biomass concentration in the influent is equal to zero. The *reaction scheme* clearly consists of one autocatalyzed growth reaction involving the two components S and X :

$$S \xrightarrow[X]{\mu} X$$

Observe that in general a component may be reactant and product at the same time. In the above scheme, X is an *autocatalyst.* This means that it is a pseudoreactant which is *not consumed* by the reaction, but which can be accumulated in the bioreactor.

Application of straightforward mass balances leads to the following set of equations :

Biomass accumulation in the bioreactor

$$\frac{dX}{dt} = \mu X - F_{out}\frac{X}{V}$$

Substrate accumulation in the bioreactor

$$\frac{dS}{dt} = -\frac{1}{Y_{x/s}}\mu X - F_{out}\frac{S}{V} + F_{in}C_{s,in} \qquad (1.1)$$

Variation of volume

$$\frac{dV}{dt} = F_{in} - F_{out}$$

Using concentrations instead of absolute quantities, we obtain the following equivalent dynamic model :

$$\begin{aligned}\frac{dC_x}{dt} &= \mu C_x - DC_x \\ \frac{dC_s}{dt} &= -\frac{1}{Y_{x/s}}\mu C_x - DC_s + DC_{s,in} \qquad (1.2)\\ \frac{dV}{dt} &= DV - F_{out}\end{aligned}$$

with the *dilution rate* D defined as

$$D \triangleq \frac{F_{in}}{V}$$

We define the *specific substrate consumption rate* σ as

$$\sigma \triangleq \frac{1}{Y_{x/s}}\mu \qquad (1.3)$$

Note that the dynamic model can represent any mode chosen for bioreactor operation. Consider the following three particular cases.

Batch reactor

During this mode of operation there is neither inflow nor outflow. Clearly the culture volume is constant. The dynamic model is given by equations (1.1) using

$$F_{in} = F_{out} = 0$$

or by equations (1.2) using

$$D = 0$$

Continuous stirred tank reactor CSTR

During this mode of operation substrate is continuously added and product continuously removed, the total culture volume remaining constant. In the above models we have

$$\begin{aligned}F_{in} = F_{out} &= F \\ D &= F/V\end{aligned}$$

Fed–batch reactor

A fed–batch reactor has no outflow. The tank initially contains a small amount of both substrate and biomass and is filled either intermittently or continuously with the influent substrate. In the above dynamic models we must use

$$F_{out} = 0$$

1.1.1.2 Extensions to the basic dynamics

Cell death and maintenance

Additional terms can be included in the model equations (1.1) or (1.2) to account for the natural death of biomass and for that part of the substrate and the biomass used for biomass maintenance. Using e.g. model (1.2) we obtain :

$$\begin{aligned}
\frac{dC_x}{dt} &= (\mu_{substr} - m_x - k_d)\, C_x \;-\; DC_x \\
\frac{dC_s}{dt} &= -(\frac{1}{Y_{x/s}}\mu_{substr} + m_s)\, C_x \;+\; D(C_{s,in} - C_s) \\
\frac{dV}{dt} &= DV - F_{out}
\end{aligned}$$

with

k_d : specific rate of cell death
m_s : specific maintenance demand of substrate by the cells
m_x : specific maintenance demand of cell mass by the cells

μ_{substr} represents the specific substrate to biomass conversion rate, previously denoted with μ. The difference between m_s and m_x rests in assumptions about the nature of the maintenance metabolism for biomass survival.

$m_s = 0, m_x > 0$
If $m_s = 0$ then *endogenous* metabolism is assumed to account for the maintenance requirements of growth [Herbert 1958]. The energy supply for maintenance purposes is assumed due to combustion of part of the biomass.

$m_s > 0, m_x = 0$
If $m_x = 0$ then *maintenance* metabolism is assumed : maintenance energy is assumed to be provided by consumption of a part of the external substrate [Pirt 1965].

$m_s > 0, m_x > 0$
The generic case of a mixed endogenous–maintenance metabolism can be formulated as follows. Let m denote the *overall specific maintenance* demand of the living cells. Then we define the *endogenous fraction* $f_m \in [0, 1]$ of the overall specific maintenance demand as follows :

$$\begin{aligned}
m_x &\triangleq f_m\, Y_{x/s}\, m \\
m_s &\triangleq (1 - f_m)\, m
\end{aligned}$$

We define the *overall* specific growth rate μ and the *overall* specific substrate consumption rate σ as

$$\mu \triangleq \mu_{substr} - m_x \tag{1.4}$$

$$\sigma \triangleq \frac{1}{Y_{x/s}}\mu_{substr} + m_s \tag{1.5}$$

Clearly, we have

$$\sigma = \frac{1}{Y_{x/s}}\mu + m \tag{1.6}$$

which is a generalization of (1.3). Note that $f_m = 1$ represents endogenous metabolism, $f_m = 0$ maintenance metabolism.

Formation of a synthesis product

The mass balance relative to the product P (with concentration C_p) in the bioreactor of Figure 1.1 is

$$\frac{dP}{dt} = \pi X - F_{out}\frac{P}{V} - Q_{out}V \tag{1.7}$$

or

$$\frac{dC_p}{dt} = \pi C_x - DC_p - Q_{out} \tag{1.8}$$

with π being the specific production rate, and Q_{out} the rate of mass outflow (per unit volume) of the product from the reactor in gaseous form.

According to [Gaden 1959] and [Roels 1983], three types of product formation processes can be distinguished. In Class 1, the product is directly associated to the generation of energy by the organism. In Class 2, the product is a result of primary energy metabolism but indirectly. Class 3 contains the remaining product formation processes, in which there is no clear direct or indirect coupling to energy generation. These classes are then kinetically characterized with the help of the appearance of product in relation to that of biomass, and this subsequently gives rise to the concept of *growth associated* and *non growth associated* product formation.

In general, we have [Luedeking and Piret 1959] :

$$\pi = Y_{p/x}\mu + m_p$$

The first term represents the *growth associated* specific production rate, with $Y_{p/x}$ the corresponding yield coefficient. The second term represents the *non growth associated* part.

Analogous to the endogenous fraction f_m of the overall specific maintenance demand, we introduce the endogenous fraction $f_p \in [0,1]$ of the energy supply for product synthesis. A natural extension of the overall specific growth rate μ (1.4) and substrate consumption rate σ (1.5) is :

$$\mu \triangleq \mu_{substr} - Y_{x/s}(f_m m + f_p \frac{\pi}{Y_{p/s}}) \tag{1.9}$$

$$\sigma \triangleq \frac{1}{Y_{x/s}}\mu_{substr} + (1-f_m)m + (1-f_p)\frac{\pi}{Y_{p/s}} \tag{1.10}$$

with $Y_{p/s}$ the substrate to product yield coefficient.

A further generalization of (1.3) and (1.6) is then

$$\sigma = \frac{1}{Y_{x/s}}\mu + m + \frac{1}{Y_{p/s}}\pi \tag{1.11}$$

Observe that $f_p = 1$ represents an endogenous metabolism; $f_p = 0$ a maintenance metabolism.

Due to the introduction of the new concept of endogenous fraction, we are able to describe all kinds of metabolic behavior within one unifying frame. Observe that equation (1.11) holds true independent of the value of the fractions f_m and f_p.

This unifying frame will prove very useful in comparing models which are based on different metabolic assumptions. An example will be given in Chapter 4 where we analyze in detail two models for the penicillin G fed–batch fermentation process. This new concept will be at the basis of the construction of a unifying model for this type of fermentation process presented in Chapter 5.

Dissolved oxygen dynamics

In aerobic fermentation processes, oxygen is needed for growth (and in general also for product formation) : dissolved oxygen plays the role of an additional substrate. Typical examples are the baker's yeast fermentation process and the activated sludge wastewater treatment process. A straightforward mass balance for the bioreactor of Figure 1.1 leads to

$$\frac{dC_o}{dt} = OTR - OUR - DC_o$$

with C_o the dissolved oxygen concentration, OTR the oxygen transfer rate and OUR the oxygen uptake rate.
The postulation of balance (1.11) for the rate of substrate consumption leads to an expression of exactly the same structure for the oxygen uptake rate OUR, i.e. including a growth rate, a biomass concentration and a product formation associated part :

$$OUR = [\frac{1}{Y_{x/o}}\mu + m_o + \frac{1}{Y_{p/o}}\pi]C_x \tag{1.12}$$

in which $Y_{x/o}$ is the yield for biomass growth on oxygen consumed, $Y_{p/o}$ is the yield for product formation on oxygen, and m_o is the specific rate of oxygen consumption in maintenance processes.

The oxygen transfer rate OTR is expressed as follows :

$$OTR = k_L a\ (C_{o,sat} - C_o)$$

where $k_L a$ is the mass transfer coefficient and $C_{o,sat}$ is the saturation concentration of dissolved oxygen. However, in many applications both

parameters are unknown and time varying. Assuming that both the input and output oxygen flow rates (per unit volume) are available and neglecting the liquid–gas transfer dynamics, the *OTR* may be calculated from the oxygen balance in the gaseous phase :

$$OTR = Q_{in} - Q_{out}$$

Dissolved carbon dioxide dynamics

The dynamics of the dissolved carbon dioxide production during fermentation can be described by the *carbon dioxide evolution rate CER*. As CO_2 plays the role of an additional product, application of balance (1.8) for product formation leads to

$$\frac{dC_c}{dt} = CER - DC_c - Q_{out}$$

with C_c the dissolved carbon dioxide concentration and Q_{out} the rate of outflow of carbon dioxide from the reactor in gaseous form. Analogous to relations (1.11) and (1.12) the carbon dioxide evolution rate *CER* can be expressed as

$$CER = [Y_{c/x}\mu + m_c + Y_{c/p}\pi]C_x \qquad (1.13)$$

under suitably controlled conditions for *pH*. At any time during the fermentation, carbon dioxide arises from growth (yield coefficient $Y_{c/x}$), maintenance energy (specific rate m_c) and product synthesis (yield coefficient $Y_{c/p}$).

The practical importance of the last two extensions is the following. In most applications, the value of the basic variables S, X and P can not be measured on–line. However, it has been shown several times that these variables may be estimated using on–line measurements of easily accessible auxiliary variables such as oxygen and carbon dioxide in the inlet and outlet gas streams of the bioreactor. An example will be given in Chapter 6.

1.1.1.3 Models for the specific reaction rates

The specific reaction rates μ_{substr} and π are in general very complex functions of the environmental factors such as substrate concentration C_s, biomass concentration C_x, product concentration C_p, dissolved oxygen concentration C_o, *pH*, temperature T, ...

It is common practice to express a specific rate as a multiplication of individual factors. Each of them models the influence of one environmental factor, e.g.

$$\mu(C_s, C_x, C_p, C_o, pH, T, \ldots) \triangleq \mu(C_s)\mu(C_x)\mu(C_p)\mu(C_o)\mu(pH)\mu(T)\ldots$$

where we have omitted the subscript '$_{substr}$' everywhere. An overview of analytical expressions proposed in the literature for the different factors is given in [Bastin and Dochain 1990]. We limit ourselves to the models that we will use frequently in the subsequent chapters.

Models of the specific growth rate

Influence of the substrate concentration C_s

The Monod law [Monod 1942]

$$\mu_{substr}(C_s) = \mu_{max}\frac{C_s}{K_M + C_s} \qquad (1.14)$$

This is a mathematical homologue of the Michaelis–Menten equation, which expresses the reaction rate of enzyme–catalyzed reactions with a single substrate. Monod applied this law to micro–organism growth without any physical justification. As a result, this model has black box characteristics. In fact, there are many other sigmoidal functions which can fit the same experimental growth data, such as the *Tessier law*, *the Blackman law*, ...

The Tessier law [Tessier 1942]

$$\mu_{substr}(C_s) = \mu_{max}[1 - \exp(-\frac{C_s}{K_M})] \qquad (1.15)$$

The Blackman law [Blackman 1905]

$$\mu_{substr}(C_s) = \begin{cases} \mu_{max}\ C_s/K_M & \text{if } C_s \leq K_M \\ \mu_{max} & \text{if } C_s > K_M \end{cases} \qquad (1.16)$$

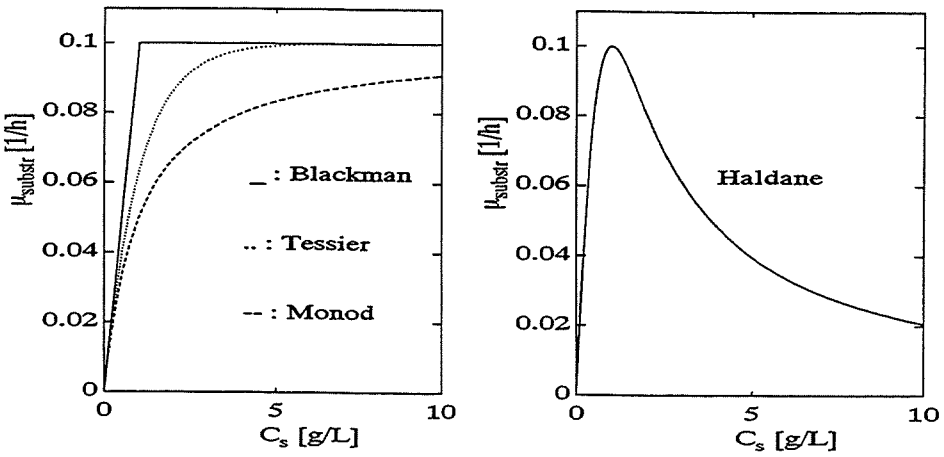

Figure 1.2: Monod, Tessier, Blackman and Haldane kinetics

To describe the inhibition of growth by high concentrations of a substrate, Andrews proposed to use the law derived by Haldane to model inhibition in enzyme–substrate reactions.
The Haldane law [Andrews 1968]

$$\mu_{substr}(C_s) = \mu_m \frac{C_s}{K_p + C_s + C_s^2/K_i} \tag{1.17}$$

This expression reaches its maximum value

$$\mu_{max} = \mu_m \frac{1}{1 + 2(K_p/K_i)^{1/2}}$$

at the substrate concentration

$$C_s^* = (K_p K_i)^{1/2}$$

Model equations (1.14), (1.15), (1.16) and (1.17) are shown in Figure 1.2 using $K_M = 1$ g/L, $K_p = 10$ g/L, $K_i = 0.1$ g/L, $\mu_{max} = 0.1$ 1/h and $\mu_m = 2.1$ 1/h.

Influence of the biomass concentration C_x

At high cell densities, serious diffusional limitations can be expected (and this has been experimentally observed in particular instances) which would cause the apparent value of the saturation constant in e.g. Monod kinetics (1.14) to be higher than its value at lower densities. In other words, biomass growth may slow down at high biomass concentrations. This can be expressed by the Contois model which is function of both C_s and C_x.
The Contois law [Contois 1959]

$$\mu_{substr}(C_s, C_x) = \mu_{max} \frac{C_s}{K_x C_x + C_s} \tag{1.18}$$

Influence of the temperature T

If it is assumed that growth is the end product of a sequence of enzymic reactions and that the rate of the sequence is determined by one rate limiting step, the temperature dependence of the maximum specific growth rate can be assumed to be represented by an Arrhenius relationship of the following type :

$$\mu(T) = A C_e \exp(-\frac{\Delta h_e}{RT})$$

in which A is a constant, C_e is the concentration of the rate limiting enzyme in the biomass, Δh_e is the activation enthalpy of the rate limiting reaction, and R is the gas constant. This model is valid only in a limited range of temperatures, i.e. below the so–called optimum temperature above which the growth rate decreases continuously with increasing temperature.

Observe that all yield coefficients $Y_{i/j}$ and specific maintenance coefficients m_k may depend on temperature as well.

In most engineering calculations in the field of (fed–batch) fermentation processes, the temperature dependence is considered less important than the substrate dependence, and is therefore most often neglected.

However, in the field of food processing, temperature is one of the most important environmental factors influencing the (undesired) growth of micro–organisms (see e.g. [Teixeira and Shoemaker 1989]), while substrate is considered non–limiting. At

present, much more research effort is needed in modeling a microbial population in foods, in particular under time varying temperature conditions. Chapter 2 is entirely devoted to a new dynamic model for microbial growth and cell death in chilled prepared food products (see also [Van Impe *et al.* 1992a]).

Models of the specific production rate

As an example, we mention two analytic expressions presented in the literature modeling the specific production rate π of penicillin G by *Penicillium chrysogenum* in a fed–batch fermentation process.

Influence of the specific growth rate μ

Heijnen *et al.* [1979] propose the following relation between π and the overall growth rate μ :

$$\pi(\mu) = \begin{cases} \pi_{max}\ \mu/\mu_{crit} & \text{if } \mu \leq \mu_{crit} \\ \pi_{max} & \text{if } \mu > \mu_{crit} \end{cases}$$

This is a homologue of the Blackman law (1.16).

Influence of the substrate concentration C_s

Bajpai and Reuß [1980,1981] use a homologue of the Haldane model (1.17) to describe π as function of C_s :

$$\pi(C_s) = \pi_m \frac{C_s}{K_p + C_s + C_s^2/K_i}$$

1.1.2 Structured models

As already mentioned, in an *unstructured* fermentation model the culture is assumed to consist of a single, homogeneously growing organism. Moreover, it is often assumed that there is a single growth limiting substrate. Such a model will be successful if all relevant adaptational mechanisms inside the organism are at steady state with respect to the environmental conditions.

However, an unstructured model will probably fail if the time constants of the relevant environmental changes become of the order of magnitude of those of relevant adaptational mechanisms inside the organism. Hence, *structured* models in which changes in the composition of the organism are considered, are sometimes needed.

In general, a *structured* model takes into account the various cellular processes which are important to the process. The activities of specific

enzymes in the cell as well as structures such as ribosomes, macromolecular components (e.g. proteins, DNA/RNA, ...) may all be included in a highly structured model. Furthermore, the age distribution of e.g. the growing cells in the culture can be characterized by a system of partial differential equations, sometimes simplified to ordinary differential equations.

An advantage of such models is the potential for modeling the interrelationship of the metabolic processes and predicting the effects of disturbances on the overall microbial process. The disadvantages of the highly structured model are the difficulty in determining the various kinetic constants to describe the individual reactions and the computational difficulty posed by large sets of equations that result. Such models are thus generally of little use to the control engineer.

Although the extremely complex nature of the biological system may require complicated models, oversophistication of models should be avoided. This tends to defy the very purpose of modeling by obscuring the essence of the model, and makes the prediction of microbial behavior exceedingly difficult.

A subclass of potentially useful structured models results from a simple *extension* of the unstructured approach, in which the amount and the properties of the biomass are specified by up to three or four variables. Those models, generally termed *compartment* models, combine a better description of the behavior of the system with moderate mathematical complexity and sufficiently low number of parameters in order to permit experimental verification.

Our recent work on the design of estimation and control algorithms for an activated sludge wastewater treatment process using a structured compartment model for the biotransformation processes is not included in this text. Some results can be found in [Vanrolleghem et al. 1991] and [Van Impe et al. 1991e, 1991f, 1992f].

1.1.3 Physiological models

It should be sufficiently clear that constructing an accurate mathematical model of a biotechnological process is a formidable task. Moreover, suitable values must be found for the model parameters. Therefore, in the past considerable attention has been paid to developing controllers *without* the need for a mathematical model.

In a *physiological* (or *verbal*) *model* knowledge of the biological processes is expressed in consecutive, but usually non–mathematical, statements. Models based upon an understanding of the Pasteur, Crabtree, ... effects are important here [Roels 1983].

Physiological control attempts to emulate the routine process control of e.g. the chemical industry where process variables are held at *set–points* by means of regulators. Controller design reduces to *selecting the 'appropriate' set–points.*

EXAMPLE : BAKER'S YEAST FED–BATCH FERMENTATION

The mechanism of yeast growth on glucose with ethanol production is described by the following set of autocatalytic microbiological reactions.

Respiratory growth on glucose

$$S + O \xrightarrow[X]{\phi_1} X + C$$

Fermentative growth on glucose

$$S \xrightarrow[X]{\phi_2} X + E + C$$

Respiratory growth on ethanol

$$E + O \xrightarrow[X]{\phi_3} X + C$$

where S, O, X, C, E represent glucose, dissolved oxygen, yeast, dissolved carbon dioxide and ethanol respectively.

This reaction scheme can be interpreted as follows. The above three reactions represent three metabolic pathways from glucose to yeast. If the glucose concentration in a well–aerated bioreactor (high dissolved oxygen concentration) is sufficiently low, then primarily the first pathway is activated (respiratory growth of biomass on glucose). The yield of yeast production with respect to glucose is high, but the reaction rate ϕ_1 is very low. On the other hand, at high glucose concentrations, respiratory growth is

inhibited or repressed. Instead the second pathway is activated, where fermentative growth appears with a high reaction rate ϕ_2 but a low yield, while ethanol is produced at the expense of some glucose. The ethanol produced by this fermentative reaction can be consumed for respiratory yeast growth in the third pathway if oxygen is present. Needless to say that in reality the three reactions can take place simultaneously. Their relative importance is determined by the level of glucose and dissolved oxygen concentrations.

Based on this physiological model, we could think of the following control objectives :

1. Yeast growth rate is maximal without ethanol production if substrate concentration is held at its critical value.
2. Yeast growth is optimal when the specific growth rate follows a predetermined trajectory.
3. Yeast growth is optimal when the ethanol concentration is constant.
4. Maximum yeast growth occurs when there is pure respiratory growth without ethanol production and simultaneously maximum substrate feed.

As already mentioned, one of the main contributions of this work is to provide a theoretical frame for developing optimal adaptive controllers for biotechnological processes which can be easily implemented.

However, our approach will be based not on a physiological (verbal) model but on a mathematical unstructured model. Using optimal control theory, we try to characterize the optimal control strategy in terms of model characteristics and kinetic parameters. This optimal strategy will then be translated into an adaptive suboptimal controller, which consists basically of some set–point or reference profile and a tracking mechanism. In choosing an appropriate set–point or reference, the results gained during the preliminary optimal control study will prove to be very useful.

This approach will be illustrated in Chapter 3 for a general fed–batch fermentation process and in Chapters 4 to 6 for the penicillin G fed–batch fermentation process.

1.1.4 General state space model

Application of modern control techniques in general requires the knowledge of a *state space description* of the process.

If we define a biotechnological process as a set of m reactions involving n components within a *reaction scheme*, then a general state space model for a biotechnological process in a perfectly mixed stirred tank reactor (STR) is given by (see [Bastin and Dochain 1990]) :

$$\frac{d\mathbf{x}}{dt} = \mathbf{K}\,\boldsymbol{\phi}(\mathbf{x},t) - D\mathbf{x} - \mathbf{q}(\mathbf{x}) + \mathbf{f} \tag{1.19}$$

with

$\mathbf{x}$: $n \times 1$ state vector of concentrations of components in the liquid phase
$\mathbf{K}$: $n \times m$ matrix containing the yield coefficients
$\boldsymbol{\phi}$: $m \times 1$ vector of reaction rates
may depend in general on the process state $\mathbf{x}$ and the time t
D : the dilution rate
$\mathbf{q}$: $n \times 1$ vector
q_i is the rate of mass outflow of the corresponding x_i from the reactor in gaseous form, in general depending on $\mathbf{x}$
$\mathbf{f}$: $n \times 1$ vector
f_i is the feed rate of the corresponding x_i if it is an external substrate

We recognize clearly the two kinds of phenomena occurring in a biotechnological process :

1. the first term at the right–hand side represents the *kinetics* of all microbiological, chemical and biochemical reactions occurring in the bioreactor,

2. the remaining terms represent the *transport phenomena* occurring at the boundaries of the bioreactor.

This state space model for single–tank systems can be generalized to describe *complex* biotechnological systems occurring in interconnected bioreactors [Chen 1992].

It is a basic tool in designing model–based estimation and adaptive control algorithms for biotechnological processes ([Bastin and Dochain 1990] and [Chen 1992]).

Observe that the general state space model can represent both unstructured and structured compartment models.

As an example, consider the simple microbial growth process including cell death and maintenance metabolism. The reaction scheme involves $n = 3$ components (substrate S, living biomass X and dead biomass X_d) and $m = 3$ reactions (growth, cell death and maintenance) :

$$S \xrightarrow[X]{\mu} X$$

$$S \xrightarrow[X]{m_s} X$$

$$X \xrightarrow[]{k_d} X_d$$

The state space model for this system is (C_{xd} is the concentration of dead biomass X_d) :

$$\frac{d}{dt}\begin{pmatrix} C_s \\ C_x \\ C_{xd} \end{pmatrix} = \begin{pmatrix} -1/Y_{x/s} & -1 & 0 \\ 1 & 0 & -1 \\ 0 & 0 & 1 \end{pmatrix}\begin{pmatrix} \mu C_x \\ m_s C_x \\ k_d C_x \end{pmatrix} - D\begin{pmatrix} C_s \\ C_x \\ C_{xd} \end{pmatrix} + \begin{pmatrix} D\,C_{s,in} \\ 0 \\ 0 \end{pmatrix}$$

Obviously, we could write an equivalent state space model using absolute amounts instead of concentrations.

1.1.5 Minimal modeling

Once the biotechnological process is described within the frame of a general state space model, we must select appropriate models for both the reaction kinetics and the transport phenomena. Obviously, modeling the reaction kinetics is the most difficult of the two.

In general, a modeling procedure for the reaction rates consists of two steps.

First, we choose an appropriate analytical expression for each reaction rate, most often a rational function of both the state variables and a set of kinetic coefficients. Some examples have been given above.

Second, the unknown kinetic parameters must be calibrated from experimental data.

However, in modeling of e.g. a growth curve the choice of an analytical expression is a priori virtually unlimited. Monod himself recognized that [Monod 1942]

> " ... toute courbe d'allure sigmoïde pourrait être ajustée aux données expérimentales."

Furthermore, Holmberg and Ranta [1982] illustrated that the parameters μ_{max} and K_M used in Monod–kinetics (1.14) are not practically identifiable : they can not be uniquely determined from noisy batch measurements. Another illustration of the non–uniqueness of kinetic parameters will be given in Chapter 5 for the penicillin G fed–batch fermentation.

Therefore, we will *design control algorithms for biotechnological processes with a minimal modeling of the kinetics* (see also [Bastin and Dochain 1990]).

REMARK

The practical non–identifiability does not mean that analytical models for the reaction rates should not be used at all. Since one of the main purposes of this thesis is to design robust controllers with nearly optimal performance, we first have to characterize the optimal controller under the assumption of a completely known model. As an example, we will show in Chapter 5 that certain kinetic parameters may play a vital role in answering the question whether optimization of the substrate feed rate profile to the penicillin G fed–batch fermentation process is useful or not.

Furthermore, although we are building simulation models for biotechnological processes for control purposes, we should not neglect their potential use in studying the physiological properties of the organisms. From Chapter 3 on, it will be illustrated that the study of model building and parameter estimation on the one hand, and experimental results on the other, raises many questions that can not be solved without further microbiological research. Also the usefulness of simulation models in connection with experimental planning will be shown.

In summary, modeling and simulation can be valuable tools in both control and microbiological research by directing investigators towards a search for quantifiable results. ■

1.1.6 The singular perturbation technique

In reducing the complexity of a state model for a biotechnological process (1.19), we may use the singular perturbation technique. This technique is suitable when certain substrates or products have low solubility in the liquid phase of the bioreactor. The basic idea is to replace the differential equation for these components by a simple algebraic equation.

We limit ourselves here to a practical example. A more detailed treatment can be found in e.g. [Bastin and Dochain 1990] and [Van Breusegem and Bastin 1992].

SINGULAR PERTURBATION TECHNIQUE FOR A PRODUCT

Recall the dynamic equation for dissolved carbon dioxide produced during a fermentation

$$\frac{dC_c}{dt} = CER - DC_c - Q_{out}$$

This model is valid only if the carbon dioxide concentration C_c is lower than the saturation concentration $C_{c,sat}$ representative of the CO_2 solubility :

$$C_c \triangleq \Pi\, C_{c,sat} \qquad \Pi \in [0,1]$$

The differential equation can then be written as

$$C_{c,sat}\frac{d\,\Pi}{dt} = CER - \Pi D C_{c,sat} - Q_{out} \tag{1.20}$$

In several applications, the CO_2 solubility is very low, which means that carbon dioxide appears almost completely under gaseous form. Thus, letting $C_{c,sat} = 0$ is a meaningful singular perturbation. We obtain the following algebraic equation [using (1.13)] :

$$Q_{out} = CER = [Y_{c/x}\mu + m_c + Y_{c/p}\pi]C_x$$

Note that we do *not* assume that $C_{c,sat}$ is equal to zero. We only assume that $C_{c,sat}$ is small enough to neglect the terms $C_{c,sat}(d\,\Pi/dt)$ and $\Pi D C_{c,sat}$ in differential equation (1.20).

1.2 Optimal control theory

1.2.1 Statement of the problem

Consider a dynamical system governed by the following ordinary differential equation for the *state vector* $\mathbf{x}(t) \in \mathbb{R}^{n\times 1}$

$$\frac{d\mathbf{x}(t)}{dt} = \mathbf{f}[\mathbf{x}(t), \mathbf{u}(t), t],\ t_0 \leq t \leq t_f \tag{1.21}$$

where the real valued $n \times 1$ function $\mathbf{f}$ may depend on the state, the vector of *control inputs* $\mathbf{u}(t) \in \mathbb{R}^{m\times 1}$ and the time t. t_0 is the *initial time* (usually $t_0 = 0$), while t_f denotes the *final time* (either free or fixed).
Physically *realizable controls* generally have magnitude limitations

$$U_{i,MIN} \leq u_i(t) \leq U_{i,MAX}$$

The thrust of a rocket engine cannot exceed a certain value; motors, which provide torque, saturate. *State constraints* often arise because of safety, or structural restrictions : the current in an electric motor cannot exceed a certain value without damaging the windings; a concentration in a chemical reactor is by definition always positive. Specifying an initial (and/or final) state further reduces the admissible region in the state space. A control (respectively state) vector satisfying all constraints of the problem is called an *admissible control* (respectively *admissible state*).

The general problem of optimal control is to *find an admissible history of the control vector* [$\mathbf{u}^*(t)$ for $t_0 \leq t \leq t_f$] *which forces the state from its initial value* $\mathbf{x}_0$ (usually given) *to its final value* $\mathbf{x}_f$ (either fixed or free) *and,* at the same time, *minimizes a cost function.* The resulting state history [$\mathbf{x}^*(t)$ for $t_0 \leq t \leq t_f$] is an *optimal trajectory.* Seeking to *maximize* the same cost function but with opposite sign is another way of expressing the same problem; hence the distinction between optimizing to achieve a maximum or a minimum is mathematically trivial.

A cost function or *performance index* in general consists of two parts, a scalar algebraic function of the final state and time, and a scalar integral function of the state and control :

$$J[\mathbf{u}] = g[\mathbf{x}(t_f), t_f] + \int_{t_0}^{t_f} \mathcal{L}[\mathbf{x}(t), \mathbf{u}(t), t]\ dt \tag{1.22}$$

A cost function containing only a terminal penalty is of the *Mayer type*, while one with just the integral term is of the *Lagrange type.* If both terms

are present, the cost index is of the *Bolza type.* Note that a cost function of one type can easily be transformed into either of the two other types. For the *minimum time problem* for instance, the appropriate cost function is ($t_0 = 0$) :

$$J[\mathbf{u}] = \int_0^{t_f} 1\ dt = t_f$$

1.2.2 Parametric optimization

In many problems, the *admissible control histories* [$\mathbf{u}^*(t)$ for $t_0 \leq t \leq t_f$] are assumed to have *known shapes but unknown magnitudes.* The specified control functions are given by $\mathbf{u}(\mathbf{k}, t)$, where the constant vector $\mathbf{k}$ contains the *control parameters.* The dimension of $\mathbf{k}$ is in general greater than or equal to the control vector dimension m.

The objective is to find the value of $\mathbf{k}$ that minimizes the cost function J (1.22) while satisfying the dynamic constraint (1.21). Observe that there is no guarantee that a *parametric–optimal* solution is truly optimal or, for that matter, that it is unique in minimizing J.

If control settings must be constant during $[t_0, t_f]$, the admissible controls are described by

$$\mathbf{u}(\mathbf{k}, t) = \mathbf{k}$$

If they increase or decrease linearly,

$$\mathbf{u}(\mathbf{k}, t) = \mathbf{k}_1 + \mathbf{k}_2 t$$

where $\mathbf{k}^{\mathbf{T}} \triangleq [\mathbf{k}_1^{\mathbf{T}} \mathbf{k}_2^{\mathbf{T}}]$ and has dimension $2m$ ($^{\mathbf{T}}$ denotes the *transpose* of a vector). Higher powers of t could be added, leading to a *truncated power series.* Similarly, one could employ *truncated Fourier series*

$$\mathbf{u}(\mathbf{k}, t) = \sum_{i=1}^{N} [\mathbf{k}_{1i} \sin \frac{i\pi t}{t_f - t_0} + \mathbf{k}_{2i} \cos \frac{i\pi t}{t_f - t_0}]$$

or other orthogonal functions, e.g. *Walsh functions,* ... It should be clear that the parametric–optimal solutions obtained in each case might be very different. It often is desirable to use as few control parameters as possible to minimize computations, although increasing the number of parameters may improve the optimality of the result.

Having chosen the functional form of $\mathbf{u}(\mathbf{k}, t)$, the optimizing value of $\mathbf{k}$ must be determined. A *necessary* condition for $\mathbf{k}$ to minimize J is that

$$\frac{\partial J}{\partial \mathbf{k}} = 0$$

If, in addition,

$$\frac{\partial^2 J}{\partial \mathbf{k}^2} > 0$$

the two equations provide *necessary and sufficient* conditions for a *local minimum*. The *global minimum* is defined by the locally minimizing $\mathbf{k}$ that produces the lowest value of J.

The preceding discussion pertains to optimization of the parameters of control *time* functions, i.e. *open loop parametric optimization*. In *closed loop parametric optimization*, the given control structure is some function of the state $\mathbf{x}$, such as

$$\mathbf{u} = \Psi[\mathbf{k}, \mathbf{x}(t), t]$$

If e.g.

$$\mathbf{u} = -\mathbf{C}\mathbf{x}(t)$$

the optimization problem has as degrees of freedom the $m \times n$ elements of the gain matrix $\mathbf{C}$.

1.2.3 The Minimum Principle of Pontryagin

1.2.3.1 Problem without constraints on the control vector

Suppose that both the initial time t_0 and the initial state $\mathbf{x}(t_0) = \mathbf{x}_0$ are given. Define a scalar function $\mathcal{H}$ (the *Hamiltonian*), as follows :

$$\mathcal{H}[\mathbf{x}(t), \mathbf{u}(t), t] \triangleq \mathcal{L}[\mathbf{x}(t), \mathbf{u}(t), t] + \boldsymbol{\lambda}^{\mathrm{T}} \mathbf{f}[\mathbf{x}(t), \mathbf{u}(t), t]$$

where $\mathcal{L}$ is the integrand of the performance index (1.22), and $\boldsymbol{\lambda}(t)$ is the vector of *adjoint variables* (or *costates*) of the same dimension as the state $\mathbf{x}$.

Necessary conditions for an optimal control $\mathbf{u}^*(t)$ are [Pontryagin *et al.* 1962; Athans and Falb 1966; Kirk 1970; Bryson and Ho 1975]

$$\forall\, t \in [t_0, t_f] :$$

$$\begin{aligned} \frac{d\mathbf{x}^*(t)}{dt} &= \frac{\partial \mathcal{H}}{\partial \boldsymbol{\lambda}}[\mathbf{x}^*(t), \mathbf{u}^*(t), \boldsymbol{\lambda}^*(t), t] \\ \frac{d\boldsymbol{\lambda}^*(t)}{dt} &= -\frac{\partial \mathcal{H}}{\partial \mathbf{x}}[\mathbf{x}^*(t), \mathbf{u}^*(t), \boldsymbol{\lambda}^*(t), t] \\ \mathbf{0} &= \frac{\partial \mathcal{H}}{\partial \mathbf{u}}[\mathbf{x}^*(t), \mathbf{u}^*(t), \boldsymbol{\lambda}^*(t), t] \end{aligned} \qquad (1.23)$$

This is a set of $2 \times n$ first order ordinary differential equations (the *state* and *costate* equations), together with m algebraic equations. The solution of the state and costate equations will contain $2 \times n$ constants of integration. To evaluate these constants we use the n equations

$$\mathbf{x}^*(t_0) = \mathbf{x}_0$$

and an additional set of n or $n+1$ relationships —depending on whether or not t_f is specified— derived from the following *transversality* condition [g is the first term of the performance index (1.22)] :

$$\begin{aligned} &[\frac{\partial g}{\partial \mathbf{x}}(\mathbf{x}^*(t_f), t_f) - \boldsymbol{\lambda}^*(t_f)]^{\mathrm{T}}\, \delta\mathbf{x}_f \\ &\quad + [\mathcal{H}(\mathbf{x}^*(t_f), \mathbf{u}^*(t_f), \boldsymbol{\lambda}^*(t_f), t_f) + \frac{\partial g}{\partial t}(\mathbf{x}^*(t_f), t_f)]\, \delta t_f = 0 \end{aligned} \qquad (1.24)$$

where $\delta\mathbf{x}_f$ is the *variation* of the state at the final time, and δt_f is the variation of the final time itself. Notice that we are confronted by a *two-point boundary-value problem* (TPBVP). The *existence and continuity of the partial derivatives* of the functions g, $\mathcal{L}$ and $\mathbf{f}$ with respect to their arguments is tacitly assumed in the above equations.

Let us consider now some boundary conditions that may occur.

Final time and final state fixed

$\delta\mathbf{x}_f = 0$, $\delta t_f = 0$, and the transversality condition (1.24) is replaced by the following n conditions

$$\mathbf{x}^*(t_f) = \mathbf{x}_f$$

and

t_f fixed

Final time fixed and final state free

$\delta t_f = 0$, so condition (1.24) reduces to the following n conditions

$$\boldsymbol{\lambda}^*(t_f) = \frac{\partial g}{\partial \mathbf{x}}[\mathbf{x}^*(t_f), t_f]$$

and

t_f fixed

Final time free and final state fixed

$\delta \mathbf{x}_f = 0$ and (1.24) provides *one* condition

$$\mathcal{H}[\mathbf{x}^*(t_f), \mathbf{u}^*(t_f), \boldsymbol{\lambda}^*(t_f), t_f] + \frac{\partial g}{\partial t}[\mathbf{x}^*(t_f), t_f] = 0$$

and we have also

$$\mathbf{x}^*(t_f) = \mathbf{x}_f$$

Final time and final state free

In this case, (1.24) provides the following $n+1$ conditions

$$\boldsymbol{\lambda}^*(t_f) = \frac{\partial g}{\partial \mathbf{x}}[\mathbf{x}^*(t_f), t_f]$$

$$\mathcal{H}[\mathbf{x}^*(t_f), \mathbf{u}^*(t_f), \boldsymbol{\lambda}^*(t_f), t_f] + \frac{\partial g}{\partial t}[\mathbf{x}^*(t_f), t_f] = 0$$

1.2.3.2 Problem with constraints on the control vector

Suppose that the control vector $\mathbf{u}$ must take on values in a closed and bounded region. In that case, only necessary condition (1.23) must be altered, leading to the *Minimum Principle of Pontryagin* [Pontryagin *et al.* 1962; Athans and Falb 1966; Kirk 1970; Bryson and Ho 1975] :

$$\forall\, t \in [t_0, t_f], \text{ for all admissible } \mathbf{u}(t) :$$

$$\begin{aligned} \frac{d\mathbf{x}^*(t)}{dt} &= \frac{\partial \mathcal{H}}{\partial \boldsymbol{\lambda}}[\mathbf{x}^*(t), \mathbf{u}^*(t), \boldsymbol{\lambda}^*(t), t] \\ \frac{d\boldsymbol{\lambda}^*(t)}{dt} &= -\frac{\partial \mathcal{H}}{\partial \mathbf{x}}[\mathbf{x}^*(t), \mathbf{u}^*(t), \boldsymbol{\lambda}^*(t), t] \\ \mathcal{H}[\mathbf{x}^*(t), \mathbf{u}(t), \boldsymbol{\lambda}^*(t), t] &\leq \mathcal{H}[\mathbf{x}^*(t), \mathbf{u}^*(t), \boldsymbol{\lambda}^*(t), t] \end{aligned} \qquad (1.25)$$

The transversality condition (1.24) remains unchanged. Notice again that the above conditions constitute a set of *necessary* conditions for optimality; these conditions are not, in general, sufficient.

In addition, this Minimum Principle, although derived for bounded controls, can also be applied to problems in which the admissible controls are

not bounded. This can be done by viewing the unbounded control region as having arbitrarily large bounds, thus ensuring that the optimal control will not be constrained by the boundaries. In this case, for $\mathbf{u}^*(t)$ to minimize the Hamiltonian it is necessary (but not sufficient) that

$$\frac{\partial \mathcal{H}}{\partial \mathbf{u}}[\mathbf{x}^*(t), \mathbf{u}^*(t), \boldsymbol{\lambda}^*(t), t] = \mathbf{0} \qquad (1.26)$$

If this equation is satisfied, then a *sufficient condition* for a *local minimum* is that the matrix

$$\frac{\partial^2 \mathcal{H}}{\partial \mathbf{u}^2}[\mathbf{x}^*(t), \mathbf{u}^*(t), \boldsymbol{\lambda}^*(t), t]$$

is *positive definite.* If the Hamiltonian can be expressed in the form

$$\begin{aligned} \mathcal{H}[\mathbf{x}(t), \mathbf{u}(t), \boldsymbol{\lambda}(t), t] &= \rho[\mathbf{x}(t), \boldsymbol{\lambda}(t), t] \\ &\quad + \mathbf{c}^{\mathbf{T}}[\mathbf{x}(t), \boldsymbol{\lambda}(t), t]\ \mathbf{u}(t) + \frac{1}{2}\mathbf{u}^{\mathbf{T}}(t)\mathbf{R}(t)\mathbf{u}(t) \end{aligned}$$

where $\mathbf{c}$ is an $m \times 1$ array independent of $\mathbf{u}(t)$, then satisfaction of (1.26) and $\partial^2 \mathcal{H}/\partial \mathbf{u}^2 \equiv \mathbf{R}(t) > 0$ are *necessary and sufficient* for $\mathcal{H}[\mathbf{x}^*(t), \mathbf{u}^*(t), \boldsymbol{\lambda}^*(t), t]$ to reach a *global* minimum in $\mathbf{u}^*(t) = -\mathbf{R}^{-1}(t)\ \mathbf{c}[\mathbf{x}^*(t), \boldsymbol{\lambda}^*(t), t]$.

Pontryagin *et al.* [1962] have also derived other necessary conditions for optimality that we will find very useful. We now state two of these necessary conditions :

Necessary condition 1

If the Hamiltonian does not depend explicitly on time, then the Hamiltonian must be constant when evaluated on an extremal trajectory :

$$\forall\, t \in [t_0, t_f] \ : \quad \mathcal{H}[\mathbf{x}^*(t), \mathbf{u}^*(t), \boldsymbol{\lambda}^*(t)] = c_1$$

Necessary condition 2

If the terminal cost $g[\mathbf{x}(t_f)]$ and the Hamiltonian do not depend explicitly on time and if the final time t_f is free, then the Hamiltonian must be identically zero when evaluated on an extremal trajectory :

$$\forall\, t \in [t_0, t_f] \ : \quad \mathcal{H}[\mathbf{x}^*(t), \mathbf{u}^*(t), \boldsymbol{\lambda}^*(t)] = 0$$

1.2.3.3 Problem with path constraints

Integral (or isoperimetric) constraints

Suppose there is an additional constraint that a certain integral must have a specified value along the optimal path, such as

$$\int_{t_0}^{t_f} N[\mathbf{x}^*(t), \mathbf{u}^*(t), t]\, dt = N_f$$

with N_f a given number. A straightforward way to handle this problem is to add another system equation, namely

$$\frac{dx_{n+1}(t)}{dt} = N[\mathbf{x}(t), \mathbf{u}(t), t]$$

with two prescribed boundary conditions

$$x_{n+1}(t_0) = 0 \quad \text{and} \quad x_{n+1}(t_f) = N_f$$

Let μ be the costate associated with x_{n+1}. Then the Hamiltonian for the augmented system is

$$\mathcal{H}[\mathbf{x}(t), \mathbf{u}(t), t] = \mathcal{L}[\mathbf{x}(t), \mathbf{u}(t), t] + \boldsymbol{\lambda}^T \mathbf{f}[\mathbf{x}(t), \mathbf{u}(t), t] + \mu N[\mathbf{x}(t), \mathbf{u}(t), t]$$

The costate differential equations then become

$$\begin{aligned} \frac{d\boldsymbol{\lambda}^*(t)}{dt} &= -\frac{\partial \mathcal{H}}{\partial \mathbf{x}}[\mathbf{x}^*(t), \mathbf{u}^*(t), \boldsymbol{\lambda}^*(t), t] = -\frac{\partial \mathcal{L}}{\partial \mathbf{x}} - \boldsymbol{\lambda}^{\mathbf{T}} \frac{\partial \mathbf{f}}{\partial \mathbf{x}} - \mu \frac{\partial N}{\partial \mathbf{x}} \\ \frac{d\mu^*}{dt} &= -\frac{\partial \mathcal{H}}{\partial x_{n+1}} = 0 \quad \Rightarrow \quad \mu^* \text{ is constant} \end{aligned}$$

Note that there is no boundary condition for the costate μ, as both the initial and final value of the corresponding state x_{n+1} are given.

Other path constraints

For a complete treatment of other types of path constraints (such as state variable constraints) we refer to the literature. Observe that from the numerical point of view, it is often useful to convert a *bounded* optimal control problem into an *unbounded* optimal control problem, so that the easy to use necessary condition (1.23) can be used. This transformation is most often done by using the *linear* or the *nonlinear* (most often quadratic) *penalty function technique.*

1.2.4 Singular control problems

We consider the class of time invariant systems that are *linear* in the (scalar) control input $u(t)$

$$\frac{d\mathbf{x}(t)}{dt} = \mathbf{f}[\mathbf{x}(t)] + \mathbf{b}[\mathbf{x}(t)]\, u \tag{1.27}$$

where $\mathbf{b} \in \mathbb{R}^{n\times 1}$. This is not the most general case, but it includes most of the important cases that have appeared in applications to date. Furthermore, we consider only the case of a scalar control input, since all the developments in this section apply individually to components of $\mathbf{u}$ in the vector case. Given the initial time and initial state

$$\mathbf{x}(t_0) = \mathbf{x}_0$$

we treat the problem of minimizing

$$J[\mathbf{u}] = g[\mathbf{x}(t_f)]$$

subject to the dynamical constraints (1.27) and the following inequality constraint on the input $u(t)$

$$U_{MIN} \le u(t) \le U_{MAX}$$

The final time t_f is free.
The Hamiltonian $\mathcal{H}$ for this problem is given by

$$\mathcal{H} = \boldsymbol{\lambda}^{\mathbf{T}}(\mathbf{f}(\mathbf{x}) + \mathbf{b}(\mathbf{x})u) \triangleq \phi + \psi u$$

Necessary conditions for a stationary solution include

$$\begin{aligned} \frac{d\boldsymbol{\lambda}(t)}{dt} &= -\boldsymbol{\lambda}^{\mathbf{T}}\left(\frac{\partial \mathbf{f}}{\partial \mathbf{x}} + \frac{\partial \mathbf{b}}{\partial \mathbf{x}} u\right) \\ \boldsymbol{\lambda}(t_f) &= \frac{\partial g}{\partial \mathbf{x}}[\mathbf{x}(t_f)] \end{aligned}$$

Because the Hamiltonian $\mathcal{H}$ is *linear* in the control u, application of Pontryagin's Minimum Principle (1.25) leads to the following *Bang-Singular-Bang* control :

$$u(t) = \begin{cases} U_{MAX} & \text{if } \psi < 0 \\ u_{sing} & \text{if } \psi = 0 \quad t_i \le t \le t_{i+1} \\ U_{MIN} & \text{if } \psi > 0 \end{cases}$$

On any *singular* interval $[t_i, t_{i+1}]$, we have

$$\psi \equiv \boldsymbol{\lambda}^{\mathbf{T}}\mathbf{b} = 0 \tag{1.28}$$

so the Minimum Principle fails to provide the optimal solution. In that case, the *singular* control can be determined as follows. As $\psi = 0$ for all t in $[t_i, t_{i+1}]$, all of its derivatives with respect to t must vanish on the same interval, i.e. :

$$\frac{d^k\psi}{dt^k} = 0,\ k = 1, 2, \ldots,\ \forall\ t \in [t_i, t_{i+1}]$$

So we differentiate the function ψ repeatedly until u appears explicitly. We obtain :

$$\frac{d\psi}{dt} = \dot{\boldsymbol{\lambda}}^{\mathbf{T}}\mathbf{b} + \boldsymbol{\lambda}^{\mathbf{T}}\dot{\mathbf{b}} = -\boldsymbol{\lambda}^{\mathbf{T}}\left(\frac{\partial \mathbf{f}}{\partial \mathbf{x}} + \frac{\partial \mathbf{b}}{\partial \mathbf{x}}u\right)\mathbf{b} + \boldsymbol{\lambda}^{\mathbf{T}}\frac{\partial \mathbf{b}}{\partial \mathbf{x}}(\mathbf{f} + \mathbf{b}u) \triangleq \boldsymbol{\lambda}^{\mathbf{T}}\mathbf{d} = 0 \tag{1.29}$$

where

$$\mathbf{d} = \frac{\partial \mathbf{b}}{\partial \mathbf{x}}\mathbf{f} - \frac{\partial \mathbf{f}}{\partial \mathbf{x}}\mathbf{b}$$

Note that the terms in u canceled out of (1.29). Hence, we try again to find some relations that determine u by differentiating (1.29) with respect to time :

$$\begin{aligned}\frac{d^2\psi}{dt^2} &= \dot{\boldsymbol{\lambda}}^{\mathbf{T}}\mathbf{d} + \boldsymbol{\lambda}^{\mathbf{T}}\dot{\mathbf{d}} = -\boldsymbol{\lambda}^{\mathbf{T}}\left(\frac{\partial \mathbf{f}}{\partial \mathbf{x}} + \frac{\partial \mathbf{b}}{\partial \mathbf{x}}u\right)\mathbf{d} + \boldsymbol{\lambda}^{\mathbf{T}}\frac{\partial \mathbf{d}}{\partial \mathbf{x}}(\mathbf{f} + \mathbf{b}u) \\ &= \boldsymbol{\lambda}^{\mathbf{T}}\left(\frac{\partial \mathbf{d}}{\partial \mathbf{x}}\mathbf{f} - \frac{\partial \mathbf{f}}{\partial \mathbf{x}}\mathbf{d}\right) + \boldsymbol{\lambda}^{\mathbf{T}}\left(\frac{\partial \mathbf{d}}{\partial \mathbf{x}}\mathbf{b} - \frac{\partial \mathbf{b}}{\partial \mathbf{x}}\mathbf{d}\right)u = 0\end{aligned} \tag{1.30}$$

Now, provided that we have

$$\boldsymbol{\lambda}^{\mathbf{T}}\left(\frac{\partial \mathbf{d}}{\partial \mathbf{x}}\mathbf{b} - \frac{\partial \mathbf{b}}{\partial \mathbf{x}}\mathbf{d}\right) \neq 0$$

equation (1.30) can be solved for u :

$$u_{sing}(t) = -\frac{\boldsymbol{\lambda}^{\mathbf{T}}[(\partial \mathbf{d}/\partial \mathbf{x})\mathbf{f} - (\partial \mathbf{f}/\partial \mathbf{x})\mathbf{d}]}{\boldsymbol{\lambda}^{\mathbf{T}}[(\partial \mathbf{d}/\partial \mathbf{x})\mathbf{b} - (\partial \mathbf{b}/\partial \mathbf{x})\mathbf{d}]} \tag{1.31}$$

The control law (1.31) maintains the stationarity condition (1.28) *if* (1.28) and (1.29) were satisfied at the beginning (or the end) of the singular arc. Thus, singular arcs (with a scalar control variable) are *not possible at all points of the* $2n$ *dimensional* $(\mathbf{x}, \boldsymbol{\lambda})$ *space*; they are restricted, via (1.28) and (1.29), to a hypersurface of dimension $2n - 2$, called a *singular surface.*

For *stationary* systems with *unspecified final time*, the singular surface is of dimension $2n - 3$ since the Hamiltonian is zero over the whole time period (Necessary condition 2) :

$$\mathcal{H} \equiv \phi + \psi u = 0$$

or, using (1.28),

$$\phi \equiv \boldsymbol{\lambda}^{\mathbf{T}}\mathbf{f} = 0 \tag{1.32}$$

For stationary systems with unspecified terminal time and $n = 3$, equations (1.28), (1.29) and (1.32) are *linear* and *homogeneous* in λ_1, λ_2 and λ_3. Consistency among these equations requires the vanishing of the determinant of the coefficients λ_1, λ_2 and λ_3. This yields a relation that defines a singular surface *in the state space.*

However, it may happen that $d^2\psi/dt^2$ is again *independent* of u, or more generally, that

$$\left(\frac{d}{dt}\right)^k\psi = 0 \quad k = 0, 1, \ldots, m-1 \tag{1.33}$$

We can prove that for some (finite) m :

$$\left(\frac{d}{dt}\right)^m\psi = v(\mathbf{x}, \boldsymbol{\lambda}) + w(\mathbf{x}, \boldsymbol{\lambda})u \tag{1.34}$$

In addition, the following facts can be shown [Tait 1965; Kelley, Kopp and Moyer 1966; Robbins 1966] :

> *The variable m is always even. We call the problem a singular problem of order m if it fulfills (1.33) and (1.34).*
>
> *The singular surface in the* $(\mathbf{x}, \boldsymbol{\lambda})$ *space in this case is of dimension* $2n - m$.

1.2.5 Optimization of the initial state

In most optimal control problems, the initial state is specified a priori. However, in the subsequent chapters we will formulate many optimization problems where some components of the initial state can be manipulated as well to minimize the performance measure (1.22).

In this section we derive the *necessary boundary conditions* if the initial state is not given in an explicit way. Consider again the continuous dynamic system (1.21)

$$\frac{d\mathbf{x}(t)}{dt} = \mathbf{f}[\mathbf{x}(t), \mathbf{u}(t), t],\ t_0 \leq t \leq t_f$$

Let $J[u]$ (1.22) be the cost index to be minimized :

$$J[\mathbf{u}] = g[\mathbf{x}(t_f), t_f] + \int_{t_0}^{t_f} \mathcal{L}[\mathbf{x}(t), \mathbf{u}(t), t]\, dt$$

Then $\overline{J}(u)$ denotes the *augmented* cost, i.e. the cost to which the system differential equations have been adjoined using multiplier functions $\boldsymbol{\lambda}(t)$:

$$\overline{J}[u] \triangleq J[u] + \int_{t_0}^{t_f} \boldsymbol{\lambda}^{\mathbf{T}}(t)(\mathbf{f}[\mathbf{x}(t), \mathbf{u}(t), t] - \dot{\mathbf{x}})\, dt \tag{1.35}$$

Now consider the *variation* in $\overline{J}(u)$ due to *admissible* variations in the control vector $u(t)$ for fixed time t_0 (see e.g. [Bryson 1975])

$$\delta\overline{J}(u) = \boldsymbol{\lambda}^{\mathbf{T}}(t_0)\, \delta\mathbf{x}(t_0) + \ldots \tag{1.36}$$

where only the term on $t = t_0$ is mentioned. For an extremum, $\delta\overline{J}$ must be zero for any admissible $\delta u(t)$. Observe that the range of admissible control variations $\delta u(t)$ is *not* influenced by any constraint on the initial state $\mathbf{x}(t_0)$. As a consequence, all necessary conditions at times $t > t_0$ to make $\delta\overline{J}(u)$ vanish, will still hold *independently of the constraints on* $\mathbf{x}(t_0)$. We consider the following cases.

Initial state fixed

$\delta\mathbf{x}(t_0) = 0$, so there is no contribution to $\delta\overline{J}$ in (1.36). We have the following n initial conditions

$$\mathbf{x}(t_0) = \mathbf{x}_0$$

Initial state free

There will be an optimal value for $\mathbf{x}(t_0)$ such that $\delta\overline{J} = 0$ for arbitrarily small variations of $\mathbf{x}(t_0)$ around this optimal value. As a consequence, we must choose :

$$\boldsymbol{\lambda}(t_0) = 0$$

which are again n initial conditions, in this case for the costate. For some initial state $x_i(t_0)$ unspecified, the others given, we must have the corresponding $\lambda_i(t_0) = 0$.

Initial state determined by a set of equality constraints

If on $t = t_0$ the initial state is only determined by a set of constraints of the form

$$\mathbf{h}[\mathbf{x}(t_0)] \triangleq \begin{pmatrix} h_1[\mathbf{x}(t_0)] \\ \vdots \\ h_k[\mathbf{x}(t_0)] \end{pmatrix} = 0 \tag{1.37}$$

then clearly, $k \leq n$. We suppose n to be greater than 1, as for $n = 1$ the initial state is completely defined by the scalar equation $h[x(t_0)] = 0$. Observe that for $k = n$ in general the initial state is also completely determined by the given constraints. For $k > n$ there are $(k - n)$ redundant conditions. So we focus on the case $k < n$, where we have to find $(n - k)$ *additional conditions on* $t = t_0$. These are derived as follows. Introducing a $k \times 1$ vector $\boldsymbol{\nu}$ of *constant Lagrange–multipliers*, we adjoin the constraints to the augmented cost function (1.35) (for simplicity we use the same notation $\overline{J}(u)$)

$$\overline{J}(u) = \boldsymbol{\lambda}^{\mathbf{T}}(t_0)\, \mathbf{x}(t_0) + \boldsymbol{\nu}^{\mathbf{T}}\mathbf{h}[\mathbf{x}(t_0)] + \ldots$$

As before, we only concentrate on terms at $t = t_0$. Then the first variation of the cost becomes

$$\delta\overline{J}(u) = (\boldsymbol{\lambda}^{\mathbf{T}}(t_0) + \boldsymbol{\nu}^{\mathbf{T}}\frac{\partial \mathbf{h}}{\partial \mathbf{x}}[\mathbf{x}(t_0)])\, \delta\mathbf{x}(t_0) + \ldots$$

where $\partial\mathbf{h}/\partial\mathbf{x}$ denotes the $k \times n$ Jacobian matrix of (1.37). Obviously, to make the term in $\delta\mathbf{x}(t_0)$ disappear, we must choose

$$\boldsymbol{\lambda}(t_0) + \frac{\partial \mathbf{h}}{\partial \mathbf{x}}^{\mathbf{T}}[\mathbf{x}(t_0)]\, \boldsymbol{\nu} = 0$$

These are n equations to determine the k Lagrange–multipliers ν_i and the $(n - k)$ additional boundary conditions.

EXAMPLE

Suppose that $n = 3$ and that the first state is fixed at $t = t_0$, while the two others are linearly related to each other. We have

$$\begin{aligned} x_1(t_0) &= x_{1,0} \\ a x_2(t_0) + b x_3(t_0) &= 1 \end{aligned}$$

The vector $\mathbf{h}$ for this case is $(k = 2)$

$$\mathbf{h}[\mathbf{x}(t_0)] \triangleq \begin{pmatrix} x_1(t_0) - x_{1,0} \\ ax_2(t_0) + bx_3(t_0) - 1 \end{pmatrix} = 0$$

and we obtain

$$\begin{pmatrix} \lambda_1(t_0) \\ \lambda_2(t_0) \\ \lambda_3(t_0) \end{pmatrix} = - \begin{pmatrix} 1 & 0 \\ 0 & a \\ 0 & b \end{pmatrix} \begin{pmatrix} \nu_1 \\ \nu_2 \end{pmatrix}$$

Or, in other words

$$b\lambda_2(t_0) - a\lambda_3(t_0) = 0$$

which is the additional equation we are looking for. Note that ν_1, and thus $\lambda_1(t_0)$, remains undetermined, as $x_1(t_0)$ is given explicitly! ν_2 is only implicitly needed.

1.2.6 A conjecture

We end this overview of optimal control theory by formulating a new, rather simple but very powerful conjecture.

Conjecture 1.1

Suppose we have a convergent sequence of models $\mathcal{M}(\mathbf{p})$ where $\mathbf{p}$ is a set of parameters :

$$lim_{\mathbf{p}\to\mathbf{p_0}} \mathcal{M}(\mathbf{p}) \triangleq \mathcal{M}_\mathbf{0}$$

Suppose that for every model $\mathcal{M}(\mathbf{p})$, with $\mathbf{p} \neq \mathbf{p_0}$, we can determine the optimal control $u(\mathbf{p}, t)$ that minimizes some cost index $J[u]$ with standard optimal control theory.
Then the sequence of optimal controls $u(\mathbf{p}, t)$ is convergent :

$$lim_{\mathbf{p}\to\mathbf{p_0}} u(\mathbf{p}, t) \triangleq u_\mathbf{0}(t)$$

Moreover, this limit $u_0(t)$ is the optimal control for model $\mathcal{M}_\mathbf{0}$ minimizing $J[u]$.

In this Conjecture, the symbol $\mathcal{M}(\mathbf{p})$ stands for any model of the form (1.21), parameterized by a vector $\mathbf{p}$, i.e. :

$$\mathcal{M}(\mathbf{p}) \; : \; \frac{d\mathbf{x}(t)}{dt} = \mathbf{f}[\mathbf{x}(t), \mathbf{u}(t), \mathbf{p}, t], \; t_0 \leq t \leq t_f$$

Similarly, the notation

$$lim_{\mathbf{p}\to\mathbf{p_0}} \mathcal{M}(\mathbf{p}) \triangleq \mathcal{M}_\mathbf{0}$$

must be interpreted as :

$$lim_{\mathbf{p}\to\mathbf{p_0}} f_i[\mathbf{x}(t), \mathbf{u}(t), \mathbf{p}, t] = f_i[\mathbf{x}(t), \mathbf{u}(t), \mathbf{p_0}, t], \; i = 1, \ldots, n$$

with n the dimension of the state vector $\mathbf{x}$.

It can be easily illustrated that proving the Conjecture is not possible without imposing *additional conditions.*

Consider for instance the one dimensional static case. The problem then reduces to the minimization with respect to an independent variable u of a sequence of functions $\{J_n\}$, induced by a parameter sequence $\{p_n\}$. As an example, consider the parameter sequence defined by :

$$\{p_n\} \; : p_n = \frac{1}{n}, \; n = 1, \ldots, \infty$$

which clearly converges to $p_n \to 0$, and the following sequence of functions induced by $\{p_n\}$:

$$\{J_n\} \; : J_n[u, p_n] = \frac{1}{2} p_n u^2 - u$$

Some members of this sequence are shown in Figure 1.3. Clearly, this sequence converges to $J_n \to J = -u$. Setting the derivative of J_n with respect to u equal to zero, leads to :

$$p_n u - 1 = 0$$

As a result, J_n reaches its (global) minimum at :

$$u_n^* = \frac{1}{p_n} \equiv n$$

Obviously, the sequence $\{u_n^*\}$ is *not* convergent.

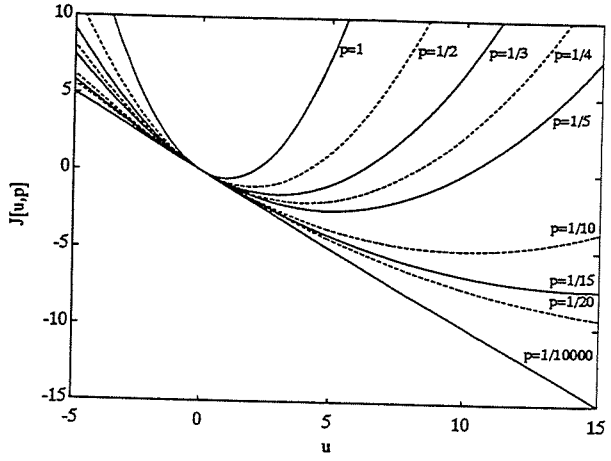

Figure 1.3: A counter–example in the static case

As a result, in order to prove the above Conjecture, some *additional assumptions* are required. First we introduce some definitions.

Definition 1

$\mathcal{U}$ is the set of control functions $u(t)$ defined over the interval $[t_0, t_f]$ with values in the interval $[U_{MIN}, U_{MAX}]$:

$$\mathcal{U} = \{u \ : \ [t_0, t_f] \rightarrow [U_{MIN}, U_{MAX}]\}$$

A sequence $\{u_n\}$ *is pointwise convergent to* u *if :*

$$\forall\, t \in [t_0, t_f] \ : \lim_{n\rightarrow\infty} u_n(t) \rightarrow u(t)$$

Definition 2

A sequence of real–valued functions $\{f_n : X \rightarrow \mathbb{R}\}$ *on a topological space* X *is equicontinuous if :*

$$\begin{aligned} \forall\, x \in X, \forall\, \varepsilon > 0 \ &: \\ \exists\, V_x \ &: \ (V_x \text{ is a neighborhood of } x) \\ \forall\, n, \forall\, y \in V_x \ &: \quad | f_n(x) - f_n(y) | < \varepsilon \end{aligned}$$

Now we are able to give an outline of the proof of the conjecture in two parts, provided we impose the following assumptions.

PART 1

We make the following assumptions.

Assumption 1. Assume on the set $\mathcal{U}$, defined above, the topology of pointwise convergence.

Assumption 2. $J[u] : \mathcal{U} \rightarrow \mathbb{R}$ is a real–valued functional over the set $\mathcal{U}$. Assume that there exists an equicontinuous sequence of functionals $\{J_n[u] : \mathcal{U} \rightarrow \mathbb{R}\}$ such that :

$$\forall\, u \ : \ \lim_{n\rightarrow\infty} J_n[u] = J[u]$$

Note that this sequence $J_n[u]$ is induced by the parameter vector sequence $\{\mathbf{p}_n\}$ in the following way. Referring to the statement of the Conjecture, the functional $J[u]$ must be minimized under a dynamic constraint, namely the sequence of state space models $\mathcal{M}_n$, which in turn is induced by the parameter vector sequence $\{\mathbf{p}_n\}$.

Assumption 3. Assume that every functional $J_n[u]$ of this sequence has a unique, global minimum, at $u = u_n^*$.

Under these assumptions we prove the following result :

If the sequence $\{u_n^*\}$ *is pointwise convergent to* u^**, then the functional* $J[u]$ *reaches a global minimum at* $u = u^*$.

From Assumption 3, we know that for all values of n :

$$\forall\, u \in \mathcal{U} \ : \quad J_n[u_n^*] \leq J_n[u]$$

On the other hand, we must prove that :

$$\forall\, u \in \mathcal{U} \ : \quad J[u^*] \leq J[u]$$

We now prove that this second inequality follows from the first inequality by considering the limit for $n \rightarrow \infty$. For the right–hand side, this follows immediately from Assumption 2. For the left–hand side, we must prove that :

$$J[u^*] \stackrel{?}{=} \lim_{n\rightarrow\infty} J_n[u_n^*]$$

In other words, we must show that :

$$\begin{aligned} &\forall\, \varepsilon > 0 \ : \\ &\exists\, M \in \mathbb{N} \ : \\ &\forall\, n > M \ : \ \mid J_n[u_n^*] - J[u^*] \mid < \varepsilon \end{aligned}$$

Consider an arbitrary but fixed value of $\varepsilon > 0$. Since $\{J_n[u]\}$ is equicontinuous on the set $\mathcal{U}$ (Assumption 2), and thus also at $u = u^*$, there exists a neighborhood V_{u^*} of u^* such that :

$$\forall\, k, \forall\, v \in V_{u^*} \ : \ \mid J_k[v] - J_k[u^*] \mid < \frac{1}{2}\varepsilon$$

Since the sequence $\{u_n^*\}$ is (pointwise) convergent to u^*, there exists a (positive) number n_1 such that :

$$\forall\, n > n_1 \ : \ u_n^* \in V_{u^*}$$

As a result, we have :

$$\forall\, k, \forall\, n > n_1 \ : \ \mid J_k[u_n^*] - J_k[u^*] \mid < \frac{1}{2}\varepsilon$$

This holds $\forall\, k$, thus also for $k = n$:

$$\forall\, n > n_1 \ : \ \mid J_n[u_n^*] - J_n[u^*] \mid < \frac{1}{2}\varepsilon \qquad (1.38)$$

In addition, we know from Assumption 2 that there exists a (positive) number n_2 such that :

$$\forall\, n > n_2 \ : \ \mid J_n[u^*] - J[u^*] \mid < \frac{1}{2}\varepsilon \qquad (1.39)$$

Combining inequalities (1.38) and (1.39), we obtain :

$$\begin{aligned} \forall\, n > M \triangleq \max(n_1, n_2) \ &: \\ \mid J_n[u_n^*] - J[u^*] \mid \ &\leq \ \mid J_n[u_n^*] - J_n[u^*] \mid + \mid J_n[u^*] - J[u^*] \mid \\ &\leq \ \frac{1}{2}\varepsilon + \frac{1}{2}\varepsilon \end{aligned}$$

which proves the result.

PART 2

If we make the following additional assumption :

Assumption 4. Assume that the sequence of functionals considered in Assumption 2, $\{J_n[u] : \mathcal{U} \to \mathbb{R}\}$, converges *uniformly* on the set $\mathcal{U}$, i.e. :

$$\begin{aligned} &\forall\, \varepsilon > 0 \ : \\ &\exists\, N \in \mathbb{N} \ : \\ &\forall\, n > N, \forall\, u \in \mathcal{U} \ : \ \mid J_n[u] - J[u] \mid < \varepsilon \end{aligned}$$

then we can prove the following result :

If the functional $J[u]$ reaches a unique global minimum at $u = u^*$, then the sequence $\{u_n^*\}$, where u_n^* minimizes J_n globally, is convergent to u^*.

We give a prove by contradiction. So suppose that the sequence $\{u_n^*\}$ *does not* converge to u^*. Then there exists a subsequence $\{u_{n_k}^*\}$, and a non–empty open neighborhood W_{u^*} of u^*, such that $\{u_{n_k}^*\}$ lies completely outside W_{u^*}.

Since $J[u]$ has a *unique* global minimum at $u = u^*$, we can argue that :

$$\begin{aligned} &\exists\, \varepsilon_0 > 0 \ : \\ &\forall\, u \notin W_{u^*} \ : \ J[u] > J[u^*] + \varepsilon_0 \qquad (1.40) \end{aligned}$$

Indeed, suppose that (1.40) would *not* hold. Then, for every $n \in \mathbb{N}_0$ one could find a $v_n \notin W_{u^*}$ such that :

$$J[u^*] < J[v_n] < J[u^*] + \frac{1}{n}$$

Since $\mathcal{U}$ is compact for the topology of pointwise convergence and since W_{u^*} is open, we have that $\mathcal{U} \backslash W_{u^*}$ is compact. Therefore, the sequence $\{v_n\}$ must have at least one accumulation point, say v^*, in $\mathcal{U} \backslash W_{u^*}$. By the continuity of J, one has that $J[v^*] = J[u^*]$, which is in contradiction with the assumption that J has a unique global minimum.

Using (1.40), we can write :

$$J[u^*_{n_k}] > J[u^*] + \varepsilon_0 \tag{1.41}$$

On the other hand, since the sequence $\{J_{n_k}\}$ is uniformly convergent to J, there exists a (positive) number k_0 (which depends on ε_0) such that :

$$\forall\, n_k > k_0, \forall\, u \in \mathcal{U} \;:\; |\, J_{n_k}[u] - J[u]\,| < \frac{1}{4}\varepsilon_0$$

This leads to :

$$J_{n_k}[u^*] < J[u^*] + \frac{1}{4}\varepsilon_0 \tag{1.42}$$

but also :

$$J_{n_k}[u^*_{n_k}] > J[u^*_{n_k}] - \frac{1}{4}\varepsilon_0$$

Using inequality (1.41), this leads to :

$$J_{n_k}[u^*_{n_k}] > J[u^*] + \frac{3}{4}\varepsilon_0$$

Using inequality (1.42), we obtain :

$$J_{n_k}[u^*_{n_k}] > J_{n_k}[u^*] + \frac{1}{2}\varepsilon_0$$

In other words, $u^*_{n_k}$ does not globally minimize the functional J_{n_k}, which is a contradiction.

Combining the results of Part 1 and Part 2 proves the conjecture under the Assumptions 1 to 4. ■

Obviously, the application of Conjecture 1.1 does not make much sense in cases where we can obtain the optimal control for the limit model in a *direct* way. However, its practical importance is the following. It provides a useful methodology to calculate optimal controls for models to which standard techniques are *not* applicable. This is e.g. the case when some element f_i of $\mathbf{f}$ [which is the right–hand side of the state space model (1.21)] exhibits a *corner* : f_i is continuous, but its derivative is not. To circumvent this problem, we replace the *piecewise–smooth* function f_i by a family of *completely smooth* curves that converge as a function of e.g. one parameter to the original function.

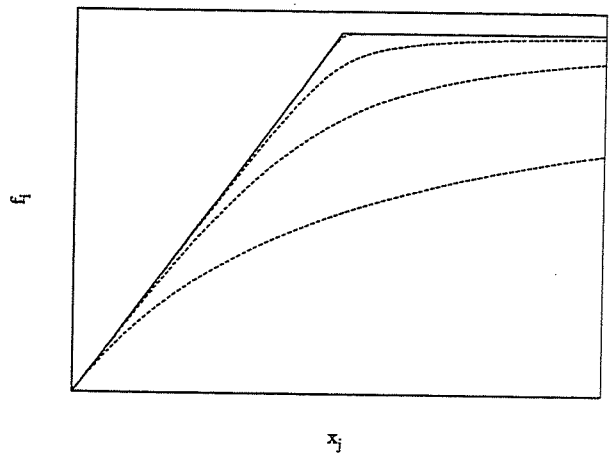

Figure 1.4: Approximation of a piecewise–smooth function by a family of smooth functions

A typical example is plotted in Figure 1.4 : a *Blackman type function* (1.16) is approximated by a family of smooth functions, starting from a *Monod type function* (1.14). This example will be studied in more detail in Chapter 4.

Note however that the application of this Conjecture is not limited to piecewise smooth models of biotechnological processes only. It can also prove useful when dealing with *friction* in mechanical systems, *hysteresis* phenomena, ...

Since in practice it may be very difficult to verify all assumptions that were made in the above proof, it is an interesting question whether or not they can be relaxed. Furthermore, we have only shown that these assumptions are *sufficient conditions.*

Consider again the (static) example of Figure 1.3. In the above proof, we assume that the admissible control functions u take on values in a closed finite interval (see Definition 1). As a result, if we take $\mathcal{U} = \mathbb{R}$, which is not compact, then we are not allowed to apply the above results. However, if we take $\mathcal{U} = [U_{MIN}, U_{MAX}]$, say $\mathcal{U} = [-5, 15]$, then it can be easily

seen that all assumptions are satisfied. For instance, from Figure 1.3 we conclude immediately that, over the interval $[-5, 15]$, the sequence $\{J_n\}$ converges *uniformly* to $J = -u$ which reaches its unique global minimum at $u = U_{MAX} = 15$.

Because at this time more general results are still lacking, we can proceed as follows for a particular optimal control problem characterized by a model $\mathcal{M}_0$. We *assume* a priori that the Conjecture holds. Then we select a model $\mathcal{M}(\mathbf{p}_n)$ *sufficiently close* to the limit model $\mathcal{M}_0$, i.e. we choose n sufficiently large. If we are able to determine the optimal control solution using model $\mathcal{M}(\mathbf{p}_n)$, then this solution will be at least an excellent approximation for the optimal control to the limit model $\mathcal{M}_0$. Note that the validity of this Conjecture can always be verified *a posteriori*. An example will be given in Chapter 4.

1.3 Conclusions

In this chapter we presented the background material and mathematical tools used throughout this work.

We discussed the modeling of biotechnological processes from a control engineering viewpoint. The introduction of the new concept of *endogenous fraction* allows to describe all kinds of metabolism for biomass maintenance and product biosynthesis within one unifying frame. This concept is at the basis of the results presented in Chapter 5.

We also presented a brief overview of optimal control theory. The singular control problem has been studied in some detail for the class of systems studied in subsequent chapters. Finally, we presented a new conjecture that allows to determine the optimal control profile in the case of a piecewise smooth state space model (Conjecture 1.1).

Chapter 2

A dynamic mathematical model to predict microbial growth and inactivation during food processing

Nowadays, there is an increased consumer interest in chilled prepared food products. However, the shelf life of this kind of foods is usually limited due to spoilage by common micro–organisms, such as Pseudomonas and Lactobacillus spp., and the increased risk for food pathogens.

In predicting the shelf life, the use of mathematical models gains more and more attention to increase insight in the different subprocesses and their interactions. For process design and optimization, simulation studies can be very useful to reduce the number of expensive and time consuming experiments.

Predictive microbiology is the term used to describe the mathematical modeling of the effects of temperature (T), water activity (a_w), pH and other environmental influences on the rate of microbial growth or the time to reach specified numbers of micro–organisms or their metabolites. The potential benefits of predictive food microbiology depend entirely on the selection of appropriate models to describe the effects of environmental factors on the microbial growth rate. Substrate consumption is not modeled, as substrate is considered to be a non–limiting growth factor : the amount of substrate available is assumed high enough.

In this chapter, we consider food products for which the value of both pH and a_w is such that these factors do not influence microbial growth. As a result, temperature is the only significant factor affecting the growth rate. Foods in this category include e.g. fresh meat, poultry, fish and milk stored aerobically at chill temperatures.

In section 2.1, we give an overview of explicit mathematical models presented in the literature describing bacterial growth as a function of both time and temperature. Many sigmoidal functions have been reported to describe a bacterial growth curve as an explicit function of time. Furthermore, several expressions have been proposed to model the influence of temperature on the main characteristics of this growth curve : maximum specific growth rate, lag time and asymptotic level. However, as the predictive value of such explicit models is most often only guaranteed at a constant temperature within the temperature range of microbial growth, they are less appropriate in optimization studies of a whole production and distribution chain.

In section 2.2, we present a new dynamic mathematical model (a first order differential equation) describing the bacterial population as a function of both time and temperature. Furthermore, the inactivation of the population at temperatures above the maximum temperature for growth has been incorporated. In the special case of a constant temperature, the solution coincides exactly with the corresponding Gompertz model, which has been validated in several recent reports. However, the main advantage of this dynamic model is its ability to deal with time varying temperatures, over the whole temperature range of growth and inactivation. As such, it is an essential building block in (time saving) simulation studies to design e.g. optimal time–temperature profiles with respect to microbial safety of a production and distribution chain of chilled foods.

We wish to emphasize from the outset that the principal aim of this chapter is to introduce more advanced concepts of mathematical modeling into the field of predictive microbiology. More specifically, the model developed here is a first step towards a realistic and consistent description of the evolution of a microbial population under time varying temperature conditions. The experimental validation of the model under such temperature conditions is the subject of an ongoing project within our research group.

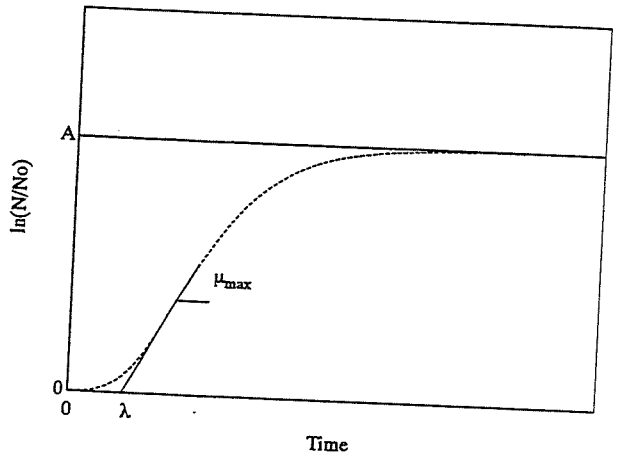

Figure 2.1: A microbial growth curve

2.1 Explicit bacterial growth models

2.1.1 Modeling bacterial growth as a function of time

As a generic property, most microbial growth curves can be characterized by the following three features : the *maximum specific growth rate* μ_{max}, the *lag time* λ, and the *asymptotic value* A. If we define the growth curve as the logarithm of the relative population size [$y = \ln(N/N_0)$] (N is the number of micro–organisms per unit volume) as a function of time (t), we obtain the typical *sigmoidal* behavior as shown in Figure 2.1. A number of growth models are found in the literature, describing the number of organisms as a function of time. Substrate consumption is not modeled, as substrate is considered to be a *non–limiting* growth factor : the amount of substrate available is assumed high enough. Schnute proposed a new comprehensive model which includes numerous historical models as special cases [Schnute 1981]. Possible submodels include not only *asymptotic* growth (such as *von Bertalanffy*, *Richards*, *Gompertz*, or *logistic* growth), but also *linear*, *quadratic*, or *exponential* growth.

Recently, Zwietering *et al.* compared several explicit models for bacterial growth, either reported in the literature or newly developed, using a lot of experimental data [Zwietering *et al.* 1990]. The objective was to evaluate

similarities and differences between the models and to deal with the question of which model(s) can be used, on the basis of statistical reasoning. Note that they use the models to relate the logarithm of the relative population size $y = \ln(N/N_0)$ with time, while most models were originally developed to describe the evolution of the absolute population size N with time!

Different models were compared statistically, as well as with respect to their ease of use. They reparameterized the models in order to obtain biologically significant parameters such as the maximum specific growth rate (μ_{max}), the lag time (λ) and the asymptotic level (A) of the growth curve. Furthermore, this facilitates the problem of finding adequate starting values and calculating confidence intervals during curve fitting. The different models were fitted to growth data by nonlinear regression with a Marquardt algorithm.

Using extensive experimental data, Zwietering *et al.* concluded that, in almost all the cases tested, the three–parameter *modified Gompertz equation* is statistically sufficient (using the t test and the F test) to describe the growth data. Moreover, the fourth parameter in any four–parameter model is a *shape* parameter, which is difficult to explain biologically. The original Gompertz model [Gompertz 1825] with parameters a, b and c is reparameterized as follows.
Original Gompertz equation :

$$y = a \exp[-\exp(b - ct)] \tag{2.1}$$

Modified Gompertz equation [$e = \exp(1)$] [Zwietering *et al.* 1990] :

$$y = A \exp[-\exp(\frac{\mu_{max} e}{A}(\lambda - t) + 1)] \tag{2.2}$$

The conversion formulas are :

$$a = A \tag{2.3}$$
$$c = \frac{\mu_{max} e}{A} \tag{2.4}$$
$$b = \frac{\mu_{max} e}{A}\lambda + 1 \tag{2.5}$$

2.1.2 Modeling bacterial growth as a function of temperature

The *temperature* of chilled foods is a very important factor for microbial safety in a production and distribution chain. In order to predict the influence of temperature, it is essential to model the three characteristics μ_{max}, A and λ in model (2.2) as a function of T.

Again, the literature provides us with a large number of models. In a second recent paper Zwietering *et al.* selected for μ_{max}, A and λ the most appropriate model, either existing or newly developed, by systematic and statistical analysis of a large amount of experimental data. The models were compared using an F test, by which the lack of fit was compared with the measuring error [Zwietering *et al.* 1991].

Growth – Temperature relations

Ratkowsky *et al.* proposed an empirical *square root* relationship between the maximum specific growth rate μ_{max} and the temperature T.
Square root model of Ratkowsky *et al.* [1982] :

$$\sqrt{\mu_{max}} = b_1(T - T_{min})$$

where T_{min} is the theoretical minimum temperature for growth and b_1 is a parameter.

Ratkowsky *et al.* expanded their model to describe the growth rate around the optimum and the maximum temperatures.
Expanded square root model of Ratkowsky *et al.* [1983] :

$$\sqrt{\mu_{max}} = b_2[T - T_{min}][1 - \exp\{c_2(T - T_{max})\}] \tag{2.6}$$

where T_{min} is the minimum temperature at which growth is observed, T_{max} is the theoretical maximum temperature for growth and b_2 and c_2 are parameters.

To avoid positive values for μ_{max} at temperatures $T > T_{max}$, Zwietering *et al.* proposed the following modification.
Modified Ratkowsky model [Zwietering *et al.* 1991] :

$$\mu_{max} = b_3^2[T - T_{min}]^2[1 - \exp\{c_3(T - T_{max})\}] \tag{2.7}$$

where T_{min} and T_{max} have the same meaning as above, and b_3 and c_3 are parameters.

These models do not have a biological basis. The model of Schoolfield *et al.* is based on Arrhenius' and Eyring's equations. As a result, all parameters have a clear biological and graphical interpretation.
Model of Schoolfield *et al.* [1981] :

$$\mu_{max} = \frac{\mu_{25}\frac{T}{298}\exp(\frac{H_a}{R}(\frac{1}{298} - \frac{1}{T}))}{1 + \exp(\frac{H_l}{R}(\frac{1}{T_l} - \frac{1}{T})) + \exp(\frac{H_h}{R}(\frac{1}{T_h} - \frac{1}{T}))}$$

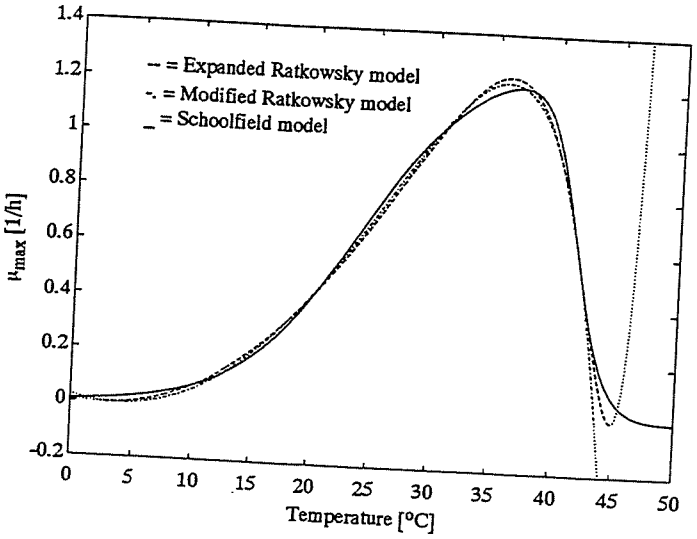

Figure 2.2: Maximum specific growth rate as a function of temperature

with

μ_{25} : specific growth rate at 25 °C
T_l : temperature at which the enzyme is 50 % inactivated due to low temperature
T_h : temperature at which the enzyme is 50 % inactivated due to high temperature
H_a : enthalpy of activation of the reaction catalyzed by the enzyme
H_l : change in enthalpy associated with low temperature inactivation
H_h : change in enthalpy associated with high temperature inactivation
R : gas constant

The last three models are shown in Figure 2.2, using the parameters reported in [Zwietering *et al.* 1991]. It can be seen that the expanded and the modified Ratkowsky models make realistic predictions of μ_{max} for temperatures T *inside* the interval $[T_{min}, T_{max}]$ only. Only the model of Schoolfield *et al.* has the following desired behavior : $\mu_{max} > 0\ \forall T$; $\mu_{max} \to 0$ if $T > T_{max}$; $\mu_{max} \to 0$ if $T < T_{min}$; where the last transitions are required to be sufficiently *smooth*. Although this model has the largest number of parameters (6), these have all a sound biological interpretation. Moreover, the model can be *simplified* if we focus only on high or low temperatures.

However, Zwietering *et al.* found that, from a statistical point of view, the experimental growth rate data are best described by the Ratkowsky model based equations (2.6) and (2.7). They preferred model equation (2.7), as it had the lowest residual sum of squared errors. However, the difference with the expanded Ratkowsky model is almost negligible.

Asymptote – Temperature model

As compared with the maximum specific growth rate, there are not so many experimental asymptote data reported in the literature. Zwietering *et al.* [1991] tested a large number of models, including the Ratkowsky and Schoolfield models mentioned. These equations must be regarded as *empirical fit* models only. As the asymptote data did not differ much in the low temperature range, and the measuring errors were too large to discriminate statistically, Zwietering *et al.* proposed the following *second modified Ratkowsky model* :

$$A = b_4[1 - \exp\{c_4(T - T_{A,max})\}] \tag{2.8}$$

where b_4 is the final level at low temperatures, and $T_{A,max}$ is the maximum temperature at which growth is observed. Assuming that the final population N_∞ is independent of the inoculum level, b_4 depends on the inoculum level N_0 as follows :

$$b_4 = \ln(N_\infty) - \ln(N_0)$$

Model equation (2.8) is shown in Figure 2.3, using the parameters reported in [Zwietering *et al.* 1991].

Lag time – Temperature model

Zwietering *et al.* [1991] tried to fit the logarithm of the available experimental data with the logarithm of the inverse of the growth rate equations. They also proposed a *hyperbolic* equation :

$$\ln(\lambda) = \frac{p}{T - q} \tag{2.9}$$

This hyperbola model (with only 2 parameters) had the lowest residual sum of squares, and has been selected therefore. This model is shown in Figure 2.4, using the parameters reported in [Zwietering *et al.* 1991].

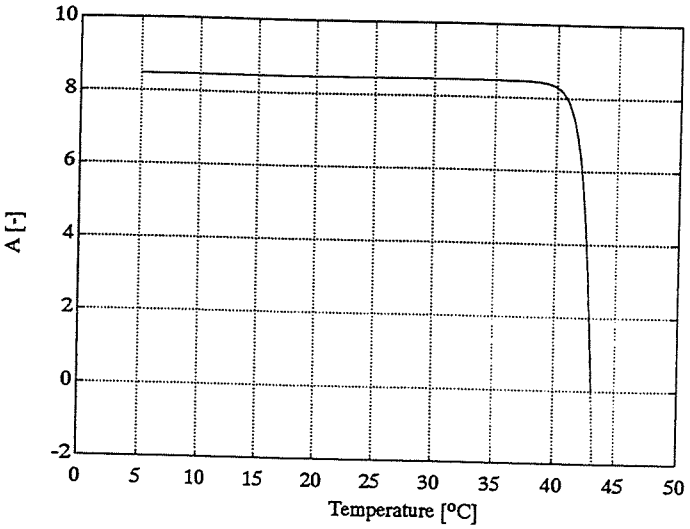

Figure 2.3: Asymptote as a function of temperature

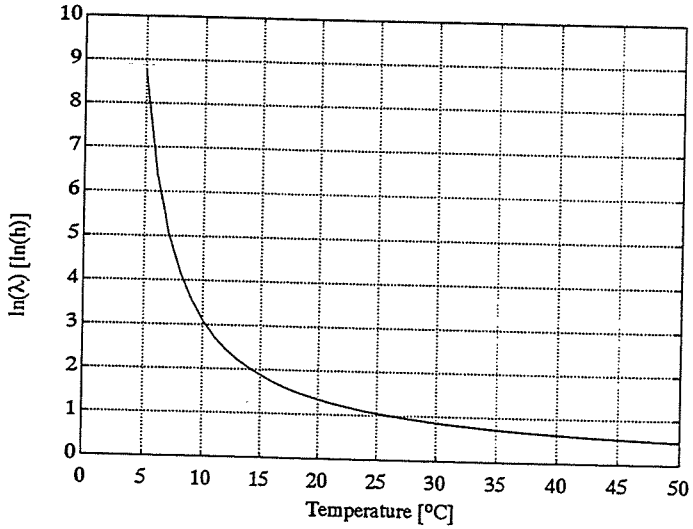

Figure 2.4: Lag time as a function of temperature

Expanded Ratkowsky model (2.6)		*Modified Ratkowsky model (2.7)*	
Parameter	Estimate	Parameter	Estimate
b_2	0.0377	b_3	0.0410
T_{min}	2.82	T_{min}	3.99
c_2	0.250	c_3	0.161
T_{max}	44.9	T_{max}	43.7
Asymptote A (2.8)		*Lag time λ (2.9)*	
Parameter	Estimate	Parameter	Estimate
b_4	$21.58 - \ln(N_0)$	p	23.9
c_4	1.25	q	2.28
$T_{A,max}$	43.1		

Table 2.1: Parameters reported by Zwietering *et al.* [1991]

2.1.3 The model of Zwietering et al.

Using equation (2.7), equation (2.8), and equation (2.9), the growth rate, asymptote, and lag time at every desired temperature can be calculated, and using equation (2.2), a growth curve at that temperature can be described [Zwietering *et al.* 1991]. The parameters for the models shown by equations (2.6), (2.7), (2.8) and (2.9) are summarized in Table 2.1. In most cases the model predictions agreed very well with the measured values.

2.2 A dynamic mathematical model

2.2.1 Limitations of the current explicit model

The predictive value of the model of Zwietering *et al.* [equations (2.2) and (2.7)–(2.9)] is only guaranteed at a constant temperature within the temperature range of bacterial growth. Zwietering *et al.* [1991] reported an excellent agreement with measured values.

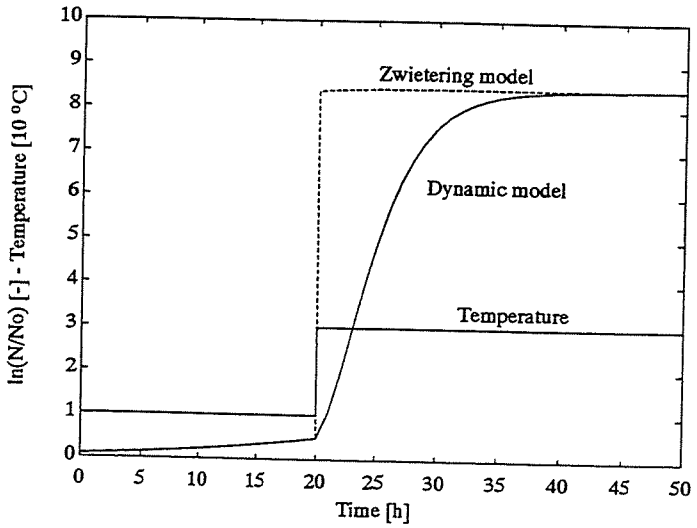

Figure 2.5: Prediction of the explicit model of Zwietering *et al.* versus the dynamic model for a step in the temperature profile

However, in practice the food product may be subjected to wide temperature variation during the subsequent stages of processing, storage, distribution, ..., and finally consumption, thus hampering an efficient prediction and control of the microbial safety. It can be easily illustrated that the proposed model, and in fact *any* explicit model, cannot be used under time varying temperature conditions. Consider, e.g., the following temperature profile. From $t = 0$ h to $t = 20$ h, T equals 10°C; at $t = 20$ h, the temperature jumps to $T = 30$°C. In Figure 2.5, the output of the explicit model of Zwietering *et al.* is compared with the result of the dynamic model we shall present in the next sections. Although the solutions coincide during the first phase, the model of Zwietering *et al.* cannot handle the temperature shock in a consistent way : at the moment of the temperature shock, the population makes also a (discontinuous) jump which is, of course, impossible. On the other hand, the prediction of the dynamic model coincides with what might be expected intuitively : from the temperature shock on, the population starts growing faster but remains continuous. In other words, the new dynamic model can take into account the previous history of the product at hand.

Observe that both model equations (2.7) and (2.8) predict unrealistic negative values for, respectively, μ_{max} and A at temperatures above the maximum temperature for growth (see also Figures 2.2 and 2.3). At temperatures below the minimum temperature for growth, model equation (2.7) predicts unrealistic positive values for μ_{max}.

In addition, Zwietering *et al.* [1990,1991] use the Gompertz model as an empirical model for describing the logarithm of the relative population size [$y = \ln(N/N_0)$] with time, while the original Gompertz model [Gompertz 1825] was developed to describe the evolution of the absolute population size N. Their approach can be justified by the excellent fitting results of experimental data. However, there is some inconsistency from the mathematical point of view. At time $t = 0$, we have $N(t = 0) = N_0$, so $y(0) = 0$. On the other hand, from model equation (2.1) or (2.2) it is readily seen that $y \to 0$ for $t \to -\infty$ only. At $t = 0$, we have :

$$y(0) = a\exp[-\exp(b)] = A\exp[-\exp(\frac{\mu_{max}e}{A}\lambda + 1)] \qquad (2.10)$$

which is not equal to zero. For the values of the parameters estimated by Zwietering *et al.*, $y(0)$ only approaches zero. This has some consequences in developing a consistent dynamic model, as we shall see further on.

2.2.2 Design requirements for a dynamic model

It is well known that temperature T, pH and water activity a_w are the main factors influencing the microbial stability of chilled prepared food products. Unlike the pH and the water activity, the temperature may vary extensively throughout the complete production and distribution chain.

The development of control strategies based on modern control techniques in general requires the knowledge of a sufficiently accurate dynamic mathematical model for heat transfer, microbial load and other process variables (e.g. sensory quality) at any location in the food.

A model based approach was pioneered in the sterilization of canned foods, for which an optimization methodology already exists (e.g. [Saguy and Karel 1979], [Nadkarni and Hatton 1985], [Teixeira and Shoemaker 1989]). In sterilization processes a drastic thermal treatment results in a complete inactivation of vegetative cells and a considerable reduction of spores of pathogenic thermoresistent sporulating micro–organisms at the expense of the sensory quality. The kinetics of thermal inactivation are well documented (e.g. [Stumbo 1973]). Under normal storage conditions and in the absence of post contamination, usually no further microbial growth occurs.

However, the construction of a dynamic model for the microbial load in chilled prepared foods presents some specific problems. The objective of the thermal treatment is to obtain an optimal textural and sensory quality, while the reduction of pathogenic and spoiling vegetative cells is a derived benefit. The latter is less intensive than in canning, and thermoresistent micro–organisms (or their spores) may survive. During the subsequent stages of chilling, transport, storage, and distribution, the temperature within the product can fluctuate between 0°C and 30°C, and the surviving micro–organisms may start growing. To our knowledge, there are up to now no mathematical models available which are capable of predicting microbial growth in foods under dynamically changing temperature conditions.

Without loss of generality, we consider food products for which the possible influence of pH and water activity can be neglected. An appropriate dynamic mathematical model describing the bacterial population evolution with respect to time and temperature should meet some design requirements.

DESIGN REQUIREMENTS

1. The dynamic model should be able to deal with *time varying temperature profiles* in a consistent way, over the whole biokinetic temperature range of growth and inactivation. All variables must take on physically acceptable values under all conditions.

2. The model should be able to simulate a *transition* (whether smooth or not) *between growth and inactivation*, using as few additional parameters as possible (in order to avoid unnecessary complications in parameter estimation studies).

3. The *previous history* of the food product under consideration should be taken into account. At the beginning of a growth phase after a phase of inactivation, the reference population level N_0 should be modified accordingly. This will be explained later on.

4. The model should *reduce to the validated existing explicit model*, in the special case of a constant temperature within the range of growth.

5. Besides microbial soundness, the model should meet some *mathematical requirements*, such as differentiability for all values, in order to make some nonlinear parameter estimation algorithms and modern optimization techniques easily applicable.

2.2.3 A dynamic model for growth

From the mathematical point of view, the main reason why the model of Zwietering *et al.* [1991] fails under time varying temperature conditions (Figure 2.5) is that this model must be considered as the explicit solution of a more general (dynamic) differential equation in the special case of a constant temperature. The underlying differential equation for model equation (2.1) [or (2.2)] can be easily obtained by differentiating y with respect to t. We have :

$$\begin{aligned} \frac{dy}{dt} &= a(\exp[-\exp(b-ct)])(-\exp(b-ct))(-c) \\ \frac{dy}{dt} &= cy\ln(\frac{a}{y}) \end{aligned} \tag{2.11}$$

Unfortunately, the parameter b, and thus the influence of the lag time λ due to equation (2.5), has disappeared completely from this dynamic model. Furthermore, an initial condition, $y(t=0)=0$, as required by the definition of y itself, causes a numerical problem in the right hand side of equation (2.11), although the limit for $y \to 0$ is zero using de l'Hôpital's rule.

Both problems can be circumvented by using the initial condition as given by equation (2.10). By using conversion formulas (2.3) to (2.5) and model equations (2.7) to (2.9), this dynamic model becomes function of T also. By doing so, we also guarantee the complete equivalence of dynamic model (2.11) with explicit model (2.1) in the case of a constant temperature.

It is now easily seen that the jump in the temperature profile of Figure 2.5 causes a discontinuity in the values of μ_{max} and λ and, as a consequence, in the value of y modeled by equation (2.1). However, by using dynamic model (2.11), there is a jump only in the derivative of y, y itself remaining continuous. The influence of the temperature shock is smoothed through the integration process, which results in a more realistic time profile $y(t)$. This is one of the main advantages of the new dynamic model.

In order to handle the third model design requirement on N_0 in an easy way, we define the following variable :

$$n \triangleq \ln(N)$$

Note that $dy/dt = dn/dt$. With $n_0 = \ln(N_0)$, we obtain the following dynamic model for n [the initial condition follows immediately from (2.10)] :

$$\begin{aligned} \frac{dn}{dt} &= c(n-n_0)\ln(\frac{a}{n-n_0}) \\ n(t=0) &= n_0 + a\exp[-\exp(b)] \end{aligned} \tag{2.12}$$

2.2.4 A dynamic model including inactivation

As a first step, we make the model for growth consistent outside the interval $[T_{min}, T_{max}]$. Kohler *et al.* [1991] proposed the following modification of the expanded Ratkowsky model (2.6) :

$$\begin{aligned} \mu_{max} &= 0 \quad \text{if} \quad T < T_{min} \\ \mu_{max} &= b_2^2[T - T_{min}]^2[1 - \exp\{c_2(T - T_{max})\}]^2 \quad \text{if} \quad T_{min} \leq T \leq T_{max} \\ \mu_{max} &= 0 \quad \text{if} \quad T > T_{max} \end{aligned} \tag{2.13}$$

Because of conversion formula (2.4), c equals 0 outside the interval $[T_{min}, T_{max}]$. As a result, y remains then constant [see equation (2.11)], which is the desired behavior. Note that this model is both continuous and differentiable for all values of T, which makes it attractive from the mathematical point of view also.

Furthermore, the prediction by model equation (2.8) of negative asymptote values A for $T > T_{A,max}$ (see also Figure 2.3) can be circumvented as follows. It is clear that around the transition temperature $T_{A,max}$, there are two phenomena occurring at the same time : microbial growth and high temperature inactivation. A realistic model should exhibit some transition point (or even a transition zone), where the net effect of both reactions is almost zero : growth and inactivation compensate each other almost completely. The most consistent and elegant solution is to model both competing processes independently of each other. As a result, we propose the asymptote A to be independent of the temperature T :

$$A = b_4 = A_0 - \ln(N_0) = A_0 - n_0 \tag{2.14}$$

As a second step, we include high temperature inactivation. In the food engineering literature, it is common practice to model the high temperature inactivation rate constant k [1/h] with an Arrhenius–type model proposed by Bigelow [1921] :

$$k(T) = 60\frac{2.303}{D_{ref}}\exp[\frac{2.303}{z}(T - T_{ref})] \tag{2.15}$$

where D_{ref} is the time [minutes] required to reduce the bacterial concentration by a factor of 10, at the reference temperature T_{ref}, while z is the increase in temperature necessary to reduce this time requirement by the same factor. In order to model a possible transition zone between growth

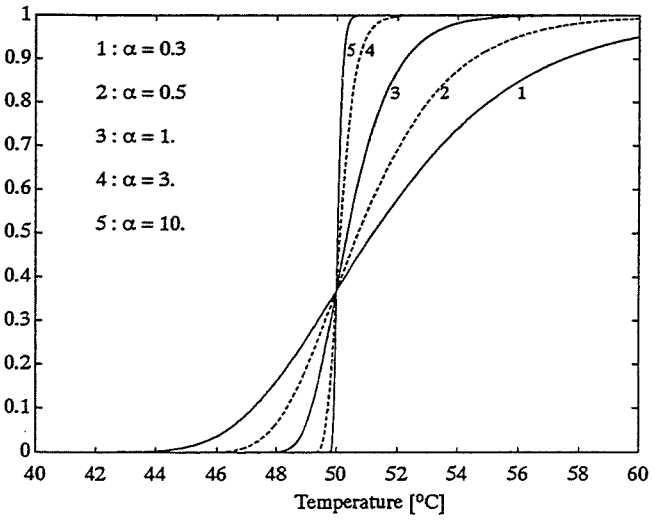

Figure 2.6: Value of the transition function $f_{trans}(T)$ for some values of the parameter α and $T_{trans} = 50°C$

and inactivation in which y remains constant, we propose the following modification of the model of Bigelow :

$$\begin{aligned} k_{mod}(T) &\triangleq f_{trans}(T)k(T) \\ f_{trans}(T) &\triangleq \exp[-\exp\{\alpha(T_{trans} - T)\}] \end{aligned} \tag{2.16}$$

The temperature T_{trans} determines the length of the transition zone ($T_{trans} - T_{max}$), while the parameter α determines the transition velocity around T_{trans} from growth to inactivation. Both parameters depend on the bacterial population under consideration. The function $f_{trans}(T)$ is plotted in Figure 2.6 for $T_{trans} = 50°C$ and some values of α. It can be seen that for $\alpha \to \infty$, $f_{trans}(T)$ approaches a unit step function at $T = T_{trans}$. In the special case of $T_{trans} = T_{max}$, there is no transition zone at all.

The overall specific growth rate μ [1/h] is defined as follows :

$$\frac{dN}{dt} \triangleq \mu N$$

It follows that :

$$\frac{dn}{dt} = \mu \tag{2.17}$$

Observe that the overall rate μ includes both growth and inactivation. We obtain the following dynamic model :

$$\frac{dn}{dt} = (1 - f_{trans}(T))c(n - n_0)\ln(\frac{A_0 - n_0}{n - n_0}) - f_{trans}(T)k(T) \tag{2.18}$$

$$n(t = 0) = \ln(N_0) + a\exp[-\exp(b)] \tag{2.19}$$

Note that in this model equation, the sum of the weighting factors for growth and inactivation is equal to 1, thus assuring a smooth transition if α is low.

The third model design requirement can be explained as follows. It can be expected that at the beginning of a new growth phase after an inactivation phase, the organism has to adapt again during some time to the lower temperature conditions. This results in a new lag time. In order to make consistent predictions using model equation (2.18), the value of $n_0 = \ln(N_0)$ —which plays the role of a reference level— must be changed accordingly. It follows that n_0 must be variable with time t. By doing so, we take into account the previous history of the food product in a natural way. The desired behavior can be modeled by the following dynamic model for n_0 :

$$\frac{dn_0}{dt} = \gamma f_{zero}(T)(n - n_0 - a\exp[-\exp(b)]) \tag{2.20}$$

$$n_0(t = 0) = \ln(N_0) \tag{2.21}$$

$$f_{zero}(T) = \exp[-\exp\{\beta(T_{zero} - T)\}] \tag{2.22}$$

This can be explained as follows. $f_{zero}(T)$ is a switching function similar to $f_{trans}(T)$. The temperature T_{zero} is the temperature at which the overall specific growth rate μ [equations (2.17) and (2.18)] changes sign. Observe that in general T_{zero} depends on the (logarithmic) population size n. In Figure 2.7 some curves are shown for $T_{max} = 44.9°C$ and some values of T_{trans} and α. If $T_{trans} = T_{max}$ (upper plot), i.e. if there is no transition zone, then T_{zero} approximates T_{max} only for very large values of α. However, in the generic case $T_{trans} > T_{max}$, the lower plot indicates that for all values of n, T_{zero} almost equals T_{max} from $\alpha = 2$ on and needs not to be determined numerically anymore.

β is set equal to a very large positive value [e.g. $\beta = 100$], so that $f_{zero}(T)$ approaches a unit step function at $T = T_{zero}$. Note that, in contrast with parameter α in equation (2.16), β does not depend on the microbial

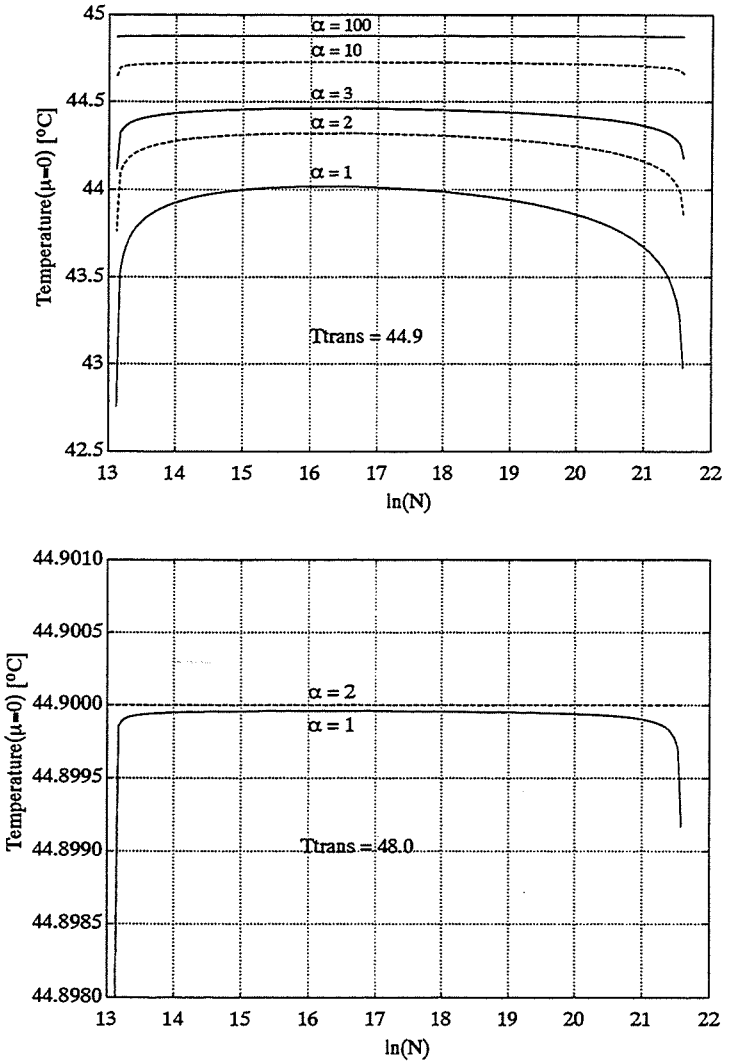

Figure 2.7: T_{zero} as a function of $n = \ln(N)$ for some values of T_{trans} and α, and $T_{max} = 44.9°C$

population under consideration. During a growth phase ($T < T_{zero}$) $f_{zero}(T)$ equals 0 (at least from the numerical point of view), so n_0 remains constant. During an inactivation phase ($T > T_{zero}$) $f_{zero}(T)$ equals 1, so n_0 moves towards $(n - a\exp[-\exp(b)])$ with a velocity determined by the factor γ (which is at the disposal of the user) and then tracks this value. At the beginning of a subsequent growth phase, the difference $(n - n_0)$ —needed in model equation (2.18)— is at its desired value $a\exp[-\exp(b)]$ with an accuracy determined by γ. This is equivalent with the initial condition (2.12) for the dynamic model for growth only. Note that $a\exp[-\exp(b)]$ contains the lag time λ in an implicit way through equation (2.5). From the mathematical point of view, $(n - n_0)$ never becomes negative, thus making the right hand side of model equation (2.18) always computable.
The complete dynamic model is summarized in Table 2.2

2.2.5 Simulation results and discussion

In this section we check whether the design requirements for a dynamic model as stated above are sufficiently fulfilled by the proposed model. During all simulations mentioned, the following parameter set was used : for growth, $A_0 = 21.58$ and $\gamma = 100$; for inactivation (taken from the work of Stumbo [1973]), $D_{ref} = 1.00$, $z = 10$, and $T_{ref} = 65.6$; and for transition, $T_{trans} = 44.9$, $\alpha = 1$, and $\beta = 100$. For the parameters concerning growth reference is made to Table 2.1. Observe that in the model of Kohler *et al.* (2.13) the parameters of the expanded square root model (2.6) can be used immediately. The parameters given in Table 2.1 are from *Lactobacillus plantarum* [Zwietering *et al.* 1991]. Since no parameters describing high temperature inactivation are available, the parameters for a *Lactobacillus sp.* (reported by Stumbo [1973]) are given above. The value of the inoculum level N_0 is set equal to $5\ 10^5$.

2.2.5.1 Verification of model design requirements

First of all, a transition zone between growth and inactivation can be easily simulated by using the transition function $f_{trans}(T)$ (2.16). The overall specific growth rate μ as a function of temperature is given by the right–hand side of equation (2.18). In Figure 2.8, some of the possibilities are illustrated. In this plot, n is chosen such that $\max(\mu) = \mu_{max}$. The first curve, obtained by letting $T_{trans} = T_{max}$ and $\alpha = 1$, represents a micro–organism with no transition zone at

$$\frac{dn}{dt} = (1 - f_{trans})c(n - n_0)\ln(\frac{A_0 - n_0}{n - n_0}) - f_{trans}k \quad (2.18)$$

$$n(t = 0) = \ln(N_0) + a\exp[-\exp(b)] \quad (2.19)$$

$$\frac{dn_0}{dt} = \gamma f_{zero}(n - n_0 - a\exp[-\exp(b)]) \quad (2.20)$$

$$n_0(t = 0) = \ln(N_0) \quad (2.21)$$

growth

$$c = \mu_{max}e/A \quad (2.4)$$

$$b = \mu_{max}e\lambda/A + 1 \quad (2.5)$$

$$\ln(\lambda) = \frac{p}{T - q} \quad (2.9)$$

$$A = A_0 - n_0 \quad (2.14)$$

$$\mu_{max} = \quad (2.13)$$

$$\begin{cases} 0 & T < T_{min} \\ b_2^2[T - T_{min}]^2[1 - \exp\{c_2(T - T_{max})\}]^2 & T_{min} \leq T \leq T_{max} \\ 0 & T > T_{max} \end{cases}$$

inactivation

$$k(T) = 60\frac{2.303}{D_{ref}}\exp[\frac{2.303}{z}(T - T_{ref})] \quad (2.15)$$

transition

$$f_{trans}(T) = \exp[-\exp\{\alpha(T_{trans} - T)\}] \quad (2.16)$$

$$f_{zero}(T) = \exp[-\exp\{\beta(T_{zero} - T)\}] \quad (2.22)$$

Table 2.2: Dynamic model equations

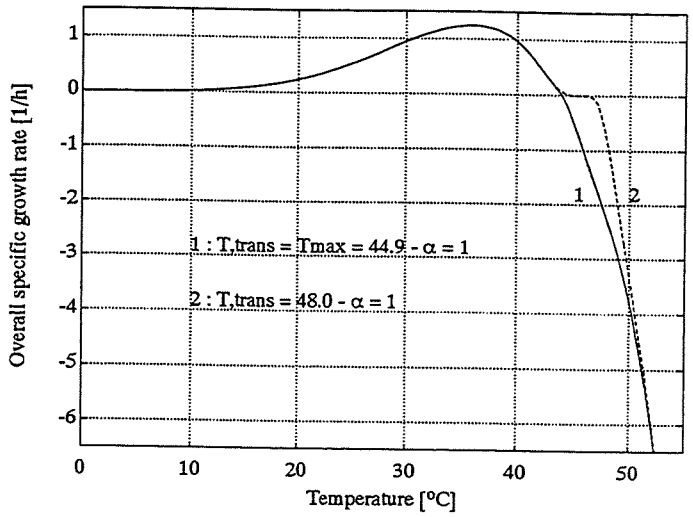

Figure 2.8: The overall specific growth rate as a function of temperature

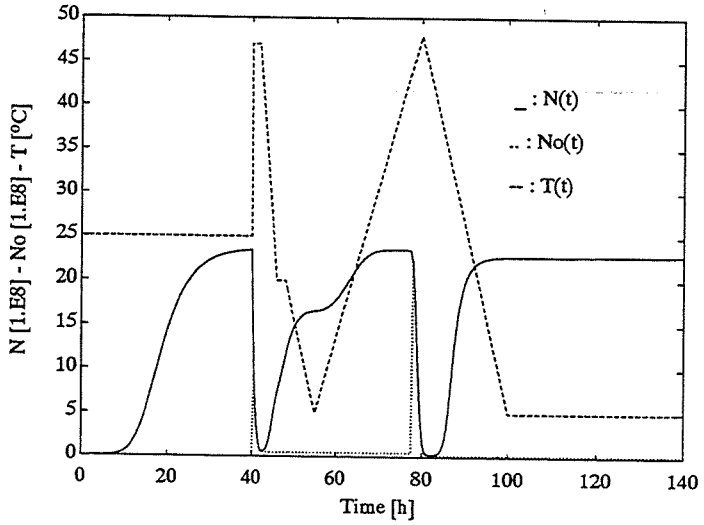

Figure 2.9: Predicted response of a microbial population to a hypothetic time–temperature profile

all. The very smooth behavior around the transition point T_{max} is obtained with a low value of α. The second curve exhibits a transition zone with zero overall specific growth rate between T_{max} and T_{trans}. The low value of α results again in a smooth behavior at temperatures near T_{trans}. Observe that both parameters T_{trans} and α depend on the microbial population under consideration : α is a curve fitting parameter, and T_{trans} has a clear physical interpretation. Obviously, the shape of the transition zone in the overall specific growth rate is rather sensitive to the value of T_{trans}. This indicates that T_{trans} can be determined uniquely if sufficient experimental data around T_{trans} are available.

Differentiability for all times and temperatures is guaranteed by the construction of the model itself. Note that we proposed a smooth transition function $f_{zero}(T)$ [equation (2.22)] instead of a simple unit step function. As a result, derivation with respect to temperature can be done analytically for all values of T. As such, modern optimization techniques (such as optimal control theory) become easily applicable.

Furthermore, the proposed model can deal with time varying temperature profiles in a consistent way, over the whole temperature range of growth and inactivation. In Figure 2.9, the predicted response of a microbial population to a hypothetic time–temperature profile is shown [$N = \exp(n)$ is the absolute population size per unit volume]. This plot sufficiently illustrates the capabilities of the model. After a phase of inactivation, the value of the reference level $N_0 = \exp(n_0)$ is indeed at the value required in the subsequent growth phase. In the second growth phase, there is an additional lag around $t = 50$ h, due to the very low temperatures, as could be expected.

Finally, it can be easily seen that the dynamic model reduces by construction to the experimentally validated explicit model as proposed by Zwietering *et al.* [1990,1991] in the special case of a constant temperature within the range of microbial growth. This is also illustrated in Figure 2.5 for values of t lower then 20 h, and in Figure 2.9 for values of t lower then 40 h.

2.2.5.2 Notes on parameter sensitivity

As for the parameter sensitivity, the following observations can be made.

First, all parameters concerning growth are taken from Zwietering *et al.* [1991]. More details concerning the practical identifiability and the determination of confidence intervals starting from experimental data are reported there and are not repeated here. Suffice it to say that all parameters describing μ_m, λ and A can be determined from experiments carried out at a lot of different but constant temperatures. In addition, Kohler *et al.* [1991] demonstrated that when modeling the maximum specific growth rate μ_m with equation (2.13) instead of using the expanded Ratkowsky model (equation 2.6) —in other words, using μ_m as the dependent variable instead of $\sqrt{\mu_m}$—, best fit estimates of the parameters can easily be obtained by employing a standard implementation of the Marquardt–Levenberg algorithm. Model equation (2.13) is a close–to–linear model [Kohler *et al.* 1991]. This means that a least square estimator, even when sample sizes are relatively small, comes close to being an unbiased, normally distributed, minimum–variance estimator. As a result, confidence intervals for the parameters can be readily constructed.

Second, the sensitivity of the transition zone to variations in T_{trans} has been illustrated in Figure 2.8.

Third, the values for the parameters D_{ref} and z (describing high temperature inactivation) given above are in fact the maximum values, for which Stumbo [1973] reported the following range for a *Lactobacillus sp.* : D_{ref} in the interval $[0.50, 1.00]$, and z in the interval $[8, 10]$. A detailed analysis of the practical identifiability of these parameters is beyond the scope of this paper. Reference is made to, e.g., the work of Stumbo [1973] and the references therein. In Figure 2.10, the sensitivity of the predictions by the new model towards different values for D_{ref} and z by using the same hypothetic time–temperature profile as in Figure 2.9 is illustrated. Clearly, both parameters have a large influence on the evolution of the total population number N with respect to time. On the other hand, these simulation results suggest that both parameters may be determined uniquely if designing an experiment using a similar dynamic time–temperature profile.

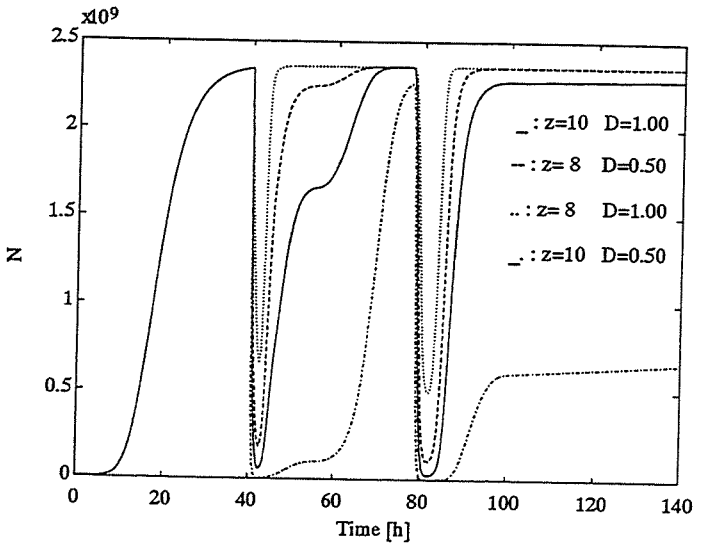

Figure 2.10: Sensitivity of the predicted response of a microbial population to variations in D_{ref} and z

Therefore, we suggest the following two–step procedure for the estimation of the parameters of the new dynamic model.

Step 1. In a first step, experiments are carried out at a lot of different but constant temperatures. This allows to model the growth characteristics μ_m, λ and A as functions of temperature using the model equations given in Table 2.2. In addition, experimental data of the specific growth rate at temperatures around T_{trans} allow for the estimation of T_{trans} and α.

Step 2. In a second step, experiments carried out using a dynamic time–temperature profile as illustrated in Figure 2.10 can be helpful to refine the value of the parameters D_{ref} and z (taken from e.g. literature data). As already mentioned, T_{zero} can then be calculated numerically from the right–hand side of equation (2.18) if all parameters are known.

Remember that the parameters β [equation (2.22)] and γ [equation (2.20)] are independent of the microbial population under consideration and are set at a large (positive) value.

2.3 Conclusions

As already mentioned in the introduction, the principal aim of this chapter was to introduce more advanced modeling concepts into the field of predictive microbiology. The new dynamic model presented establishes a general framework for describing a microbial population under time varying conditions in a consistent way : the simulations indicate that the predicted population evolution coincides with what may be expected intuitively.

The main features of this dynamic model can be summarized as follows.

1. As the model is in the form of a first order differential equation instead of an explicit function, it can deal with time varying temperatures in a consistent way. As an additional feature, the previous history of the product under consideration is taken into account in a natural way. Although not yet validated in practice, the model predictions are very meaningful.

2. Both microbial growth and inactivation are described within a single expression. The model can easily simulate micro–organisms with a quite different behavior at temperatures around the transition from growth to inactivation, by using a simple transition function with clear parameters.

3. In the special case of a constant temperature within the range of growth, the model predictions coincide exactly with the experimentally validated explicit Gompertz model as proposed by Zwietering *et al.* [1990,1991].

4. Finally, the complete model has suitable mathematical properties to make advanced nonlinear parameter estimation schemes and modern optimization techniques easily applicable.

As such, this model is an appropriate building block of a global model, useful for prediction and control of microbial growth during thermal treatment and storage of chilled foods.

We wish to emphasize again that further refinements will be certainly required after an experimental validation study. This is one of the research topics of the ongoing FLAIR (Food Linked Agro–Industrial Research) project AGRF–DT91–0047 (DTEE), supported by the European Commission. More specifically, the validity of the model equations (2.9), (2.13), (2.14) and (2.15) under time varying temperature conditions must be checked. For instance, it

can be expected that for the same initial population size, the lag time λ will depend on whether or not the growth phase follows an inactivation phase. Furthermore, the possible influence of pH and water activity must be considered. This can be done e.g. by multiplying the temperature–dependent maximum specific growth rate, asymptote, and lag time, with additional factors, as explained in Chapter 1.

However, as these refinements are only at the level of modeling the main characteristics λ, μ_m, A and k, the general approach presented in this chapter will remain valid.

Chapter 3

Optimal control of fed-batch fermentation processes

In this chapter the optimization of fed–batch bioreactors is under study. An increasing number of papers in recent years are devoted to the theoretical investigation of optimal control problems in fed–batch fermentations. These are of particular importance when the products are secondary metabolites. Fed–batch operation enables superior control as it provides different avenues in the substrate plane for control through distinct phases of biomass growth and metabolite production. By programming substrate feeding, one can control important phenomena such as substrate inhibition, glucose effect and catabolite repression. Control opportunities in fed–batch operated fermentations have been reviewed in detail in a number of articles (see e.g. [Parulekar and Lim 1985], [Johnson 1987], ...).

The results we present here are general in this way that they are written in terms of the specific reaction rates. In other words, an exact analytical expression for these rates is not required a priori. In addition, no assumptions are made concerning the metabolism involved for biomass survival and possibly product synthesis. Much attention is given to carefully motivating from a microbiological viewpoint both the methods used and the results obtained. As such, even results already partially reported in the literature are given additional interpretations.

In Section 3.1 we describe some marked advantages of fed–batch operation mode. We also include a review of the literature about the application of (optimal) control techniques to fed–batch fermentation processes.

In Section 3.2 we present a general unstructured model for a fed–batch bioreactor characterized by one limiting substrate, a single micro–organism, and possibly one product of interest. A general optimization problem is then formulated with the volumetric substrate feed rate considered as the control input. We consider performance indices of both the yield type and the productivity type. The optimization of the initial substrate concentration is also included.

In Section 3.3 this general optimization problem is then reformulated in the framework of optimal control theory, leading to a two point boundary value problem. It is shown that the solution reduces to the determination of the optimal control sequence —possibly including a singular interval— and the corresponding switching times.

As an introductory example, the microbial growth process is considered in Section 3.4. Although the solution has been reported already elsewhere [Parulekar and Lim 1985], we include an analysis of this example for three reasons. First, the deduced control sequences are justified here based on biochemical insight in the process. Second, the extension to processes with growth associated product formation is straightforward. Third, a similar line of reasoning will be adopted for fed–batch fermentations characterized by a decoupling between growth and product formation considered in Section 3.5.

According to Modak et al. [1986], fermentation processes with a decoupling between growth and production are classified following the qualitative behavior of the specific growth and production rates with respect to substrate concentration. As an example, we derive the optimal control sequence for processes with monotonic growth rate and non–monotonic production rate. We are able to prove that the deduced control sequence minimizes the performance index globally. In addition, we present for the first time a complete solution in the realistic case of substrate and biomass inequality constraints. The resulting straightforward computational algorithm has some advantages over the algorithm proposed by Lim et al. [1986]. First, there is no need for costate variables —which have in general no clear physical interpretation— independent of the performance measure considered. Second, as a result this algorithm proves to be numerically more reliable.

In Section 3.6 the singular arc is analyzed very carefully. The results obtained —summarized in Theorems 3.1 and 3.2— are at the basis of a heuristic optimization methodology described in Section 3.7. These heuristic controllers play a central role throughout this thesis. They are also motivated from the biochemical viewpoint. In contrast to the optimal control solution they are the translation of a more realistic control objective, namely set–point control, for which adaptive model–independent control algorithms can be developed (see Chapter 6).

Some concluding remarks are summarized in Section 3.8

3.1 Fed-batch fermentations

3.1.1 Advantages of fed-batch fermentations

In a fed–batch operation (also referred to as a *zulauf* process) the nutrients necessary for microbial growth are fed either intermittently or continuously during the course of an otherwise batch operation. The reaction mixture broth is then harvested either fully or partially at the end of the operational period, and this whole process may be repeated several times (*repeated fed–batch*).

Fed–batch bioreactors are well suited for processes in which the cell growth and/or product formation are significantly sensitive to the concentration of the so–called limiting substrate. These reactors offer large flexibility with respect to control of the limiting substrate. In particular, the fed–batch operation has been found to be very effective for processes in which effects such as *glucose effect*, *substrate inhibition* and *catabolite repression* are important.

1. Overfeeding of nutrients often leads to the production of undesired by–products. Consider e.g. the production of baker's yeast with glucose as the substrate (see Chapter 1). When the glucose concentration in the aerobic culture medium exceeds a certain critical value, then the second pathway is activated and glucose is partially metabolized to ethanol. This is the so–called Crabtree effect or the glucose effect [Roels 1983]. Overfeeding of nutrients has also been observed to reduce production of non–biomass products (such as antibiotics and enzymes) due to excessive cell growth [Giona *et al.* 1976b].

On the other hand, an underfeeding of nutrients results in cell starvation and reduced specific growth rates, thereby lowering the productivities of biomass and metabolite products.

The fed–batch mode of operation provides an excellent means of regulating the nutrient feed rate to optimize the productivity while at the same time obviating over– and underfeeding of nutrients.

2. Ethanol and methanol severely inhibit the growth of micro–organisms when present in the culture medium either as a substrate or as a product [Yamane *et al.* 1976; Kishimoto *et al.* 1981a and b; Lee and Wang 1982; ...]. If the concentration of ethanol or methanol in the culture broth is high, there is a considerable loss of substrate due to evaporation.

   In a fed–batch culture, concentrations of these species in the broth can be kept low and the inhibition and evaporation problem can be overcome.

3. Synthesis of many metabolite products is repressed when the cells are grown rapidly on a readily utilizable carbon source such as glucose. This catabolite repression may be caused by the limiting substrate, an intermediate, or the product. A typical example is the penicillin production by *Penicillium chrysogenum* grown on glucose.

   By operating the bioreactor in fed–batch mode, it is possible to obtain maximum productivity while at the same time circumventing catabolite repression by optimal (slow) feeding of the carbon source.

Following successful application to yeast production, fed–batch cultures have been tried in the industrial production of antibiotics, amino acids, enzymes, vitamins, single–cell proteins, biomass, and various organic compounds of commercial importance.

3.1.2 Review of the literature

An increasing number of studies in recent years are devoted to the theoretical and experimental investigation of optimal control problems in fed–batch fermentations. The main advantages of such systems over other modes of operation have been discussed in Section 3.1.1. Control opportunities in fed–batch operated fermentations have been reviewed in detail in a number of articles (see e.g. [Parulekar and Lim 1985], [Johnson 1987], ...). Yet the

determination of an optimal operating strategy is not a straightforward matter and is often further complicated by the presence of constraints imposed on the state variables.

Optimization of fed–batch fermentations has been traditionally sought with respect to the volumetric substrate feed rate while keeping the substrate concentration in the feed fixed. Formulating the problem with the feed rate as the control variable yields a *singular* optimal control problem. Fishman and Biryukov [1974] considered the problem of optimal glucose feed strategy for penicillin production. However, they did not give any general characteristics nor a numerical scheme and ignored volume changes arising from the feed. Ohno *et al.* [1976] used a method based on Greens' theorem for the production of lysine. This method is applicable only to problems with two mass balance equations and fixed boundary conditions.

When the fermentation process is described by no more than three mass balance equations, one can take advantage of the structure of a particular problem. Weigand *et al.* [1979] reduced the problem of optimal feed rate determination for single cell protein production (three dimensional problem) to one in which the time to switch from the maximum rate to a singular feed rate is iterated. This approach provides the optimal solution with relative ease [Weigand 1981; San and Stephanopoulos 1984].

Due to limited success in singular control theory, most of the fed–batch fermentation processes considered so far have been limited to low–order processes, described by no more than four mass balance equations (see e.g. [Staniškis and Levišauskas 1984; Hong 1986]). General computational algorithms have been developed by Lim *et al.* [1986] and Modak *et al.* [1986] for the optimal volumetric feed rate profiles for such fermentation processes.

A number of techniques have been proposed to convert the singular control problem into a nonsingular one. To avoid a singular control problem, variables other than the feed flow rate may be taken as the control variable. Yamane *et al.* [1977] considered the specific growth rate as the control variable. However, this can lead to a problem in physically realizing the flow rate from the optimum specific growth rate unless proper physical constraints are placed on the specific growth rate. If the specific growth rate is a non–monotonic function of substrate concentration or depends on other component concentrations as well, this approach cannot be used. Furthermore, constraints on the flow rate cannot taken into account. Guthke and Knorre [1981] considered the substrate concentration as the manipulated variable and omitted the substrate and the overall mass balance equations.

This method runs into a problem of realizing the optimal substrate concentration profile due to the physical constraints on feeding rate and volume that were ignored. Modak and Lim [1989] proposed an alternative set of state variables and used the culture volume as the control variable. This approach may be useful to optimize fed–batch cultures described by any number of mass balance equations involving different kinds of constraints. However, the success of the method depends greatly on the ability to numerically solve highly nonlinear nonsingular control problems with constraints on the manipulated variable and its time derivative. San and Stephanopoulos [1989] proposed to solve the problem in two steps. First the optimal control problem with the fermentor substrate concentration as the control variable must be solved to yield an optimal substrate trajectory. State inequalities on both substrate and biomass concentration can be included with relative ease. In a second step they propose to realize the optimal reactor substrate profile by manipulating the substrate concentration in the feed while keeping the volumetric feed rate fixed. However, they do not solve this second step. Kurtanjek [1991] also proposed a two step procedure for a multidimensional optimization problem with constraints imposed on control and state variables based on the use of the orthogonal collocation technique. The first step is the nonsingular optimization of temperature and substrate profiles. The second part is the determination of the optimal substrate concentration in the feed rate and the optimal volumetric substrate feeding rate. However, this method critically relies on an exact knowledge of the specific growth and production rates.

As a matter of fact, these methods all suffer from problems with respect to practical implementation. Therefore, in this thesis we adopt the traditional point of view, i.e. singular optimal control with the volumetric substrate feed rate as the manipulated variable. We will show in the following that the determination of the switching times in the feed rate profile can be simplified a lot by incorporating as much as possible microbiological knowledge concerning the process under consideration. We will also present for the first time a complete general solution in the case of substrate and biomass inequality constraints.

A detailed analysis of the singular arc will lead to the design of heuristic control strategies which play a central role throughout this thesis. They are at the basis of the design of model–independent control strategies which combine nearly optimal performance with excellent robustness properties : optimal adaptive control (see Chapter 6).

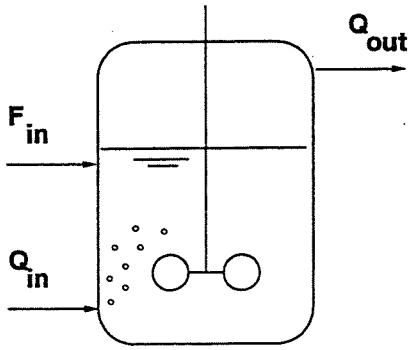

Figure 3.1: Fed–batch bioreactor

3.2 General optimization problem

3.2.1 General unstructured model for fed-batch reactors

Consider the stirred tank reactor of Figure 3.1 operated in fed–batch mode. As in Chapter 1 we assume that the process is in a completely mixed condition and can be characterized by the macroscopic variables S (amount of substrate), X (amount of biomass) and P (amount of product), S being the only limiting substrate for cell mass growth and production. All other nutrients are present in excess but not in toxic quantities throughout the fermentation period. We do not consider gaseous flow rates Q_{in} and Q_{out}, while we suppose that the product remains completely in the liquid phase. Constant environmental conditions are assumed to be maintained. A general unstructured dynamic model involving substrate S, biomass X, product P and reactor volume V is (see also Chapter 1) :

$$\begin{aligned} \frac{dS}{dt} &= -\sigma X + C_{s,in}F_{in} \\ \frac{dX}{dt} &= \mu X \\ \frac{dP}{dt} &= \pi X - k_h P \\ \frac{dV}{dt} &= F_{in} \end{aligned} \tag{3.1}$$

or, using concentrations instead of absolute quantities :

$$\begin{aligned}
\frac{dC_s}{dt} &= -\sigma C_x - C_s\frac{F_{in}}{V} + C_{s,in}\frac{F_{in}}{V} \\
\frac{dC_x}{dt} &= \mu C_x - C_x\frac{F_{in}}{V} \\
\frac{dC_p}{dt} &= \pi C_x - C_p\frac{F_{in}}{V} - k_h C_p \\
\frac{dV}{dt} &= F_{in}
\end{aligned} \tag{3.2}$$

where σ is the specific substrate consumption rate, μ is the specific growth rate, and π is the specific production rate. Note that decay of product P is explicitly taken into account using a first order model, where k_h denotes the *specific product decay rate*. There is no dynamic equation for dissolved oxygen, as dissolved oxygen is considered non–limiting by maintaining a sufficiently high aeration level. At this point we allow the specific rates σ, μ and π to be arbitrary functions which may depend on substrate, cell and product concentrations, interrelated by (1.11) :

$$\sigma = \frac{\mu}{Y_{x/s}} + m + \frac{\pi}{Y_{p/s}} \tag{3.3}$$

where $Y_{x/s}$ and $Y_{p/s}$ are yield coefficients and m is the overall maintenance coefficient.

As already mentioned, fed–batch fermentation processes have been found to be most effective in overcoming such effects as substrate inhibition, catabolite repression, and glucose effects. In other words, whenever the specific rates of growth (μ) and/or product formation (π) are *non–monotonic* functions of the substrate concentration, a fed–batch operation may be superior and it is then necessary to determine the *optimal feed rate of substrate* (nutrients and precursors).

3.2.2 Statement of the problem

In this section we formulate a general optimization problem for fed–batch reactors.

We use the volumetric substrate feed rate F_{in} as control input u :

$$u \triangleq F_{in}$$

If we use *absolute quantities* as in model (3.1), an obvious choice for a state space vector $\mathbf{x}$ is given by :

$$\mathbf{x} = \begin{pmatrix} x_1 \\ x_2 \\ x_3 \\ x_4 \end{pmatrix} \triangleq \begin{pmatrix} S \\ X \\ P \\ V \end{pmatrix}$$

and with the definition of :

$$\mathbf{f} = \begin{pmatrix} f_1 \\ f_2 \\ f_3 \\ f_4 \end{pmatrix} \triangleq \begin{pmatrix} -\sigma X \\ \mu X \\ \pi X - k_h P \\ 0 \end{pmatrix} \qquad \mathbf{b} = \begin{pmatrix} b_1 \\ b_2 \\ b_3 \\ b_4 \end{pmatrix} \triangleq \begin{pmatrix} C_{s,in} \\ 0 \\ 0 \\ 1 \end{pmatrix}$$

we obtain the following state space model linear in the control input u :

$$\frac{d\mathbf{x}}{dt} = \mathbf{f}(\mathbf{x}) + \mathbf{b}\, u \tag{3.4}$$

Observe that we can obtain a completely equivalent state space model using *concentrations* [as in (3.2)] as state variables. However, it is easily seen that the corresponding column vector $\mathbf{b}$ then becomes an explicit function of the state variables. In order to facilitate further computations as much as possible, we prefer to work with the model in absolute quantities.
First, a *performance measure* to be minimized must be specified. Two general forms for the objective function are :

$$\begin{aligned}
J_1[u] &= g_1[\mathbf{x}(t_f), t_f] \\
&= -\gamma_x X(t_f) - \gamma_p P(t_f) + \gamma_t t_f
\end{aligned} \tag{3.5}$$

$$\begin{aligned}
J_2[u] &= g_2[\mathbf{x}(t_f), t_f] \\
&= -\frac{\gamma_x X(t_f) + \gamma_p P(t_f)}{t_f}
\end{aligned} \tag{3.6}$$

with γ_x, γ_p the unit 'prices' associated with the cell mass and metabolite product respectively, and γ_t the unit 'operating cost'.

The optimization problem is then to determine for the set of differential equations (3.4) the optimal volumetric substrate feed rate profile $u^*(t)$ that minimizes the performance index (3.5) or (3.6).

The initial values for X and P are *fixed*, i.e. (the initial time $t_0 = 0$) :

$$\begin{aligned} x_2(0) &= X_0 \\ x_3(0) &= P_0 \end{aligned}$$

However, in contrast to classical optimal control problems, we consider some components of the initial state as *additional control parameters* that can be manipulated to minimize the performance index. More specifically, in the sequel we assume most often that the initial value for S, $x_1(0)$, is *free*; the initial values for S and V are only constrained by a linear relation of the form :

$$x_4(0) = V_* + \frac{x_1(0)}{C_{s,in}} \tag{3.7}$$

with V_* the initial volume *without* substrate. Note that substrate is added as a solution with concentration $C_{s,in}$.
As a result, the performance indices (3.5) and (3.6) should be written as :

$$J_1[u, x_1(0)] = -\gamma_x X(t_f) - \gamma_p P(t_f) + \gamma_t t_f \tag{3.8}$$

$$J_2[u, x_1(0)] = -\frac{\gamma_x X(t_f) + \gamma_p P(t_f)}{t_f} \tag{3.9}$$

Note that minimizing performance index (3.9) is equivalent to *maximizing the average productivity* $\mathcal{P}$, weighted by the unit prices of cell mass and product.
The performance index (3.8) or (3.9) must be minimized subject to an additional set of *constraints.*

1. The final time t_f is *fixed or free.*

2. As all state and control variables represent non–negative physical quantities, we must have :

   $$\forall t \in [0, t_f] : \quad x_i(t) \geq 0, \text{ for } i = 1, \ldots, 4 \quad \wedge \quad u(t) \geq 0$$

   Observe that in an appropriate fermentation process model, the first part of this constraint (i.e., all state variables are non–negative) should be satisfied automatically. In other words, this constraint must be seen as a *model design requirement.* However, if the process model does not satisfy this condition a priori (this is for instance the case for a complete maintenance metabolism), it should be included explicitly as a constraint in the optimization, or the model should be modified accordingly.

3. The total amount of substrate available for the fermentation (denoted with α) is *fixed or free* :

   $$x_1(0) + \int_0^{t_f} C_{s,in} u(t)\, dt = \alpha \tag{3.10}$$

   If α is fixed, then the last *isoperimetric* constraint is equivalent to a *physical* constraint of the form (see the differential equation for V) :

   $$x_4(t_f) \equiv V(t_f) = V_f, \; V_f \text{ fixed} \tag{3.11}$$

It can be easily seen that specifying both the final time t_f and the total amount of substrate available α may lead to an ill conditioned optimal control problem. On the other hand, letting both t_f and α free does not lead to a well posed problem either. As a result, it is necessary to *specify either* t_f *or* α.
In the following, we always *fix* α, while letting t_f *free.* This choice can be motivated as follows :

1. By fixing α, we can easily take into account the physical constraint on the fermentor volume (3.11).

2. By letting t_f free, we can derive more general properties of the optimal control profile in terms of microbial knowledge of the process under consideration. This will be illustrated in the following sections.

3. From an industrial point of view the final time t_f is very often the most important factor. This can be taken into account in two ways. First, we can increase the unit operating cost γ_t in cost index (3.8). Second, we can use the additional degree of freedom $x_1(0)$ to calculate a *trade off* between the value of the cost J and the final time t_f. Some examples will be given in the next chapters.

The average *yield* $\mathcal{Y}$ is defined as the ratio of the final amount of biomass and product weighted by their unit prices to the total amount of substrate consumed during fermentation α. If we neglect the unit operating cost γ_t and fix the total substrate amount α, then minimizing performance index (3.8) is equivalent to *maximizing the average yield* $\mathcal{Y}$.

3.3 Necessary conditions for optimality

The general optimization problem presented in the previous section is now formulated within the framework of optimal control theory.

3.3.1 Statement of the two point boundary value problem

The Minimum Principle (see Section 1.2.3) states that the following Hamiltonian $\mathcal{H}$ must be minimized over all admissible control inputs $u(t)$:

$$\mathcal{H} = \boldsymbol{\lambda}^{\mathbf{T}}(\mathbf{f}(\mathbf{x}) + \mathbf{b}u) \triangleq \phi + \psi u \tag{3.12}$$

with

$$\phi = \lambda_1 f_1 + \lambda_2 f_2 + \lambda_3 f_3 \qquad \psi = C_{s,in}\lambda_1 + \lambda_4$$

The adjoint vector $\boldsymbol{\lambda}$ satisfies the following system of differential equations :

$$\frac{d\boldsymbol{\lambda}}{dt} = -\frac{\partial \mathcal{H}}{\partial \mathbf{x}} = -\frac{\partial \mathbf{f}}{\partial \mathbf{x}}^{\mathbf{T}} \boldsymbol{\lambda} \tag{3.13}$$

Together with the state equations (3.4), we obtain a system of $2n$ first order differential equations —where n denotes the dimension of the state vector $\mathbf{x}$, here $n = 4$— which needs of course $2n$ boundary conditions. These can be specified as follows :

- $x_2(0)$ and $x_3(0)$ are given
- $x_1(0)$ and $x_4(0)$ are interrelated by equation (3.7)
- $x_4(t_f)$ is given due to equation (3.11)
- $\lambda_i(t_f)$, $i = 1, \ldots, 3$ are given by :

$$\lambda_i(t_f) = \frac{\partial g}{\partial x_i}[\mathbf{x}(t_f), t_f]$$

As $x_1(0)$ and $x_4(0)$ are not given in an explicit way, we need an additional boundary condition. Application of the result of Section 1.2.5 leads to :

$$C_{s,in}\lambda_1(0) + \lambda_4(0) \equiv \psi(0) = 0 \tag{3.14}$$

Since the boundary conditions are specified either at the initial time $t = 0$ or at the final time $t = t_f$ this is a *two point boundary value problem (TPBVP).*

Observe that the Hamiltonian $\mathcal{H}$ does not depend explicitly on time t. Then we know that on an extremal trajectory (see Necessary condition 1 in Section 1.2.3) :

$$\forall t \in [0, t_f] \; : \; \mathcal{H} \equiv \boldsymbol{\lambda}^{*\mathbf{T}}(t)(\mathbf{f}[\mathbf{x}^*(t)] + \mathbf{b}\; u^*(t)) = \mathcal{H}^*$$

with $\mathcal{H}^*$ a constant. If in addition the cost index is independent of the final time t_f [e.g. a cost index of the form (3.8) with $\gamma_t = 0$] we have (see Necessary condition 2 in Section 1.2.3) :

$$\forall t \in [0, t_f] \; : \; \mathcal{H} \equiv \boldsymbol{\lambda}^{*\mathbf{T}}(t)(\mathbf{f}[\mathbf{x}^*(t)] + \mathbf{b}\; u^*(t)) = 0$$

3.3.2 Extremal controls

Following Pontryagin's Minimum Principle (Section 1.2.3) an *extremal* control $u^*(t)$ follows from the minimization of the Hamiltonian $\mathcal{H}$ (3.12) over all *admissible* control functions :

$$\min_{\text{all admissible } u} \mathcal{H}(\mathbf{x}^*, \boldsymbol{\lambda}^*, u) = \mathcal{H}(\mathbf{x}^*, \boldsymbol{\lambda}^*, u^*)$$

while $\mathbf{x}$ and $\boldsymbol{\lambda}$ satisfy the above two point boundary value problem.

Minimization of the Hamiltonian $\mathcal{H}$ is considerably simplified since the control $u(t)$ appears *linearly* in it. In other words, an extremal control $u^*(t)$ can be determined by examining the coefficient of u in (3.12), $\psi \equiv \boldsymbol{\lambda}^{\mathbf{T}}\mathbf{b}$.

In a real life application, there is a constraint on the feeding pump capacity $u(t)$:

$$0 \equiv U_{MIN} \leq u(t) \leq U_{MAX}, \quad U_{MAX} \text{ given}$$

In that case, an extremal control $u^*(t)$ can be characterized as follows. If ψ is positive we set $u = 0$, while if ψ is negative we have $u = U_{MAX}$. However, if over a finite time interval $[t_i, t_{i+1}]$ the coefficient ψ remains identically zero, the Minimum Principle fails to provide $u(t)$ during this interval. Such intervals are called *singular* intervals. In summary, we have :

$$u^*(t) = \begin{cases} U_{MAX} & \text{if} \quad \psi < 0 \\ u_{sing} & \text{if} \quad \psi = 0 \quad t_i \leq t \leq t_{i+1} \\ 0 & \text{if} \quad \psi > 0 \end{cases} \tag{3.15}$$

which represents a *bang–singular–bang* solution.

As explained in Section 1.2.4, on any singular interval $[t_i, t_{i+1}]$ the *singular* control $u_{sing}(t)$ is obtained by repeatedly differentiating the function ψ until u appears explicitly. We obtain successively :

$$\frac{d\psi}{dt} = \dot{\boldsymbol{\lambda}}^{\mathbf{T}}\mathbf{b} = -\boldsymbol{\lambda}^{\mathbf{T}}\frac{\partial \mathbf{f}}{\partial \mathbf{x}}\mathbf{b} \triangleq \lambda^{\mathbf{T}}\mathbf{d} = 0$$

$$\frac{d^2\psi}{dt^2} = \dot{\boldsymbol{\lambda}}^{\mathbf{T}}\mathbf{d} + \boldsymbol{\lambda}^{\mathbf{T}}\frac{\partial \mathbf{d}}{\partial \mathbf{x}}\dot{\mathbf{x}} = -\boldsymbol{\lambda}^{\mathbf{T}}\frac{\partial \mathbf{f}}{\partial \mathbf{x}}\mathbf{d} + \boldsymbol{\lambda}^{\mathbf{T}}\frac{\partial \mathbf{d}}{\partial \mathbf{x}}(\mathbf{f} + \mathbf{b}u) = 0$$

The last equation can be solved for u_{sing} :

$$u_{sing}(t) = \frac{\boldsymbol{\lambda}^{\mathbf{T}}[(\partial \mathbf{f}/\partial \mathbf{x})\mathbf{d} - (\partial \mathbf{d}/\partial \mathbf{x})\mathbf{f}]}{\boldsymbol{\lambda}^{\mathbf{T}}[\partial \mathbf{d}/\partial \mathbf{x}]\mathbf{b}} \tag{3.16}$$

We wish to emphasize that this quite compact expression represents a lot of analytic calculations on the right–hand side of state equations (3.4), as the partial derivatives of first and second order with respect to all state variables are needed. A necessary condition for existence of a singular arc can be shown to be [Bryson and Ho 1975] :

$$\frac{\partial}{\partial u}\left[\frac{d^2\psi}{dt^2}\right] \geq 0$$

We conclude that the TPBVP has been reduced to the determination of the *optimal control sequence* $[U_{MAX}, U_{MIN}, u_{sing}]$ and the corresponding *switching times.*

REMARKS

1. In all examples we consider in this work the denominator of the singular control (3.16) is indeed different from zero. Obviously, this problem is a *singular problem of order 2.*

2. In expression (3.16) both the numerator and the denominator are *linear* in the costate vector $\boldsymbol{\lambda}$. On any singular interval, there exist three linear algebraic equations between the costate variables. These equations are :

$$\begin{aligned} \psi \equiv \boldsymbol{\lambda}^T\mathbf{b} &= 0 \\ \frac{d\psi}{dt} \equiv \boldsymbol{\lambda}^T\mathbf{d} &= 0 \\ \phi \equiv \boldsymbol{\lambda}^T\mathbf{f} &= \mathcal{H}^* \end{aligned} \tag{3.17}$$

with $\mathcal{H}^*$ a constant. If the cost index is independent of final time t_f [e.g. a cost index of the form (3.8) with $\gamma_t = 0$] then $\mathcal{H}^* = 0$. The homogeneous system (3.17) specifies three costates as functions of the remaining fourth one. As a corollary, the singular control (3.16) is a *nonlinear feedback law of the state variables* $\mathbf{x}$ *only.*
For the state space model (3.4) it can be seen that λ_4 has disappeared from u_{sing}, as $f_4 \equiv 0$. So the first equation in (3.17) can be omitted, and the last two can be solved as follows :

$$\begin{pmatrix} f_1 & f_2 \\ \beta_1 & \beta_2 \end{pmatrix}\begin{pmatrix} \lambda_1 \\ \lambda_2 \end{pmatrix} = -\begin{pmatrix} f_3 - \mathcal{H}^* \\ \beta_3 \end{pmatrix}\lambda_3 \tag{3.18}$$

with

$$\beta_i \triangleq b_1\frac{\partial f_i}{\partial x_1} + b_4\frac{\partial f_i}{\partial x_4},\ i = 1, \ldots, 3$$

■

3.4 Example : microbial growth process

In some situations a complete analytical solution of the given two point boundary value problem is possible. To illustrate this, we consider the microbial growth process introduced in Section 1.1.1 in which biomass is the major product. So in the general state space model (3.1) we omit the equation for product formation :

$$\begin{aligned} \frac{dS}{dt} &= -\sigma X + C_{s,in}u \\ \frac{dX}{dt} &= \mu X \\ \frac{dV}{dt} &= u \end{aligned}$$

The specific substrate consumption rate σ and the specific growth rate μ are interrelated by (1.6) :

$$\sigma = \frac{1}{Y_{x/s}}\mu + m$$

which can represent a maintenance, an endogenous or a mixed metabolism. Furthermore, we assume that μ_{substr} is function of the limiting substrate concentration C_s only. Remember that μ_{substr} represents the specific substrate to biomass conversion rate. This is equal to the specific growth rate

μ up to the endogenous fraction m_x of the overall specific maintenance demand m [see equation (1.4)]. We consider the minimization of the following performance measure :

$$J[u] = -X(t_f)$$

i.e. maximization of the final biomass amount, which is of the form (3.8) with $\gamma_p = \gamma_t = 0$. For reasons of compatibility with the notations introduced, we denote the state and costate vectors as :

$$\mathbf{x} \triangleq \begin{pmatrix} x_1 \\ x_2 \\ x_4 \end{pmatrix} \qquad \boldsymbol{\lambda} \triangleq \begin{pmatrix} \lambda_1 \\ \lambda_2 \\ \lambda_4 \end{pmatrix}$$

The two point boundary value problem stated in Section 3.3.1 reads as follows.

- The Hamiltonian is expressed as :

$$\mathcal{H} = \phi + \psi u$$

with

$$\phi = (-\lambda_1\sigma + \lambda_2\mu)x_2 \qquad \psi = C_{s,in}\lambda_1 + \lambda_4$$

Clearly, $\mathcal{H} = 0$ for all t.

- The adjoint variables satisfy (the prime denotes derivation with respect to substrate concentration C_s) :

$$\begin{aligned} \dot{\lambda_1} &= -(-\lambda_1\sigma' + \lambda_2\mu')x_2/x_4 \\ \dot{\lambda_2} &= -(-\lambda_1\sigma + \lambda_2\mu) \\ \dot{\lambda_4} &= (-\lambda_1\sigma' + \lambda_2\mu')x_1x_2/x_4^2 \end{aligned}$$

with

$$\begin{aligned} \lambda_1(t_f) &= 0 \\ \lambda_2(t_f) &= -1 \end{aligned} \tag{3.19}$$

An extremal control is then given by (3.15). On a *singular* interval, the conditions (3.17) must be satisfied :

$$\phi = 0 \;:\; -\lambda_1\sigma + \lambda_2\mu = 0 \tag{3.20}$$

$$\psi = 0 \;:\; C_{s,in}\lambda_1 + \lambda_4 = 0$$

$$\frac{d\psi}{dt} = 0 \;:\; (-\lambda_1\sigma' + \lambda_2\mu')(\frac{x_1}{x_4} - C_{s,in})\frac{x_2}{x_4} = 0$$

Clearly, $x_1/x_4 \equiv C_s$ can not be equal to $C_{s,in}$, while $x_2/x_4 \equiv C_x > 0$. The last condition is thus equivalent to :

$$-\lambda_1\sigma' + \lambda_2\mu' = 0 \tag{3.21}$$

Substituting these relations in the costate differential equations, we conclude that *on a singular interval the costate remains constant.*

After all substrate available α (3.10) has been added, the process continues in *batch* mode [$u(t) = 0$] consuming the remaining amount of substrate in the fermentor. During this phase, we have :

$$\mathcal{H} \equiv \phi = 0$$

Evaluation of this expression at $t = t_f$ using the costate boundary conditions (3.19) and relation (1.4) leads to :

$$\mu(C_s(t_f)) \equiv \mu_{substr}(C_s(t_f)) - Y_{x/s}f_m m = 0$$

which determines the final substrate concentration $C_s(t_f)$ and the final time t_f. In other words, the fermentation is stopped when the *net biomass growth rate equals zero*, as could be expected. In case of a *maintenance* metabolism (endogenous fraction $f_m = 0$), this means for most expressions reported for the specific substrate to biomass conversion rate :

$$C_s(t_f) = 0$$

Suppose now that if a singular arc occurs, it immediately precedes the terminating batch phase. Another result is then that the second costate variable λ_2 remains constant from the beginning of the singular interval on : $\lambda_2 = \lambda_2(t_f) = -1$. As a result, on the singular arc the linear homogeneous system (3.20) and (3.21) has a nontrivial solution $\boldsymbol{\lambda}$. Therefore, it is necessary and sufficient that

$$\sigma'\mu - \sigma\mu' = 0 \quad \text{or} \quad \frac{d}{dC_s}(\frac{\mu}{\sigma}) = 0$$

In the case of a constant yield coefficient $Y_{x/s}$ this is equivalent to :

$$\frac{d\mu}{dC_s} = 0 \tag{3.22}$$

which means that *on the singular arc the feed rate keeps the substrate concentration at the value at which the specific growth rate μ is maximum.* The corresponding singular control follows from the evaluation of $d^2\psi/dt^2 = 0$:

$$u_{sing} = \frac{\sigma X}{C_{s,in} - C_s} \tag{3.23}$$

which keeps indeed the substrate concentration constant. Note that *equation (3.22) is a necessary condition for the existence of a singular interval.* We can distinguish between the following two cases.

Case 1 : μ_{substr} monotonic

If the specific substrate to biomass conversion rate μ_{substr} [and thus the specific growth rate μ also due to definition (1.4)] is a monotonically increasing function of the substrate concentration C_s [e.g. a Monod kinetics (1.14)], there is no singular control interval.

- If there is an upper boundary U_{MAX} on the feed rate u, the optimal control is of *bang-bang* type :

$$u^*(t) = \begin{cases} U_{MAX} & \text{for} \quad 0 < t < t_1 \\ 0 & \text{for} \quad t_1 \leq t < t_f \end{cases}$$

where the switching time t_1 follows from constraint (3.10) or equivalently (3.11) :

$$t_1 = \frac{V_f - V_0}{U_{MAX}}$$

This can be explained as follows. The final biomass amount will be maximized if the specific growth rate μ is maximized. To do so, the feed rate must increase the substrate concentration C_s as much as possible.

- If there is no upper boundary on the feed rate u and the initial substrate concentration $C_s(0)$ is free, then all substrate available α (3.10) should be added at time $t = 0$ (thus $V_0 = V_f$), whereafter the process is operated in *batch* mode. Clearly, this ensures the highest possible substrate concentration during fermentation.
This solution can also be seen as a limiting case of the bounded input solution with the upper boundary on the feeding pump capacity going to infinity :

$$U_{MAX} \to \infty \quad \Rightarrow \quad t_1 \to 0$$

In the limit, t_1 goes to zero while the input becomes a *Dirac* impulse at $t = 0+$ satisfying

$$t_1 \times U_{MAX} = V_f - V_0$$

Obviously, this impulse can be replaced by an equivalent initial substrate amount $x_1(0)$.

- Another interpretation in view of condition (3.22) can be given as follows. In general, a monotonically increasing specific growth rate reaches an asymptote for substrate concentration going to infinity. In other words, necessary condition (3.22) is satisfied for $C_s \to \infty$: the optimal substrate concentration along a singular arc is $C_s \to \infty$. Obviously, in practice this optimal situation can only be approximated. In case of a bounded input, the interval $[0, t_1]$ can thus be considered as a *degenerate* singular arc. In case of an unbounded input, C_s is maximized using a Dirac impulse, the singular 'arc' becoming infinitesimally small.

Case 2 : μ_{substr} non-monotonic

As a generic case, the specific substrate to biomass conversion rate [and thus the specific growth rate due to definition (1.4)] exhibits a maximum due to effects such as glucose effect, inhibition, and catabolite repression as described earlier. An example is the Haldane kinetics (1.17). Then we know from the above analysis that on the singular arc the substrate concentration C_s remains constant at the value C_s^* which maximizes the specific growth rate μ.

The optimal control sequence then depends on the initial substrate concentration $C_s(0) = x_1(0)/x_4(0)$.

- $C_s(0) < C_s^*$. In this case, the substrate concentration is brought to the singular arc using the maximum value of the feed rate. If C_s reaches C_s^*, singular control (3.23) takes over at $t = t_1$. When all substrate available α (3.10) is added at time $t = t_2$, the process continues in batch until the net biomass growth rate equals zero at time $t = t_f$. Therefore :

$$u^*(t) = \begin{cases} U_{MAX} & \text{for} \quad 0 \leq t < t_1 \\ u_{sing} & \text{for} \quad t_1 \leq t < t_2 \\ 0 & \text{for} \quad t_2 \leq t \leq t_f \end{cases}$$

- $C_s(0) > C_s^*$. Obviously, the substrate concentration must be brought to the singular arc using an initial batch phase $[0, t_1]$. The process then continues as in the previous case.
- $C_s(0) = C_s^*$. Clearly, as the initial state is already on the singular hyperplane, singular feeding can start from $t = 0$ on. Obviously, this results in the highest possible final biomass amount.

Note that both switching times t_1 and t_2 are known in closed loop as functions of state variables only. The complete optimal solution is in state feedback form, so there is no need for any costate variable at all.

If the initial substrate concentration can be included in the optimization, the optimal value is $C_s(0) = C_s^*$.

REMARKS

1. Observe that the above results can also be applied to fermentation processes in which *the synthesis of a product of interest P is directly associated to biomass growth, i.e.* $\pi = Y_{p/x}\mu$. *P is a so-called primary metabolite.*

2. A detailed numerical analysis shows that the deduced control sequences for this microbial growth process satisfy indeed all necessary conditions for optimality. However, we preferred to justify them here using arguments based on biochemical insight in the process. A similar line of reasoning will be adopted in determining the optimal control sequence for fed–batch fermentation processes characterized by a decoupling between biomass growth and product synthesis. ■

3.5 Optimal control sequence for fed-batch fermentation processes with growth/production decoupling

In this section we consider the determination of the *optimal control sequence* $[U_{MAX}, U_{MIN}, u_{sing}]$ and the corresponding *switching times* for fed–batch bioreactors used for metabolite production.

The solution for fermentation processes with growth associated product formation (*primary metabolites*) has been given in the previous section.

3.5.1 Fermentations with growth/production decoupling

We consider the production of so–called *secondary metabolites*. Secondary metabolites are compounds produced by certain micro–organisms through special enzymatic reactions that apparently have no direct relation to growth of biomass : the enzyme catalyzed production is *not associated* to microbial growth.
As a result, these processes are characterized by a *decoupling* between growth and product formation. The first phase is characterized by rapid cell growth with almost no product synthesis (the *growth phase* or *trophophase*), while during the *production phase* (*idiophase*) the product is formed with only limited growth.

As mentioned in Section 3.1, fed–batch operation mode is most effective in overcoming such effects as substrate inhibition, catabolite repression, and glucose effects.

- From the *mathematical point of view*, this means that fed–batch operation may be superior whenever the specific rates of growth (μ) and/or product formation (π) are *non–monotonic* functions (exhibiting maxima) of the substrate concentration. A straightforward extension of the result of Section 3.4 is that under this condition singular intervals are feasible. As a matter of fact, it is the behavior of the specific substrate to biomass conversion rate μ_{substr} (instead of the specific growth rate μ) which must be taken into account. However, as already indicated in Section 3.4, in most applications these specific rates have similar behavior with respect to substrate concentration C_s independent of the endogenous fractions f_m and f_p [see definition (1.9)].

- From the *biochemical point of view*, since the specific rates μ and π are optimal at different values of the substrate concentration C_s —clearly 'optimal' depends on the performance index under consideration—, this means that growth and production are decoupled.

We can distinguish between the following three cases.

Case 1 : monotonic μ and non–monotonic π

This type is most common, in which the cell growth is not inhibited or repressed and follows a Monod type kinetics while the product formation is inhibited or repressed. Typical examples are production of

amino–acids (see e.g. [Ohno *et al.* 1976]) and production of pharmaceuticals, such as penicillin (see Chapters 4 to 6). The general shape of the specific rates μ_{substr} and π as functions of the limiting substrate concentration C_s is as depicted in Figure 3.2.

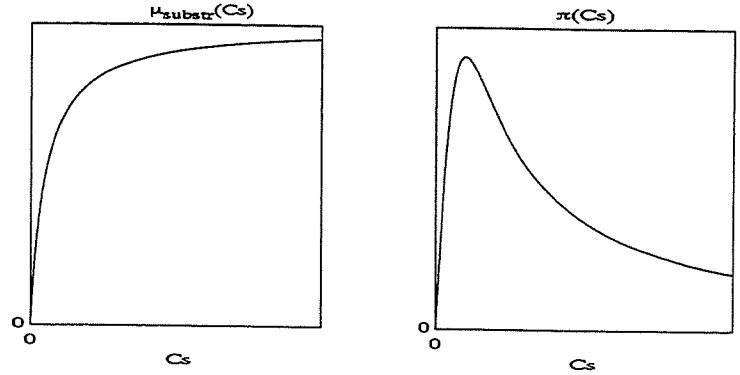

Figure 3.2: Process with monotonic μ_{substr} and non–monotonic π

Case 2 : non–monotonic μ and monotonic π

This type is less common. Examples reported in the literature include glutamic acid fermentation on ethanol (see [Kishimoto *et al.* 1981a and b]) and vitamin B_{12} fermentation (see [Yamane *et al.* 1976]). The specific rates μ_{substr} and π behave as in Figure 3.3.

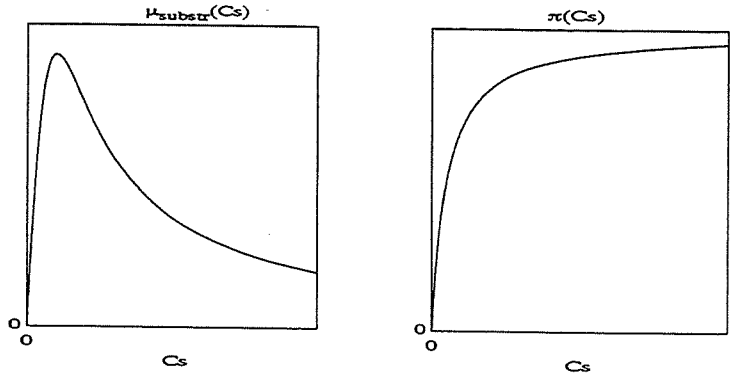

Figure 3.3: Process with non–monotonic μ_{substr} and monotonic π

Case 3 : non–monotonic μ and non–monotonic π

In this least common case, both μ_{substr} and π are Haldane type kinetics as shown in Figure 3.4. An example reported by Jain *et al.* [1985] is ethanol fermentation from fructose. Observe that a further distinction can be made according to the relative position of the maxima of μ_{substr} and π.

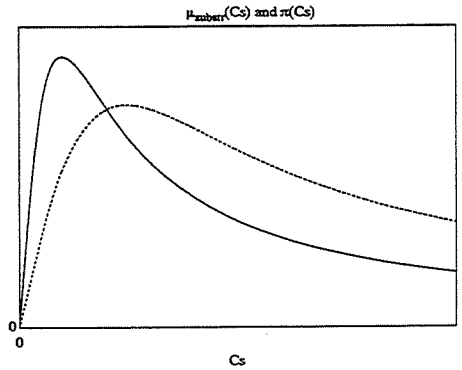

Figure 3.4: Process with non–monotonic μ_{substr} and non–monotonic π

At this point, we allow the specific rates to be functions of other component concentrations as well. In the following we focus on fermentation processes of the first type, i.e. *monotonic* μ and *non–monotonic* π. This case includes the penicillin G fermentation process which is the subject of Chapters 4 to 6. The optimal sequence for the two other types can be determined using a similar line of reasoning as presented for the first type.

3.5.2 Optimal control sequence for monotonic μ and non-monotonic π

In determining the optimal control sequence $[U_{MAX}, U_{MIN}, u_{sing}]$ the decoupling between growth and production is a quite useful feature. Initial work along the same lines has been reported by Modak *et al.* [1986] and Lim *et al.* [1986]. The computational algorithms presented here are at the basis of the development of suboptimal, but easier to implement *heuristic* control strategies (see Section 3.7).

As already mentioned in Section 3.4, the derivation of extremal control sequences can always be done without using *a priori* biochemical knowledge

concerning the process, i.e. by only using the necessary conditions for optimality. More specifically, equations (3.15) and (3.16) in principle fully specify the optimal control profile. However, a complete verification of all necessary conditions for optimality is in general a very tedious job, which provides little additional insight useful in designing suboptimal controllers. Therefore, we limit the numerical analysis of an extremal solution to one particular case : optimization of final product amount with unbounded substrate feed rate and free initial substrate concentration (see Section 3.5.4). In the following, we will exploit the available biochemical knowledge —more specifically, the experimentally observed biphasic behavior— in order to deduce extremal solutions as fast as possible.

At this point, it is very helpful to interpret the differential equation for product formation [see model equations (3.1)] within the concept of a biphasic fermentation process :

$$\frac{dP}{dt} = \pi X - k_h P \tag{3.24}$$

Clearly, product synthesis is a result of two effects : (i) formation of biomass X (during a first *growth* phase), and (ii) product formation (during a second *production* phase) with specific rate π. A performance index of type (3.8) or (3.9) can then be optimized as follows.

1. During a first *growth* phase, we want to produce as much as possible biomass X. From the differential equation for biomass X [model equations (3.1)] we know that growth is governed by the specific growth rate μ. As a result, during the growth phase the feed rate must be determined so as to realize the values for μ as a function of C_s —observe that in general μ may depend on other component concentrations as well— which result in an optimal biomass accumulation.

2. During a second *production* phase, we want the cells to produce the desired product as much as possible. As a result, the feed rate must be used to optimize the specific production rate π.

REMARKS

1. The optimal *switching time* between these phases —given the total amount of substrate available for fermentation α (3.10)— is obviously dictated by a *trade off* between the gain in product P by increasing the biomass X, and the gain in P by optimizing the specific production rate π. This can be readily seen from equation (3.24).

2. Up to this point, the above reasoning is independent of the exact analytical expression of the specific rates μ and π. In fact this scheme holds true for the three types of fermentation processes with decoupling presented in Section 3.5.1. ■

In Section 3.5.2.1, we determine the optimal control sequence in the case of a bounded input u and fixed initial state $\mathbf{x}_0$. The corresponding optimal switching times can then be calculated using the computational algorithm presented in Section 3.5.2.2. In Section 3.5.2.3, we generalize the results obtained to the case of an unbounded input u and free initial substrate concentration $C_s(0)$.

3.5.2.1 Bounded input u and fixed initial state $\mathbf{x}_0$

As a first step, we determine the optimal control sequence in the case of a constraint on the input

$$0 \equiv U_{MIN} \leq u(t) \leq U_{MAX}, \quad U_{MAX} \text{ given}$$

while we consider the complete initial state $\mathbf{x}_0$ as given : $x_1(0)$ is fixed, while $x_4(0)$ follows from relation (3.7). As a result, condition (3.14) is redundant.

As in the example of Section 3.4, the optimal sequence depends on the initial substrate concentration $C_s(0) = x_1(0)/x_4(0)$. Furthermore, we tacitly assume that the initial biomass amount $x_2(0)$ is low. If $x_2(0)$ is high, the growth phase can be skipped, while the feed rate during the production phase can be determined as explained in Section 3.4 in the case of a non–monotonic specific rate. We can distinguish between the following three cases.

Case 1 : Low initial substrate concentration $C_s(0)$

As the specific growth rate μ is monotonically increasing with respect to substrate concentration C_s, it is clear that at time $t = 0$ the control must take on its maximum possible value $u(t) = U_{MAX}$ to realize the maximum possible biomass accumulation (see also Section 3.4). At some time instant $t = t_1$, the control is set equal to its minimum value $u(t) = 0$, until the production phase starts at time $t = t_2$. During this batch phase $[t_1, t_2]$, the substrate concentration decreases, until at time $t = t_2$ singular substrate feeding starts using a control law of the form (3.16). This can be motivated as follows. We already mentioned that during the production phase the specific production rate

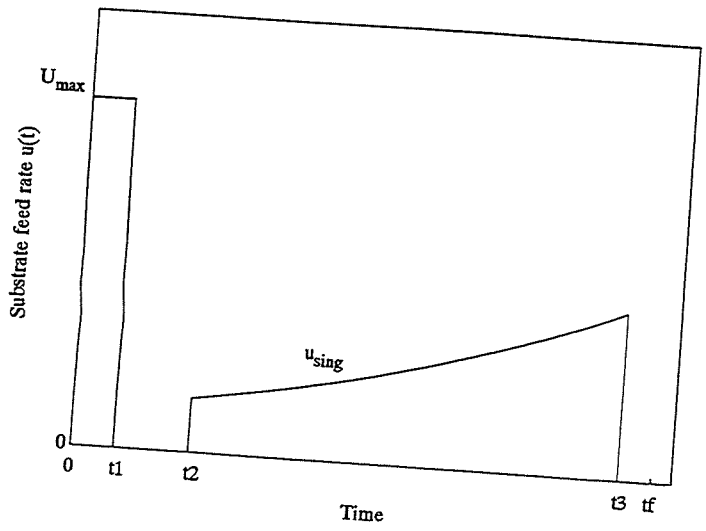

Figure 3.5: General feed rate profile for low initial substrate concentration

π is optimized. We will show that under certain limiting conditions, the substrate concentration during production remains constant at the value C_s^* which maximizes π/σ (see Section 3.6). This is similar to the result of Section 3.4. In cases where these conditions are not satisfied, we can expect that the optimal substrate concentration —although time varying— will be at least in a neighborhood of the value C_s^*. Obviously, the substrate concentration can not be kept in this neighborhood using a simple bang–bang type control, but instead a singular feed rate profile will be required. This singular control is stopped at time $t = t_3$ when all substrate available α (3.10) is used, or equivalently, when the fermentor volume reaches its final level $x_4(t_3) = V_f$ (3.11). As there may be some substrate left in the reactor, the fermentation continues in batch mode $[u(t) = 0]$ until the stopping condition —depending on the performance index under consideration— is met at time $t = t_f$. This substrate feeding scheme has been summarized in Figure 3.5.

Case 2 : High initial substrate concentration $C_s(0)$

If the initial substrate concentration is high enough, the first interval $[0, t_1]$ of feeding at the maximum rate should be omitted. The growth phase is then a complete batch phase, until at time $t = t_2$ the substrate concentration is small enough and the biomass concentration is high enough so that singular feeding can start.

Case 3 : Initial state $\mathbf{x}_0$ on the singular hyperplane

In this case the growth phase can be omitted completely, while singular feeding starts from $t = 0$ on. Clearly, this situation will result in the lowest value of the performance index. However, the comparison with both previous cases is not completely fair, as we start with a biomass concentration high enough to omit the growth phase so that all substrate available can be used for product synthesis. Therefore, in the following this case will not be considered anymore.

REMARKS

1. We can assign the following interpretation to the first switching time t_1. It is a measure for the fraction α_{growth} of the total amount of substrate available α (3.10) which is consumed during the growth phase :

$$\alpha_{growth} \triangleq C_{s,in} \times U_{MAX} \times t_1$$

Note that in general the switching times t_1 and t_2 are *not* known as functions of the state $\mathbf{x}$.

2. In the control sequence as shown in Figure 3.5 we tacitly assumed that the upper bound on the feed rate U_{MAX} is never violated on the singular arc $[t_2, t_3]$. The singular control (3.16) must be set equal to U_{MAX} if this upper bound is reached before all substrate available is added at $t = t_3$. Of course, the optimal switching times t_1 and t_2 will be changed, as compared with the values obtained without taking the upper bound into account.

3. The last batch phase $[t_3, t_f]$ $[u(t) = 0]$ is terminated if some *stopping condition* —depending on the performance index under consideration— is satisfied.

We already know from Section 3.3.1 that the Hamiltonian $\mathcal{H}$ (3.12) remains constant along an extremal trajectory. Using the transversality condition of Section 1.2.3 we have :

$$\forall t \in [0, t_f] \ :$$

$$\mathcal{H}[\mathbf{x}(t), \boldsymbol{\lambda}(t), u(t), t] = \mathcal{H}^* \equiv \phi + \psi u = -\frac{\partial g}{\partial t}[\mathbf{x}(t_f), t_f]$$

with $\mathcal{H}^*$ a constant and

$$\phi = (-\lambda_1 \sigma + \lambda_2 \mu + \lambda_3 \pi) x_2 - \lambda_3 k_h x_3$$

Using

$$\lambda_i(t_f) = \frac{\partial g}{\partial x_i}[\mathbf{x}(t_f), t_f]$$

evaluation of the above expression at $t = t_f$ for a performance index of the form (3.8) leads to :

$$\gamma_x \frac{dX}{dt}(t_f) + \gamma_p \frac{dP}{dt}(t_f) = \gamma_t$$

This can be interpreted as follows. The fermentation is stopped when *the average gain of producing an additional unit of biomass and product (i.e. weighted by their unit prices) has become equal to the unit operational cost.*
As a special case, if we want to optimize the final product amount $P(t_f)$ (so $\gamma_x = \gamma_t = 0$), then the fermentation is stopped if :

$$\frac{dP}{dt}(t_f) = 0$$

as could be expected.
If the performance index is of the form (3.9), the process is stopped if :

$$\gamma_x \frac{dX}{dt}(t_f) + \gamma_p \frac{dP}{dt}(t_f) = \frac{\gamma_x X(t_f) + \gamma_p P(t_f)}{t_f}$$

which means that the fermentation is stopped when *the average gain of producing an additional unit of biomass and product has become equal to the average productivity* $\mathcal{P}$. ■

3.5.2.2 Computational algorithm

Once the optimal control sequence has been determined, the corresponding optimal switching times can be obtained using the following straightforward computational algorithm. We consider the generic case shown in Figure 3.5.

Algorithm

Step 1 : Make a guess of t_1, or equivalently, determine the amount of substrate α_{growth} consumed during the growth phase. Integrate the state equations (3.4) from $t = 0$ to $t = t_1$ with $u(t) = U_{MAX}$.

Step 2 : Make a guess of t_2. Integrate the state equations (3.4) from $t = t_1$ to $t = t_2$ with $u(t) = 0$. This completes the *growth* phase.

Step 3 : Integrate the state equations (3.4) using the above determined singular control (3.16) until all substrate available α (3.10) is added, or equivalently, until the bioreactor is completely filled (3.11) at $t = t_3$.

Step 4 : Complete the integration with $u(t) = 0$ until the stopping condition —depending on the cost index— is satisfied at time $t = t_f$. This completes the *production* phase. Store the value of the cost index $J[u, \mathbf{x}_0]$ (3.8) or (3.9).

Step 5 : Repeat Steps 2 to 4, considering $t_{2,new} = t_{2,old} \pm \delta t$, with δt as small as required. Save the time t_2 at which the cost index $J[u, \mathbf{x}_0]$ (3.8) or (3.9) reaches its minimum.

Step 6 : Repeat Steps 1 to 5 with a new guess of t_1 in order to minimize $J[u, \mathbf{x}_0]$.

REMARKS

1. Obviously, the optimal solution of the two point boundary value problem is obtained using a *straightforward* computational algorithm. Due to the incorporation of all a priori knowledge available, there is no need for an integration backwards in time, as required in e.g. gradient type methods for solving optimal control problems (e.g. [Kirk 1970]).

2. An initial guess of the switching times t_1 and t_2 can be obtained as follows. For t_1, an upper boundary is of course

$$t_1 \leq \frac{V_f - V_0}{U_{MAX}}$$

This condition is very conservative, but in fact the starting value for t_1 is much less crucial than the corresponding starting value for t_2. If e.g. t_2 is chosen too large, the substrate concentration may become so small that the singular control is unable to bring it back within the region which is optimal for production. As we will show in Section 3.6, under certain limiting conditions the switching time t_2 can be obtained as a function of state variables. In a general case, a good initial guess is therefore the time t_2 at which the substrate concentration $C_s(t_2)$ maximizes either the specific production rate π or the ratio π/σ. Note that in general the specific rates may depend on other component concentrations as well.

3. Calculation of the singular control (3.16) as required in Step 3 in general needs a complete knowledge of both the state $\mathbf{x}$ and the costate $\boldsymbol{\lambda}$. As already noted, λ_4 is not required since in the fourth state equation $f_4 \equiv 0$. Furthermore, we can make use of equations (3.18), which define λ_1 and λ_2 in function of λ_3 and $\mathcal{H}^*$. We can distinguish between the following two cases.

   - *The performance index is independent of final time t_f.*
     Then we know that $\mathcal{H}^* = 0$ along an extremal trajectory so that (3.18) specifies two costates in function of the third one. Since both the numerator and the denominator of the singular control law (3.16) are linear in the costate $\boldsymbol{\lambda}$, the costate cancels out and the singular control is a *nonlinear feedback law of state variables only*. An example is a performance index of the form (3.8) with $\gamma_t = 0$.
   - *The performance index depends on final time t_f.*
     If the performance index has the form (3.8) we know that $\mathcal{H}^* = -\gamma_t$ which is known. The third costate equation in (3.13) can be solved using $\lambda_3(t_f) = -\gamma_p$:

$$\lambda_3(t) = -\gamma_p \exp[k_h(t - t_f)]$$

     which we can use in equations (3.18). As a result, all costates are known up to the unknown final time t_f. In other words, the singular feed rate is a *nonlinear feedback law of the state and the final time*. The above algorithm is then modified as follows. For each couple of switching times (t_1, t_2), the final time t_f must be determined iteratively in order to obtain agreement between the estimated and calculated value.

     If on the other hand the performance index has the form (3.9), we have :

$$\mathcal{H}^* = -\frac{\gamma_x X(t_f) + \gamma_p P(t_f)}{t_f^2}$$

     Solving the third costate equation using boundary condition $\lambda_3(t_f) = -\gamma_p/t_f$ leads to :

$$\lambda_3(t) = -\frac{\gamma_p}{t_f} \exp[k_h(t - t_f)]$$

     Both expressions are used in equations (3.18) to obtain all costates in function of the unknowns t_f and $\mathcal{H}^*$, or equivalently t_f, $X(t_f)$ and $P(t_f)$. As a result, the singular feed rate is a *nonlinear feedback law of the state and the unknowns t_f, $X(t_f)$ and $P(t_f)$*. Again, for each couple of switching times (t_1, t_2) these unknowns must be determined iteratively.

   In summary, in all cases the complete optimal control can be calculated *without an explicit need for any costate variable.*

4. The algorithm proposed by Lim *et al.* [1986] makes explicitly use of the costates. During singular control $[t_2, t_3]$ some costate equations must be integrated together with the state equations, while during the terminating batch phase $[t_3, t_f]$ all costate equations must be integrated. Furthermore, at the switching time t_2 an initial guess for some costate variables is required. We believe that our algorithm represents a significant improvement for the following reasons.

   - First, it is well–known (see e.g. [Kirk 1970]) that integrating the costate equations (3.13) in the forward direction of time t can give rise to (numerical) instabilities. From this point of view, our algorithm is numerically very reliable since it does not use any costate variable at all. An example will be given in Section 4.3.
   - Second, in the algorithm of Lim *et al.* some costates must be guessed at the beginning of the singular arc. Obviously, since

we cannot assign a clear physical interpretation to the costate variables of this problem, it may be very difficult to obtain a good initial guess. In our algorithm, we sometimes need an initial guess for quantities with a clear physical interpretation such as final time t_f and final product amount $P(t_f)$. As a result, good starting values can be obtained e.g. from knowledge about the process before optimization.

■

In summary, this algorithm reduces to a *two dimensional optimization problem of switching times* t_1 *and* t_2.

3.5.2.3 Unbounded input u and free initial substrate concentration

Following a similar way of reasoning as presented in Section 3.4, the case of an unbounded input $u(t)$ can be seen as a limiting case of the previous bounded input problem with $U_{MAX} \to \infty$.

The only place where the upper limit U_{MAX} is active is during the time interval $[0, t_1]$ (see Figure 3.5). Suppose now that the value of U_{MAX} becomes larger by installing more or larger feeding pumps. As a consequence, the value of t_1 will decrease. In the limit, when $U_{MAX} \to \infty$, $t_1 \to 0$, and the control during the interval $[0, t_1]$ becomes a *Dirac* impulse at time $t = 0+$ satisfying

$$t_1 \times U_{MAX} = \frac{\alpha_{growth}}{C_{s,in}}$$

Obviously, this impulse can be replaced by an equivalent set of *initial conditions* with the same effects on future time histories of all states :

$$\begin{cases} x_1(0) \equiv \alpha_{growth} \text{ which will be optimized} \\ x_4(0) = V_* + x_1(0)/C_{s,in} \end{cases}$$

where the last equation is constraint (3.7). In other words, omitting the upper bound on the input leads to the injection of all substrate consumed during growth at the beginning of the fermentation, the growth phase becoming a *batch* phase. Of course, if the initial substrate concentration is free, this is the way to achieve the maximum amount of biomass X with a given amount of substrate α_{growth}, as C_s and thus μ take on their highest possible value for all t during growth.

In the computational algorithm presented for the bounded input problem, the only modification is to replace the optimization of the first switching time t_1 by the optimization of the *equivalent* initial substrate concentration $C_s(0) \equiv x_1(0)/x_4(0)$ under constraint (3.7). In other words, if the input is unbounded and the initial substrate concentration is free, the two point boundary value problem is reduced to the *two dimensional optimization of initial substrate concentration* $C_s(0)$ *and switching time* t_2.

Obviously, this represents also the optimal control sequence in case of a *bounded input with free initial substrate concentration.*

3.5.3 Optimal control sequence with state inequality constraints

3.5.3.1 Substrate concentration constraint $C_s(t) \leq C_{s,MAX}$

In many practical applications, too high values for the substrate concentration C_s can lead to a lot of undesired effects, such as a *solubility* problem, an *inhibition* problem, *unproductive side–reactions*, ... This suggests the introduction of an upper limit on the substrate concentration during process optimization :

$$\forall t \in [0, t_f] \; : \quad C_s(t) \leq C_{s,MAX}$$

Needless to say that for the type of fermentations under consideration, this constraint can only be violated during the growth phase.

As a general result, if C_s reaches its upper limit $C_{s,MAX}$, we use a control of the form (provided $C_{s,in} > C_{s,MAX}$)

$$u_{C_s}(t) = \frac{\sigma X}{C_{s,in} - C_s} \tag{3.25}$$

which keeps C_s constant at its upper bound $C_s = C_{s,MAX}$ [see model equations (3.2)].

As an example, consider the case of a free initial substrate concentration $C_s(0)$. If the optimization as described above results in an optimal initial concentration higher than the upper boundary $C_{s,MAX}$, the control sequence must be modified as follows. The best we can do in order to ensure the highest possible growth rate without violating the constraint is to start with $C_s(0) = C_{s,MAX}$. The initial conditions are then, using (3.7) :

$$x_1(0) = \frac{C_{s,in}C_{s,MAX}V_*}{C_{s,in} - C_{s,MAX}}$$
$$x_4(0) = \frac{x_1(0)}{C_{s,MAX}}$$

We then apply a control of the form (3.25) which keeps the substrate concentration level constant. This control is shut off when all substrate for growth α_{growth} has been added at time $t = t_1$, whereafter the fermentation continues as described higher. If the input is bounded and the control resulting from expression (3.25) should exceed the upper limit U_{MAX} before $t = t_1$, obviously the control must be set equal to $u(t) = U_{MAX}$ until $t = t_1$, resulting in a substrate concentration decrease.

3.5.3.2 Biomass concentration constraint $C_x(t) \leq C_{x,MAX}$

Under certain conditions the optimal control sequence as described here may result in high biomass concentrations in the bioreactor. Some examples will be shown in the next chapters. However, it is well known that the volumetric mass transfer coefficient in e.g. penicillin fermentations drops by as much as a factor of 10 with biomass concentrations in the region of 20 g dry weight/L (see e.g. [Deindoerfer and Gaden 1953]). As a result, for a given mounted power, the oxygen transfer capacity of the fermentor will drop substantially as the biomass builds up. Hence, very often these fermentations can be continued only to a limit dictated by the oxygen transfer capacity. The correct way to include the oxygen limitation would be to incorporate additional terms into the model equations (3.1) or (3.2), and to take an oxygen balance around the fermentor. An example for the penicillin fermentation process can be found in [Bajpai and Reuß 1980].

However, since at present accurate oxygen limitation kinetics models are not available, we impose an upper limit $C_{x,MAX}$ on the biomass concentration C_x in order to get an idea about the productivities in fermentors with limited oxygen transfer capacity :

$$\forall t \in [0, t_f] \; : \quad C_x(t) \leq C_{x,MAX}$$

To cope with this inequality constraint, we could at first sight adopt a similar line of reasoning as presented for bounded substrate concentration. From model equations (3.2) we can easily deduce the control law which keeps biomass concentration C_x constant :

$$u_{C_x}(t) = \mu V \tag{3.26}$$

However, we now show that *the optimal control sequence under biomass concentration limitation is characterized by a biomass concentration profile C_x which is tangent to the upper bound $C_{x,MAX}$ at at most one time instant.* In other words, $C_x = C_{x,MAX}$ for at most one value of time t. As an example, consider again the case of a free initial substrate concentration $C_s(0)$. For another case a similar argumentation can be given. From Section 3.5.2, the optimal control sequence can be summarized as : (i) high initial substrate concentration, (ii) batch growth phase, (iii) singular production phase, and (iv) batch terminating phase. Suppose that, without taking the biomass inequality constraint into account, this sequence is characterized by the optimal couple $(C_s^*(0), t_2^*)$. We can distinguish between the following four cases.

Case 1 : The constraint is not violated

Clearly, in this case the optimal control sequence characterized by $(C_s^*(0), t_2^*)$ remains optimal under biomass limitation.

Case 2 : The constraint is violated during the batch growth phase

As a result, for some value of t within the interval $[0, t_2]$ the control must switch from zero to a positive value given by (3.26). The differential equation for the substrate concentration then reduces to [see model equations (3.2)] :

$$\frac{dC_s}{dt} = -\sigma C_{x,MAX} + (C_{s,in} - C_s)\mu$$

Depending on the specific rates, the substrate concentration C_s will decrease at a lower rate or may even start increasing. As a result, the singular conditions will either be reached only at some time $t_2 > t_2^*$, or will never be reached at all. More substrate will be added during the growth phase, in the first place to keep C_x constant due to dilution, which is then lost for the production phase, resulting in a higher value of the performance index to be minimized.

Case 3 : The constraint is violated during the singular production phase

During the production phase, a singular control of the form (3.16) keeps the substrate concentration within the region of optimal productivity. If the biomass concentration is decreasing, there is no problem. If however the biomass increases, then the upper bound may be violated. At this time the feed rate should switch from the singular control to the control (3.26). In general, the input (3.26) required to keep biomass concentration constant is larger than the singular control (3.16). As an example, if the product decay rate k_h equals zero and the specific rates are functions of the substrate concentration C_s only, then we will show (see Theorems 3.1 and 3.2) that during singular control C_s remains constant at the value C_s^* which maximizes π/σ. The singular control is then of the form

$$u_{sing}(t) = \frac{\sigma X}{C_{s,in} - C_s} \equiv \frac{\sigma C_x}{C_{s,in} - C_s} V$$

In general, we have

$$\frac{\sigma(C_s^*) C_{x,MAX}}{C_{s,in} - C_s^*} < \mu(C_s^*)$$

As a result, the substrate concentration will move away from the singular hyperplane, resulting in a decreasing performance.

Case 4 : The constraint is violated during the terminating batch phase

Obviously, this situation must be avoided also since there is no substrate available anymore to dilute the liquid phase.

From this more or less intuitive discussion, we can deduce the following procedure to obtain the optimal sequence under biomass limitation.

- First, we determine the optimal couple $(C_s^*(0), t_2^*)$ without taking the biomass constraint into account.
- Second, we verify if the constraint is violated for some value of t. If so, the optimal substrate concentration $C_s^*(0)$ must be decreased to such a level that the resulting biomass concentration profile and the constraint are tangent to each other for at most one value of t, or :

$$\exists!\ \hat{t} \in [0, t_f] \ : C_x(\hat{t}) = C_{x,MAX}$$

Then the control (3.26) will never become active. Of course, the corresponding optimal switching time t_2^* will decrease accordingly.

Some examples involving state inequality constraints will be given in Section 4.3.

3.5.4 Verification of all necessary conditions for optimality

As already mentioned, we limit ourselves to a verification of all necessary conditions for optimality as stated in Section 3.3 for a problem with unbounded input u and free initial substrate concentration $C_s(0)$, without state inequality constraints. Furthermore, we assume that the performance index is of the form (3.8) with $\gamma_t = 0$, i.e. independent of final time t_f.

As described in Section 3.5.2, the optimal control sequence consists of : (i) high initial substrate concentration, (ii) batch growth phase, (iii) singular production phase, and (iv) batch terminating phase. It can be characterized by the optimal couple $(C_s^*(0), t_2^*)$ in a unique way. Clearly, the control is either zero or singular.

As the computational algorithm presented in Section 3.5.2 does not make use of the costate variables $\boldsymbol{\lambda}$, the following necessary conditions remain to be verified along the trajectory generated by $(C_s^*(0), t_2^*)$.

1. At $t = t_f$, $\boldsymbol{\lambda}$ must satisfy the boundary conditions :

$$\begin{pmatrix} \lambda_1(t_f) \\ \lambda_2(t_f) \\ \lambda_3(t_f) \end{pmatrix} = \begin{pmatrix} 0 \\ -\gamma_x \\ -\gamma_p \end{pmatrix}$$

2. The Hamiltonian $\mathcal{H}$ (3.12) must be equal to zero along the whole trajectory, or in other words :

$$\begin{array}{rcll} \phi & = & 0 & \forall t \\ \psi & = & 0 & \text{on the singular interval} \\ \psi & > & 0 & \forall t \text{ satisfying } u(t) = 0 \end{array}$$

These conditions can be verified efficiently as follows.

1. As a simulation result we obtain t_3^* and t_f^* together with $\mathbf{x}(t_2^*)$, $\mathbf{x}(t_3^*)$ and $\mathbf{x}(t_f^*)$.
2. $\boldsymbol{\lambda}(t_3^*)$ is obtained as follows. At $t = t_3^*$, the control switches from $u(t_3^*-) = u_{sing}$ to $u(t_3^*+) = 0$. This causes a jump in $\dot{\mathbf{x}}(t_3^*)$, but all

states and costates remain continuous. Therefore, we can approach t_3^* from the left and calculate all costates from the singular conditions.

- Solving the third costate equation in (3.13) using the boundary condition leads to :

$$\lambda_3(t) = -\gamma_p \exp[k_h(t - t_f^*)] \tag{3.27}$$

so $\lambda_3(t_3^*)$ can be calculated.

- $\lambda_1(t_3^*)$, $\lambda_2(t_3^*)$ and $\lambda_4(t_3^*)$ are then calculated using relations (3.18).

3. Integrate the state equations (3.4) together with the costate equations (3.13) [using (3.27)] from $t = t_3^*$ to $t = t_f^*$ using $u(t) = 0$. Verify if $\phi(t) = 0$ and $\psi(t) > 0$. Verify also the terminal conditions on the costate. Observe that, as already mentioned, this integration of the costate equations forwards in time may cause numerical difficulties. For this reason, we propose this only as a possible verification, not as a way to actually compute extremal solutions.

4. Along the singular interval $[t_2^*, t_3^*]$ we calculated the complete costate out of $\phi = 0$ and $\psi = 0$, so $\mathcal{H} = 0$ by definition. We obtain the costate at $t = t_2^*$ in the same way as at $t = t_3^*$.

5. Integrate the state equations (3.4) together with the costate equations (3.13) [using (3.27)] backwards in time from $t = t_2^*$ to $t = 0$ using $u(t) = 0$. Verify if $\phi(t) = 0$ and $\psi(t) > 0$. Verify also all conditions at $t = 0$, more specifically $\psi(0) = 0$ (3.14). In practice, the last condition proved to be rather insensitive to variations in $C_s(0)$ and t_2 around the extremal values. Therefore, we only use it for verifying and not for detecting an extremal solution.

Note that this procedure can be seen as a test on the accuracy of t_2^* corresponding to $C_s^*(0)$.

Of course, we have tacitly assumed that the previously determined *control sequence batch–singular–batch* is the only extremal one, i.e. the only one for which all necessary conditions are satisfied. In fact, it can be easily checked (using e.g. simulations) that for the given problem this sequence is indeed the only feasible one : an interruption of e.g. the singular phase to include an additional batch phase will always result in lower performance. In addition, a detailed numerical analysis of any other control sequence will show that it does not satisfy all necessary conditions.

Therefore, we conclude that the determined extremal control $u^*(t)$ characterized by $(C_s^*(0), t_2^*)$ is an optimal control minimizing the performance measure $J[u, \mathbf{x}_0]$ at least locally.

If we consider now a *fixed* initial condition $C_s(0)$ —so condition (3.14) is redundant— in a neighborhood of $C_s^*(0)$ and determine the corresponding switching time t_2, then clearly $(C_s(0), t_2)$ characterizes the unique optimal solution. If however $C_s(0)$ is *free*, we have to investigate the behavior of the performance index $J[u, \mathbf{x}_0]$ with respect to $C_s(0)$. We will illustrate with some examples in Chapter 4 that for this type of fermentation $J[u, \mathbf{x}_0]$ behaves in a first approximation as a quadratic function over the whole admissible range of initial substrate concentrations. The optimal value can be detected by e.g. a simple linear search method for $C_s(0)$. As a result, $(C_s^*(0), t_2^*)$ determines the *unique optimal control minimizing the performance index globally.*

3.6 Physical interpretation of singular control

In this section we analyze in detail the singular arc occurring during the production phase. The results, which have a clear physical interpretation, will prove very useful in deducing suboptimal control profiles in Section 3.7.

3.6.1 The generic case : maintenance coefficient $m > 0$

Consider a fed–batch fermentation process described by model equations (3.4)

$$\frac{d\mathbf{x}}{dt} = \mathbf{f}(\mathbf{x}) + \mathbf{b}\, u$$

with $\mathbf{x}$, $\mathbf{f}$ and $\mathbf{b}$ as defined higher.
Consider first the following performance index :

$$J[u] = g[\mathbf{x}(t_f)] = -P(t_f) \tag{3.28}$$

which is of the form (3.8) with $\gamma_x = 0$ and $\gamma_t = 0$, i.e. maximization of the final product amount. The total amount of substrate α (and thus the final volume) is fixed (3.10), while the final time t_f and the initial substrate concentration $C_s(0)$ are *free*.

We now prove the following Theorem, inspired by a less general result reported in [Modak *et al.* 1986]. Furthermore, the proof we present here is more rigorous.

Theorem 3.1

Consider the minimization of performance index (3.28) subject to the dynamic constraint (3.4). Suppose that

1. *σ, μ and π are functions of the substrate concentration C_s only, with continuous derivatives up to second order,*
2. *the maintenance coefficient m is strictly positive.*

Then during singular control

1. *the substrate concentration C_s remains constant if and only if the specific product decay rate $k_h = 0$,*
2. *in which case this constant value maximizes the yield π/σ.*

PROOF

In the following, a prime denotes derivation with respect to substrate concentration C_s. The Hamiltonian $\mathcal{H}$ is given by (3.12) :

$$\mathcal{H} \equiv \phi + \psi u = 0 \tag{3.29}$$

where

$$\phi = (-\lambda_1\sigma + \lambda_2\mu + \lambda_3\pi)x_2 - \lambda_3 k_h x_3$$

and

$$\psi = C_{s,in}\lambda_1 + \lambda_4$$

The adjoint equations can be written as follows :

$$\begin{aligned}
\dot{\lambda}_1 &= (\lambda_1\sigma' - \lambda_2\mu' - \lambda_3\pi')x_2/x_4 \\
\dot{\lambda}_2 &= \lambda_1\sigma - \lambda_2\mu - \lambda_3\pi = -(\phi + \lambda_3 k_h x_3)/x_2 \\
\dot{\lambda}_3 &= \lambda_3 k_h \\
\dot{\lambda}_4 &= -(\lambda_1\sigma' - \lambda_2\mu' - \lambda_3\pi')x_1 x_2/x_4^2
\end{aligned}$$

with boundary conditions (see Section 1.2.3)

$$\boldsymbol{\lambda}(t_f) \equiv \frac{\partial g}{\partial \mathbf{x}}[\mathbf{x}(t_f)] = \begin{pmatrix} 0 \\ 0 \\ -1 \\ - \end{pmatrix} \tag{3.30}$$

On the singular interval, we know that $\phi = 0$, $\psi = 0$ and $\dot{\psi} = 0$:

$$\begin{aligned}
-\lambda_1\sigma + \lambda_2\mu + \lambda_3\pi &= \lambda_3 k_h x_3/x_2 \\
C_{s,in}\lambda_1 + \lambda_4 &= 0 \\
(\lambda_1\sigma' - \lambda_2\mu' - \lambda_3\pi')(C_{s,in} - \frac{x_1}{x_4}) &= 0
\end{aligned} \tag{3.31}$$

The case $x_1/x_4 \equiv C_s = C_{s,in}$ can be excluded as C_s is then unrealistic high during production. So the last equation is equivalent to :

$$\lambda_1\sigma' - \lambda_2\mu' - \lambda_3\pi' = 0 \tag{3.32}$$

Substituting these relations into the adjoint differential equations, we find (with C_i, $i = 1$ & 4, a *constant*) :

$$\begin{aligned}
\lambda_1 &= C_1 \\
\dot{\lambda}_2 &= -\lambda_3 k_h x_3/x_2 = -\dot{\lambda}_3 x_3/x_2 \\
\lambda_3 &= -e^{k_h(t-t_f)} \\
\lambda_4 &= C_4
\end{aligned} \tag{3.33}$$

Observe that the differential equation for λ_3 has been solved using the boundary condition $\lambda_3(t_f) = -1$ (3.30). If the initial substrate concentration $C_s(0)$ is free, then we know from the optimal control sequence that the product $\psi(t)u(t) = 0$ for all t. It follows from (3.29) that $\phi = 0$ for all t, so equation (3.33) holds for all t, with boundary condition $\lambda_2(t_f) = 0$ due to (3.30).

For the complete costate to be constant on the singular interval, obviously it is *necessary and sufficient that the specific product decay rate $k_h = 0$.*

We now evaluate $d^2\psi/dt^2 = 0$ on the singular interval. We obtain after some calculations :

$$\dot{C}_s = k_h \frac{\lambda_3(\pi' x_2 - \mu' x_3)}{x_2(\lambda_1\sigma'' - \lambda_2\mu'' - \lambda_3\pi'')} \tag{3.34}$$

$$= -\sigma\frac{X}{V} + \frac{u_{sing}}{V}(C_{s,in} - C_s) \tag{3.35}$$

the second equality being due to the system equations (3.4). Let us first verify that the denominator in equation (3.34) is different from zero. We give a demonstration by contradiction. So suppose that:

$$\lambda_1\sigma'' - \lambda_2\mu'' - \lambda_3\pi'' = 0 \tag{3.36}$$

Then together with equations (3.31) and (3.32) we obtain the homogeneous linear system :

$$\begin{pmatrix} -\sigma & \mu & \pi - k_h x_3/x_2 \\ -\sigma' & \mu' & \pi' \\ -\sigma'' & \mu'' & \pi'' \end{pmatrix} \begin{pmatrix} \lambda_1 \\ \lambda_2 \\ \lambda_3 \end{pmatrix} = \begin{pmatrix} 0 \\ 0 \\ 0 \end{pmatrix} \tag{3.37}$$

We know that there exists a nontrivial solution $\boldsymbol{\lambda}(t)$ since at least $\lambda_3(t) \neq 0$. So for assumption (3.36) to be true, a necessary and sufficient condition is that the above system matrix has its determinant equal to zero. We have using (3.3) :

$$\begin{aligned} \mathbf{A} &\triangleq \begin{pmatrix} -\sigma & \mu & \pi - k_h x_3/x_2 \\ -\sigma' & \mu' & \pi' \\ -\sigma'' & \mu'' & \pi'' \end{pmatrix} \\ &= \begin{pmatrix} -\mu/Y_{x/s} - m - \pi/Y_{p/s} & \mu & \pi - k_h x_3/x_2 \\ -\mu'/Y_{x/s} - \pi'/Y_{p/s} & \mu' & \pi' \\ -\mu''/Y_{x/s} - \pi''/Y_{p/s} & \mu'' & \pi'' \end{pmatrix} \end{aligned}$$

Obviously, $\mathbf{A}$ has no zero rows or columns, nor any identical rows or columns. The only possibility for $det(\mathbf{A})$ to be zero is that *both* k_h and m are zero, which is in contradiction with $m > 0$.

From equation (3.34) we conclude now immediately that a *necessary and sufficient condition for C_s to be constant on the singular interval is $k_h = 0$.* Let us determine that constant value. Solving the first two equations of (3.37) for λ_2/λ_3 delivers:

$$\frac{\lambda_2}{\lambda_3} = -\frac{\pi'\sigma - (\pi - k_h x_3/x_2)\sigma'}{\mu'\sigma - \mu\sigma'} \tag{3.38}$$

From $k_h = 0$ it follows that $\lambda_2(t)$ and $\lambda_3(t)$ are constant for all t, so from boundary conditions (3.30) we obtain:

$$\begin{aligned} \lambda_2(t) = \lambda_2(t_f) &= 0 \\ \lambda_3(t) = \lambda_3(t_f) &= -1 \end{aligned}$$

As a consequence, equation (3.38) reduces to:

$$\pi'\sigma - \pi\sigma' = 0$$

or, in other words, the singular control extremizes the *product yield* :

$$\frac{d}{dC_s}\left(\frac{\pi}{\sigma}\right) = 0 \tag{3.39}$$

which completes the proof. ■

REMARKS

1. The specific rates σ, μ and π are required to be *smooth* functions of C_s, in order to ensure the existence and continuity of at least the first two derivatives with respect to C_s, thus enabling the calculation of $u_{sing}(t)$ from equations (3.34) and (3.35). Note that the singular control is *linear* in the specific product decay rate k_h :

$$u_{sing}(t) = \frac{\sigma X}{C_{s,in} - C_s} + k_h \frac{V\lambda_3(\pi' x_2 - \mu' x_3)}{x_2(C_{s,in} - C_s)(\lambda_1\sigma'' - \lambda_2\mu'' - \lambda_3\pi'')} \tag{3.40}$$

2. It follows from the above Theorem that the condition $k_h = 0$ is also *necessary and sufficient to obtain the complete optimal control for any given value of S_0 —or equivalently $C_s(0)$— as a closed loop solution* : clearly the switch from *batch* to *singular* control is then dictated by the condition $C_s = C_s^*$, C_s^* denoting the value of C_s for which π/σ has its optimum.

3. As an example, consider the penicillin G fermentation process which is the subject of the following chapters. For the kinetics σ, μ and π reported in literature for this fermentation, there is only one extremal value for the yield π/σ which is indeed a *maximum.* ■

At this point we can generalize the above results to performance indices of the form :

$$J[u] = g[\mathbf{x}(t_f)] \tag{3.41}$$

Following a similar way of reasoning, we obtain that the *singular control keeps the substrate concentration at a constant level if and only if $k_h = 0$,* where that constant level satisfies

$$\lambda_2(t_f)(\mu'\sigma - \mu\sigma') + \lambda_3(t_f)(\pi'\sigma - \pi\sigma') = 0 \tag{3.42}$$

which generalizes (3.39).

REMARKS

1. As an example, if the performance index is taken to be a profit function of the form (3.8) with $\gamma_t = 0$

$$J[u] = -\gamma_x X(t_f) - \gamma_p P(t_f)$$

the final conditions on λ_2 and λ_3 are, using (3.30),

$$\lambda_2(t_f) = -\gamma_x \qquad \lambda_3(t_f) = -\gamma_p$$

Substitution in condition (3.42) yields

$$\frac{d}{dC_s}(\gamma_x \frac{\mu}{\sigma} + \gamma_p \frac{\pi}{\sigma}) = 0$$

which can be interpreted as that the *singular control maximizes the average yield, weighted by the unit prices of cell mass and product.*

2. Let us check whether the results of Theorem 3.1 can be extended to a performance index which depends explicitly on final time t_f

$$J[u] = g[\mathbf{x}(t_f), t_f]$$

Using the transversality condition

$$\mathcal{H}[\mathbf{x}(t_f), \boldsymbol{\lambda}(t_f), u(t_f), t_f] + \frac{\partial g}{\partial t}[\mathbf{x}(t_f), t_f] = 0$$

and Necessary Condition 1 of Section 1.2.3 we have :

$$\forall t \in [0, t_f] \; : \quad \mathcal{H}[\mathbf{x}(t), \boldsymbol{\lambda}(t), u(t), t] \equiv \phi + \psi u = -\frac{\partial g}{\partial t}[\mathbf{x}(t_f), t_f]$$

On a singular arc the following conditions hold :

$$\psi = 0 \; : \qquad C_{s,in}\lambda_1 + \lambda_4 = 0$$

$$\dot{\psi} = 0 \; : \qquad \lambda_1 \sigma' - \lambda_2 \mu' - \lambda_3 \pi' = 0$$

$$\phi + \frac{\partial g}{\partial t}[\mathbf{x}(t_f), t_f] = 0 \; :$$

$$(-\lambda_1 \sigma + \lambda_2 \mu + \lambda_3 \pi) x_2 - \lambda_3 k_h x_3 + \frac{\partial g}{\partial t}[\mathbf{x}(t_f), t_f] = 0$$

Substituting these relations into the adjoint differential equations, we obtain :

$$\begin{aligned} \dot{\lambda}_1 &= 0 \\ \dot{\lambda}_2 &= -\lambda_3 k_h \frac{x_3}{x_2} + \frac{\partial g}{\partial t}[\mathbf{x}(t_f), t_f] \frac{1}{x_2} \\ \dot{\lambda}_3 &= \lambda_3 k_h \\ \dot{\lambda}_4 &= 0 \end{aligned}$$

Evaluating $d^2\psi/dt^2 = 0$ on the singular interval, we obtain :

$$\dot{C}_s = (k_h \lambda_3 (\pi' x_2 - \mu' x_3) + \frac{\partial g}{\partial t}[\mathbf{x}(t_f), t_f] \mu') \frac{1}{x_2(\lambda_1 \sigma'' - \lambda_2 \mu'' - \lambda_3 \pi'')}$$

which generalizes (3.34).

We conclude that for the results of Theorem 3.1 to hold, an additional necessary and sufficient condition is that *the performance index is independent of the final time t_f :*

$$\frac{\partial g}{\partial t}[\mathbf{x}(t_f), t_f] = 0$$

■

3.6.2 Special case : maintenance coefficient $m = 0$

The results of Theorem 3.1 have been obtained under the somewhat artificial condition $m > 0$. We now consider the limiting case of negligible energy demands for maintenance ($m = 0$). From the proof of Theorem 3.1 we know that only the case where *both m and k_h equal zero* needs additional justification.
Equation (3.3) reduces to

$$\sigma(C_s) = \frac{\mu(C_s)}{Y_{x/s}} + \frac{\pi(C_s)}{Y_{p/s}} \tag{3.43}$$

It is not quite difficult to show that in this case the dimension of the state vector can be reduced by one. Using state equations (3.4), equation (3.43) can be written as :

$$C_{s,in} u dt = dS + \frac{1}{Y_{x/s}} dX + \frac{1}{Y_{p/s}} dP$$

Integrating from $t = t_0$ delivers :

$$C_{s,in}(V(t) - V_0) = S(t) - S_0 + \frac{1}{Y_{x/s}}(X(t) - X_0) + \frac{1}{Y_{p/s}}(P(t) - P_0)$$

Using (3.7) :

$$V_0 = V_* + S_0/C_{s,in}$$

we obtain :

$$P(t) - P_0 = Y_{p/s}[C_{s,in}(V(t) - V_*) - S(t) - \frac{1}{Y_{x/s}}(X(t) - X_0)]$$

As $P(t)$ does not appear explicitly in the differential equations for S and X, we can omit the differential equation for P, $P(t)$ being determined for all t by the above *algebraic* equation.
Furthermore, as the total amount of substrate α is limited (3.10), we have using the last state equation :

$$C_{s,in}(V_f - V_*) = \alpha$$

So we obtain at $t = t_f$:

$$P(t_f) = P_0 + Y_{p/s}[\alpha + X_0/Y_{x/s}] - Y_{p/s}[S(t_f) + X(t_f)/Y_{x/s}] \qquad (3.44)$$

As a result, maximizing the final amount of product $P(t_f)$ is equivalent to minimizing the performance measure :

$$J[u] = S(t_f) + X(t_f)/Y_{x/s}$$

For reasons of compatibility with the above notations, we denote the costate vector as :

$$\boldsymbol{\lambda}(t) \triangleq \begin{pmatrix} \lambda_1(t) \\ \lambda_2(t) \\ \lambda_4(t) \end{pmatrix}$$

with boundary conditions :

$$\boldsymbol{\lambda}(t_f) = \frac{\partial g}{\partial \mathbf{x}}[\mathbf{x}(t_f)] = \begin{pmatrix} 1 \\ 1/Y_{x/s} \\ - \end{pmatrix} \qquad (3.45)$$

The Hamiltonian $\mathcal{H}$ is given by (3.29), where the functions ϕ and ψ reduce to :

$$\phi = (-\lambda_1\sigma + \lambda_2\mu)x_2 \qquad \psi = C_{s,in}\lambda_1 + \lambda_4$$

The adjoint equations become :

$$\begin{aligned} \dot{\lambda}_1 &= (\lambda_1\sigma' - \lambda_2\mu')x_2/x_4 \\ \dot{\lambda}_2 &= \lambda_1\sigma - \lambda_2\mu \\ \dot{\lambda}_4 &= -(\lambda_1\sigma' - \lambda_2\mu')x_1x_2/x_4^2 \end{aligned}$$

On the singular interval, we obtain :

$$\begin{aligned} C_{s,in}\lambda_1 + \lambda_4 &= 0 \\ \lambda_1\sigma - \lambda_2\mu &= 0 \\ \lambda_1\sigma' - \lambda_2\mu' &= 0 \end{aligned}$$

which again results in a *constant* costate vector on the singular interval. We also have from the start of the singular arc on :

$$\lambda_2(t) = \lambda_2(t_f) = \frac{1}{Y_{x/s}}$$

For the above system to have a nontrivial solution $\boldsymbol{\lambda}$, it is *necessary and sufficient* that :

$$\sigma'\mu - \sigma\mu' = 0$$

or, in other words :

$$\frac{d}{dC_s}(\frac{\sigma}{\mu}) = 0$$

or, using relation (3.43) :

$$\frac{d}{dC_s}(\frac{\pi}{\sigma}) = 0$$

which determines the *constant* value of C_s during singular control. Note that $d^2\psi/dt^2 = 0$ leads to :

$$(\lambda_1\sigma'' - \lambda_2\mu'')\dot{C}_s = 0$$

Clearly, $\lambda_1\sigma'' - \lambda_2\mu''$ cannot be zero, so we obtain indeed :

$$\dot{C}_s = 0$$

resulting in

$$u_{sing}(t) = \frac{\sigma X}{C_{s,in} - C_s}$$

The final time t_f for this case is obtained as follows. During the last batch phase, we have $u = 0$, so from (3.29) we obtain :

$$\phi(t_f) = 0 \tag{3.46}$$

Using boundary conditions (3.45) this results in :

$$-\sigma(t_f) + \mu(t_f)/Y_{x/s} = 0$$

or using equation (3.43) :

$$\pi(t_f) = 0$$

This is equivalent with :

$$\frac{dP}{dt}(t_f) = 0$$

as we might expect on *physical* grounds. Note that for most analytical expressions for the specific production rate this means that :

$$C_s(t_f) = 0$$

Again, we can generalize these results to a more general performance measure (3.41), wherein $P(t_f)$ has to be replaced by expression (3.44). Note that the analytical expression for $g[\mathbf{x}(t_f)]$ does *not* influence the (constant) level of C_s during singular control. It only determines the final time t_f through condition (3.46).

■

The above results can be summarized in a more general theorem.

Theorem 3.2

Consider the minimization of performance index $J[u] = g[\mathbf{x}(t_f)]$, subject to the dynamic constraint (3.4). Suppose that

σ, μ and π are functions of the substrate concentration C_s only, with continuous derivatives up to second order.

Then during singular control

1. *the substrate concentration C_s remains constant if and only if the specific product decay rate $k_h = 0$,*
2. *this constant value satisfies*

   if $m > 0$:

   $$\frac{\partial g}{\partial x_2}[\mathbf{x}(t_f)](\mu'\sigma - \mu\sigma') + \frac{\partial g}{\partial x_3}[\mathbf{x}(t_f)](\pi'\sigma - \pi\sigma') = 0$$

   if $m = 0$:

   $$\pi'\sigma - \pi\sigma' = 0$$

Furthermore, the optimal feed rate $u^*(t)$ is obtained in closed loop for any given value of S_0.

3.7 Heuristic control strategies

In Sections 3.5 and 3.6 we described in detail the optimal substrate feed rate profile for a type of fed–batch fermentation processes with growth/production decoupling (monotonic specific growth rate μ, non–monotonic specific production rate π).

However, although the application of optimal control theory has lead to the characterization of the feed rate profile which *minimizes the performance index globally*, this technique has some important drawbacks with respect to a real life implementation.

1. It is well–known that putting an optimal control solution into practice may be hampered by a lot of problems. If the control law is not obtained in complete closed loop form —as is the case here, unless certain

limiting conditions are satisfied—, it cannot compensate for unmodeled disturbances, parameter variations, ... A simple *feedforward* will not generate the predicted results. In other words, it is *not robust.*

2. Optimal control is a highly model sensitive technique : it requires full knowledge of an analytic expression of all specific rates. Since for most applications a sufficiently accurate model is not available, the determined profiles can be used only to obtain a greater qualitative insight in the process.

This motivates the search for suboptimal control strategies which are easier to implement and more robust against modeling uncertainties and process disturbances. In this section, we propose *heuristic* control strategies based on microbial and mathematical knowledge. These heuristic controllers can be considered as limiting cases of the optimal control profiles : under certain conditions they coincide with the optimal solutions. They can be motivated from both the *microbiological* and *mathematical* point of view.

Using *microbiological and experimental knowledge* the construction of a suboptimal profile can be based on the concept of a *biphasic* fermentation, as has been done also for the optimal solution (see Section 3.5).

growth phase $[0, t_2]$

During the growth phase we focus on the specific growth rate μ. For the control needed we refer to the optimal control results. For instance, in the case of an unbounded input u, an unconstrained state vector $\mathbf{x}$, and a free initial substrate concentration $C_s(0)$, the growth phase is a *batch* phase. In case of a constraint on the input or the state and/or a fixed initial state, some minor modifications are required. A general strategy is that *the fraction α_{growth} of the total amount of substrate available α (3.10) which is consumed for biomass accumulation during the growth phase must be added as fast as possible in order to obtain the highest possible value of μ.*

production phase $[t_2, t_3]$

During production we focus on the specific production rate π.

- As shown in Figure 3.2, π exhibits a maximum as function of the substrate concentration C_s. So, it is a reasonable control objective to keep the substrate concentration during the production

phase constant at the level C_s^* which maximizes π. Therefore, the control during production is of the form :

$$u_{production}(t) = \frac{\sigma X}{C_{s,in} - C_s} \tag{3.47}$$

This control is shut off when all substrate α has been added at time $t = t_3$. The final time t_f of the terminating batch phase $[t_3, t_f]$ is determined by the stopping condition which depends on the performance measure under consideration (see Section 3.5.2). Obviously, the switching time t_2 is known in closed loop : the production phase starts when the substrate concentration C_s becomes equal to C_s^*. As a result, the optimization problem has been reduced to the *one dimensional optimization of the fraction α_{growth} of the total substrate amount available.*

- A further refinement of this strategy consists of optimizing the switching time t_2, and thus the value of the substrate concentration C_s during production. In other words, C_s is kept constant, but not necessarily at the value $C_s = C_s^*$. As in the case of optimal control a *two dimensional optimization of α_{growth} and t_2 is obtained.*

The proposed suboptimal control sequence agrees very well with the optimal one : the only change is the substitution of the *singular control* (3.16) by a control of the form (3.47). As a *mathematical justification*, it follows immediately from the analysis presented in Section 3.6 that this suboptimal control profile reduces to the optimal profile if (and only if) (i) the performance index is independent of final time t_f, (ii) the specific rates μ and π are functions of C_s only, and (iii) $k_h = 0$ (see Theorems 3.1 and 3.2). In cases where these conditions are not satisfied, it is at least a very good approximation of the optimal solution, as will be illustrated with several examples in the following chapters.

The main advantages of these suboptimal profiles as compared with the optimal control solution can be summarized as follows.

1. They are the translation of a more realistic control objective, namely *setpoint* control, for which even model–independent adaptive control algorithms can be developed. More specifically, there will be no need for an analytic expression of the specific rates.

2. There is no need for a complete measurement of the state, a problem which has not been solved completely up to now.

This will be illustrated with a case study in Chapter 6.

3.8 Conclusions

In this chapter we have analyzed the optimization of fed–batch bioreactors with respect to the volumetric substrate feeding rate. In general this yields a *singular* optimal control problem. However, due to state inequality constraints —which reflect physical limitations— complete solutions are especially hard to obtain and almost nonexistent in the literature.

To circumvent this, a lot of techniques have been proposed in the literature to convert a singular problem into a nonsingular one by considering variables other than the feed flow rate as the control variable. As a matter of fact, these methods all suffer from problems with respect to practical implementation.

Therefore, in this chapter we have adopted the traditional point of view, i.e. *singular optimal control* with the volumetric substrate feed rate as the manipulated variable. We have considered performance indices of both the yield type and the productivity type. The optimization of the initial substrate concentration has been included also.

A general optimization problem has been formulated within the framework of optimal control theory, leading to a two point boundary value problem. It is shown that the solution reduces to the determination of the optimal control sequence —possibly including a singular interval— and the corresponding switching times.

We have illustrated that the determination of the switching times in the feed rate profile can be simplified a lot by incorporating as much as possible microbiological knowledge concerning the process under consideration. As an introductory example, optimization of a microbial growth process has been considered. The deduced control sequences have been justified based on biochemical insight in the process. The extension to processes with growth associated product formation is straightforward.

A similar line of reasoning has been adopted for optimization of fed–batch fermentations characterized by a decoupling between growth and product formation. As an example, we have derived the optimal control sequence for processes with monotonic growth rate and non–monotonic production rate. We have been able to prove that the deduced control sequence *minimizes the performance index globally.* In addition, we have presented for the first time a *complete solution in the realistic case of both substrate and biomass inequality constraints.* The resulting straightforward computational algorithm has some advantages over the algorithm proposed by Lim *et al.* [1986]. First, there is no need for costate variables —which have in general no clear physical interpretation— independent of the performance measure considered. Second, as a result this algorithm proves to be numerically more reliable. The results we have presented here are general in this way that they are written in terms of the specific reaction rates. In other words, an exact analytical expression for these rates is not required a priori. In addition, no assumptions have been made concerning the metabolism involved for biomass survival and possibly product synthesis.

A detailed analysis of the singular arc —summarized in Theorems 3.1 and 3.2— is at the basis of a *heuristic optimization methodology* which plays a central role throughout this thesis. These heuristic controllers have been motivated from the biochemical viewpoint also. In contrast to the optimal control solution they are the translation of a more realistic control objective, namely set–point control, for which adaptive model–independent control algorithms can be developed with nearly optimal performance : *optimal adaptive control* (see Chapter 6).

Chapter 4

Analysis of two unstructured models for the penicillin G fed-batch fermentation process

The tools and methods developed in Chapter 3 are applied to the optimization of the penicillin G fed–batch fermentation process. In Section 4.1, we briefly introduce this fermentation process.

In Section 4.2, we consider the unstructured model of Heijnen, Roels and Stouthamer [1979], characterized by a continuous but non–differentiable growth associated specific production kinetics and an endogenous metabolism viewpoint. We first show that in the weight balance of the original model all terms except the one representing substrate input have negligible influence on the dynamics and final value of the product, so they can be omitted. The use of this simplified model facilitates a lot the analytical computations. Based on Conjecture 1.1, we derive for the first time the optimal substrate feed rate profile for this model resulting in the maximum amount of product for a given amount of substrate. The simulation results illustrate the efficiency of the computational algorithm developed in Chapter 3, even for these more or less degenerate kinetics. Based on the same conjecture, we prove an additional theorem (Theorem 4.1) characterizing the singular arc which is the analogon of the theorems of Chapter 3. The realizable gain due to feed profile optimization is in the region of some hundred percents. Furthermore, the model is very sensitive towards different feeding policies. These results, together with the fact that the commonly observed biphasic behavior of the penicillin fed–batch fermentation has dis-

appeared after optimization, raise some questions concerning the validity of this model.

In Section 4.3, we analyze the unstructured model proposed by Bajpai and Reuß [1980,1981], characterized by a monotonic specific growth rate and non–monotonic specific production rate within a maintenance metabolism viewpoint. In solving the same optimization problem as formulated for the Heijnen et al. model, we compare different suboptimal strategies with the optimal control solution. As an extension of the results of Bajpai and Reuß —they only investigated control strategies with predefined structure— we conclude that using any of these strategies, a performance similar to the optimal one can be obtained provided the associated degrees of freedom are at their optimal values. Using this model the realizable gain is in the region of only a few percents up to several hundred percents depending on the parameter set used. We also consider the optimization of the productivity. The yield–productivity conflict in fed–batch reactors is clearly illustrated. Again, the proposed computational algorithm proves to be very reliable and efficient for both performance measures considered. A comparison with the results obtained by Lim et al. [1986] is also given.

Apart from the derivation of optimal control profiles for both models —which are important on their own—, we believe that the most important results from this chapter are the following. First, although both models have a more or less similar behavior using a constant feed rate profile and have been validated using experimental data reported in the literature, clearly they exhibit a quite different behavior after feed profile optimization. As a result, this optimal control study can prove to be very useful in model characterization as will be illustrated in Chapter 5 : optimization for model discrimination. Second, although the optimal profile and the resulting realizable gain strongly depend on the model used, the heuristic controllers introduced in Chapter 3 have an excellent performance in all cases. As such, they can serve indeed as a basis for the development of model–independent control algorithms. This will be elaborated in detail in Chapter 6 : optimal adaptive control. Some concluding remarks are summarized in Section 4.4.

4.1 The penicillin G fermentation process

The category of secondary metabolites includes a large number of extremely valuable compounds whose mass production has revolutionized public health in modern society. In this chapter the penicillin G fed–batch fermentation process is under study.

Nowadays penicillin G is an almost common antibiotic; nevertheless the fermentation technology and the mathematical description of the production process are still a subject of interest. The optimization of product formation during fermentation as a part of total process control has gained a renewed attention.

According to Gaden's classification (see Section 1.1.1 and [Gaden 1959]) secondary metabolites would fall under the third category —where the main product has no relation to the primary energy metabolism— and therefore follow a non growth associated kinetics. Most of the antibiotics in fact follow a typical *trophophase* (high growth rates resulting in rapid biomass build–up) – *idiophase* (appearance of product in the broth with no or little increase in the amount of biomass) relationship.

However, in the light of our present knowledge it seems that the growth and/or non growth associated kinetic interpretation of Gaden's classification is not enough to explain the diverse experimental observations concerning product forming systems. A typical example is the penicillin G production which follows a non growth associated kinetics under batch conditions, and a more or less growth independent kinetics in a chemostat [Pirt and Righelato 1967].

The last few decades studies by several authors clearly point out that the production of secondary metabolites takes place in a cell in a carefully controlled fashion (see e.g. [Martin and Liras 1989] for a state–of–the–art review). This information concerning the regulation of product formation in the micro–organisms, coupled with the concept of limiting reactions, can be used to develop models for a better mathematical representation of these systems.

For an overview of the current knowledge about the penicillin synthesis pathway we refer to Section 5.1.2. The most important mathematical models reported in the literature for this fermentation process are the following.

Constantinides *et al.* [1970a,b] investigated several unstructured models. The best fit on experimental data has been obtained using a logistic law for biomass growth. The penicillin production rate is supposed to be proportional to the amount of biomass present. Penicillin is also assumed to be hydrolyzed at a rate proportional to the total amount of product. Based on the temperature dependence of the parameters, represented by second degree polynomial or Arrhenius–type relationships, optimal fermentation temperature profiles were derived using Pontryagin's Minimum Principle.

Giona *et al.* [1976a and b] derived an unstructured model involving sub-

strate, biomass and penicillin for a semi–continuous fermentation process based on mass balances. They assumed a linear relationship (including a maintenance term) between substrate consumption and growth rate as suggested by Rhigelato *et al.* [1968]. Penicillin synthesis is assumed to be well correlated with the oxygen concentration. A comparison of industrial fermentation data and simulation results confirms the hypothesis that penicillin production is very sensitive towards the oxygen level, which is explained by the biochemical function of oxygen in penicillin biosynthesis [White *et al.* 1982]. They also investigated the influence of different fermentation conditions on total biomass and penicillin production. The main conclusion was that there exists an optimal oxygen concentration.

Hegewald *et al.* [1981] constructed an unstructured model based on mass balances with equations for biomass, glucose, oxygen, ammonia nitrogen, amino nitrogen and penicillin. Maintenance requirements are fulfilled by endogenous respiration; penicillin synthesis occurs at the expense of substrate. Penicillin hydrolysis has not been taken into account. Simulations showed that disturbances of the volumetric oxygen transfer rate might have a tremendous influence on final penicillin yield. Unfortunately the authors did not provide numerical values for the parameters of their model.

The models of Heijnen *et al.* [1979] and of Bajpai and Reuß [1980,1981] are analyzed in detail in the next sections. They allow for optimization of the final product amount with respect to the substrate feeding rate.

Nestaas and Wang [1983] postulated three different cell types in the penicillin fermentation : growing tips, penicillin producing cells and degenerated non–producing cells. Starting from the observation that penicillin fermentation usually exhibits a biphasic behavior, they proposed for each of both phases a structured compartment model. In the first phase only growing tips and penicillin producing cells are assumed to be present. During the production phase degenerated cells are also present. The delay in penicillin production is assumed to be caused by a hypothetic intermediary precursor, while penicillin is subjected to hydrolysis. Furthermore, they assumed maintenance metabolism. Glucose consumption is modeled using a semi–empirical substrate balance. The authors developed a control algorithm which was able to track a certain prespecified biomass concentration profile.

Recently another structured model has been proposed by Aynsley *et al.* [1990]. These authors established a very interesting analogy between growing hyphae and a tubular reactor. A drawback of their model is the fact that no expression for penicillin synthesis has been provided. Moreover, their model contains a large number of parameters which might be difficult to estimate.

4.2 The model of Heijnen, Roels and Stouthamer

4.2.1 The original model equations

Heijnen *et al.* [1979] used the following steps in the construction of a simple unstructured model for the penicillin G fed–batch fermentation process : (i) definition of relevant compounds in the penicillin fermentation, (ii) specification of chemical composition and specific enthalpies, (iii) formulation of elemental balances and the enthalpy balance (one of the most interesting features of this approach), (iv) formulation of mass balances for individual compounds, (v) formulation of the weight balance, and (vi) selection of the kinetic equations (in this case based on a literature survey). Their research resulted in the following continuous time model which they believe to be of great possible help in the optimization of the process :

$$\begin{aligned}
\frac{dS}{dt} &= -\sigma X + u \\
\frac{dX}{dt} &= \mu X \\
\frac{dP}{dt} &= \pi X - k_h P \\
\frac{dG}{dt} &= \frac{1}{C_{s,in}} u - 0.0008G - 0.044 r_c \\
&\quad + 0.068 r_n + 0.392 r_{su} + 0.032 r_o + 0.68 \pi X
\end{aligned} \tag{4.1}$$

with

S	: amount of substrate (glucose) in broth	[mol]
X	: amount of cell mass in broth	[mol dry weight]
P	: amount of product (penicillin) in broth	[mol]
G	: total broth weight	[kg]
u	: substrate feed rate	[mol/h]
$C_{s,in}$	: glucose concentration in feed stream	[mol/kg]
σ	: specific substrate consumption rate	[mol/mol dry weight h]
μ	: specific growth rate	[1/h]
π	: specific production rate	[mol/mol dry weight h]
k_h	: penicillin hydrolysis constant	[1/h]
r_c	: net rate of CO_2 conversion	[mol/h]
r_n	: net rate of nitrogen source conversion	[mol/h]
r_o	: net rate of oxygen conversion	[mol/h]
r_{su}	: net rate of sulphate source conversion	[mol/h]

Observe that this model is written in a [mol,kg] unit system : concentrations are expressed with respect to total broth weight G (instead of volume V). In the last equation, terms with a positive sign are due to the input of respectively glucose, nitrogen source, sulphate source, oxygen and precursor. Terms with a negative sign represent respectively evaporation and carbon dioxide production. For more details see [Heijnen *et al.* 1979].
The specific rates are specified as follows :

1. The specific substrate consumption rate σ is modeled using a *Monod*–type relationship (1.14) :

$$\sigma = Q_{s,max}\frac{C_s}{K_s + C_s} \tag{4.2}$$

with

$Q_{s,max}$: maximum specific sugar uptake rate [mol/mol dry weight h]
K_s : Monod constant for sugar uptake [mol/kg]

2. The specific production rate π is assumed to be directly coupled with the specific growth rate μ, following a *Blackman*–type relation (1.16) :

$$\pi(\mu) = Q_{p,max}\begin{cases} \mu/\mu_{crit} & \text{for } \mu \leq \mu_{crit} \\ 1 & \text{for } \mu \geq \mu_{crit} \end{cases} \tag{4.3}$$

with

$Q_{p,max}$: maximum specific production rate [mol/mol dry weight h]
μ_{crit} : critical specific growth rate [1/h]

3. The specific growth rate is given by

$$\mu = Y_{x/s}(\sigma - m - \pi/Y_{p/s}) \tag{4.4}$$

which clearly satisfies relation (1.11).

This represents an *endogenous* metabolism [Herbert1958], as can be easily seen comparing this expression with equation (1.9). We have :

$$\begin{aligned} \mu_{substr} &\triangleq Y_{x/s}\sigma \\ f_m &= 1 \\ f_p &= 1 \end{aligned}$$

parameters			
$Q_{s,max}$	0.0245	$Q_{p,max}$	$3.3\ 10^{-4}$
K_s	0.0056	μ_{crit}	0.01
$Y_{x/s}$	3.67	k_h	0.002
$Y_{p/s}$	0.46	$C_{s,in}$	1/0.36
m	0.0034		
initial conditions			
X_0	4000	S_0	*to be specified*
P_0	0	G_0	$98020 + S_0/C_{s,in}$
t_0	0	α	205500

Table 4.1: Parameters and initial conditions used in simulations

Table 4.1 shows the parameters and initial conditions used in all simulations. The expressions for the rates r_c, r_n, r_o and r_{su} can be found in [Heijnen *et al.* 1979].

The specific substrate consumption rate σ (4.2) is a function of C_s only. Substitution of equations (4.2) and (4.3) in equation (4.4) delivers an implicit relationship between μ and C_s, the solution for μ of which can be used in equation (4.3). We conclude that the three *specific rates σ, μ and π are functions of C_s only.* Figures 4.1 and 4.2 show the results of these manipulations. As π has a discontinuity in the derivative with respect to μ at $\mu = \mu_{crit}$, it is quite clear that π as a function of C_s exhibits a corner at the corresponding value of C_s, say $C_{s,crit}$. Notice that both the (overall) specific growth rate μ and the specific production rate π become zero at a positive value for substrate concentration C_s. Obviously, this is due to the endogenous metabolism assumption. As a result, these kinetics represent a degenerate version of the first type fermentation processes introduced in Section 3.5.1, i.e. *monotonic μ and non–monotonic π*. They can also be interpreted as a degenerate case of a *fermentation process with growth associated product formation.*

4.2.2 A simplified weight balance

We now show that in the right–hand side of differential equation (4.1) for total broth weight G all terms except the first one (which represents the input of glucose) have negligible influence on the dynamics and final value of the product P.

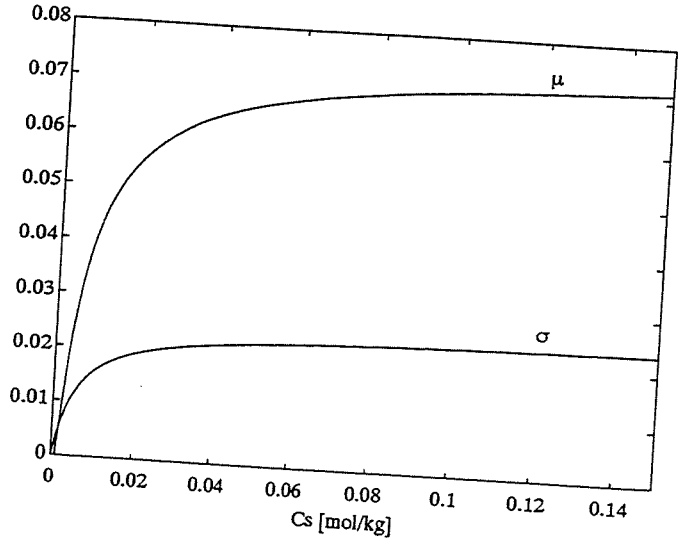

Figure 4.1: The specific rates σ and μ as functions of C_s

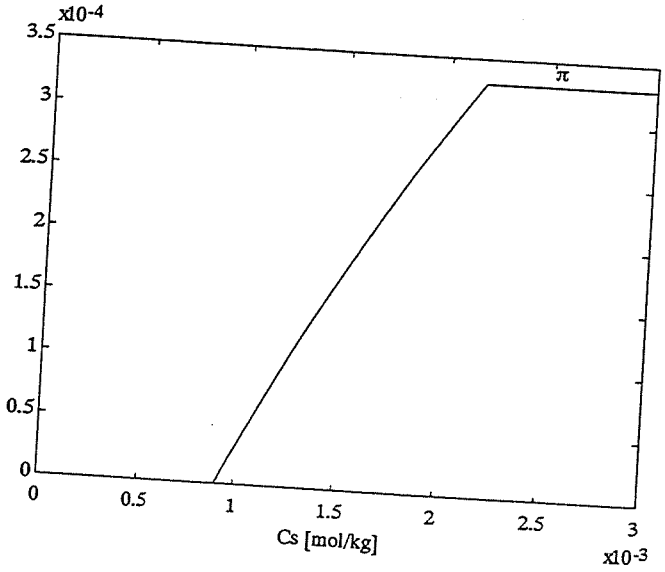

Figure 4.2: The specific rate π as a function of C_s

This can be seen as follows. As all specific rates are functions of C_s only, it is useful to derive the differential equation for C_s :

$$\frac{dC_s}{dt} = \frac{1}{G}\frac{dS}{dt} - \frac{C_s}{G}\frac{dG}{dt}$$

For π out of saturation, typical orders of magnitude are : $C_s = O(10^{-3})$, $\mu = O(10^{-3})$, $\pi = O(10^{-4})$. Using the exact expressions for the specific rates r_c, r_n, r_o and r_{su} (see [Heijnen *et al.* 1979]) in the right-hand side of equation (4.1), it can be verified that under these conditions, the second most important contribution comes from the term representing evaporation. So the above dynamic equation for C_s can be written as :

$$\frac{dC_s}{dt} = -\sigma C_x + (1 - \frac{C_s}{C_{s,in}})\frac{u}{G} + 0.0008C_s + \text{l.o.t.}$$

With u in the order of magnitude of 1000 mol/h, the term $0.0008C_s$ has negligible influence on the dynamics of C_s, and thus on the dynamics of all specific rates.

So in optimizing the final product amount $P(t_f)$ with respect to the glucose feeding policy, we will omit all these terms to simplify the analytical developments. The original model then reduces to :

$$\begin{aligned}
\frac{dS}{dt} &= -\sigma X + u \\
\frac{dX}{dt} &= \mu X \\
\frac{dP}{dt} &= \pi X - k_h P \\
\frac{dG}{dt} &= \frac{1}{C_{s,in}} u
\end{aligned} \tag{4.5}$$

Defining F_{in} as

$$F_{in}\ [kg/h] \triangleq \frac{u}{C_{s,in}}\ \frac{[mol/h]}{[mol/kg]}$$

this model has the general structure (3.1).

Another advantage of this model structure is that we can take care of an isoperimetric constraint on the input *without* introducing an additional state equation.

As an example, using $S_0 = 5500$ mol and a constant input $u = 1000$ mol/h during 200 hours, we obtain $P(t_f) = 3001.12$ mol using the complete equation for G (4.1), and a value which is only 0.03% smaller when

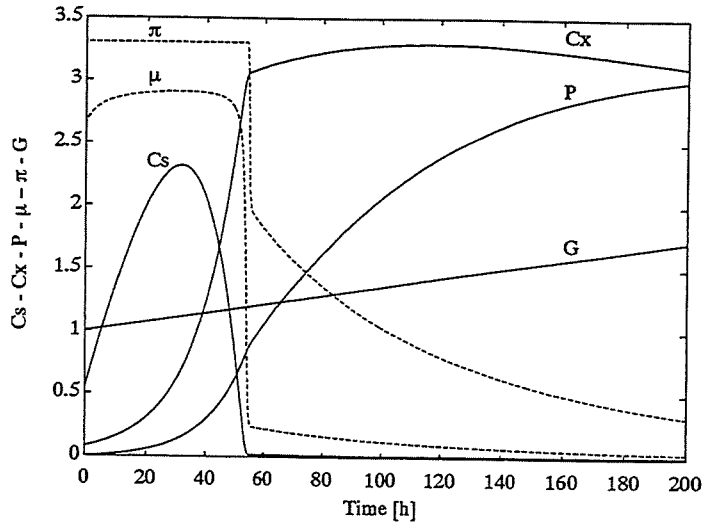

Figure 4.3: Constant glucose feed rate and corresponding cell, glucose, product, μ and π profiles
Scaling: $Cs * 10$, $Cx * 2$, $P/10^3$, $G/10^5$, $\mu * 40$, $\pi * 10^4$

using only the first term as in (4.5). The simulation results using the simplified model are shown in Figure 4.3. Some comments are in order here.

1. Up to now the penicillin fermentation —when operated in fed–batch mode— is most often classified in the group of product formation processes of the non growth associated type. In agreement with the experimentally observed behavior, the process is assumed to consist of two phases : a phase of rapid growth with almost no product formation (*trophophase*) and a phase with limited growth in which the product is formed (*idiophase*). The simulation results for $S(t)$, $X(t)$ and $P(t)$ are obviously in agreement with this biphasic description. However, Heijnen *et al.* obtained these results on the assumption of a direct coupling between specific growth rate and specific rate of product formation [see equation (4.3)]. The μ and π profiles in Figure 4.3 illustrate some of these ideas. Heijnen *et al.* therefore concluded that *the apparent separation between production and growth phases does not necessarily mean that penicillin production is of the non growth associated type.*

2. Another feature of the simulation results is an apparent *lag phase* in the penicillin production curve of about 20 hrs. Observe that this was not introduced *a priori* in the model. Heijnen *et al.* concluded that it remains possible that there is in reality no real lag in the beginning of penicillin production.

3. Another modeling approach that has been followed is the assumption of a *relationship between mycelial age and its productivity.* Most often the product activity is assumed to decrease at high mycelial age [Fishman and Biryukov 1974]. In this way the decreasing π curve (Figure 4.3) during the production phase can be modeled. However, Heijnen *et al.* did not model such an age dependency. In their viewpoint, the decreasing π profile may very well be explained from either dilution due to increasing broth weight or hydrolysis of penicillin to penicilloic acid.

Heijnen *et al.* concluded that with their growth–coupled penicillin production most of the phenomena observed in practice —which have often lead to the assumption of non growth associated or age dependent penicillin productivity— can be adequately described. We will come back to these interpretations in Chapter 5. However, from the mathematical point of view, the commonly observed separation between growth and production phase is a quite useful feature in optimizing the process.

4.2.3 Statement of the optimization problem

Heijnen *et al.* [1979] used their model to illustrate that the *feed rate profile during fermentation is of vital importance in the realization of a high production rate throughout the duration of the fermentation.* This statement was based on the following set of controls : a constant input (the results of which are shown in Figure 4.3), a linearly increasing input and a linearly decreasing input. The initial state was fixed, as well as the final time and the total amount of substrate available. Table 4.2 summarizes the results we have obtained using the simplified model.

Although Heijnen *et al.* did not consider other feeding strategies in an attempt to obtain the optimal feeding profile, the above results indicate that the present model allows indeed for the optimization of the glucose feed rate scheme with respect to the final amount of product $P(t_f)$.

Following the lines presented in Chapter 3, we formulate the problem of optimizing the final product amount as an optimal control problem. Intro-

Operational conditions	
S_0 5500	P_0 0
X_0 4000	G_0 100000
t_f 200	α 205500
Control $u(t)$	$P(t_f)$
$u(t) = 1000$	3001.
$u(t) = 500 + 5t$	5883.
$u(t) = 1500 - 5t$	89.

Table 4.2: Simulation results with the controls of Heijnen *et al.*

ducing a state space vector $\mathbf{x}$

$$\mathbf{x} = \begin{pmatrix} x_1 \\ x_2 \\ x_3 \\ x_4 \end{pmatrix} \triangleq \begin{pmatrix} S \\ X \\ P \\ G \end{pmatrix}$$

and defining

$$\mathbf{f} = \begin{pmatrix} f_1 \\ f_2 \\ f_3 \\ f_4 \end{pmatrix} \triangleq \begin{pmatrix} -\sigma X \\ \mu X \\ \pi X - k_h P \\ 0 \end{pmatrix} \qquad \mathbf{b} = \begin{pmatrix} b_1 \\ b_2 \\ b_3 \\ b_4 \end{pmatrix} \triangleq \begin{pmatrix} 1 \\ 0 \\ 0 \\ 1/C_{s,in} \end{pmatrix}$$

we obtain a state space model linear in the control u of the form (3.4)

$$\frac{d\mathbf{x}}{dt} = \mathbf{f}(\mathbf{x}) + \mathbf{b}\, u \tag{4.6}$$

Observe that considering the mass flow rate u [mol glucose/h] as the control input is equivalent to controlling the 'volumetric' flow rate F_{in} [kg feed/h] (as proposed in Chapter 3), since the substrate concentration $C_{s,in}$ is assumed constant. Numerical values for the initial conditions are given in Table 4.1. $x_2(0)$ and $x_3(0)$ are given; the initial amount of substrate $x_1(0)$ is *free*. $x_1(0)$ and $x_4(0)$ are related by :

$$x_4(0) = G_* + x_1(0)/C_{s,in} \tag{4.7}$$

where G_* denotes the given initial weight *without* substrate [$G_* = 98020$ kg (Table 4.1)].

The optimization problem is to determine for the given set of differential equations (4.6) the optimal initial state $\mathbf{x}_0^*$ and the optimal feed rate profile $u^*(t)$ that minimize the performance index

$$J[u, \mathbf{x}_0] = g[\mathbf{x}(t_f)] \triangleq -x_3(t_f) \tag{4.8}$$

i.e. maximize the final amount of product, subject to the following constraints :

1. $t_0 = 0$, t_f is *free*.

2. All variables have to be kept positive :

$$\forall t \in [0, t_f] : \quad x_i(t) \geq 0, \text{ for } i = 1, \ldots, 4 \quad \wedge \quad u(t) \geq 0$$

3. The total amount of substrate available α is fixed, i.e. :

$$x_1(0) + \int_{t_0}^{t_f} u(t)\, dt = \alpha \tag{4.9}$$

The last *isoperimetric* constraint on the input is equivalent to a *physical* constraint of the form [see the simplified differential equation for total broth weight G (4.5)] :

$$x_4(t_f) \equiv G(t_f) = G_f, \; G_f \text{ fixed} \tag{4.10}$$

4.2.4 A modified model

As can be easily seen from equation (4.3) and Figure 4.2, the specific production rate π exhibits a *corner* at $\mu = \mu_{crit}$ or equivalently at $C_s = C_{s,crit}$. As a result some partial derivatives $\partial f_i / \partial x_j$ are not continuous. So we can not apply standard optimal control theory (see e.g. [Athans and Falb 1966]). To circumvent this problem, we replace the piecewise smooth Blackman–type kinetics $\pi(\mu)$ (4.3) by a family of completely smooth curves that converge as a function of one parameter to the original kinetics. This is basically inspired by the result of Conjecture 1.1.

Consider the following relationship between μ and π, a *Dabes*–type kinetics [Dabes *et al.* 1973], with A and B parameters :

$$\mu = A\pi + \frac{B\pi}{Q_{p,max} - \pi} \tag{4.11}$$

or, in another way :

$$A\pi^2 - (Q_{p,max}A + B + \mu)\pi + Q_{p,max}\mu = 0$$

Solving this quadratic equation for π and taking the root with negative sign —we want $\pi = 0$ at $\mu = 0$ as in the original kinetics (4.3)— leads to :

$$\pi(\mu) = \frac{(Q_{p,max}A + B + \mu) - \sqrt{(Q_{p,max}A + B + \mu)^2 - 4AQ_{p,max}\mu}}{2A}$$

We now eliminate one parameter, say A, by solving :

$$\frac{d\pi}{d\mu}(\mu = 0) = \frac{Q_{p,max}}{\mu_{crit}}$$

which imposes that the derivative of π at $\mu = 0$ must be equal to the value derived from equation (4.3). The solution is :

$$A = \frac{\mu_{crit} - B}{Q_{p,max}}$$

and thus we obtain :

$$\pi(\mu) = Q_{p,max}\frac{(\mu + \mu_{crit}) - \sqrt{(\mu + \mu_{crit})^2 - 4(\mu_{crit} - B)\mu}}{2(\mu_{crit} - B)} \tag{4.12}$$

which is the desired family of smooth curves, where B, which must lie between $0 < B < \mu_{crit}$, is the only parameter.

Let us consider now the boundaries for the parameter B. For $B \to \mu_{crit}$, A tends to 0, and the above equation becomes undetermined. However, solving the original relation (4.11) for π with $A = 0$ delivers the following *Monod*–type law :

$$\pi(\mu) = Q_{p,max}\frac{\mu}{\mu_{crit} + \mu} \tag{4.13}$$

which is of course also a completely smooth relationship.

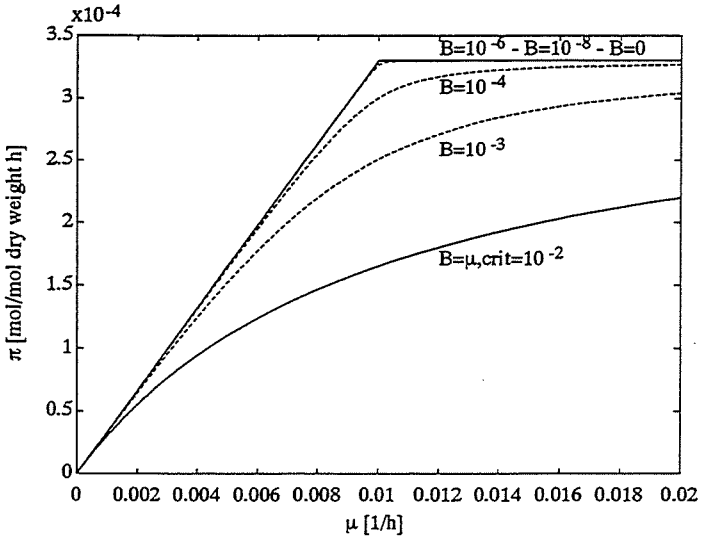

Figure 4.4: Dabes–type kinetics $\pi(\mu)$ for some values of the parameter B

On the other hand, as $B \to 0$ equation (4.12) reduces to :

$$\pi(\mu) = Q_{p,max}\frac{(\mu + \mu_{crit}) - \sqrt{(\mu - \mu_{crit})^2}}{2\mu_{crit}} = \frac{Q_{p,max}}{2\mu_{crit}}(\mu + \mu_{crit} - \mid \mu - \mu_{crit} \mid)$$

which is in fact another form of the original model (4.3). So we can refine the boundaries for B to $0 < B \leq \mu_{crit}$. We conclude that we have constructed a one dimensional family of curves —and thus a family of models— that are completely smooth within the given boundaries of the parameter B, thus assuring the continuity of $\partial f_i/\partial x_j$ for all i and j. Moreover, as $B \stackrel{>}{\to} 0$, we come arbitrarily close to the original model. In Figure 4.4 we show some members of the family (4.12) for different values of B. From the numerical point of view, setting $B = 10^{-11}$ in equation (4.12) is a very accurate approximation in simulating the original Blackman type kinetics (4.3).
Obviously, we can determine the optimal control $u^*(B,t)$ for every B within the given boundaries $]0, \mu_{crit}]$, using standard optimal control theory. For the original model —corresponding to $B = 0$— we will make use of Conjecture 1.1.

4.2.5 Optimal control using the modified model

The given optimization problem can be formulated within the frame of the Minimum Principle as a *two point boundary value problem* (TPBVP), as shown in Section 3.3.1.
The Hamiltonian $\mathcal{H}$ for this problem is :

$$\mathcal{H} = \boldsymbol{\lambda}^{\mathbf{T}}(\mathbf{f}(\mathbf{x}) + \mathbf{b}u) \triangleq \phi + \psi u \tag{4.14}$$

with

$$\phi = \lambda_1 f_1 + \lambda_2 f_2 + \lambda_3 f_3 \qquad \psi = \lambda_1 + \lambda_4 / C_{s,in}$$

The adjoint vector $\boldsymbol{\lambda}$ satisfies the following system of differential equations :

$$\frac{d\boldsymbol{\lambda}}{dt} = -\frac{\partial \mathcal{H}}{\partial \mathbf{x}} = -\frac{\partial \mathbf{f}}{\partial \mathbf{x}}^{\mathbf{T}} \boldsymbol{\lambda} \tag{4.15}$$

or

$$\begin{pmatrix} \dot{\lambda}_1 \\ \dot{\lambda}_2 \\ \dot{\lambda}_3 \\ \dot{\lambda}_4 \end{pmatrix} = \begin{pmatrix} -\partial f_1/\partial x_1 & -\partial f_2/\partial x_1 & -\partial f_3/\partial x_1 & 0 \\ \sigma & -\mu & -\pi & 0 \\ 0 & 0 & k_h & 0 \\ -\partial f_1/\partial x_4 & -\partial f_2/\partial x_4 & -\partial f_3/\partial x_4 & 0 \end{pmatrix} \begin{pmatrix} \lambda_1 \\ \lambda_2 \\ \lambda_3 \\ \lambda_4 \end{pmatrix}$$

Note that in order to compute $\partial f_i/\partial x_1$ and $\partial f_i/\partial x_4$, $i = 2, 3$, we need $\partial \mu/\partial x_1$ and $\partial \mu/\partial x_4$. These can be obtained by substituting equation (4.12) in equation (4.4) and calculating the *implicit* partial derivatives with respect to x_1 and x_4 respectively.

The state equations (4.6) together with the costate equations (4.15) constitute a set of 2×4 first order differential equations. The required boundary conditions are :

- $x_2(0)$ and $x_3(0)$ are given
- $x_1(0)$ and $x_4(0)$ are interrelated by equation (4.7)
- Application of the result of Section 1.2.5 leads to :

$$\lambda_1(0) + \lambda_4(0)/C_{s,in} \equiv \psi(0) = 0$$

- $x_4(t_f)$ is given due to equation (4.10)

- $\lambda_i(t_f)$, $i = 1, \ldots, 3$ are given by :

$$\lambda_i(t_f) = \frac{\partial g}{\partial x_i}[\mathbf{x}(t_f)]$$

or, using (4.8) :

$$\begin{pmatrix} \lambda_1(t_f) \\ \lambda_2(t_f) \\ \lambda_3(t_f) \end{pmatrix} = \begin{pmatrix} 0 \\ 0 \\ -1 \end{pmatrix}$$

As stated in the Minimum Principle [see Section 1.2.3], an *extremal* control follows from the minimization of the Hamiltonian $\mathcal{H}$ (4.14) over all *admissible* control functions while satisfying the given TPBVP :

$$\min_{\text{all admissible } u} \mathcal{H}(\mathbf{x}^*, \boldsymbol{\lambda}^*, u) = \mathcal{H}(\mathbf{x}^*, \boldsymbol{\lambda}^*, u^*)$$

Note that as all conditions are only *necessary* conditions, we can only obtain *extremal* solutions $(\mathbf{x}^*, \boldsymbol{\lambda}^*, u^*)$ which must be checked for optimality.
Since the state equations (4.6) and the cost index (4.8) are time invariant, the Hamiltonian $\mathcal{H}$ remains constant along an extremal trajectory. As the final time t_f is free, we know that $\mathcal{H} = 0$ [see Necessary condition 2 in Section 1.2.3].

As already mentioned, the original kinetics (4.2), (4.3) and (4.4) represent a degenerate case of a fermentation process with monotonic specific growth rate μ and non–monotonic specific production rate π —the corner point is a degenerate maximum—, for which the optimal control algorithm has been derived in Chapter 3. However, since the original model is only piecewise smooth, this algorithm can not be used directly.

> *We verify now that the algorithm can be used for any model with a specific production rate kinetics within the family of completely smooth curves (4.12). The optimal solution using the original model is then obtained considering the limit*
>
> $$\lim_{B \gtrsim 0} u^*(B, t) \triangleq u^*(B = 0, t)$$
>
> *as stated in Conjecture 1.1.*

As the Hamiltonian $\mathcal{H}$ is *linear* in the control input u, the Minimum Principle can fail to provide the solution on any singular interval $[t_i, t_{i+1}]$ where the

function ψ remains zero. In that case, the singular control can be calculated by solving

$$\frac{d^2\psi}{dt^2} = 0$$

for u (see Chapter 3) :

$$u_{sing}(t) = \frac{\boldsymbol{\lambda}^{\mathbf{T}}[(\partial \mathbf{f}/\partial \mathbf{x})\mathbf{d} - (\partial \mathbf{d}/\partial \mathbf{x})\mathbf{f}]}{\boldsymbol{\lambda}^{\mathbf{T}}(\partial \mathbf{d}/\partial \mathbf{x})\mathbf{b}}$$

with

$$\mathbf{d} = -\frac{\partial \mathbf{f}}{\partial \mathbf{x}}\mathbf{b}$$

It can be verified that for all kinetics (4.12) the denominator of the singular control $u_{sing}(t)$ is different from zero. Obviously, this is a singular control problem of *order 2*. Since both the numerator and the denominator are *linear* in the costate variables $\boldsymbol{\lambda}$ and there exist 3 linear homogeneous equations between them, we know that the optimal control along a singular arc is a *nonlinear feedback law of the state variables* $\mathbf{x}$ *only*. These 3 equations are :

$$\begin{aligned} \psi \equiv \boldsymbol{\lambda}^T\mathbf{b} &= 0 \\ \frac{d\psi}{dt} \equiv \boldsymbol{\lambda}^T\mathbf{d} &= 0 \\ \phi \equiv \boldsymbol{\lambda}^T\mathbf{f} &= 0 \end{aligned}$$

For this problem, it can be seen that λ_4 has disappeared from $u_{sing}(t)$, as $f_4 \equiv 0$. So the first equation can be omitted, and the last two can be solved as follows :

$$\begin{pmatrix} f_1 & f_2 \\ \beta_1 & \beta_2 \end{pmatrix} \begin{pmatrix} \lambda_1 \\ \lambda_2 \end{pmatrix} = -\begin{pmatrix} f_3 \\ \beta_3 \end{pmatrix} \lambda_3$$

with

$$\beta_i \triangleq b_1\frac{\partial f_i}{\partial x_1} + b_4\frac{\partial f_i}{\partial x_4},\ i = 1, \ldots, 3$$

Consider the case of an unbounded input u and an unconstrained state vector $\mathbf{x}$. As shown in Chapter 3 the problem reduces to the *two dimensional optimization of the initial amount of substrate* S_0 *and the time instant* t_2 *at which the switch from batch to singular control occurs*, the optimal control sequence being *batch – singular arc – batch*. In case of a constraint on u and/or $\mathbf{x}$, only some minor modifications are required, the algorithm itself remaining a two dimensional search.

S_0	t_2	t_3	t_f	P_f
200000	68.064	69.373	69.440	2962.88
205000	68.384	68.501	68.568	2795.38
205500	68.482	68.482	68.482	2778.63

Table 4.3: Extremal values for S_0 near α for $B = 10^{-11}$

SIMULATION RESULTS

We now present some results obtained with the computational algorithm of Chapter 3. We concentrate on 2 specific values of the parameter B : $B = 10^{-11}$ as an approximation of the original Blackman type kinetics (4.3), and the other extremal value $B = \mu_{crit} = 10^{-2}$ where $\pi(\mu)$ reduces to the Monod type law (4.13).

$\boxed{B = 10^{-11}}$

In Figure 4.5 we have visualized the actions taken by the computational algorithm for $B = 10^{-11}$. For every S_0, the optimal switch time t_2 has been calculated. As a consequence, we obtain the corresponding values for $P(t_f)$ and t_f. Clearly, the optimal couple (S_0^*, t_2^*) is the one which maximizes $P(t_f)$. Observe the quadratic behavior of $P(t_f)$ as a function of S_0, so that there exists a *unique optimal* solution to this problem.

Observe that there exists a lower limit S_{min} on the possible values for S_0, corresponding to $t_2 = 0$. In that case, the complete initial state $\mathbf{x}_0$ is on the singular hyperplane, so singular control starts immediately.

The results for S_0 near to its maximum value α are summarized in Table 4.3. We note that the last row corresponds to a process operated completely in batch mode : $t_f \equiv t_3 \equiv t_2$, while $\forall t : u(t) = 0$. Furthermore, it can be checked that even for these large values of S_0, the condition $dP/dt = 0$ is never met *before* $t = t_2$. As a result, the algorithm of Chapter 3 can indeed be applied to the whole possible range $S_0 \in [S_{min}, \alpha]$. A derived benefit is of course that *a good starting value for* S_0 *is not required for the algorithm to converge.*

Some numerical values for the optimal control are summarized in Table 4.4. Figure 4.6 shows the corresponding time profiles.

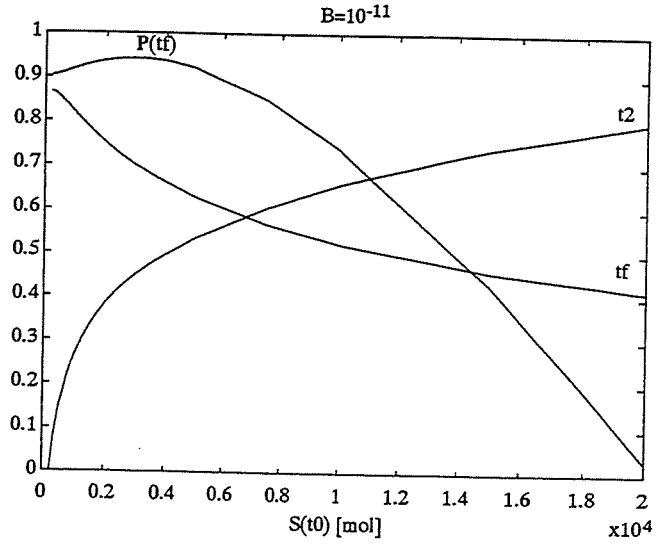

Figure 4.5: Extremal values for $P(t_f)$, t_2 and t_f as functions of S_0 for $B = 10^{-11}$ — Scaling: $t_2/50$, $t_f/500$, $(P(t_f) - 8150)/180$

S_0	G_0	t_2	t_3	t_f	P_f
optimal control					
3000	99100	22.321	349.987	350.101	8319.461
heuristic control					
3000	99100	22.337	350.037	350.151	8319.239

Table 4.4: Optimal and heuristic control results for $B = 10^{-11}$

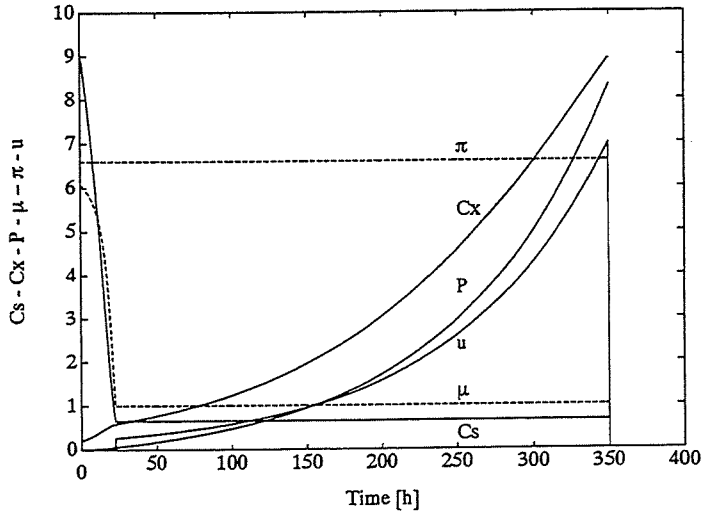

Figure 4.6: Optimal glucose feed rate and corresponding cell, glucose, product, π and μ profiles for $B = 10^{-11}$
Scaling: $C_s * 300$, $C_x * 5$, $P/10^3$, $\mu * 100$, $\pi * 2\ 10^4$, $u/300$

Let us draw the following remarks.

1. From Table 4.4 we note that the optimal initial substrate amount S_0 is rather low as compared with the total amount available $\alpha = 205500$ mol, resulting in a small first batch phase $[0, t_2]$ of 22.32 hrs. In fact the singular interval $[t_2, t_3]$ takes most of total fermentation time t_f. The terminating batch phase $[t_3, t_f]$ is negligible small.
2. From the profiles for $X(t)$ and $P(t)$ (Figure 4.6) we conclude that, although the optimal control algorithm is based on the conjecture of a *biphasic* process, this biphasic behavior has disappeared almost completely, as compared with e.g. the results for the *constant* strategy of Figure 4.3. Principally this is due to the structure of the specific production rate π (4.3), which represents a direct coupling between product synthesis and biomass growth.
3. On the singular arc $[t_2, t_3]$, the optimal control seems to maintain μ at the lowest possible value ($\mu \approx \mu_{crit}$) which still guarantees

the maximum possible value for π. From Theorem 3.1 we know that during singular control $C_s(t)$ [and thus $\mu(t)$ and $\pi(t)$] is time varying as $k_h \neq 0$. However, k_h is so small that the resulting variations in C_s (and thus in μ and π) are in fact negligible so that they cannot be detected on this plot.

4. It is important to see that the optimal control keeps π on its maximum value for all $t < t_3$. This will be at the basis of *suboptimal* profiles presented in one of the next sections.
5. In order to evaluate the performance of the optimal control $u^*(t)$, we need some *reference*. As we do not penalize the total fermentation time t_f in the cost index $J[u, \mathbf{x}_0]$ (4.8), a good choice might be the outcome of a *constant* control with $t_f = t_f^*$, t_f^* denoting the optimal fermentation time. As for convenience, we take $S_{0,ref} = 0$ mol. Then we define the *gain* $\mathcal{G}$ [%] as follows :

$$\mathcal{G} \triangleq 100 \times \frac{J[u^*, \mathbf{x}_0^*] - J[u_{ref}, \mathbf{x}_{0,ref}](t_f = t_f^*)}{J[u_{ref}, \mathbf{x}_{0,ref}](t_f = t_f^*)} \ \% \qquad (4.16)$$

For $B = 10^{-11}$, a constant control during 350.101 hrs with $S_0 = 0$ produces 1981.283 mol penicillin. So for the optimal control $u^*(t) \equiv u^*(B = 0, t)$ we obtain a *gain* $\mathcal{G} = 319.9$ %.
Consider now a constant feed rate strategy. Optimizing the initial substrate amount S_0 and the final time t_f leads to : $S_0 = 90.156$ mol, $t_f = 129.688$ hrs, and $P_f = 3779.012$ mol. Observe that the optimal final amount is still far away from the optimal control result. From this simple parametric optimization (see also Section 1.2.2) we can conclude that *this model is very sensitive towards different feeding policies.* ■

Observe the enormous increase in the final product amount $P(t_f)$, which may suggest some questions concerning the validity of the model of Heijnen *et al.* [1979] under conditions imposed by applying the optimal feed rate. As up to now the penicillin fermentation has been recognized through all experiments as an intrinsically *biphasic* process, it seems unlikely that the obtained control put into practice would result in a quasi *monophasic* fermentation, producing such a high gain. We conclude that the results obtained using optimal control theory suggest some possible shortcomings in this model. A deeper study of this model in comparison with the model of Bajpai and Reuß [1980,1981] (to be discussed in Section 4.3) is the subject of Chapter 5.

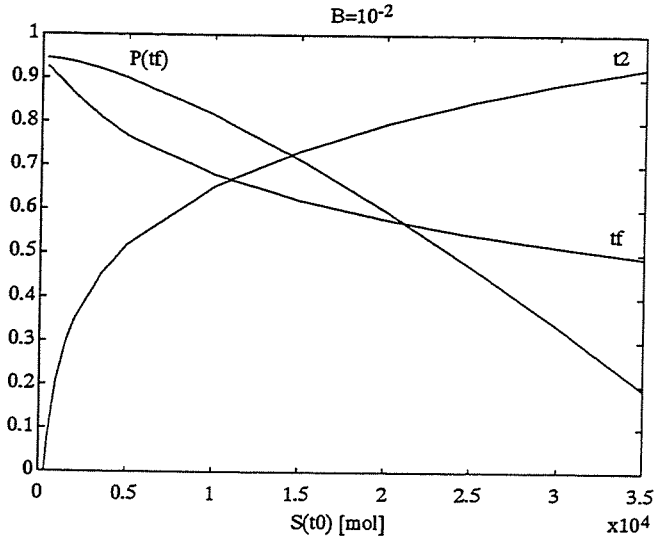

Figure 4.7: Extremal values for $P(t_f)$, t_2 and t_f as functions of S_0 for $B = \mu_{crit} = 10^{-2}$
Scaling: $t_2/50$, $t_f/300$, $(P(t_f) - 4300)/280$

$\boxed{B = \mu_{crit} = 10^{-2}}$

We now give the analogous results for the other extreme $B = \mu_{crit} = 10^{-2}$, in order to demonstrate that the algorithm presented in Chapter 3 can be applied to *every* model with B between $0 < B \leq \mu_{crit}$. Figure 4.7 shows the evolution of t_2, and thus $P(t_f)$ and t_f, as functions of S_0. Observe that the optimal couple (S_0^*, t_2^*) corresponds to $t_2 = 0$, in other words the optimal initial state lies on the singular hyperplane itself. As a consequence, the separation between *growth*– and *production*–phase has disappeared completely. This is also illustrated by the time profiles of Figure 4.8. In this case, both σ (and thus μ_{substr}) and π are of Monod type : the corner point in π has disappeared completely (see Figure 4.4). However, the optimal solution does *not* consist of adding all substrate available at $t = 0$ followed by a batch phase, as could be expected at first sight from the results of Section 3.4. The main reason

S_0	t_2	t_3	t_f	P_f
200000	67.833	69.114	69.184	2505.80
205000	68.152	68.267	68.335	2442.59
205500	68.252	68.252	68.252	2436.26

Table 4.5: Extremal values for S_0 near α for $B = \mu_{crit} = 10^{-2}$

S_0	G_0	t_2	t_3	t_f	P_f
optimal control					
326	98137.36	0.	277.205	277.320	4564.455
heuristic control with $\mu_{switch} = \mu_{crit}$					
7000	100540	29.573	292.890	292.995	4399.589
heuristic control with μ_{switch} *free*					
1000	98380	12.225	304.665	304.792	4553.437

Table 4.6: Optimal and heuristic control results for $B = \mu_{crit} = 10^{-2}$

is the following. Combining equations (4.2) and (4.4) with (4.13), we can verify that the resulting expression for π as a function of C_s does *not* satisfy an equation of the form :

$$\pi(C_s) = Y_{p/x}\mu(C_s)$$

For this value of B the lower limit S_{min} is equal to the optimal value S_0^*. Table 4.5 shows the results for S_0 near to its maximum value α. Note again that the condition $dP/dt = 0$ is never met *before* $t = t_2$, so we can indeed apply the proposed algorithm to the whole interval $S_0 \in [S_{min}, \alpha]$. Some numerical values for the optimal control are summarized in Table 4.6.

Observe that on the singular arc, the variations of π and μ (and thus of C_s) with respect to time are more pronounced than in the case of $B = 10^{-11}$, although k_h has not been changed. We conclude that the *model structure* itself plays also an important role in the amplitude of these variations.

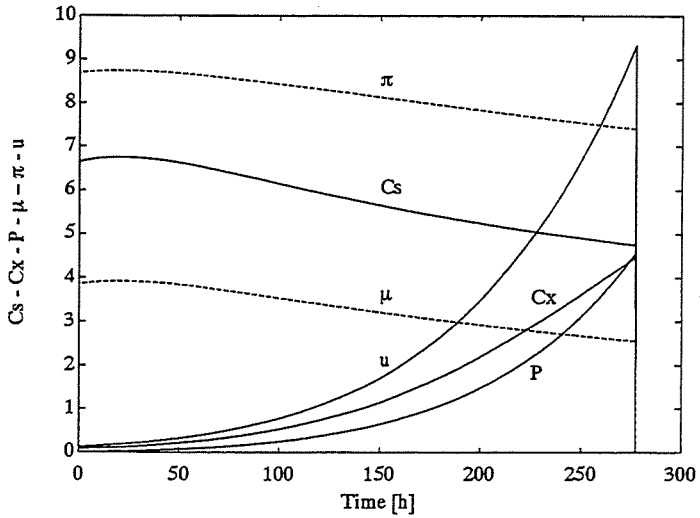

Figure 4.8: Optimal glucose feed rate and corresponding cell, glucose, product, π and μ profiles for $B = \mu_{crit} = 10^{-2}$
Scaling: $C_s * 2\ 10^3$, $C_x * 2$, $P/10^3$, $\mu * 200$, $\pi * 4\ 10^4$, $u/300$

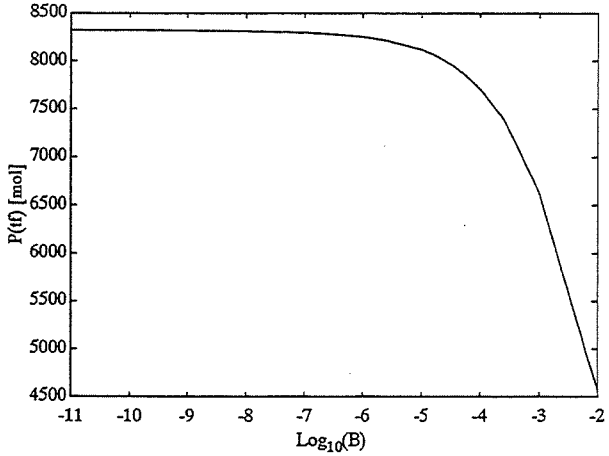

Figure 4.9: Optimal production $P(t_f)$ as a function of B

A *constant* strategy during 277.320 hrs with $S_0 = 0$ mol produces 1978.425 mol penicillin, so the gain using the optimal control is $\mathcal{G} = 130.7$ %.

$\boxed{0 < B \leq \mu_{crit}}$

As already mentioned, we can repeat these calculations for every B within the given boundaries. The result for the optimal production $P(t_f)$ as a function of parameter B is shown in Figure 4.9, as an illustration of Conjecture 1.1. From this plot we conclude that the sequence of optimal controls $u^*(B,t)$ is indeed convergent. Note also that for $B < 10^{-9}$ the cost has almost reached its limit value.

4.2.6 Physical interpretation of singular control

We already pointed out that the three specific rates σ (4.2), π (4.3) and μ (4.4) are functions of the substrate concentration C_s only. However, due to the corner point in π, these kinetics are not continuously differentiable for every value of C_s. As a result, the Theorems of Section 3.6 can not be used to characterize the singular control arc when using the original Heijnen *et al.* model.

On the other hand, the family of production kinetics (4.12) is sufficiently smooth to guarantee the applicability of these Theorems. For the original model we prove the following Theorem.

Theorem 4.1

Consider the minimization of performance index (4.8) subject to the dynamic constraint (4.6). Suppose that the specific rates are modeled by equations (4.2), (4.3) and (4.4) which are continuous piecewise smooth functions of the substrate concentration.

Then during singular control the substrate concentration remains constant if and only if the hydrolysis constant $k_h = 0$, and is determined by the equation :

$$\mu = \mu_{crit}$$

This constant value maximizes the yield π/σ.

PROOF

In the following, a prime denotes derivation with respect to substrate concentration C_s.
For every value of the parameter B in the half open interval $]0, \mu_{crit}]$, the specific rates (4.2), (4.4) and (4.12) are smooth functions of the substrate concentration C_s only.

Following the results of Theorem 3.1, we know that on the singular interval C_s remains constant if and only if $k_h = 0$. C_s satisfies :

$$\pi'\sigma - \sigma'\pi = 0 \tag{4.17}$$

We have :

$$\frac{d\pi}{dC_s} = \frac{d\pi}{d\mu}\frac{d\mu}{dC_s}$$

Using equation (4.4)

$$\frac{d\mu}{dC_s} = Y_{x/s}\left(\frac{d\sigma}{dC_s} - \frac{1}{Y_{p/s}}\frac{d\pi}{dC_s}\right)$$

we obtain a relation between π' and σ', which can be written as follows:

$$\pi' = F(\mu, B)\sigma' \tag{4.18}$$

with

$$F(\mu,B) \triangleq \frac{Q_{p,max}Y_{x/s}[1-(\mu-\mu_{crit}+2B)/R(\mu,B)]/[2(\mu_{crit}-B)]}{1+Q_{p,max}Y_{x/s}[1-(\mu-\mu_{crit}+2B)/R(\mu,B)]/[2(\mu_{crit}-B)Y_{p/s}]}$$

$$R(\mu,B) \triangleq \sqrt{(\mu+\mu_{crit})^2 - 4(\mu_{crit}-B)\mu}$$

Substituting (4.18) in (4.17) and noting that $\sigma' \neq 0$ we obtain :

$$F(\mu,B)\left(\frac{\mu}{Y_{x/s}} + m + \frac{\pi}{Y_{p/s}}\right) = \pi$$

We now follow a similar way of reasoning as used in the determination of the optimal control for the model involving the original kinetics (4.3) starting from a model with smooth kinetics (4.12) (see Conjecture 1.1). So we consider the limit for $B \stackrel{>}{\to} 0$ in both sides of the above equation to obtain :

$$Y_{x/s}[\mid \mu - \mu_{crit} \mid -(\mu - \mu_{crit})][\frac{\mu}{Y_{x/s}} + m + \frac{Q_{p,max}}{2Y_{p/s}\mu_{crit}}(\mu + \mu_{crit} - \mid \mu - \mu_{crit} \mid)] =$$

$$[\mu + \mu_{crit} - \mid \mu - \mu_{crit} \mid][\mid \mu - \mu_{crit} \mid + \frac{Y_{x/s}Q_{p,max}}{2Y_{p/s}\mu_{crit}}(\mid \mu - \mu_{crit} \mid -(\mu - \mu_{crit}))]$$

Solving for μ obviously leads to:

$$\mu = \mu_{crit}$$

Using equation (4.4), the substrate concentration during singular control is :

$$C_{s,sing} = K_s \frac{\mu_{crit}/Y_{x/s} + m + Q_{p,max}/Y_{p/s}}{Q_{s,max} - (\mu_{crit}/Y_{x/s} + m + Q_{p,max}/Y_{p/s})} \equiv C_{s,crit}$$

Figure 4.10 shows values of π/σ as a function of C_s, for different values of B. We conclude that for $B = 0$, π/σ takes on its maximum value at $C_s = C_{s,crit}$.

■

In Figure 4.11 we show the optimal value for μ and the corresponding value C_s [calculated using (4.17)] at which to switch from batch to singular control, for different values of B with $k_h = 0$. Observe the convergence to $\mu \to \mu_{crit}$, $C_s \to C_{s,crit}$ as $B \to 0$ as indicated by Theorem 4.1. Observe that for $B = \mu_{crit} = 10^{-2}$, π/σ exhibits a (very smooth) maximum, corresponding to a finite value of $C_{s,switch}$. This is a simple verification that the optimal control in this case is not a simple batch process while adding all available substrate α at $t = 0$, as might have been expected.

These plots also illustrate again that setting $B = 10^{-11}$ in (4.12) is a very accurate approximation of the original kinetics (4.3).

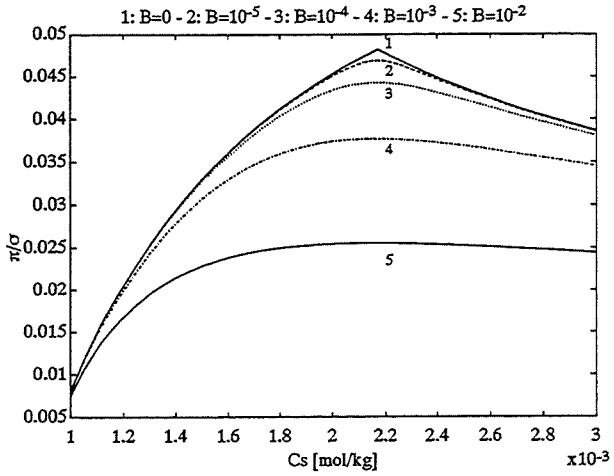

Figure 4.10: π/σ as a function of C_s for some values of B

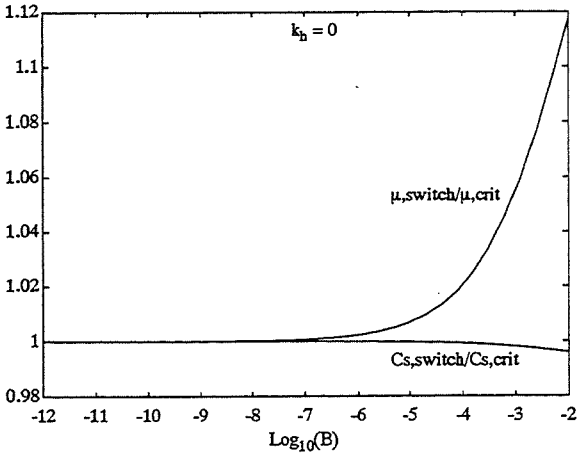

Figure 4.11: Optimal switch values for μ and C_s as a function of B with $k_h = 0$

In general, hydrolysis $k_h \neq 0$, so we do not know the switch time t_2 in *closed loop* form, i.e. as function of state variables only. However, the above Theorem provides a good initial guess for t_2 if k_h is sufficiently small. It also indicates that during singular control, the substrate concentration will be time varying. Of course for small k_h, this time dependence will be small also, as illustrated by the simulation results presented earlier.

4.2.7 Heuristic control strategies

In this section we propose *heuristic* control strategies based on microbial and mathematical knowledge, following a same line of reasoning as presented in Section 3.7. We indicate the conditions under which the suboptimal solution coincides with the *optimal* one.

As there is no need for partial derivatives, the original model ($B = 0$) can be handled directly without any difficulty : as a matter of fact, the presence of a corner in the production kinetics (4.3) facilitates the design of a suboptimal controller.

From the *microbiological and experimental* point of view, the construction of a suboptimal profile can be based on the concept of a *biphasic* fermentation process.

growth phase $[0, t_2]$

During the growth phase we focus on the specific growth rate μ (4.4). For the control needed we refer to the optimal control results : in case of an unbounded input and an unconstrained state vector the growth phase is a *batch* phase. All substrate consumed for growth is added all at once at time $t = 0$ in order to obtain the highest possible value of μ. Note that for the original specific production rate (4.3) this results in maximizing π also. In case of a constraint on the input and/or the state some minor modifications are required.

production phase $[t_2, t_3]$

During production we focus on the specific production rate π.

- *Original model.* Equation (4.3) indicates that the lowest value of μ which still guarantees the maximum value of π is $\mu = \mu_{crit}$. Note that this is equivalent to $C_s = C_{s,crit}$, so the control during production is of the form :

$$u_{production}(t) = \frac{C_{s,in}\sigma X}{C_{s,in} - C_s} \tag{4.19}$$

maintaining C_s (and thus μ) at their critical values. This choice can also be motivated from the analysis of the optimal control result (see Figure 4.6). As a consequence, the conjunction point t_2 of growth and production follows from the condition :

$$C_s(t_2) = C_{s,crit} \qquad \text{or} \qquad \mu(t_2) = \mu_{crit}$$

The control (4.19) is stopped at $t = t_3$ when all substrate is used [see (4.9) and (4.10)]. As in the optimal case, the final *batch* phase $[t_3, t_f]$ is stopped when $dP/dt = 0$. Note that the complete suboptimal control is obtained in *closed loop* for a given initial substrate amount S_0. As a result, the optimization problem is reduced to the *one dimensional optimization of* S_0.

- *Modified model.* For values of B in the interval $0 < B \leq \mu_{crit}$ it is less clear how to determine a heuristic control during production as the specific production rate π (4.12) has no corner point anymore. However, we will verify that keeping C_s, and thus μ, *constant* using a control of the form (4.19) is an appropriate choice for this case also.

  The switch from growth to production could be determined as follows. As a first guess, we can still switch on $C_s = C_{s,crit}$ and thus $\mu = \mu_{crit}$. However, we know from Section 4.2.6 and Figure 4.11 that this guess is only appropriate for B near 0. For B near μ_{crit}, we will simply optimize the switch time t_2. As in the optimal control case, we obtain a *two dimensional optimization of* S_0 *and* t_2.

As a *mathematical justification*, it follows immediately from Theorem 4.1 that the suboptimal control profile for the original model reduces to the optimal profile if (and only if) $B = 0$ and $k_h = 0$.

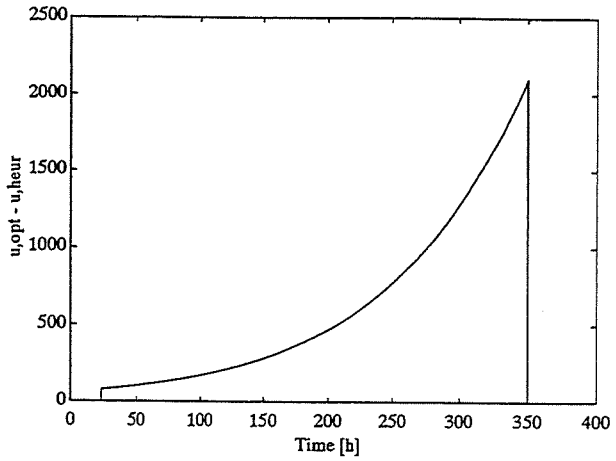

Figure 4.12: Optimal and suboptimal glucose feed rate for $B = 10^{-11}$
Legend: —: optimal control, – –: heuristic control

SIMULATION RESULTS

$\boxed{B = 10^{-11}}$

Some numerical values are summarized in Table 4.4. Figure 4.12 compares the suboptimal and optimal control profiles. From these we conclude that for the original model, the *suboptimal control results almost coincide with the optimal values*, thanks to the low value of k_h.

$\boxed{B = \mu_{crit} = 10^{-2}}$

For $\pi(\mu)$ modeled by the Monod type kinetics (4.13), the results are summarized in Table 4.6 and Figures 4.13 to 4.15. We have done the optimization with $\mu_{switch} = \mu_{crit}$ (Figure 4.13) and μ_{switch} considered *free* (Figure 4.14). Optimal and suboptimal feed rates are compared in Figure 4.15. Note that —in contrast with the *optimal* profile— for both suboptimal profiles there is still an initial batch–phase. For $\mu_{switch} = \mu_{crit}$ the final amount P_f reaches 96.39 % of the optimal value. For μ_{switch} considered *free* we obtain as much as 99.77 % of the

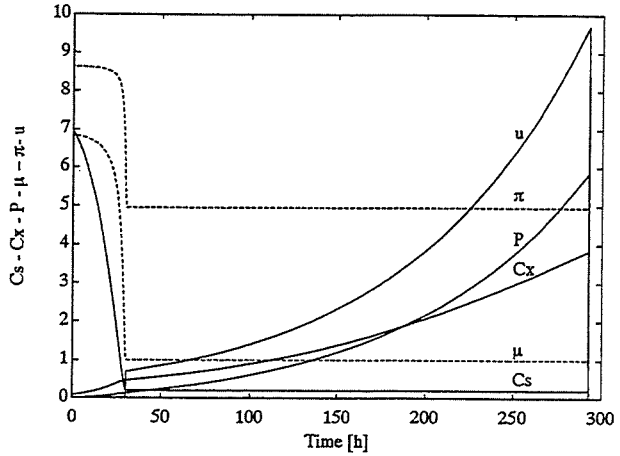

Figure 4.13: Suboptimal glucose feed rate and corresponding cell, glucose, product, π and μ profiles for $B = \mu_{crit} = 10^{-2}$ and $\mu_{switch} = \mu_{crit}$
Scaling: $C_s * 10^2$, $C_x * 2$, $P/750$, $\mu * 100$, $\pi * 3\ 10^4$, $u/220$

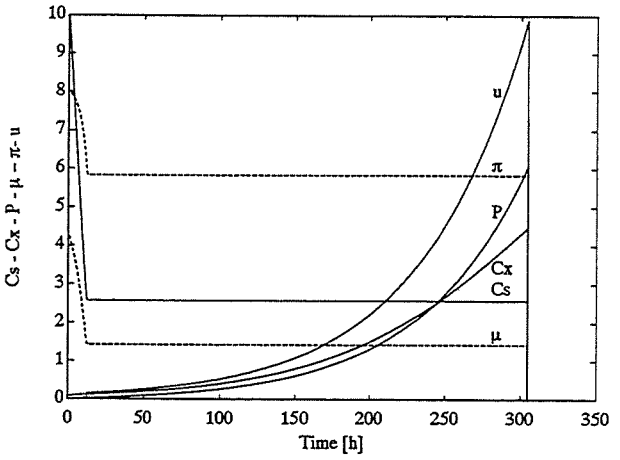

Figure 4.14: Suboptimal glucose feed rate and corresponding cell, glucose, product, π and μ profiles for $B = \mu_{crit} = 10^{-2}$ and μ_{switch} free
Scaling: $C_s * 10^3$, $C_x * 2$, $P/750$, $\mu * 100$, $\pi * 3\ 10^4$, $u/300$

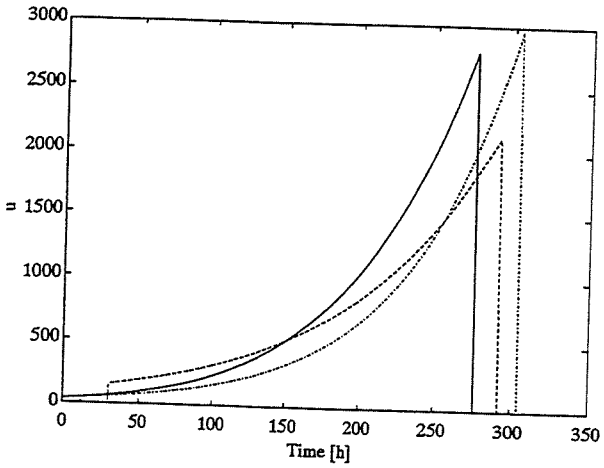

Figure 4.15: Optimal and suboptimal glucose feed rate for $B = \mu_{crit} = 10^{-2}$ Legend: —: optimal control, – –: heuristic control with $\mu_{switch} = \mu_{crit}$, – · –: heuristic control with μ_{switch} free

optimal value. These results sufficiently illustrate the performance of the suboptimal profiles over the whole range of parameter B.

Before formulating some conclusions we first give a remark. Although the only model reported in the literature is the one with $B = 0$, we also presented some simulation results for other values of B. This can be motivated as follows. First of all, from the biochemical point of view a sharp corner in π at $\mu = \mu_{crit}$ is of course only a first approximation of real life fermentation conditions. So a value for B different from zero seems more realistic. Secondly, these results make it possible to illustrate the convergence of the controls to the desired one following the basic Conjecture 1.1, see e.g. Figure 4.9. Finally, they confirm the use of the developed algorithms for optimal and suboptimal control not only for the original model, but for the whole class of models considered.

4.2.8 Conclusions

We can extract the following results from the application of optimal control theory to the penicillin G fed–batch fermentation process using the unstructured mathematical model of Heijnen *et al.* [1979] and a newly developed modified version.

1. We verified and confirmed the statement by Heijnen *et al.* that the *glucose feed scheme is of crucial importance in obtaining high penicillin yields.* In order to do so, we determined for the first time the optimal control profile for a well–defined optimization problem using their model and the modified version. We have shown that the obtained control generated the global optimum of the performance measure we have considered, using an algorithm developed in Chapter 3. Simulation results indicate a possible gain of several hundreds percents as compared with the outcome of a constant control input with zero initial substrate amount during the same time. Furthermore, this model is very sensitive towards different feeding policies.

2. From the mathematical point of view, we presented the application of a new, elegant Conjecture that allows for the determination of optimal control profiles for a class of piecewise smooth models that cannot be handled using standard optimal control theory. As this kind of models is not limited to the biotechnological field itself, this procedure can be of great use in a lot of other scientific domains also. Furthermore, we were able to include the unusual optimization of some initial states in the resulting two point boundary value problem.

3. In the field of model building, the results obtained using optimal control theory indicated some possible shortcomings in the model used, without carrying out any costly and time consuming experiments. The combination of the enormous gains in production and the vanishing of the characteristic biphasic behavior through optimization, made us conclude that the present model might be less useful for advanced control purposes than suggested by Heijnen *et al.* This motivates the deeper study of this model presented in Chapter 5.

4. We have shown that the heuristic control algorithms developed in Chapter 3 are a successful alternative for the optimal control using essentially the same computational algorithm, for the whole family of models considered. From the characterization of the singular arc in the optimal control solution, we derived conditions under which this heuristic strategy coincides with the optimal control.

4.3 The model of Bajpai and Reuß

4.3.1 Mathematical description

Bajpai and Reuß [1980,1981] describe the penicillin G fed–batch fermentation process by means of the following unstructured model which has the general form (3.1) :

$$\begin{aligned}
\frac{dS}{dt} &= -\sigma X + C_{s,in}u \\
\frac{dX}{dt} &= \mu X \\
\frac{dP}{dt} &= \pi X - k_h P \\
\frac{dV}{dt} &= u
\end{aligned}$$

with

S	: amount of substrate (glucose) in broth	[g]
X	: amount of cell mass in broth	[g dry weight]
P	: amount of product (penicillin) in broth	[g]
V	: volume of the liquid phase in the fermentor	[L]
u	: input substrate feed rate	[L/h]
$C_{s,in}$	: glucose concentration in feed stream	[g/L]
σ	: specific substrate consumption rate	[g/g dry weight h]
μ	: specific growth rate	[1/h]
π	: specific production rate	[g/g dry weight h]
k_h	: penicillin hydrolysis or degradation constant	[1/h]

This model is written in a [g,L] unit system as proposed in Chapter 3 : concentrations are expressed with respect to the volume of the liquid phase V. Dissolved oxygen is considered non–limiting, by maintaining a sufficiently high aeration level. For more details we refer to [Bajpai and Reuß 1980,1981].

The specific rates are modeled as follows.

1. The specific growth rate μ is modeled using *Contois* kinetics (1.18) :

$$\mu \equiv \mu_{substr} = \mu_C \frac{C_s}{K_x C_x + C_s} \tag{4.20}$$

with

μ_C	: maximum specific growth rate for Contois kinetics	[1/h]
K_x	: Contois saturation constant for substrate limitation of biomass production	[g/g dry weight]

2. For the specific production rate π a *Haldane* type substrate inhibition kinetics is used (1.17) :

$$\pi = \pi_m \frac{C_s}{K_p + C_s + C_s^2/K_i} \tag{4.21}$$

with

π_m	: specific production constant	[g/g dry weight h]
K_p	: Monod saturation constant for substrate limitation of product formation	[g/L]
K_i	: substrate inhibition constant for product formation	[g/L]

Even though the exact nature of the biochemical mechanism involved for regulation (catabolite repression/inhibition) is not yet completely known, Bajpai and Reuß decided to disregard the differences between time constants for the two regulation mechanisms due to relatively very long fermentations, and the inhibition kinetics was assumed to represent both. Hydrolysis of penicillin to penicilloic acid is modeled by a first order decay reaction with rate constant k_h. However, it is clear that k_h can also represent —in addition to this product decay (which is of chemical nature)— several other uncertain phenomena, e.g. reduction in synthesis rate due to gradual accumulation of some unknown toxic inhibitor produced along with the desired product.

parameters					
	Set 1	*Set 2*		*Set 1*	*Set 2*
μ_C	0.092	0.11	K_x	0.15	0.006
π_m	0.005	0.004	k_h	0.04	0.01
K_p	0.0002	0.0001	K_i	0.1	0.1
$Y_{x/s}$	0.45	0.47	$Y_{p/s}$	0.9	1.2
m	0.014	0.029	$C_{s,in}$	500	500
initial conditions					
X_0	10.5		S_0	*to be specified*	
P_0	0		V_0	$7 + S_0/C_{s,in}$	
t_0	0		α	1500	

Table 4.7: Parameters and initial conditions used in simulations

3. The specific substrate consumption rate σ follows then from (1.11) :

$$\sigma = \mu/Y_{x/s} + m + \pi/Y_{p/s} \tag{4.22}$$

which represents a *maintenance* metabolism [Pirt 1965] : $f_m = f_p = 0$ in equation (1.10).

Bajpai and Reuß have reported two *parameter sets*, according to different experimental results. They are shown in Table 4.7, together with the *initial* conditions we will use in all simulations.

The results of a simulation with a *constant* feed rate profile using parameter Set 2 are shown in Figure 4.16. With $S_0 = 0$ g and $t_f = 120$ hrs, u equals 0.025 L/h if the available amount of substrate $\alpha = 1500$ g. The final amount of penicillin is $P(t_f) = 59.65$ g. Some comments are in order here.

1. This model has been shown to exhibit most of the features of penicillin fermentation as reported in the literature. The fermentation clearly behaves as a *biphasic* process : a *growth* phase of rapid cell growth and almost no production, followed by a *production* phase with decreasing specific growth rate.

2. The functional relationships describing the specific rates (4.20) and (4.21) are essentially based on microbiological knowledge. Obviously, this is a process with monotonic specific growth rate μ and non–monotonic specific production rate π.

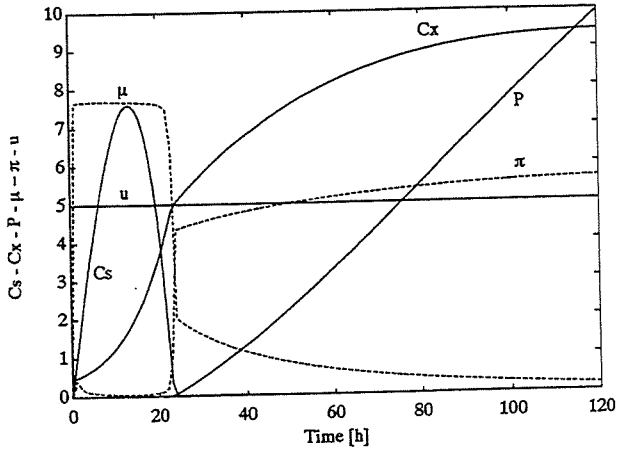

Figure 4.16: Constant glucose feed rate and corresponding cell, glucose, product, μ and π profiles, for μ Contois and parameter Set 2
Scaling: $C_x/3.5$, $C_s/1.5$, $P/6$, $\mu * 70$, $\pi * 1500$, $u * 200$

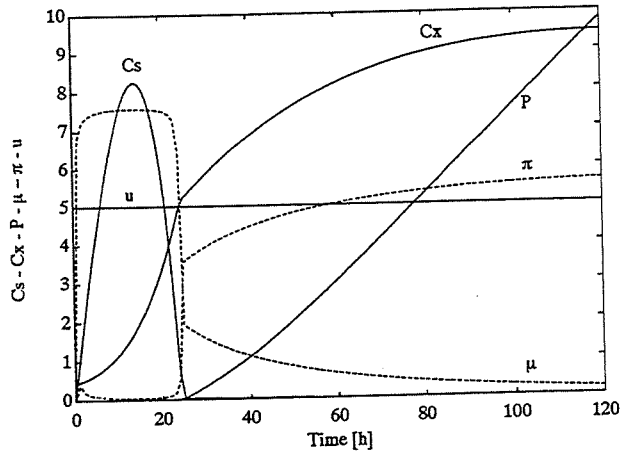

Figure 4.17: Constant glucose feed rate and corresponding cell, glucose, product, μ and π profiles, for μ Monod and parameter Set 2
Scaling: $C_x/3.5$, $C_s/1.5$, $P/6$, $\mu * 70$, $\pi * 1500$, $u * 200$

3. Bajpai and Reuß argue that their model fits adequately experimental data available in the literature. Parameter Set 1 was used to verify experimental data reported by Pirt and Righelato [1967] and Hosler and Johnson [1953], who employed a relatively simple feed rate strategy. Parameter Set 2 was used to simulate the experimental data reported by Mou [1979], who controlled the feed rate to achieve a predecided growth pattern.

As already mentioned in Section 4.2, from the mathematical point of view the commonly observed separation between growth and production phase is a quite useful feature in optimizing the process.

4.3.2 A variant for the growth kinetics

Based on some experimental evidence, Bajpai and Reuß [1980,1981] preferred Contois kinetics (4.20) over Monod kinetics (1.14) in modeling the specific growth rate μ. One reason is that at high cell densities serious diffusional limitations can be expected which would cause the apparent value of the saturation constant K_s in Monod kinetics to be higher than its value at lower cell densities. In Contois kinetics this behavior is modeled by the term $K_x C_x$ in the denominator.
However, *both* kinetics have been shown to be valid for fungal growth [Nihtilä and Virkkunen 1977]. From the *mathematical* point of view, it is interesting to consider Monod kinetics as well, as all specific rates then become functions of substrate concentration C_s only.
So a useful alternative for (4.20) is :

$$\mu = \mu_M \frac{C_s}{K_s + C_s} \tag{4.23}$$

with

μ_M	: maximum specific growth rate for Monod kinetics	[1/h]
K_s	: Monod saturation constant for substrate limitation of biomass production	[g/L]

The equivalent kinetic constants μ_M and K_s can be calculated from the following equations :

$$\mu_M = \mu_C \frac{1}{1 - Y_{x/s} K_x} \tag{4.24}$$

$$K_s = K_x \frac{Y_{x/s}}{1 - Y_{x/s} K_x} (C_s(0) + C_x(0)/Y_{x/s}) \tag{4.25}$$

This can be shown as follows.

We make the following assumptions :

1. The process is operated in *batch*, i.e. $u(t) = 0$.
2. We consider only microbial growth without product synthesis; maintenance demands are considered negligible.

Then the general model equations (3.2) can be simplified to (we prefer here to use concentrations as independent variables) :

$$\begin{aligned} \frac{dC_s}{dt} &= -\mu C_x / Y_{x/s} \\ \frac{dC_x}{dt} &= \mu C_x \end{aligned} \tag{4.26}$$

or in other words :

$$dC_x = -Y_{x/s} dC_s$$

Integrating from $t_0 = 0$ on yields :

$$C_s = (C_x(0) - C_x)/Y_{x/s} + C_s(0) \tag{4.27}$$

In case of Monod kinetics (4.23) and using (4.27), we obtain from model equation (4.26) :

$$\mu_M dt = \frac{K_s}{C_s(0) - [C_x - C_x(0)]/Y_{x/s}} \frac{dC_x}{C_x} + \frac{dC_x}{C_x}$$

Integrating from $t_0 = 0$ on yields :

$$\begin{aligned} \mu_M t = &(1 + \frac{K_s}{C_s(0) + C_x(0)/Y_{x/s}}) \ln \frac{C_x}{C_x(0)} \\ &+ \frac{K_s}{C_s(0) + C_x(0)/Y_{x/s}} \ln \frac{C_s(0)}{C_s(0) - [C_x - C_x(0)]/Y_{x/s}} \end{aligned} \tag{4.28}$$

In case of Contois kinetics analogous manipulations lead to :

$$\mu_C t = \ln \frac{C_x}{C_x(0)} + Y_{x/s} K_x \ln \frac{C_s(0)}{C_s(0) - [C_x - C_x(0)]/Y_{x/s}} \tag{4.29}$$

Requiring that for all time instants t in (4.28) and (4.29) the biomass concentration C_x must be equal we obtain the conversion formulas (4.24) and (4.25). The inverse formulas are :

$$\begin{aligned} K_s &= K_x \frac{Y_{x/s}}{1 - Y_{x/s} K_x} (C_s(0) + C_x(0)/Y_{x/s}) \\ \mu_M &= \mu_C \frac{1}{1 - Y_{x/s} K_x} \end{aligned}$$

■

Observe that K_s depends on the initial state. If for instance $S_0 = 560$ g [so from Table 4.7 $V_0 = 8.12$ L] and $X_0 = 10.5$ g, we obtain using parameter Set 2 of Table 4.7 :

$$\begin{aligned} \mu_M &= 0.110 \\ K_s &= 0.203 \end{aligned}$$

For simplicity, we will use these values in all simulations involving Monod kinetics.

Extensive simulations confirm that the transition from Contois (4.20) to Monod (4.23) kinetics does not cause fundamental changes in the dynamics of the variables, even if the reactor is not operated in batch or if the dependence of the conversion formulas on the initial state is neglected. As an example, in Figure 4.17 the simulation results using the same initial and operational conditions as in Figure 4.16 are shown. The final amount of product is $P(t_f) = 58.77$ g.

4.3.3 Statement of the optimization problem

In order to make comparison possible with the results obtained in Section 4.2 using the Heijnen *et al.* model, we will solve exactly the same optimization problem as stated in Section 4.2.3. It can be summarized as follows (see also Chapter 3) :

State space model

$$\frac{d\mathbf{x}}{dt} = \mathbf{f}(\mathbf{x}) + \mathbf{b}\, u \tag{4.30}$$

with $\mathbf{x}$, $\mathbf{f}$ and $\mathbf{b}$ as defined in Section 3.2.2.

Initial conditions

Numerical values for the initial conditions $x_2(0)$ and $x_3(0)$ are given in Table 4.7. The initial amount of substrate $x_1(0)$ and the initial volume $x_4(0)$ are related by :

$$x_4(0) = V_* + x_1(0)/C_{s,in} \tag{4.31}$$

where V_* denotes the given initial volume *without* substrate [$V_* = 7$ L (Table 4.7)]. Note that glucose is added as a solution with concentration $C_{s,in}$.

Performance index

The optimization problem is to determine for the given set of differential equations (4.30) the optimal initial state $\mathbf{x}_0^*$ and the optimal feed rate profile $u^*(t)$ that minimize the performance index

$$J[u, \mathbf{x}_0] = g[\mathbf{x}(t_f)] \triangleq -x_3(t_f) \tag{4.32}$$

i.e. maximize the final amount of product.

Constraints

1. $t_0 = 0$, t_f is *free*.
2. All variables have to be kept positive :

$$\forall t \in [0, t_f] : \quad x_i(t) \geq 0, \text{ for } i = 1, \ldots, 4 \quad \wedge \quad u(t) \geq 0$$

3. The total amount of substrate available α is fixed, i.e. :

$$x_1(0) + C_{s,in} \int_{t_0}^{t_f} u(t)\, dt = \alpha \tag{4.33}$$

$$\Updownarrow$$

$$x_4(t_f) \equiv V(t_f) = V_f, \; V_f \text{ fixed} \tag{4.34}$$

Based on simulations, Bajpai and Reuß [1981] evaluated the impact of four different strategies of glucose feeding. These were (i) constant glucose feed rate, (ii) constant specific glucose feed rate in grams of glucose per gram of cell mass per hour, (iii) controlled glucose feeding in order to obtain a constant glucose concentration in the system during production phase, and (iv) controlled glucose feeding so as to reproduce a predecided growth pattern. Their simulation results indicated that *similar penicillin productivities can*

be obtained using any of these strategies provided fermentations are carried out under optimal conditions corresponding to the strategy chosen. Application of optimal control theory to penicillin G fed–batch fermentation using the model of Bajpai and Reuß has been reported by Lim *et al.* [1986]. Penicillin fermentation was chosen as an example to illustrate the use of some computational algorithms based upon the general characteristics of optimal feed rate profiles [Modak *et al.* 1986].

In the following sections we will optimize the final amount of product with respect to the glucose feeding strategy using two techniques : *parametric optimization* (see Section 1.2.2) and *optimal control theory.* The aim is twofold. First, to verify the results obtained by Bajpai and Reuß. Second, to illustrate that the computational algorithm developed in Chapter 3 is more reliable from the numerical point of view than the one proposed by Lim *et al.* [1986]. Furthermore, the performance of heuristic control strategies as introduced in Section 3.7 will be evaluated.

4.3.4 Polynomial Control

If we propose a feeding strategy of the form :

$$C_{s,in}u(t) = \sum_{i=0}^{N} a_i t^i$$

then the optimization problem stated is equivalent to finding optimal values for the polynomial coefficients a_i, $i = 1 \ldots N$: *parametric optimization* of a controller with *predetermined structure* (see also Section 1.2.2). Observe that there is no guarantee that a parametric–optimal control history is truly optimal or, for that matter, that it is unique in minimizing the cost index J. It often is desirable to use as few control parameters as possible to minimize computations, although increasing the number of parameters may improve the optimality of the result.
Constraint (4.33) can be rewritten as

$$x_1(0) + C_{s,in} \int_{t_0}^{t_3} u(t)\, dt = \alpha$$

with t_3 the last time instant at which $u(t) > 0$ (see also Figure 3.5). Note that after all substrate available α has been added at $t = t_3$, the fermentation continues in *batch* mode [u(t)=0] until the net penicillin formation rate dP/dt becomes equal to zero at time $t = t_f$. Clearly, once α has been fixed, t_3 can

be considered as an additional degree of freedom. Optimizing t_3 implies that not all coefficients a_i are independent, as (4.33) must be satisfied. We can replace the integral constraint (4.33) by the following algebraic constraint :

$$a_0 = \frac{\alpha - x_1(0)}{t_3} - \sum_{i=1}^{N} \frac{a_i}{i+1} t_3^i \qquad (4.35)$$

Obviously, the optimization of the initial substrate amount $x_1(0)$ [and thus of $x_4(0)$ via equation (4.31)] can be easily included in the algorithm.
The combined optimization of a_i, $i = 1 \ldots N$, $x_1(0)$ and t_3 has been done —after an appropriate rescaling— with a minimization algorithm proposed by Brent [1973].

The optimal results for both parameter sets of Table 4.7 are summarized in the upper part of Table 4.8 using Contois kinetics (4.20) for growth. We have considered the following cases : (i) $N = 0$ (constant strategy) with $S_0 \equiv x_1(0)$ and t_3 free, and a_0 calculated using (4.35), and (ii) $N = 1$ (linear strategy) with $x_1(0)$, t_3 and a_1 free. From these results it can be concluded that, especially when using the second parameter set, the addition of more degrees of freedom does not improve the performance in a significant way.

Due to the biphasic behavior of the penicillin fermentation process, there is evidence for a discontinuous optimal substrate feed rate (see e.g. the results obtained for the Heijnen *et al.* model in Section 4.2). Therefore, as another application of parametric optimization, we have also used the orthogonal *Walsh functions series* as admissible control functions [Bonte *et al.* 1989]. However, the results obtained were similar and are not repeated here. This study also provided some additional insights which were helpful in deriving the *heuristic* control algorithms we are using throughout this work.

4.3.5 Optimal control

We now verify whether the performance can be improved by letting the controller structure free.

The Hamiltonian $\mathcal{H}$ for this problem is given by :

$$\mathcal{H} = \boldsymbol{\lambda}^{\mathrm{T}}(\mathbf{f}(\mathbf{x}) + \mathbf{b}u) \triangleq \phi + \psi u \qquad (4.36)$$

with

$$\phi = \lambda_1 f_1 + \lambda_2 f_2 + \lambda_3 f_3 \qquad \psi = C_{s,in}\lambda_1 + \lambda_4$$

Parameters	*Set 1*		*Set 2*	
Polynomial control				
	$N=0$	$N=1$	$N=0$	$N=1$
S_0 (g)	639	672	235	279
a_1 (g/h^2)	–	$4.29\ 10^{-3}$	–	$8.25\ 10^{-3}$
t_3 (hr)	106.093	99.281	131.941	132.042
t_f (hr)	106.094	99.288	131.942	132.044
P_f (g)	42.435	43.730	63.738	63.843
Heuristic C_s-control	$C_s(t_2) = \sqrt{K_p K_i}$			
S_0 (g)	1053		533	
t_2 (hr)	44.457		28.355	
t_f (hr)	96.636		131.323	
P_f (g)	44.926		63.597	
Heuristic C_s-control	$C_s(t_2)$ *optimized*			
S_0 (g)	–		551	
t_2 (hr)	–		28.644	
t_f (hr)	–		131.372	
P_f (g)	–		63.724	
Heuristic μ-control	$\mu(t_2)$ *optimized*			
S_0 (g)	–		551	
t_2 (hr)	–		28.644	
t_f (hr)	–		131.321	
P_f (g)	–		63.736	
Optimal control				
S_0 (g)	1053		528	
t_2 (hr)	44.457		28.271	
t_f (hr)	96.636		132.033	
P_f (g)	44.926		63.846	

Table 4.8: Numerical results for polynomial, heuristic and optimal control using the model of Bajpai and Reuß with Contois kinetics for growth

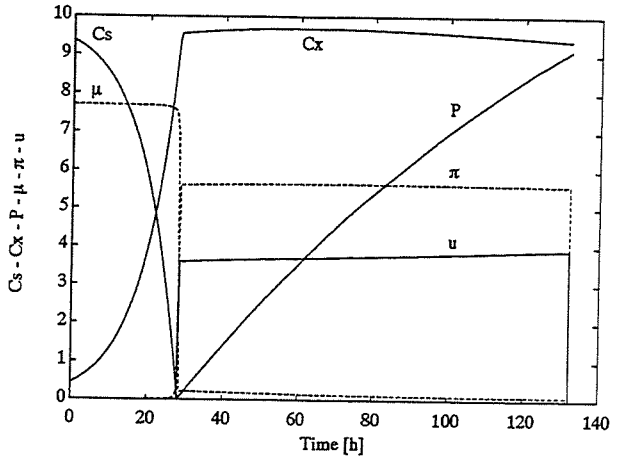

Figure 4.18: Optimal glucose feed rate and corresponding cell, glucose, product, μ and π profiles, for μ Contois and parameter Set 2
Scaling: $C_x/3$, $C_s/7$, $P/7$, $\mu * 70$, $\pi * 1500$, $u * 200$

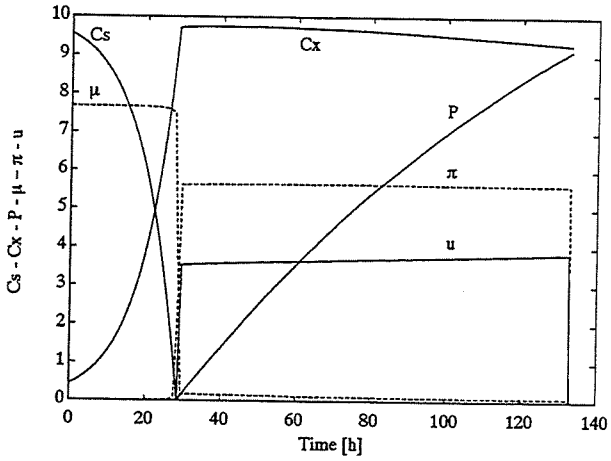

Figure 4.19: Optimal glucose feed rate and corresponding cell, glucose, product, μ and π profiles, for μ Monod and parameter Set 2
Scaling: $C_x/3$, $C_s/7$, $P/7$, $\mu * 70$, $\pi * 1500$, $u * 200$

As compared with (4.14), the expression for ψ is slightly modified due to the fact that in the Bajpai and Reuß model the substrate concentration in the feed stream $C_{s,in}$ appears in the differential equation for substrate S.

The formulation and solution to the two point boundary value problem —resulting from the application of optimal control theory to the given optimization problem— can be obtained using exactly the same steps as in Section 4.2.5, and is not repeated here. Clearly, the specific kinetics for growth (4.20) or (4.23) and production (4.21) are sufficiently differentiable to guarantee the applicability of the computational algorithm presented in Chapter 3.

First we consider the case of an unbounded input u and state $\mathbf{x}$ with free initial substrate concentration $C_s(0)$. Some numerical results using Contois kinetics (4.20) for growth are summarized in the bottom part of Table 4.8. The corresponding time profiles using parameter set 2 are shown in Figure 4.18. A constant strategy with initial substrate amount $S_0 = 0$ produces $P(t_f = 96.636) = 5.678$ g using parameter Set 1, and $P(t_f = 132.033) = 61.414$ g using parameter Set 2. As a result, the gain $\mathcal{G}$ —as defined by equation (4.16)— is equal to 691.229 % using parameter Set 1, and equals 3.961 % using parameter Set 2.

In the case of Monod kinetics (4.23) the optimal control results using parameter set 2 are : $S_0 = 540$ g, $t_2 = 28.569$ h, $t_f = 132.728$ h and $P(t_f) = 63.949$ g. The gain is then $\mathcal{G} = 5.758$ %. The corresponding time profiles are shown in Figure 4.19.

From these results we can draw the following conclusions.

1. The realizable gain $\mathcal{G}$ —defined in equation (4.16)— and the initial substrate amount S_0 depend heavily on the parameter set used. We will see in Section 5.1 that this is in the first place due to the large difference in the value of the parameter K_x (see Table 4.7).

2. However, independent of the parameter set used, the performance of the optimal polynomial controllers (see Section 4.3.4) is comparable with the optimal control results (i.e. controllers with free structure), provided the associated degrees of freedom are at their optimal values.

3. The numerical results as well as the time profiles of Figures 4.18 and 4.19 confirm that they are not determined by the analytic expression for μ, i.e. Contois (4.20) or Monod kinetics (4.23).

4. Comparing these plots with the corresponding Figures 4.16 and 4.17 for a constant feed rate profile, it can be seen that *during growth μ is optimized, while during production π is optimized.* This confirms the line of reasoning adopted in Section 3.5 in determining the optimal control sequence.

5. Using exactly the same initial and operational conditions as in Table 4.7, Lim *et al.* [1986] obtain for parameter set 2 the following optimal control results with their computational algorithm : $S_0 = 561.2$ g, $t_f = 124.9$ h and $P(t_f) = 86.99$ g. This final product amount differs a lot from the optimal and suboptimal control results given in Table 4.8, and contradicts the conclusion of Bajpai and Reuß themselves (see Section 4.3.3). As a result, we believe the difference is due to the computational algorithm proposed by Lim *et al.* [1986], as already discussed in detail in Section 3.5.2.

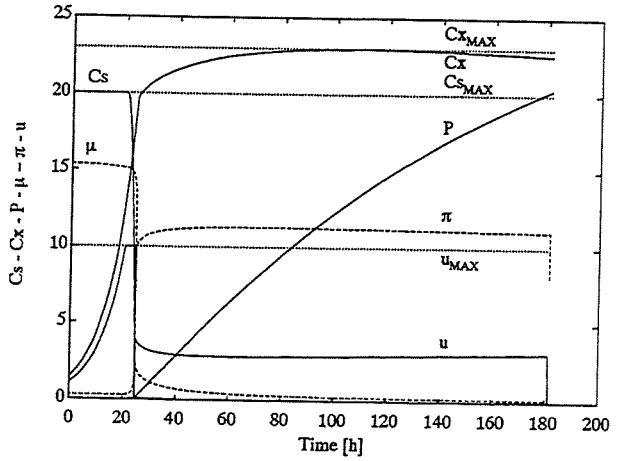

Figure 4.20: Optimal glucose feed rate and corresponding cell, glucose, product, μ and π profiles, for μ Contois and parameter Set 2, with $u_{MAX} = 0.05$ L/h, $C_{s,MAX} = 4$ g/L and $C_{x,MAX} = 23$ g/L
Scaling: $C_s * 5$, $P/3$, $\mu * 140$, $\pi * 3000$, $u * 200$

An example with bounded input u and inequality constraints on both C_s and C_x is shown in Figure 4.20 using Contois kinetics and parameter set 2. If $u_{MAX} = 0.05$ L/h, $C_{s,MAX} = 4$ g/L, and $C_{x,MAX} = 23$ g/L, then the optimal control results are : $\alpha_{growth} = 339$ g, $t_2 = 24.668$ h, $t_f = 181.407$ h and $P(t_f) = 61.015$ g.

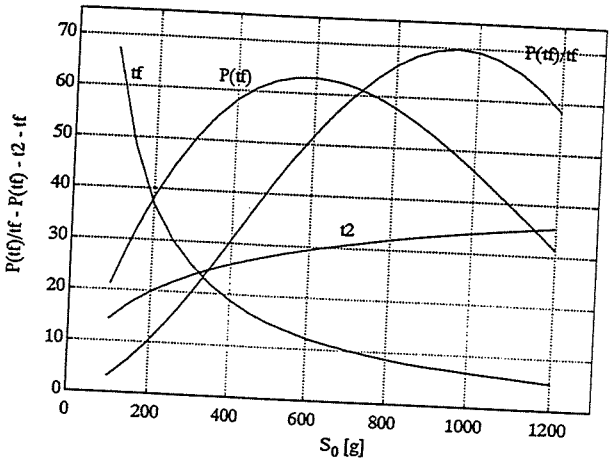

Figure 4.21: Extremal values for $P(t_f)/t_f$, $P(t_f)$, t_2 and t_f as functions of S_0
Scaling: $t_f/10$, $(P(t_f)/t_f) * 100$

Define the *yield* $\mathcal{Y}$ as the ratio of the final product amount to the total amount of substrate consumed during the fermentation :

$$\mathcal{Y} \triangleq \frac{P(t_f)}{\alpha} \tag{4.37}$$

and the *productivity* $\mathcal{P}$ as the final product amount per unit of time :

$$\mathcal{P} \triangleq \frac{P(t_f)}{t_f} \tag{4.38}$$

Observe that, since we always consider the total substrate amount α (4.33) fixed, $P(t_f)$ itself is a measure for the yield $\mathcal{Y}$.

In the above example with constraints, the *yield* decreases from $P(t_f) = 63.846$ g (see Table 4.8) to $P(t_f) = 61.015$ g, i.e. -4.43 %, while the *productivity* decreases from $\mathcal{P} = 0.484$ g/h to $\mathcal{P} = 0.336$ g/h, i.e. -30.445 %.

Let us consider now the optimization of the productivity $\mathcal{P}$ instead of the yield $\mathcal{Y}$. The performance index is then of the form (3.9) with $\gamma_x = 0$. The results obtained with the computational algorithm of Section 3.5.2 and using parameter set 2 are summarized in Figure 4.21. The optimal values

are : $S_0 = 950$ g, $t_2 = 33.430$ h, $t_f = 71.414$ h and $P(t_f) = 49.721$ g. The corresponding optimal productivity is $\mathcal{P} = 0.696$. Clearly, the optimal values of yield and productivity do not occur at the same value of S_0. This is an illustration of the well-known *yield–productivity conflict* in fed–batch reactors. A realistic process optimization strategy should consist of searching for the optimal initial substrate amount S_0, which results in the best *trade off* between *yield* and *productivity*. This represents also a trade off between *yield* and *total fermentation time*.

4.3.6 Physical interpretation of singular control

The results of Theorems 3.1 and 3.2 (see Section 3.6) have been derived under the condition that all specific rates are functions of substrate concentration only. Clearly, this is the case for Monod kinetics (4.23), not for Contois kinetics (4.20). If so, then we know that during singular control the substrate concentration remains constant at the level which maximizes π/σ if and only if $k_h = 0$.

For the values of k_h given in Table 4.7, it can be verified that for μ modeled with Monod kinetics the variations in C_s on the singular arc are in fact negligible : from Figure 4.19 for instance, it can be seen that π (and thus C_s) remains almost constant. As a result, we can obtain a very good initial guess for the switching time t_2 —as required in the computational algorithm— by maximizing the ratio π/σ with respect to substrate concentration C_s.

In fact, the same holds true for μ modeled by Contois kinetics (see Figure 4.18). The reason is that on the singular arc the variations in biomass concentration C_x are so small that in Contois kinetics (4.20) the term $K_x C_x$ can be approximated very well by a constant Monod saturation constant K_s. Note that this is in fact the basic idea behind the assumptions made in Section 4.3.2 when deriving conversion formulas between Contois and Monod kinetics.

As a conclusion, an excellent starting value for the switching time t_2 can be obtained by solving :

$$\frac{\partial}{\partial C_s}\left(\frac{\pi}{\sigma}\right) = 0$$

4.3.7 Heuristic control strategies

In this section we derive heuristic control strategies for the penicillin G fermentation process following the general ideas presented in Section 3.7. For simplicity, we consider the case of an unbounded input u and state $\mathbf{x}$ with free initial substrate concentration $C_s(0)$.

growth phase $[0, t_2]$

As already explained, the growth phase is a batch phase, while the fraction α_{growth} of all substrate available (4.33) which is consumed for biomass growth is added at time $t = 0$. This ensures the highest possible value for μ during growth.

production phase $[t_2, t_3]$

During production we focus on the specific production rate π.

- The Haldane type kinetics π (4.21) reach their maximum at :

$$C_s^* = \sqrt{K_p K_i}$$

The maximum value is :

$$\pi_{max} = \pi_m \frac{1}{1 + 2\sqrt{K_p/K_i}}$$

So during production, we keep C_s at C_s^* using a control of the form (3.47) :

$$u_{production}(t) = \frac{\sigma X}{C_{s,in} - C_s} \tag{4.39}$$

The conjunction point t_2 of growth and production is simply dictated by the condition $C_s = C_s^*$. The control is stopped at $t = t_3$ when all substrate α is used. As in the optimal case, the concluding batch phase is stopped if $dP/dt = 0$.

Note that this suboptimal control (called *heuristic C_s–control*) is in complete *closed loop* for a given S_0, or equivalently, $C_s(0)$. The optimization problem is reduced to the *one dimensional optimization of* S_0.

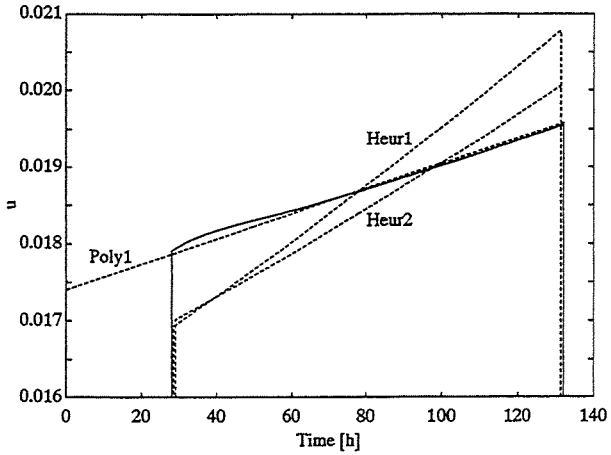

Figure 4.22: Optimal and suboptimal glucose feed rate profiles, for μ Contois and parameter Set 2
Legend: —: optimal controller, `Poly1`: polynomial controller with $N = 1$, `Heur1`: heuristic C_s-controller with $C_s^* = \sqrt{K_p K_i}$, `Heur2`: heuristic C_s-controller with $C_s(t_2)$ optimized

- As indicated in Section 3.7, a further refinement of this strategy exists in *optimizing* the set–point for C_s : during production C_s is kept constant, but not necessarily at $C_s = C_s^*$. As in the case of optimal control, a *two dimensional optimization of S_0 and t_2* is obtained.
- Observe that for μ modeled with Monod kinetics (4.23), the control (4.39) also keeps μ constant during production. In general, instead of specifying a reference profile for C_s we can select a reference profile for μ.

  In the case of Contois kinetics (4.20), a *heuristic μ–control* that keeps μ constant follows from the condition $d\mu/dt = 0$:

$$u_{production}(t) = \frac{\sigma X + \mu S}{C_{s,in}} \tag{4.40}$$

For a mathematical justification we refer to Section 4.3.6.

The performance of these heuristic controllers is illustrated in Table 4.8 for both parameter sets and using Contois kinetics. For parameter set 1, there

is almost no difference between the *heuristic C_s-control* with switching on $C_s = \sqrt{K_p K_i}$, and the *optimal control.* For this reason we do not mention the results for the other heuristic strategies. In all cases the performance is excellent, although Contois kinetics depend on biomass concentration C_x also.

In Figure 4.22, the different control strategies for parameter set 2 are shown. Since the optimal singular control increases almost linearly, it can be expected that even a simple first order polynomial control strategy performs very well.

4.3.8 Conclusions

In this section we investigated the substrate feeding rate optimization problem for the penicillin G fermentation, using the model of Bajpai and Reuß.

1. We compared different *suboptimal strategies* with the *optimal control* solution. The realizable gain as defined in (4.16) ranges from only a few percents to several hundred percents, depending on the parameter set used. However, as an extension of the results of Bajpai and Reuß, the simulation results illustrate that *using any of these strategies, we can obtain a performance similar to the optimal one, provided the associated degrees of freedom are at their optimal values.* As this holds true for the two widely different parameter sets of Table 4.7, this property seems to be related to the model *structure* rather than to the model *parameters.*

2. As a consequence, the choice for a particular feeding strategy can be based on other criteria. For instance, although at first sight a simple polynomial feed rate profile could suffice to optimize the process, such a controller is not flexible enough to take state inequality constraints into account in an efficient way.

3. We presented for the first time the optimal solution for a fed–batch fermentation process with *bounded input and state inequality constraints*, using the volumetric feed rate as control input. Of course, the heuristic controllers we derived can handle such constraints in a similar way. As a matter of fact, the results indicate that these strategies have an *excellent performance under all conditions.* For this reason, they can serve as a basis for the development of easy to implement adaptive controllers with excellent robustness properties. Furthermore, there is no need for a complete knowledge of the state, up to now one of the major bottle–necks in implementing model based control strategies for biotechnological processes. This will be illustrated with a case study in Chapter 6.

4. We clearly illustrated the *yield–productivity conflict* in fed–batch bioreactors.

5. Finally, the computational algorithm proposed in Chapter 3 proved to be very reliable for both types of performance indices.

4.4 Concluding remarks

In this chapter we have considered the optimization of the penicillin G fed–batch fermentation process with respect to the substrate feeding policy. Using optimal control theory, we have analyzed the model of Heijnen *et al.* [1979] (Section 4.2) and the model of Bajpai and Reuß [1980,1981] (Section 4.3). Although both models claim to be accurate descriptions of the penicillin G fed–batch fermentation process, the feeding strategy optimization studies indicate that the realizable gain $\mathcal{G}$ —i.e. the optimal product amount compared with the outcome of a constant feeding pattern in the same time with zero initial substrate amount— depends highly on the model and the parameter set used. The Heijnen *et al.* model predicts a gain in the region of hundred percent, while the gain predicted by the Bajpai and Reuß model depends heavily on the parameter set used. Moreover, the Heijnen *et al.* model is very sensitive towards different feeding policies, while the Bajpai and Reuß model is not. For more details we refer to the conclusions summarized in Sections 4.2.8 and 4.3.8.

Apart from the derivation of optimal control profiles for both models — which are important on their own—, we believe that the most important results from this chapter are the following.

First, although both models have a more or less similar behavior using a constant feed rate profile and have been validated using experimental data reported in the literature, clearly they exhibit a quite different behavior after feed profile optimization. As a result, this optimal control study can prove very useful in model characterization as will be illustrated in Chapter 5 : *optimization for model discrimination.*

Second, although the optimal profile and the resulting realizable gain strongly depend on the model used, the heuristic controllers introduced in Chapter 3 have an excellent performance in all cases. As such, they can serve indeed as a basis for the development of model–independent control algorithms. This will be elaborated in more detail in Chapter 6 : *optimal adaptive control.*

Chapter 5

A unifying unstructured model for the penicillin G fed-batch fermentation process

In this chapter we reconsider the model of Heijnen, Roels and Stouthamer [1979] and the model of Bajpai and Reuß [1980,1981], analyzed in Section 4.2 and Section 4.3 respectively. The need for a detailed comparison of these models from a biochemical viewpoint has originated from the following contradictory results.

The model of Heijnen et al. [1979] and the model of Bajpai and Reuß [1980, 1981], both claiming to be accurate descriptions of the penicillin G fermentation process, allow for the optimization of the final amount of product with respect to the substrate feeding rate for a given amount of substrate. However, although both models have the same general structure (3.1), they exhibit a completely different behavior towards product optimization. For instance, the analysis presented in Chapter 4 indicates that the realizable gain —i.e. the optimal product amount compared with the outcome of a constant feeding pattern in the same time with zero initial substrate amount— depends highly on the model and the parameter set used : the Heijnen et al. model predicts a gain in the region of hundred percents, while the gain predicted by the Bajpai and Reuß model ranges from only a few percents up to several hundred percents depending on the parameter set used. In

addition, we have illustrated that the Heijnen et al. model is very sensitive towards different feeding policies. However, the Bajpai and Reuß model is rather insensitive towards the structure of the feeding policy provided the associated degrees of freedom are at their optimal value.

In Section 5.1 we analyse the differences between both models from a biochemical point of view. First, the Heijnen et al. model is rewritten in a [g,L] unit system in order to facilitate comparison with the Bajpai and Reuß model. The penicillin biosynthesis pathway as known up to now is briefly summarized. Using this biosynthetic framework, the structural differences between the two models and the corresponding parameter sets are discussed. The models differ from each other in three important ways : (i) the specific production rate kinetics π, (ii) the basic assumptions about the nature of the metabolism, and (iii) the specific substrate to biomass conversion rate μ_{substr}. The model parameters not related with the above topics are discussed separately. This careful analysis reveals some physical and biochemical shortcomings in both models. In addition, the parameter estimation problem is clearly illustrated : although some model parameters can not be estimated accurately using experimental data of simple constant feed rate fermentations with low initial substrate amount, they may be key factors in concluding whether or not altering the substrate feeding strategy has an important influence upon the final amount of product. It is illustrated that feeding strategy optimization studies can be a tool in designing experiments for parameter estimation purposes.

To complete this analysis, we must investigate (i) how to determine the exact metabolism involved, and (ii) the possible effect of different metabolic assumptions —found back in model structure differences— on feeding strategy optimization results. This motivates the construction of a new unifying unstructured model in Section 5.2. This model corrects the physical and biochemical deficiencies in the previous models. The new model is essentially based on the unifying concept of endogenous fractions f_m and f_p of energy supply for biomass maintenance and product synthesis respectively, as introduced in Chapter 1. Its main features are the consistency for all values of the variables, and the ability to adequately describe different metabolic conditions of the mould. The model presented here can be considered as the translation of the latest advances in the biochemical knowledge of the penicillin biosynthesis. Simulation results obtained using a simple parametric optimization technique lead to the following important observations. First, analogous to the parameter estimation problem there also exists a model

structure characterization problem. We illustrate that a proper choice of the input feeding strategy to this new model can give indications about the metabolic nature of the mould. Second, the model structure characterization problem is in some sense decoupled from the parameter estimation problem.

Therefore, in Section 5.3 the model structure characterization problem is studied in more detail using the non–parametric optimal control technique. The results indicate that there exists a maximum realizable gain depending on the metabolism involved. However, the computational algorithm proposed in Chapter 3 can be used under all metabolic conditions. Similarly, the performance of the heuristic strategies we propose is excellent independent of the metabolism involved. The simulations illustrate that this new unifying model is an excellent tool to discriminate between different model structures (i.e. to determine the actual metabolism involved) when applying an optimal feed rate profile.

Finally, in Section 5.4 we summarize the contributions reported in this chapter. In particular, we give some further comments on our new paradigm : optimization for model discrimination.

5.1 Biochemical evaluation of two unstructured models for the penicillin G fed-batch fermentation process

5.1.1 Model equations

The model of Heijnen, Roels and Stouthamer

The unstructured model of Heijnen, Roels and Stouthamer [1979] has been described in Section 4.2.1. In the original model the dynamic equation for total broth weight G (4.1) takes into account dynamic effects resulting from the input of glucose, nitrogen source, sulphate source, oxygen and precursor, and from evaporation and carbon dioxide production. In Section 4.2.2 we concluded that the major contribution to the dynamics and final value of the most interesting variable (the product P) comes from the input of glucose. As a consequence, the other terms have been neglected, resulting in a more simple weight balance (4.5). Heijnen *et al.* use a Blackman–type kinetics for $\pi(\mu)$ (4.3) and a Monod law for $\sigma(C_s)$ (4.2) within an *endogenous* metabolism [Herbert 1958] viewpoint. The specific growth rate μ is given by (4.4).

specific rates

$$\sigma = Q_{s,max}\frac{C_s}{K_s + C_s} \tag{4.2}$$

$$\pi = Q_{p,max}\begin{cases} \mu/\mu_{crit} & \text{for } \mu \le \mu_{crit} \\ 1 & \text{for } \mu \ge \mu_{crit} \end{cases} \tag{4.3}$$

$$\mu = Y_{x/s}(\sigma - m - \pi/Y_{p/s}) \tag{4.4}$$

parameters

$Q_{s,max}$	0.18	$Q_{p,max}$	0.0045
K_s	1.	μ_{crit}	0.01
$Y_{x/s}$	0.5	k_h	0.002
$Y_{p/s}$	0.854	$C_{s,in}$	500.
m	0.025		

Table 5.1: Specific rates and parameters ([g/L] unit system) used in the model of Heijnen *et al.*

specific rates

$$\mu = \mu_C\frac{C_s}{K_x C_x + C_s} \tag{4.20}$$

$$\pi = \pi_m\frac{C_s}{K_p + C_s + C_s^2/K_i} \tag{4.21}$$

$$\sigma = \mu/Y_{x/s} + m + \pi/Y_{p/s} \tag{4.22}$$

parameters

	Set 1	*Set 2*		*Set 1*	*Set 2*
μ_C	0.092	0.11	K_x	0.15	0.006
π_m	0.005	0.004	k_h	0.04	0.01
K_p	0.0002	0.0001	K_i	0.1	0.1
$Y_{x/s}$	0.45	0.47	$Y_{p/s}$	0.9	1.2
m	0.014	0.029	$C_{s,in}$	500	500

Table 5.2: Specific rates and parameters ([g/L] unit system) used in the model of Bajpai and Reuß – Set 2 is the *nominal* set

Note that the original model is written in a [mol,kg] unit system. In order to obtain compatibility with the model of Bajpai and Reuß, we rewrite the (simplified) model in a [g,L] unit system. The resulting model has the general form (3.1) :

$$\begin{aligned} \frac{dS}{dt} &= -\sigma X + C_{s,in}u \\ \frac{dX}{dt} &= \mu X \\ \frac{dP}{dt} &= \pi X - k_h P \\ \frac{dV}{dt} &= u \end{aligned} \tag{5.1}$$

The specific rates and the corresponding parameters are summarized in Table 5.1. For an explanation of all symbols used we refer to Section 4.2 and the Nomenclature (Appendix B).

The model of Bajpai and Reuß

The unstructured model of Bajpai and Reuß [1980,1981] has been described in Section 4.3.1. This model has also the general form (5.1). Bajpai and Reuß use a Haldane–type substrate inhibition kinetics for $\pi(C_s)$ (4.21) and a Contois law for $\mu(C_s, C_x)$ (4.20) within a *maintenance* metabolism [Pirt 1965] viewpoint. The specific rates and the corresponding parameters are summarized in Table 5.2. For an explanation of all symbols used we refer to Section 4.3 and the Nomenclature (Appendix B).

Bajpai and Reuß demonstrated a close agreement between model predictions and reported fermentation data by Pirt and Rhigelato [1967] and Hosler and Johnson [1953] (using parameter Set 1 in Table 5.2) and by Mou [1979] (using parameter Set 2 in Table 5.2).

5.1.2 Biochemistry of the penicillin synthesis

During the last decade many details about the penicillin synthesis pathway have been discovered. The present knowledge about penicillin biosynthesis has been recently reviewed by Martin and Liras [1989]. In this section we only consider these steps in the pathway which are relevant with respect to a discussion of both mathematical models.

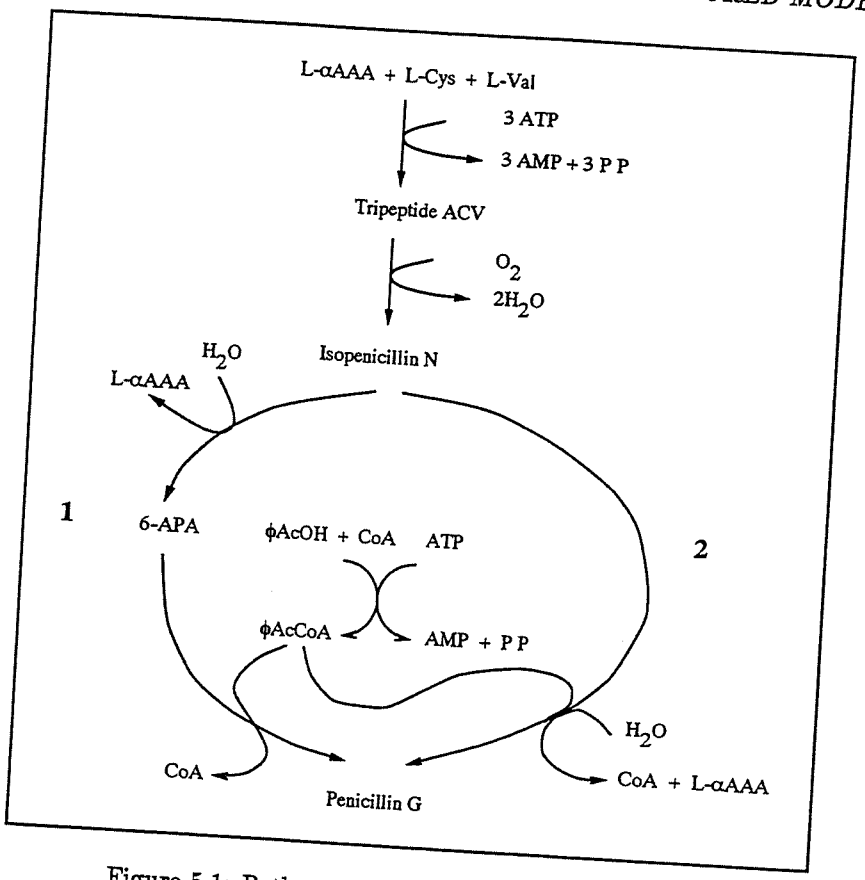

Figure 5.1: Pathway of the penicillin G biosynthesis

The penicillin biosynthesis pathway as known up to now is shown in Figure 5.1. The amino–acids L–α–aminoadipic acid (L–α–AAA), L–Cys and L–Val condensate into the tripeptide ACV, an intermediate which has been isolated and identified from *Penicillium chrysogenum* [Arnstein and Morris 1960; López–Nieto *et al.* 1985]. A first step in ACV synthesis is most probably the formation of an intermediary L–α–aminoadipyl–L–cysteine [Queener and Neuss 1982; Banko and Demain 1987] which remains enzyme bound and is converted into the tripeptide ACV by reaction with the epimerized L–valine [Delderfield *et al.* 1981]. ACV–synthetase, the enzyme responsible for the ACV–synthesis, has been recently isolated from cell–free extracts of *Cephalosporium acremonium* (*Acremonium strictum*) [Banko and Demain

1987]. The enzyme requires the presence of Mg^{2+} and ATP. The presence of phenylacetic acid, the side chain precursor of penicillin G, stimulates ACV–biosynthesis [López–Nieto *et al.* 1985]. Hersbach *et al.* [1984] assumed in their theoretical conversion yield calculations that L–α–AAA, L–cysteine and L–valine each have to be activated by ATP, yielding AMP. In contrast with these assumptions, Cooney and Acevedo [1977] supposed that each of the two peptide bonds requires ATP (consequently one molecule of ATP less than in the mechanism proposed by Hersbach *et al.*) and yields AMP.

Isopenicillin N synthetase (IPN–synthetase), the enzyme which catalyzes the second step of the pathway (the formation of isopenicillin N), has been isolated and purified from extracts of *P. chrysogenum* [Ramos *et al.* 1985]. It requires dithiotheitol (DTT), $FeSO_4$ and ascorbic acid. The oxidative cyclisation requires molecular oxygen in a 1:1 stoichiometric ratio. To our knowledge there are no reports concerning the requirements of NAD(P) and FAD as suggested by Cooney and Acevedo [1977] and Hersbach *et al.* [1984]. ATP does not seem to be necessary [White *et al.* 1982].

The last step in penicillin biosynthesis is the exchange of the L–α–AAA–sidechain of isopenicillin N for phenylacetic acid, activated by means of a phenacyl:coenzyme A ligase using Coenzyme A and ATP and yielding phenylacetyl Coenzyme A and AMP [Brunner and Röhr 1975]. The acylation is mediated by an acyltransferase complex which has been isolated and purified from *P. chrysogenum* [Preuss and Johnson 1967]. It is still an open problem whether isopenicillin N is converted into penicillin G via an *intermediary* 6–aminopenicillanic acid (6–APA) (pathway 1 in Figure 5.1) or *directly* (pathway 2 in Figure 5.1). Alvarez *et al.* [1987] isolated an AcylCoA:6–APA acyltransferase which catalyzed the reaction of both 6–APA and isopenicillin N to penicillin G, although the latter at a lower rate. The enzyme required DTT but did not require ATP or other cofactors of the IPN–synthetase.

5.1.3 Biochemical validation of the two models

Using this biosynthetic framework, the *structural* differences between the mathematical models of Heijnen *et al.* and of Bajpai and Reuß —and the corresponding *parameter* sets— are discussed here. The models differ from each other in three important ways : (i) the specific production rate kinetics π (Section 5.1.3.1), (ii) the basic assumptions about the nature of the metabolism (Section 5.1.3.2), and (iii) the specific substrate to biomass conversion rate μ_{substr} (Section 5.1.3.3). The model parameters not related with the above topics are discussed separately (Section 5.1.3.4).

5.1.3.1 Specific production rate kinetics

Heijnen *et al.* assumed that the specific penicillin production rate is directly coupled with the specific growth rate as described by equation (4.3). They based this assumption on continuous culture experiments by Pirt and Rhigelato [1967]. These results are in agreement with those obtained by Ryu and Hospodka [1980]. However, the Blackman–type kinetics is very different from the Haldane–type substrate inhibition kinetics (4.21) used by Bajpai and Reuß.

A major point of difference lies in the *value of the specific production rate π for large values of the specific growth rate μ*. In penicillin fed–batch fermentations, high μ conditions occur in the first phase (*growth phase*), which typically lasts for about 20 to 30 hours [Jarvis and Johnson 1947; Hosler and Johnson 1953; Mc Cann and Calam 1972; Calam and Ismail 1980].

First the approach of Bajpai and Reuß is commented. There seems to be some evidence that penicillin synthesis is governed by glucose repression [Aiba *et al.* 1973; Revilla *et al.* 1984]. Based on their experiments, Revilla *et al.* also concluded —although criticized by Hersbach *et al.* [1984]— that glucose *represses* biosynthesis of the necessary enzymes of the penicillin pathway, but does *not* act as an *inhibitor* of these enzymes. Banko and Demain [1987] found that fructose–1,6–diphosphate and glucose–1–phosphate inhibit ACV–biosynthesis. In the same way, López–Nieto *et al.* [1985] concluded that the time course of ACV–forming activity starts only after a lag period of about 24 hours, thus probably at the moment when the glucose amount in the fermentor has diminished substantially after the rapid growth phase. Similar lag phases were discovered in the formation of the IPN–synthetase [Ramos *et al.* 1985], Phenacyl:CoA ligase [Brunner and Röhr 1975] and AcylCoA:6–APA acyltransferase [Alvarez *et al.* 1987]. It is not clear from these reports whether *inhibition* or *repression* takes place, but nevertheless there seems to be increasing evidence that *high penicillin production rates are well correlated with low substrate concentration levels.*

At a first glance, these conclusions contradict the results of Pirt and Rhigelato [1967] —on which Heijnen *et al.* based their production kinetics— and of Ryu and Hospodka [1980]. However, these results were obtained for *continuous culture* fermentations. It is indicated

below that these experimental conditions most probably do not allow for substrate inhibition to be detected.

Because for high values of the specific growth rate μ it is most likely (as will be discussed further on) that *maintenance* metabolism occurs, the biomass concentration evolution rate for a continuous process can be described as follows :

$$\frac{dC_x}{dt} = \mu C_x - C_x D$$

with $D = u/V$ [1/h] the *dilution* rate as usual. In steady state, and with μ described by a Monod kinetics (4.23), this becomes :

$$\begin{aligned} \mu &= D \\ C_s &= K_s \frac{\mu/\mu_M}{1-\mu/\mu_M} \end{aligned}$$

where μ_M denotes the maximum specific substrate to biomass conversion rate. Pirt and Rhigelato determined π for μ between 0.023 and 0.086 [1/h]. They also reported a value $\mu_M \approx 0.095$ [1/h], so that for their experiments μ/μ_M is in the range of 0.24 to 0.9. However, if K_s is substituted with the value $K_s = 1$ g/L as used by Heijnen *et al.*, one finds with the above equation $0.3 < C_s < 9$ g/L. This agrees well with the work of Revilla *et al.* [1984], who reported that penicillin biosynthesis repression only occurs at glucose concentrations from $C_s = 10$ g/L on. The conclusion is that the *glucose concentrations in the experiments of Pirt and Rhigelato probably were too low for glucose repression to be detected.* The experimental data published by Ryu and Hospodka are not sufficiently detailed to permit a similar analysis.

These considerations are important for the time evolution of the penicillin amount during the growth phase of a fermentation operated in fed–batch for which often a considerable amount of substrate α_{growth} is provided in the beginning. During growth, most of the time the glucose concentration remains far above 10 g/L. Moreover, only when the glucose concentration falls below 10 g/L the necessary enzymes in the penicillin pathway are synthesized, resulting in an additional delay in penicillin biosynthesis. It should be noted that there is some evidence that glucose has a repressive instead of an inhibitive action above 10 g/L. From this it may be expected that *during the growth*

$S(0)$	0.	t_f	120.
$X(0)$	10.5	u	0.025
$P(0)$	0.	α	1500.
$V(0)$	7.	$C_{s,in}$	500.

Table 5.3: Initial and operational conditions used in simulations

phase virtually no production can take place, a conjecture which is in close agreement with published data on penicillin batch fermentations [Jarvis and Johnson 1947; Hosler and Johnson 1953; Mc Cann and Calam 1972; Calam and Ismail 1980]. This is in contradiction to the model of Heijnen *et al.*, which predicts that penicillin production starts *immediately* after inoculation, yielding a yet considerable amount of penicillin at the moment the production phase starts (see e.g. Figure 4.3).

As a conclusion, the use of Haldane–type *substrate inhibition* kinetics as in the Bajpai and Reuß model seems to be more appropriate. Even though there is up to now still some doubt concerning the exact nature of the biochemical mechanism involved for regulation (*repression* or *inhibition*), Bajpai and Reuß decided to disregard the differences between time constants for the two regulation mechanisms due to relatively very long fermentations, and the inhibition kinetics were assumed to represent both.

Parameters. Let us consider now the parameters used in equation (4.21). Bajpai and Reuß identified the parameters of their model using a mixture of published data, trial and error and a Nelder–Mead optimization routine. Using parameter Set 2 in Table 5.2 —which we consider as the *nominal* set used in all simulations— the maximum specific production rate occurs at $C_s = (K_p K_i)^{1/2} = 3.162\ 10^{-3}$ g/L. At $C_s = 0.9$ g/L, π falls to 10 percent of its maximum value. Clearly this is contradictory to the above mentioned lower bound for glucose repression [Revilla *et al.* 1984] of approximately $C_s = 10$ g/L. This can be explained as follows. Since there are no experimental data available for K_p and K_i, these parameters were simply *assigned* reasonable values, slightly adjusted to obtain agreement with the experimental observations [Pirt and Rhigelato 1967; Mou 1979]. Bajpai and Reuß did not look for an alternative parameter set, as the fitting was found sufficient.

#	K_p	K_i	π_m	$P(t_f)_{ref}$	$P(t_f)_{opt}$	$\mathcal{G}$	$S(0)_{opt}$
1	0.0001	0.1	0.00400	59.651	63.461	6.4	280.
2		1.0	0.00351	57.610	58.045	0.8	192.
3		10.0	0.00338	56.882	56.922	0.5	178.
4		100.0	0.00331	55.930	56.777	1.5	219.
5		1000.0	0.00330	55.842	56.954	2.0	235.
6		10000.0	0.00329	55.688	56.835	2.0	237.
7	0.0010	0.1	0.00426	58.156	58.272	0.2	56.
8		1.0	0.00374	56.069	56.069	0.0	0.
9		10.0	0.00360	55.141	55.141	0.0	0.
10		100.0	0.00352	54.439	54.439	0.0	0.
11		1000.0	0.00350	54.224	54.224	0.0	0.
12		10000.0	0.00350	54.233	54.233	0.0	0.
13	0.0100	0.1	0.00652	51.604	51.604	0.0	0.
14		1.0	0.00584	49.851	49.851	0.0	0.
15		10.0	0.00549	48.310	48.310	0.0	0.
16		100.0	0.00529	47.352	47.352	0.0	0.
17		1000.0	0.00525	47.137	47.137	0.0	0.
18		10000.0	0.00525	47.150	47.150	0.0	0.

Table 5.4: Estimation of π_m for different values of K_p and K_i for the Bajpai and Reuß model with constant feeding strategy, and corresponding final product amount – optimal initial substrate level and optimal product amount

However, a simple simulation experiment indicates that *the model predictions of biomass, substrate and penicillin are quite insensitive with respect to even large variations of K_p and especially K_i.* First, a set of 120 *reference data* for C_s, C_x and C_p is generated using the original Bajpai and Reuß model (Table 5.2), a constant feed rate strategy with zero initial substrate amount, and the initial and operational conditions as given in Table 5.3. For obvious reasons, only values of K_p and K_i greater than the nominal ones are considered. The value of π_m is adjusted so as to minimize the Euclidean distance to the reference data concentration profiles. The numerical results are summarized in Table 5.4, columns 1 to 5. The final amount of product is denoted with $P(t_f)_{ref}$. In Figure 5.2 the time profiles of biomass, substrate and penicillin are plotted for some combinations (K_p,K_i,π_m) from Table

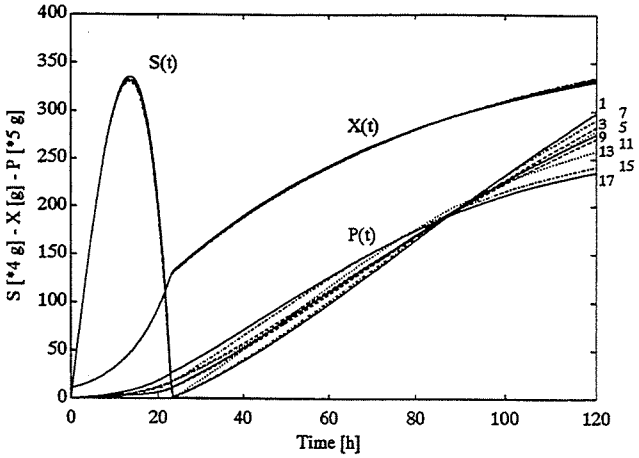

Figure 5.2: Substrate, biomass and penicillin profiles during constant feed rate fermentation for some (K_p,K_i,π_m) combinations of Table 5.4 – $S_0 = 0$ g

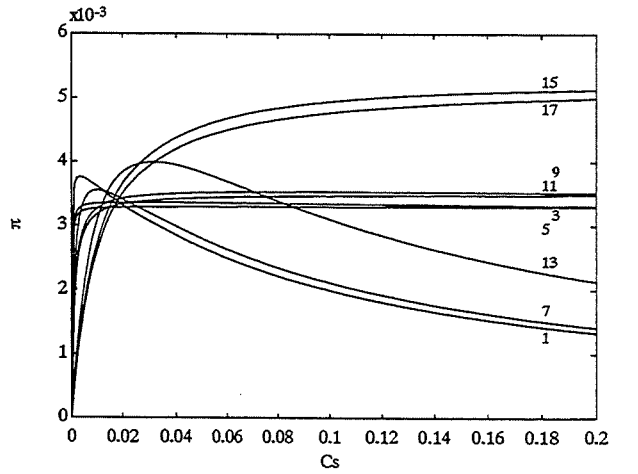

Figure 5.3: Specific production rate π for some (K_p,K_i,π_m) combinations of Table 5.4

5.4. The above results indicate that even large variations of K_p and K_i have virtually no influence on the time evolution of biomass and substrate, as could be expected also from the system equations (5.1) and the specific rates (Table 5.2) : K_p and K_i appear in the specific production rate π, which represents only a limited fraction of the specific substrate consumption rate σ. Furthermore, for a *fixed* value of K_p, extremely large variations of K_i have only a slight influence on the penicillin time profile, although for larger values of K_i the decreasing substrate inhibition results in an earlier and smoother start of product formation. For $K_p = 10^{-2}$ g/L the fit for penicillin is worse (curves 13 to 17 in Figure 5.2). Note that the necessary adjustments of π_m are small. All values are of the same order of magnitude as the reported ones : $\pi_m = 0.004$ g/g DW h (Set 2 in Table 5.2) to $\pi_m = 0.005$ g/g DW h (Set 1). In Figure 5.3 π versus C_s is plotted for the same (K_p,K_i,π_m) combinations of Figure 5.2. As could be expected, the value of K_p determines how fast π increases with increasing low values of C_s, while the K_i value reflects the importance of glucose inhibition at high values of C_s. In summary, this simulation experiment indicates that *it is impossible to estimate the correct values of K_p and K_i using experimental data obtained with this particular feeding strategy.*

From equation (4.21), the maximum specific production rate is found to be $\pi_{max} = \pi_m/(1 + 2(K_p/K_i)^{1/2})$, which is almost equal to π_m if $K_i \gg K_p$ as is the case for the values of Table 5.2. This agrees well with the value $Q_{p,max} = 0.0045$ g/g DW h used by Heijnen *et al.*, and with the value of 0.006 g/g DW h used by Nestaas and Wang [1983].

5.1.3.2 Maintenance or endogenous metabolism

The behavior of π for low values of μ —which corresponds to low values of substrate concentration C_s— depends on the metabolic properties of the mould under severe substrate limitation. This can e.g. occur at the end of the growth phase of a fermentation operated in fed–batch.

The model of Bajpai and Reuß is inconsistent when C_s falls to zero : the system equations (5.1) indicate that for $u = 0$ (e.g. during a batch growth phase) C_s decreases monotonically and may even take on *negative* values, which is of course physically impossible. The reason for this inconsistency lies in the *maintenance energy concept* adopted in this model. Bajpai and Reuß assumed that the energy for the maintenance

and production requirements of the mould is directly obtained from the combustion of substrate. However, what happens when the substrate concentration falls to zero can not be explained by this assumption. It seems reasonable that under severe environmental limiting conditions, the energy requirements of the cell are fulfilled by combustion of the cellular storage compounds themselves, i.e. *endogenous metabolism.* In this connection, Ballio *et al.* [1964] and Thevelin [1984] reported that trehalose and polyols, such as mannitol, are frequently important storage compounds in both conidia and vegetative mycelium. Many fungi also have an important lipid fraction [Moss 1987].

On the other hand, for high substrate concentrations it can be expected that organisms directly use the substrate, instead of first synthesizing the storage components and then combusting or transforming these into biomass and product. Therefore, the model of Heijnen *et al.* — which relies on the endogenous metabolism concept— can be expected to behave well for *low* C_s values, but will probably fail to make reliable predictions in *high* C_s–regions, where the Bajpai and Reuß model — with its maintenance metabolism— should behave better.

Parameters. The maintenance coefficient used by Heijnen *et al.* ($m = 0.025$ g/g DW h) corresponds well to the value $m = 0.029$ g/g DW h (Set 2 in Table 5.2 of Bajpai and Reuß), to the value $m = 0.024$ g/g DW h reported by Ryu and Hospodka [1980], and to the value used by Nestaas and Wang ($m = 0.022$ g/g DW h) [1983]. However, these values differ from the value in Set 1 of Bajpai and Reuß ($m = 0.014$ g/g DW h). It is not clear where this difference originates from. Simulations indicate that the dynamic behavior of the model is rather sensitive with respect to the value of m.

When considering the production kinetics equation (4.3) of Heijnen *et al.* at low values for μ, an additional modeling problem arises. When biomass consumption due to maintenance and production requirements exceeds the conversion of substrate into biomass, μ (4.4) may fall to zero and become even negative. For the latter case π is not defined by equation (4.3), resulting in an inconsistency. A straightforward extension of the $\pi(\mu)$ kinetics could be $\pi(\mu \leq 0) = 0$, but there are some biochemical indications that penicillin biosynthesis actually does *not* stop in that case. This statement is motivated using the penicillin synthesis pathway as shown in Figure 5.1.

From this scheme it is clear that in order to produce penicillin, there is need for the amino–acid precursors L–Cys and L–Val, L–α–AAA, ATP, ϕAc, O_2, some cofactors and of course the relevant enzymes. In living cells there is a constant *turn–over* of cell proteins into amino–acids, which results in an amino–acid pool from which new proteins are synthesized. So the amino–acid precursors L–Cys and L–Val are always present, even for $\mu \leq 0$. Furthermore, as can be seen from the pathway, it seems that L–α–AAA is released unaltered after the incorporation of ϕAc, and thus could be recycled for penicillin synthesis. This has been confirmed by the work of Friedrichs and Demain [1978], although there are also indications that not L–α–AAA but 6–oxo–piperidine–2–carboxylic acid (a cyclisation product of L–α–AAA) is released in the final step [Brundidge *et al.* 1980]. However, even when no recycling is possible, L–α–AAA can be synthesized *de novo* from α-ketoglutaric acid and Acetyl Coenzyme A, two very abundant compounds in living cells which may be produced e.g. by the catabolism of cellular storage compounds. This probably also holds true for ATP and the necessary cofactors. ϕAc and O_2 are supposed to be supplied at a sufficient rate. From this it can be concluded that *even when* $\mu \leq 0$, *all compounds necessary for the penicillin biosynthesis are present.* To our knowledge there is no biochemical evidence for regulation mechanisms that repress or inhibit the relevant enzymes at low μ conditions.

At first sight, this is contradictory to reported continuous culture data by Pirt and Righelato [1967] and Ryu and Hospodka [1980], suggesting π becoming zero for zero μ. However, Pirt and Rhigelato showed that penicillin production in continuous cultures decays linearly at a rate of only 1 or 2 percent/h (depending on the previous value of μ) when μ was decreased to zero, so that for relatively short glucose depletion periods (up to a few hours) π remains positive. The decay of penicillin production rate for larger glucose limitation periods may be a result of the decay of the enzymes involved in penicillin biosynthesis in that case. The data of Ryu and Hospodka, indicating a positive π for $\mu = 0$ (which the authors assumed to be caused by experimental error or an erroneous linearity assumption) are in fact too vague at low μ values, so they fail to give a decisive answer. Pirt [1990] recently showed that penicillin *hydrolysis* could be responsible for the apparent low π levels in low μ conditions in continuous cultures, suggesting that the real value of π is higher than the observed one.

5.1.3.3 Specific substrate to biomass conversion rate

In the model of Heijnen *et al.* the conversion of substrate to biomass is modeled with Monod kinetics, while in the Bajpai and Reuß model Contois kinetics are used.

Bajpai and Reuß motivated their choice by the argument that at high biomass concentrations the fermentation broth becomes very thick and limits either oxygen or nutrient diffusion into the fungal cells [Hosler and Johnson 1953]. From equation (4.20) it can be seen immediately that a high microbial cell density C_x decreases the substrate to biomass conversion rate, thus simulating the diffusion problem.

On the other hand, the presence of the biomass concentration in the Contois kinetics complicates analytical treatment of the governing equations for e.g. optimal control purposes. Using Monod kinetics all specific rates become functions of the substrate concentration *only*. Moreover, Monod kinetics can be clearly motivated from enzyme kinetics studies [Roels 1983]. Nihtilä and Virkkunen [1977] proved that both Monod and Contois kinetics can describe fungal growth well. The simulations with optimal and suboptimal heuristic feeding policies presented in Chapter 4 also indicated that the overall dynamics are not significantly influenced by the choice of either Monod or Contois kinetics.

Parameters. In the two parameter sets used by Bajpai and Reuß (Table 5.2), there is only a small difference in the maximum specific substrate to biomass conversion rate μ_C —which can be easily determined using continuous culture experiments—: 0.092 1/h to 0.11 1/h. These values also agree with the elsewhere reported maximum rates (0.095 1/h to 0.15 1/h) [Pirt and Rhigelato 1967; Ryu and Hospodka 1980], and with the maximum specific substrate to biomass conversion rate $Q_{s,max} \times Y_{x/s} = 0.09$ 1/h used by Heijnen *et al.* (Table 5.1). The differences are probably due to the different strains used in the experiments for parameter estimation.

A more serious difference exists between the reported K_x values. For the continuous culture experiments of Pirt and Rhigelato —on which the value $K_x = 0.15$ g/g DW (Set 1 of Bajpai and Reuß) is based—, steady–state values of $C_x = 4$ up to 14 g/L have been reported. From (4.20) it is clear that under these experimental conditions Contois kinetics can be related to an *equivalent* Monod kinetics, by setting $K_s = C_x K_x$. This results in a K_s value between 0.6 and 2.1 g/L, which agrees well with the value $K_s = 1$ g/L used by Heijnen *et al.* [Table (5.1)]. However, there is a striking difference between the K_x value of Set 1 ($K_x = 0.15$ g/g DW) and the one of Set 2 ($K_x = 0.006$ g/g DW) reported by Bajpai and Reuß. In Table 5.5 the results of a similar parameter estimation study as described above are given. K_x values greater than 0.05 g/g DW result in a rather poor fit on the reference fermentation data generated with Set 2, and in unacceptably high π_m values (> 0.01 g/g DW h). For K_x values from 0.001 to 0.05 g/g DW the π_m values are in the range of 0.003 to 0.007 g/g DW h and the fit is good, as illustrated in Figure 5.4. This is another illustration of the *parameter estimation problem* when using this feeding strategy.

The cause of the contradiction between the two sets remains unclear. However, in Section 5.1.4 it will be shown that these large differences in K_x may result in a completely different behavior of the model towards optimization.

#	K_x	π_m	$P(t_f)_{ref}$	$P(t_f)_{opt}$	$\mathcal{G}$	$S(0)_{opt}$
1	0.150	0.01322	75.641	167.858	122.9	284.
2	0.100	0.01038	72.226	150.148	107.9	305.
3	0.050	0.00720	67.703	109.734	62.1	335.
4	0.010	0.00432	60.907	68.457	12.4	314.
5	0.007	0.00408	59.988	64.735	7.9	291.
6	0.006	0.00400	59.651	63.461	6.4	280.
7	0.005	0.00392	59.281	62.159	4.9	261.
8	0.001	0.00370	57.057	57.057	0.0	0.

Table 5.5: Estimation of π_m for different values of K_x for the Bajpai and Reuß model with constant feeding strategy, and corresponding final product amount – optimal initial substrate level and optimal product amount

5.1.3.4 The remaining model parameters

Most parameters have been discussed above. The remaining ones are the substrate to biomass yield coefficient $Y_{x/s}$, the substrate to product yield coefficient $Y_{p/s}$, and the hydrolysis constant k_h.

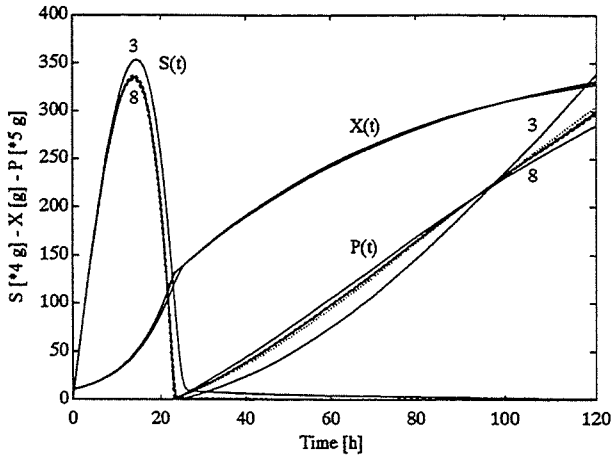

Figure 5.4: Substrate, biomass and penicillin profiles during constant feed rate fermentation for some (K_x,π_m) combinations of Table 5.5 – $S_0 = 0$ g

$Y_{x/s}$ is almost the same in both models, and corresponds to the yield coefficient measured by Ryu and Hospodka [1980] (0.45 g DW/g). Nestaas and Wang [1983] determined $Y_{x/s}$ to be 0.6 g DW/g, which is somewhat higher than typically reported. This was caused by the presence of some complex nutrients in the growth medium.

$Y_{p/s}$ varies from 0.85 g/g to 1.2 g/g. The last value was based upon the maximum theoretical value of 1.1 g/g calculated by Cooney and Acevedo [1977] —also used by Heijnen *et al.* and Nestaas and Wang [1983]— using the biochemical knowledge present at that time. Hersbach *et al.* [1984] reviewed these calculations, and based on recent biochemical evidence about cysteine–biosynthesis, they concluded that the *theoretical maximum* $Y_{p/s}$ value may be somewhere between 0.41 g/g and 0.925 g/g, depending on some additional assumptions. These authors however also assumed that NAD(P) and FAD are required for the oxidative cyclisation of ACV, which is refuted by recent research as described above. *Actual* conversion yields of the best penicillin strains would be about only 0.12 g/g [Hersbach *et al.* 1984]. In order to investigate the influence of $Y_{p/s}$ upon simulation results a similar parameter

estimation study as described above has been carried out. Several values of $Y_{p/s} < 1.2$ g/g have been considered. A larger relative weight has been assigned to the penicillin concentration fitting errors during estimation of π_m. $Y_{p/s}$ values below 0.6 g/g resulted in a very poor fit.

Similarly, a poor fit has been obtained for an increase of the hydrolysis constant k_h from 0.01 1/h (Set 2 of Bajpai and Reuß) to 0.04 1/h (Set 1). On the other hand, an acceptable fit has been obtained using $k_h =$ 0.002 1/h (Heijnen *et al.*) with a corresponding value $\pi_m = 3.18\ 10^{-3}$ g/g DW h. In the work of Nestaas and Wang [1983], k_h was given the value 0.003 1/h.

5.1.4 Effect of the model parameters on feeding strategy optimization

In this section we optimize a feeding strategy of the following form in order to investigate the possible effects of the model parameters. As usual, the total amount of substrate available for fermentation α is fixed ($\alpha = 1500$ g). The initial amount of substrate $S(0)$ is free, the initial volume $V(0)$ follows then from $V_0 = 7 + S_0/C_{s,in}$ [L] (4.31). Remember that glucose is added as a solution with concentration $C_{s,in}$. The remaining amount of substrate is fed at a constant rate from $t = 0$ on, with the final time t_f fixed at $t_f = 120$ hrs. For the other initial and operational conditions the values given in Table 5.3 are used. As a result, we obtain a *one dimensional optimization problem.* Obviously, this is a very simple example of *parametric optimization* (see also Sections 1.2.2 and 4.3.4). This simple controller structure is chosen to make the possible influence of the model parameters as clear as possible.

The biochemical evidence presented in Section 5.1.3 suggests that, as long as C_s remains positive, the Bajpai and Reuß model seems to be a better description of the actual fermentation process than the Heijnen *et al.* model. For this reason all further computations have been performed using the Bajpai and Reuß model. In order to prevent C_s from becoming negative, μ (4.20) and σ (4.22) are modified as follows :

$$\begin{aligned}
\mu_{substr} &= \mu_C \frac{C_s}{K_x C_x + C_s} \\
\mu &= \mu_{substr} - Y_{x/s}(1 - \mathcal{U}(C_s))(m + \pi/Y_{p/s}) \\
\sigma &= \mu/Y_{x/s} + m + \pi/Y_{p/s} \\
&= \mu_{substr}/Y_{x/s} + \mathcal{U}(C_s)(m + \pi/Y_{p/s})
\end{aligned}$$

with $\mathcal{U}(C_s)$ a unit step function :

$$\begin{aligned} \mathcal{U}(C_s) &= 1, \quad C_s > 0 \\ &= 0, \quad C_s \leq 0 \end{aligned}$$

In other words, as long as $C_s > 0$ these specific rates represent a pure maintenance metabolism. However, if C_s becomes equal to zero these specific rates reduce to :

$$\begin{aligned} \mu &= \mu_{substr} - Y_{x/s}(m + \pi/Y_{p/s}) \\ \sigma &= \mu_{substr}/Y_{x/s} \end{aligned}$$

which represents an endogenous metabolism as used in the Heijnen *et al.* model. Obviously, this modification prevents C_s from becoming negative.

In Table 5.4 the optimization results for the different (K_p,K_i,π_m) combinations are given in columns 6 to 8. $P(t_f)_{opt}$ denotes the final amount of penicillin for S_0 optimized. The gain $\mathcal{G}$ [%] is as defined in (4.16) :

$$\mathcal{G} = 100 \times \frac{P(t_f)_{opt} - P(t_f)_{ref}}{P(t_f)_{ref}}$$

For increasing values of K_i with K_p fixed at K_p=0.0001 g/L (i.e. the *nominal* value), the gain first decreases quickly to reach a minimum value near $K_i = 10$ g/L but increases then slightly at higher values of K_i.

In columns 5 to 7 of Table 5.5 the optimization results for the different (K_x,π_m) combinations are given. Observe that *the value of K_x has a very important influence on optimization.* K_x values above 0.05 g/g DW —which result in a possible gain of up to 123 percents— seem to be less likely because of the very high corresponding value of π_m. However, smaller K_x values — which give an excellent fit and acceptable π_m values (see also Figure 5.4)— still result in large optimization differences. In Figure 5.5 the time evolution of the (modified) Bajpai and Reuß model using the (K_x,π_m) combinations of Table 5.5 with $K_x \leq 0.05$ g/g DW is shown for an initial amount of substrate $S(0) = 335$ g, i.e. the optimal value for $K_x = 0.05$ g/g DW. Apart from the large influence of K_x on optimization itself, comparison of Figure 5.4 and Figure 5.5 also indicates that feeding strategy optimization can be useful in solving the parameter estimation problem.

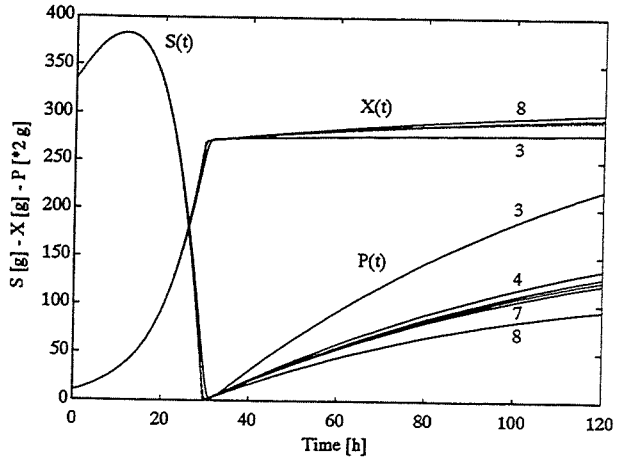

Figure 5.5: Substrate, biomass and penicillin profiles during constant feed rate fermentation for some (K_x,π_m) combinations of Table 5.5 – $S_0 = 335$ g

A decrease in m from 0.029 g/g DW h (Set 2 of Bajpai and Reuß) to 0.014 g/g DW h (Set 1) results in an increase of the realizable gain $\mathcal{G}$ from 6.4 % to 35.9 %. However, as mentioned above, the fit of the model with this low m value to the reference data is rather poor.

When the k_h value is increased from $k_h = 0.01$ 1/h to 0.04 1/h, the fit is also poor and the corresponding π_m values are unacceptable. In this case the gain has been lost completely. On the other hand, for $k_h = 0.002$ 1/h as used by Heijnen *et al.*, the fit is acceptable with a corresponding π_m value equal to 0.00318 g/g DW h. The realizable gain increases to 9.9 %.

The influence of the other parameter differences upon optimization is less important.

To conclude, some model parameters may have an important influence upon feeding strategy optimization results. Furthermore, these results suggest that feeding strategy optimization studies may be a valuable tool in the design of real life experiments for parameter estimation purposes. The simulations indicate that they may be estimated more accurately when using an optimal feed rate profile : *optimization for parameter estimation.* We give some further comments on this at the end of Section 5.4.

5.2 A unifying unstructured model

5.2.1 Deficiencies in the current models

The evaluation (see Section 5.1) of the model of Heijnen *et al.* [1979] and the model of Bajpai and Reuß [1980,1981] revealed some biochemical and physical inconsistencies with respect to the *model structure.* Observe that the structural differences between both models are due to structural differences in the specific rates μ, π, and σ, which are interrelated by $\sigma = \mu/Y_{x/s} + m + \pi/Y_{p/s}$. These deficiencies can be summarized as follows.

1. An endogenous metabolism viewpoint as adopted by Heijnen *et al.* can be justified in low substrate concentration conditions. However, at high substrate concentrations, this assumption may not be valid, and should be replaced by a maintenance metabolism viewpoint as in the Bajpai and Reuß model.

2. On the other hand, the Bajpai and Reuß model is inconsistent in low substrate concentration conditions, because the maintenance metabolism concept can lead to (physically impossible) negative substrate concentrations in cases where the glucose feeding rate becomes too small.

3. In modeling the specific production rate π Heijnen *et al.* have extrapolated continuous culture data to fed–batch conditions. This may obscure substrate inhibition or more probably repression effects. Furthermore, their model predicts penicillin production becoming zero if the net growth rate decreases to zero. This is in contradiction with some experiments of Pirt and Righelato [1967] for limited time ranges. For negative growth rates, the production rate kinetics are not defined, thus causing the model to become inconsistent in conditions of very low substrate levels.

4. The Bajpai and Reuß substrate inhibition production kinetics is believed to reflect biochemical evidence better, although an accurate set of corresponding parameters is not available up to now.

We also investigated the corresponding *model parameters.* In this context, we clearly illustrated the *parameter estimation problem* with some simulation experiments using the (slightly modified) Bajpai and Reuß model. Although a reliable estimate of e.g. K_p, K_i, and K_x can not be obtained using data

from a constant feed rate fermentation with zero initial substrate amount, these parameters (especially K_x) may have an important influence upon optimization results. In addition, the simulations indicate that they may be estimated more accurately when using an optimal feed rate profile.

To complete the analysis, we must investigate (i) how to determine the exact metabolism involved, and (ii) the possible effect of different metabolic assumptions —found back in *model structure differences*— on feeding strategy optimization results.

This motivates the construction of a *new unifying unstructured model* for this fermentation process.

5.2.2 A unifying model

5.2.2.1 Design requirements

Let us first enumerate some basic design requirements.

1. The general structure of the updated model must be the same as used by both Heijnen *et al.* and Bajpai and Reuß [equations (5.1)]. In particular, material balances have to be satisfied.

2. There must be a *smooth transition* between *maintenance* and *endogenous* metabolism as a function of substrate concentration C_s : for C_s approaching zero endogenous metabolism is required; for high C_s values maintenance metabolism must be modeled. Furthermore, it must be possible to adjust the endogenous fraction for a certain value of C_s, using as few additional parameters as possible (in order to avoid unnecessary complications in parameter estimation studies).

3. Recent biochemical evidence discussed in Section 5.1.3 suggests that biosynthesis of penicillin might be subjected to glucose repression. Although the exact mechanism (e.g. *repression* or *inhibition*) is not known yet, *glucose inhibition kinetics* as proposed by Bajpai and Reuß are chosen.

4. The specific substrate to biomass conversion rate μ_{substr} (Monod or Contois kinetics) is not fixed a priori, as both are acceptable from the biochemical point of view.

5. The new model must be consistent as to allow physically acceptable values for all variables involved, under different fermentation conditions.

6. The right–hand side of the resulting state equations must have continuous derivatives up to second order with respect to all state variables, in order to make the application of standard optimal control theory possible.

5.2.2.2 Specific rates

These requirements have been incorporated into the model equations (5.1), using the following specific rates :

$$\pi = \pi_m \frac{C_s}{K_p + C_s + C_s^2/K_i} \tag{5.2}$$

$$\mu = \mu_{substr} - Y_{x/s}(f_m(C_s)\, m + f_p(C_s)\, \pi/Y_{p/s}) \tag{5.3}$$

with the specific substrate to biomass conversion rate μ_{substr} either modeled by Contois (4.20) or Monod (4.23) kinetics :

$$\mu_{substr} = \mu_C \frac{C_s}{K_x C_x + C_s} \quad \text{or} \quad \mu_{substr} = \mu_M \frac{C_s}{K_s + C_s}$$

Note that in these specific rates we have made use of the unifying concept of *endogenous fractions* f_m and f_p of energy supply for biomass maintenance and product synthesis respectively, as introduced in Chapter 1 [see definitions (1.9) and (1.10)]. The analysis presented in Section 5.1.3 suggests that the occurrence of a particular metabolism is dictated *directly* by the limiting substrate C_s, rather than by the value of the specific growth rate μ. As a result, we consider the endogenous fractions f_m and f_p as functions of C_s only. Between a lot of possible expressions that match the desired behavior the following expressions are chosen

$$f_m(C_s) = \exp(-C_s/E_m) \qquad f_p(C_s) = \exp(-C_s/E_p)$$

as exponential functions can be easily handled analytically, in particular in computing partial derivatives as is required for optimal control (Section 5.3). As a result of balancing, the specific glucose uptake rate is given by :

$$\begin{aligned} \sigma &= \mu/Y_{x/s} + m + \pi/Y_{p/s} \\ &= \mu_{substr}/Y_{x/s} + m(1 - f_m(C_s)) + \pi(1 - f_p(C_s))/Y_{p/s} \end{aligned} \tag{5.4}$$

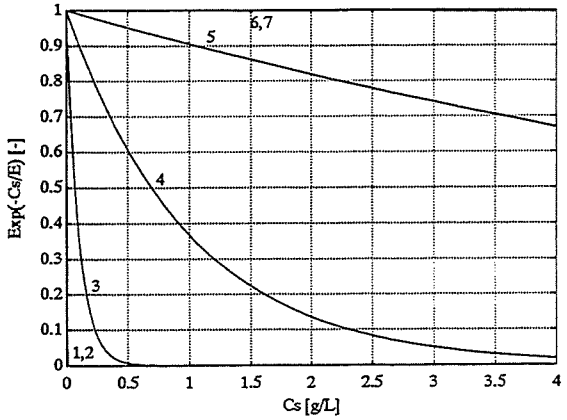

Figure 5.6: $\exp(-C_s/E)$ as a function of C_s for different values of E
Legend: (1) $E = 10^{-9}$ g/L – (2) $E = 10^{-3}$ g/L – (3) $E = 10^{-1}$ g/L (4) $E = 1$ g/L – (5) $E = 10^{+1}$ g/L – (6) $E = 10^{+3}$ g/L – (7) $E = 10^{+12}$ g/L

Observe that in the above expression $(1 - f_i(C_s))$ —with f_i as mentioned— is a Tessier–type kinetics [Tessier 1942].

In Figure 5.6 the endogenous fraction $f(C_s)$ versus C_s is shown for some values of the parameter E. A physical interpretation can be assigned to the parameters E_m and E_p as follows : they represent the *glucose concentration at which the respective endogenous fraction is equal to 36.8 percent.*

5.2.2.3 Special cases

Special Case 1 : $(E_m = E_p) \to +\infty$

Using very high values for E_i, the endogenous fractions f_m and f_p approximate 100 percent for every value of C_s. The specific rates (5.3) and (5.4) reduce to :

$$\begin{aligned} \mu &= \mu_{substr} - Y_{x/s}(m + \pi/Y_{p/s}) \\ \sigma &= \mu_{substr}/Y_{x/s} \end{aligned}$$

which represents an endogenous metabolism as adopted in the Heijnen *et al.* model.

Special Case 2 : $(E_m = E_p) \to 0$

For very low values of E_i the endogenous fractions approximate to zero for all values of $C_s > 0$, as in the original Bajpai and Reuß model. The specific rates (5.3) and (5.4) reduce to :

$$\begin{aligned} \mu &= \mu_{substr} \\ \sigma &= \mu_{substr}/Y_{x/s} + m + \pi/Y_{p/s} \end{aligned}$$

which represents a maintenance metabolism.
However, for $C_s = 0$, $f_m = f_p = 1$. In other words, the metabolism becomes completely endogenous, thus preventing C_s from becoming negative. The modified Bajpai and Reuß model as introduced in Section 5.1.4 is in fact the limit of the new model for $(E_m = E_p) \to 0$.

Although both special cases correspond to known metabolic concepts (endogenous and maintenance metabolism respectively), obviously the physical interpretation of the parameters E_m and E_p as stated above has been lost.

Additional Special Cases

Combining Special Cases 1 and 2, two additional special cases can be constructed : a first one with $E_m \to 0$ and $E_p \to +\infty$, a second with $E_m \to +\infty$ and $E_p \to 0$. For instance, in the second case the specific rates reduce to :

$$\begin{aligned} \mu &= \mu_{substr} - Y_{x/s}m \\ \sigma &= \mu_{substr}/Y_{x/s} + \pi/Y_{p/s} \end{aligned}$$

This models a process where production only occurs at the expense of substrate, while maintenance requirements of the mould are fulfilled by endogenous respiration.

A more general case : $0 < E_m < +\infty$, $0 < E_p < +\infty$

For intermediate values of E_m and E_p, there is a smooth transition between maintenance and endogenous metabolism as a function of C_s. Note that the ability to choose different values for E_m and E_p makes it possible to simulate different endogenous fractions of maintenance requirements and production respectively.

5.2.3 Simulation Results

For all simulations obtained with this unifying model the following assumptions have been made. Values of E_m are always set equal to E_p (further on simply denoted with E), as there is no a priori reason for not doing so. For μ_{substr} Contois kinetics are chosen to make the comparison with the original Bajpai and Reuß model possible. As already described in Section 5.1.3 a set of 120 *reference data* for C_s, C_x and C_p are generated using the original Bajpai and Reuß model with a zero initial amount of substrate and a constant feed rate strategy during 120 hrs. The *nominal* parameter set is Set 2 of Table 5.2, while the initial and operational conditions are summarized in Table 5.3. Since the substrate concentration C_s never becomes negative for this particular feeding strategy, the reference data can be simulated by the unifying model as well using a very low value of E, e.g. $E = 10^{-9}$ g/L.

Model parameter estimation problem

First, we check whether a similar influence of the model parameters upon optimization as described in Section 5.1.4 is obtained under different metabolic conditions. As an example, we investigate the influence of the parameter K_x in the case of a mixed maintenance–endogenous metabolism with $E = 1$ g/L. The value of π_m is adjusted so as to minimize the Euclidean distance to the reference data. The results are summarized in Table 5.6 and Figures 5.7 and 5.8.

Observe that only values $K_x \leq 0.010$ g/g DW result in an acceptable value for π_m, i.e of the same order of magnitude as the reported ones (Section 5.1.3). Therefore, only the combinations 4 to 8 are shown in the plots. From Figure 5.7 ($S_0 = 0$ g) we conclude again that it is virtually *impossible to estimate the correct value of K_x, using data obtained with this particular feeding strategy*. However, the profiles of Figure 5.8 using $S_0 = 1376$ g (i.e. the optimal initial substrate amount for the nominal value $K_x = 0.006$ g/L) indicate a very large influence of K_x upon the final penicillin amount. The results obtained for the other parameters considered in Section 5.1.4 are similar and are not included here. The following trends can be observed.

1. For all parameters a *similar effect upon optimization* is obtained when changing the metabolic assumptions, i.e. the value of E. However, the trends observed become more pronounced when

#	K_x	π_m	$P(t_f)_{ref}$	$P(t_f)_{opt}$	$\mathcal{G}$	$S(0)_{opt}$
1	0.150	0.02896	63.314	360.269	469.0	1489.
2	0.100	0.02231	62.565	302.974	384.3	1486.
3	0.050	0.01434	61.636	217.454	252.8	1478.
4	0.010	0.00606	59.800	103.227	72.6	1418.
5	0.007	0.00531	59.357	91.233	53.7	1390.
6	0.006	0.00506	59.239	87.141	47.6	1376.
7	0.005	0.00480	59.020	82.825	40.3	1356.
8	0.001	0.00377	58.009	63.770	9.9	1050.

Table 5.6: Estimation of π_m for different values of K_x for the unifying model ($E = 1$ g/L) with constant feeding strategy, and corresponding final product amount – optimal initial substrate level and optimal product amount

going from a maintenance metabolism towards an endogenous metabolism. As an example, compare the realizable gain $\mathcal{G}$ in Tables 5.5 and 5.6.

2. If the endogenous fraction increases, the optimal initial substrate amount for corresponding parameters also increases : since more and more biomass is consumed during the production phase — which can result in a decreasing biomass profile as in Figure 5.8—, a larger amount must be built up during the growth phase.

These results motivate a separate investigation of the possible effects of the metabolic assumptions themselves upon optimization results.

Model structure characterization problem

In a second simulation experiment, the model is fitted to the reference data for values of E between $E = 10^{-9}$ g/L (simulating a maintenance metabolism) and $E = 10^{+12}$ g/L (simulating an endogenous metabolism). As already explained, the value of π_m is adjusted so as to minimize the Euclidean distance to the reference data. Some numerical values are summarized in Table 5.7.

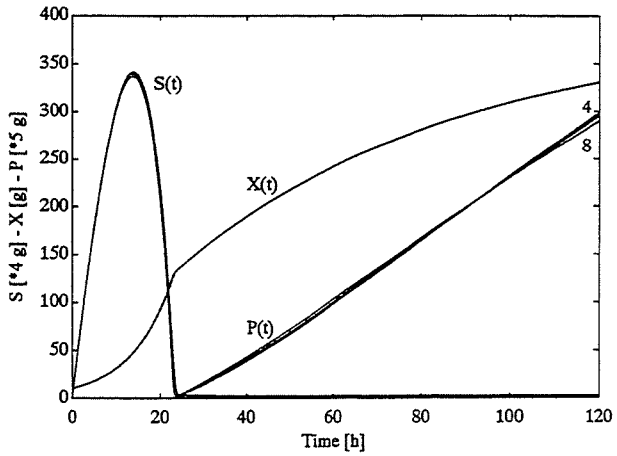

Figure 5.7: Substrate, biomass and penicillin profiles during constant feed rate fermentation for some (K_x,π_m) combinations of Table 5.6 – $S_0 = 0$ g

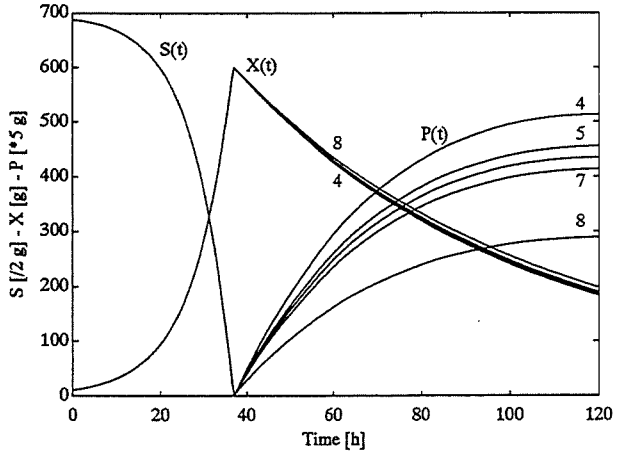

Figure 5.8: Substrate, biomass and penicillin profiles during constant feed rate fermentation for some (K_x,π_m) combinations of Table 5.6 – $S_0 = 1376$ g

#	E	π_m	$P(t_f)_{ref}$	$P(t_f)_{opt}$	$\mathcal{G}$	$S(0)_{opt}$
1	10^{-9}	$4.0000\ 10^{-3}$	59.651	63.461	6.4	280.
2	$4.5622\ 10^{-3}$	$4.0750\ 10^{-3}$	59.683	68.367	14.6	1002.
3	1.	$5.0634\ 10^{-3}$	59.277	87.141	47.0	1376.
4	10^{+12}	$5.2861\ 10^{-3}$	60.822	89.538	47.2	1378.

Table 5.7: Estimation of π_m for different values of E for the unifying model with constant feeding strategy, and corresponding final product amount – optimal initial substrate level and optimal product amount

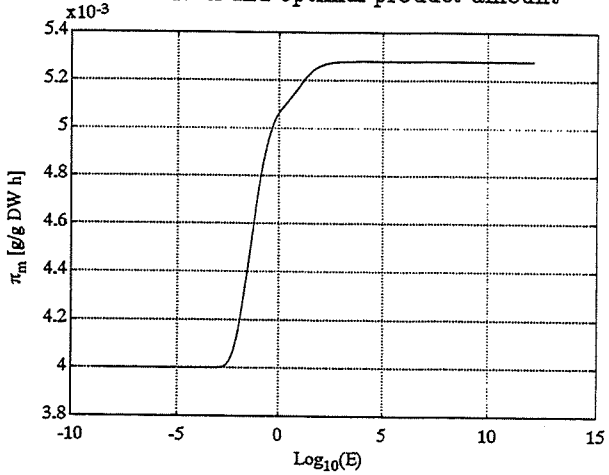

Figure 5.9: Estimation of π_m for different values of E

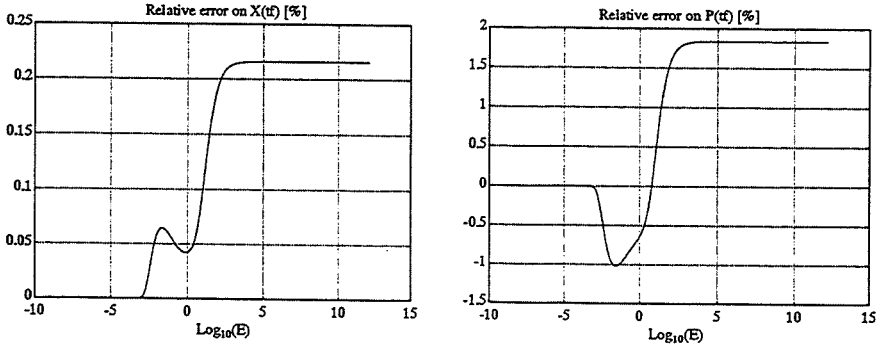

Figure 5.10: Relative error of final biomass amount $X(t_f)$ and final product amount $P(t_f)$ as functions of E

Note that $E = 4.5622\ 10^{-3}$ g/L represents a mixed maintenance–endogenous metabolism with an endogenous fraction of 50 percent at $C_s = (K_p K_i)^{1/2}$, which maximizes π. Figure 5.9 indicates that for all values of E, π_m remains within the range of reported values. The relative error (with respect to the reference data set) on the final biomass amount $X(t_f)$ and final product amount $P(t_f)$ as function of E is shown in Figure 5.10. For $P(t_f)$ the error is smaller than 2 %, for $X(t_f)$ the error becomes even less than 0.22 %. The corresponding time profiles are plotted in Figure 5.11. As already noted, the results for the maintenance model coincide with the reference data, as C_s never becomes negative for this particular feeding strategy. For $10^{-9} < E < 1.0$ g/L, the fit is almost exact. For the endogenous model, the fit of X and P is still very good, although the S–profiles differ somewhat in the growth phase. This is a very important result, as it indicates that it is virtually *impossible to make a distinction between different kinds of metabolic behavior, using data from fermentations with this particular feeding strategy.*

In Figure 5.12, the value of S_0 is increased to $S_0 = 400$ g. The resulting penicillin profiles exhibit large differences : the *maintenance* model (curve 1) predicts a much lower product synthesis in comparison with the other cases of Table 5.7. This can be explained as follows. Due to the increased initial substrate amount, a larger amount of biomass is built up during the growth phase, as compared with the results of Figure 5.11. This is favorable for the cases 2 to 4 of Table 5.7 (characterized by an increasing endogenous fraction) : during the production phase biomass is partially consumed to fulfil maintenance requirements. In these cases, the decreased value of the constant feed rate during fermentation —due to the increased initial substrate amount— has little influence. However, in the first case (i.e. the maintenance metabolism model) the consumption of substrate for maintenance requirements further amplifies the effect of the lower feed rate on the substrate concentration during production : the specific production rate $\pi(C_s)$ decreases. Comparison of Figures 5.11 and 5.12 indicates that this model may be very useful for *model structure characterization* purposes as well, when choosing an appropriate feeding strategy. The impact of more complex feeding strategies is discussed in Section 5.3.

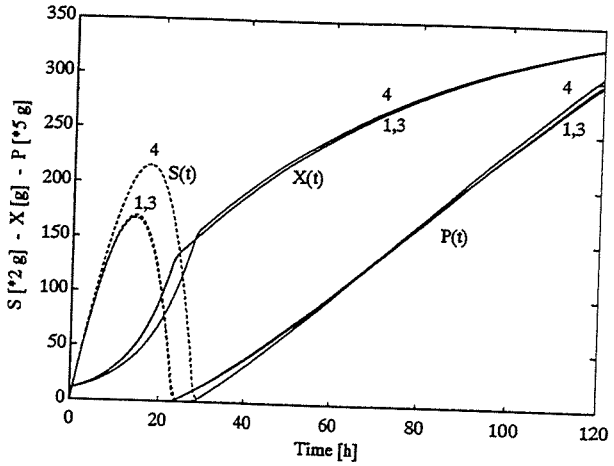

Figure 5.11: Substrate, biomass and penicillin profiles during constant feed rate fermentation for some (E,π_m) combinations of Table 5.7 – $S_0 = 0$ g

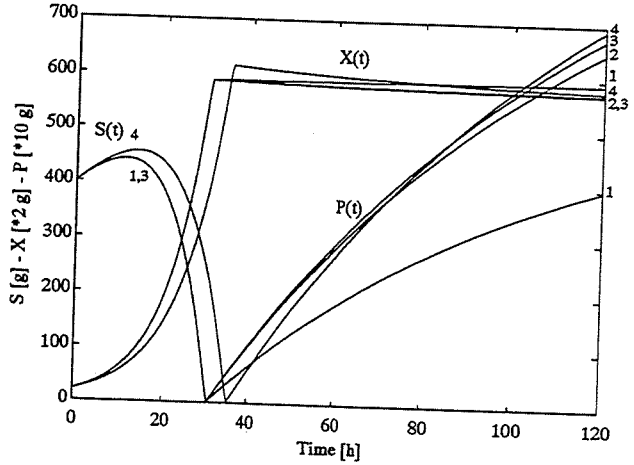

Figure 5.12: Substrate, biomass and penicillin profiles during constant feed rate fermentation for some (E,π_m) combinations of Table 5.7 – $S_0 = 400$ g

5.2.4 Conclusions

The deficiencies in the models of Heijnen *et al.* [1979] and Bajpai and Reuß [1980,1981] are corrected well in this new unifying unstructured model. It is essentially based on the unifying concept of *endogenous fractions* f_m and f_p of energy supply for biomass maintenance and product synthesis respectively, as introduced in Chapter 1.

Only two additional parameters E_m and E_p —with a clear physical interpretation— are needed to obtain a more complete model representation which can simulate a lot of different metabolic conditions.

The above preliminary simulation results —obtained with a simple parametric optimization method— indicate that a proper choice of the input feeding strategy to this model can give indications about the *metabolic nature* of the mould and about the *model parameters*. In addition, the model structure characterization problem is in some sense *decoupled* from the parameter estimation problem.

In Section 5.3, the model structure characterization problem is studied in more detail using a non–parametric optimization technique, namely optimal control.

5.3 Optimal control using the unifying model

5.3.1 Optimal control strategy

In this section we apply optimal control theory in order to solve exactly the same optimization problem as stated in Sections 4.2.3 and 4.3.3 for the models of Heijnen *et al.* and Bajpai and Reuß respectively. As the new unifying model is in some sense an extension of the original Bajpai and Reuß model using the same specific rates μ_{substr} and π, obviously this model also belongs to the class of processes with monotonic specific growth rate and non–monotonic specific production rate (see Section 3.5.1) characterized by a decoupling between growth and production. Since the specific rates are sufficiently smooth, optimal control can be applied directly without any difficulty.

For a detailed analysis of the optimal control sequence and the corresponding switching times we refer to Section 3.5. Obviously, the numerical values of the switching times and of the singular control (3.16) depend on the value of the parameter E, i.e. on the metabolism involved. However, we will illustrate that the computational algorithm proposed in Section 3.5.2 can be

used to calculate the optimal volumetric feed rate profile for any value of E in the (open) interval $]0, +\infty[$.

Simulation results are given after the presentation of *heuristic* feeding strategies, in order to make the comparison between the performance of different strategies as a function of E more easy.

5.3.2 Heuristic control strategies

Obviously, if in equation (5.3) μ_{substr} is modeled with Monod kinetics then all specific rates (5.2) to (5.4) become functions of C_s only. In that case the singular arc can be characterized as described in Theorems 3.1 and 3.2. If μ_{substr} is modeled with Contois kinetics, we refer to the comments formulated in Section 4.3.6.

Therefore, suboptimal *heuristic* control strategies based on biochemical and mathematical knowledge can be developed and justified in exactly the same way as presented in general in Section 3.7, and in Sections 4.2.7 and 4.3.7 for the Heijnen *et al.* and the Bajpai and Reuß models respectively.

growth phase $[0, t_2]$

As already explained, the growth phase is a batch phase if there are no constraints on the input u or the state $\mathbf{x}$ and if the initial substrate amount S_0 is free. The fraction α_{growth} of all substrate available α which is consumed for biomass growth is added at time $t = 0$. This ensures the highest possible value for μ (5.3) during growth.

production phase $[t_2, t_3]$

- For the heuristic C_s–controllers we refer to Section 4.3.7. We use a control of the form (4.39)

$$u_{production}(t) = \frac{\sigma X}{C_{s,in} - C_s} \tag{5.5}$$

to keep the substrate concentration C_s constant, either at the value $C_s^* = (K_p K_i)^{1/2}$ which maximizes π (5.2) or at another set–point to be optimized. We obtain a *one or two dimensional optimization problem respectively.*

- The heuristic μ–controller (4.40) developed for the Bajpai and Reuß model (with Contois kinetics)

$$u_{production}(t) = \frac{\sigma X + \mu S}{C_{s,in}} \tag{5.6}$$

which keeps μ constant during production, can be extended as follows (μ_{substr} is modeled with Contois kinetics) :

$$u_{production}(t) = \frac{\mu_{max} K_x C_x (C_s \mu + C_x \sigma)/(K_x C_x + C_s)^2 + F(E_m, E_p)\sigma X/V}{\mu_{max} K_x C_x C_{s,in}/V(K_x C_x + C_s)^2 + F(E_m, E_p)(C_{s,in} - C_s)/V} \tag{5.7}$$

with

$$F(E_m, E_p) \triangleq \exp(-C_s/E_m) m Y_{x/s}/E_m + \exp(-C_s/E_p)\frac{Y_{x/s}}{Y_{p/s}}\left(\frac{\pi}{E_p} - \frac{d\pi}{dC_s}\right)$$

Observe that controller (5.7) is a *quasi convex* combination of controllers (5.6) and (5.5) : the numerator (respectively denominator) is obtained by adding the numerators (respectively denominators) of (5.6) and (5.5) weighted by $\mu_{max} K_x C_x/(K_x C_x + C_s)^2$ and $F(E_m, E_p)/V$ respectively. For $E \to 0$ we can verify that controller (5.7) reduces to controller (5.6) as required.

- As usual, the heuristic controller is stopped at $t = t_3$ when all substrate available α is added. As in the optimal case, the concluding batch phase is stopped when $dP/dt = 0$.

We will illustrate in the following section that these control sequences —as in the case of optimal control— are independent of the metabolism involved, although the numerical values of the switching times and the control during production obviously depend on the value of the parameter E.

5.3.3 Simulation results

We limit ourselves to the case of an unbounded input u and an unconstrained state vector $\mathbf{x}$, with free initial substrate amount $S(0)$. The extension to problems involving one or more constraints is straightforward, following the same lines as presented in Section 3.5.3 for a general model and in Section 4.3.5 for the Bajpai and Reuß model. The initial and operational conditions are as specified in Section 5.1.4.

Some numerical results are summarized in Table 5.8, with the gain $\mathcal{G}$ as defined in (4.16). The corresponding time profiles for optimal control are shown in Figure 5.13. We can formulate the following conclusions :

1. The results indicate that there exists a maximum realizable gain $\mathcal{G}$ as a function of the endogenous fraction E.

2. The computational algorithm proposed in Section 3.5.2 can be used for any value of the parameter E.

3. Similarly, the performance of the heuristic strategies is excellent independent of the metabolic assumptions.

4. For the mixed maintenance–endogenous models considered and the completely endogenous model, the *overall* specific growth rate μ becomes negative. However, the specific substrate to biomass conversion rate μ_{substr} always remains positive —as biologically required— since C_s can not become negative in the unifying model. The occurrence of negative values for μ is completely due to increasing endogenous fractions of biomass maintenance and product synthesis.

In order to obtain a more detailed picture, the *one degree of freedom* heuristic C_s–control (i.e. with $C_s(t_2) = (K_p K_i)^{1/2}$) has been calculated for a large number of values of E. The results are summarized in Figure 5.14.

The optimal value of $S(0)$ increases uniformly with E : for a maintenance metabolism ($E \to 0$), 35.53 % of the available substrate amount α is needed at the beginning of the fermentation, while for an endogenous metabolism ($E \to \infty$) as much as 93.6 % is needed. This result can be explained as follows. When E increases from $E = 0$ to $E \to \infty$, the endogenous fraction of energy supply for maintenance requirements of living biomass and product synthesis increases uniformly. As a result, an increasing amount of biomass must be built up during the growth phase (requiring an increasing amount of substrate), which is then partially combusted during the production phase. Consequently, the final biomass amount $X(t_f)$ decreases with increasing values of E.

Similarly, since more substrate is consumed during growth with increasing values of E, the growth phase will last longer resulting in an increasing value of the switching time t_2. As for the final time t_f, there seems to be a minimum according to a mixed maintenance–endogenous metabolism with $\log_{10}(E) = 0.875$.

E	S_0	t_2	t_f	$P(t_f)$	$\mathcal{G}$
Optimal control					
10^{-9}	528	28.271	132.033	63.846	3.961
$4.5622\ 10^{-3}$	880	32.749	125.200	70.652	16.822
1.	1409	37.016	117.602	87.448	49.064
10^{+12}	1411	42.106	122.493	89.709	45.909
Heuristic C_s–control			$C_s(t_2) = \sqrt{K_p K_i}$		
10^{-9}	533	28.355	131.323	63.597	3.692
$4.5622\ 10^{-3}$	940	33.338	124.427	68.436	13.160
1.	1401	36.969	116.906	87.164	48.580
10^{+12}	1404	42.059	121.974	89.430	45.455
Heuristic C_s–control			$C_s(t_2)$ *optimized*		
10^{-9}	551	28.644	131.372	63.724	3.762
$4.5622\ 10^{-3}$	1124	34.926	122.252	69.263	14.527
1.	1417	37.075	117.250	87.258	48.740
10^{+12}	1418	42.165	122.189	89.511	45.587
Heuristic μ–control			$\mu(t_2)$ *optimized*		
10^{-9}	551	28.644	131.321	63.736	3.782
$4.5622\ 10^{-3}$	1113	34.838	122.727	69.439	14.817
1.	1406	36.990	117.511	87.428	49.030
10^{+12}	1407	42.069	122.445	89.686	45.870

Table 5.8: Numerical results for optimal and heuristic control for some values of E

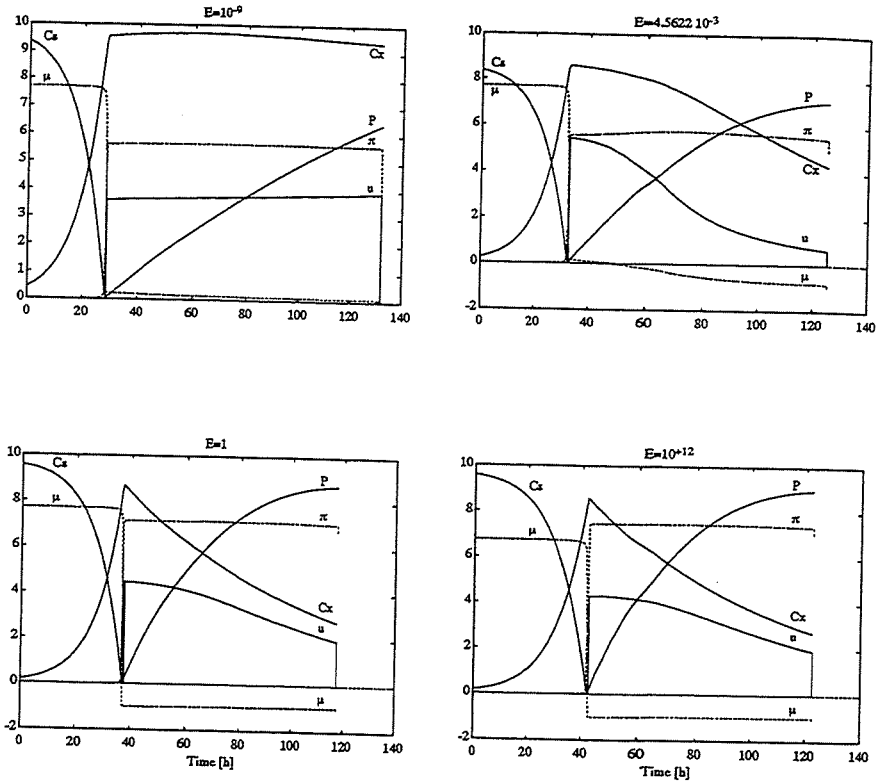

Figure 5.13: Substrate, biomass, product, μ, π and u profiles during optimal feed rate fermentation for the values of E of Table 5.8

Scaling:

$E = 10^{-9}$	:	$C_s/7$	$C_x/3$	$P/10$	$\mu * 70$	$\pi * 1500$	$u * 200$
$E = 4.5622\ 10^{-3}$	:	$C_s/12$	$C_x/5$	$P/10$	$\mu * 70$	$\pi * 1500$	$u * 200$
$E = 1$	:	$C_s/15$	$C_x/7$	$P/10$	$\mu * 70$	$\pi * 1500$	$u * 1500$
$E = 10^{12}$	:	$C_s/15$	$C_x/7$	$P/10$	$\mu * 70$	$\pi * 1500$	$u * 1500$

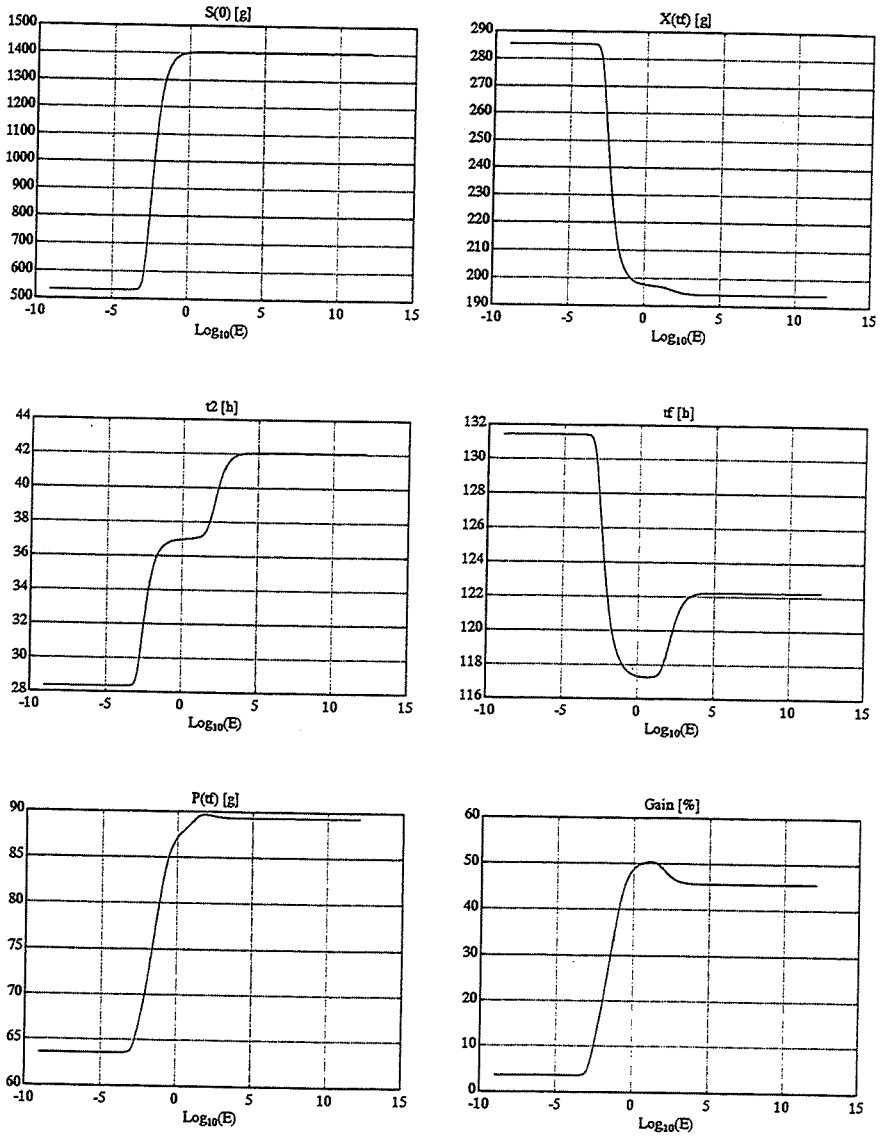

Figure 5.14: Heuristic C_s–control : $S(0)$, $X(t_f)$, t_2, t_f, $P(t_f)$ and $\mathcal{G}$ as functions of E

Observe that $P(t_f)$ has a (very smooth) maximum value $P_{f,max} = 89.68$ g, for $\log_{10}(E) = 1.875$. The gain $\mathcal{G}$ reaches its maximum value $\mathcal{G}_{max} = 50.390$ % for $\log_{10}(E) = 1.250$, while the minimum value is $\mathcal{G}_{min} = 3.692$ % for $\log_{10}(E) \to -\infty$ (which represents the model of Bajpai and Reuß).

These simulations sufficiently illustrate that the metabolic condition of the mould may be a key factor in concluding whether or not changing the glucose feeding strategy for a given amount of substrate has an effect on the final amount of product. However, in order to identify the parameter E, the glucose feeding strategy must be designed carefully : remember that it is impossible to extract E from data resulting from a constant glucose input rate.

5.3.4 Conclusions

The results of this section can be summarized as follows. As indicated by the simulations, the new unifying model for the penicillin G fed–batch fermentation process proposed in Section 5.2 is an excellent tool for studying the *model structure characterization problem*, more precisely for evaluating the importance of the metabolic nature of the mould.

We have illustrated that the assumptions about the fundamental nature of the metabolism may have a great influence on feeding strategy optimization results. For instance, a model assuming completely endogenous metabolism allows for a larger realizable gain $\mathcal{G}$ than a model assuming completely maintenance metabolism. This explains the contradictory results obtained by Heijnen *et al.* and Bajpai and Reuß respectively.

Notice however that our conclusion formulated after the analysis of the Bajpai and Reuß model (Section 4.3) remains valid for different metabolic conditions. Comparing the results of Table 5.7 (obtained using parametric optimization) and Table 5.8 (obtained using non–parametric optimization), we note that *a performance similar to the optimal one can be obtained provided the associated degrees of freedom are at their optimal values, independent of the metabolic assumptions*, i.e. the value of E.

Finally, apart from the large influence of the metabolism involved — reflected in the model structure— upon optimization, we can determine the actual metabolism by applying an optimal feed rate profile : *optimization for model structure characterization.* We give some further comments on this at the end of the following Section.

5.4 Conclusions

In Section 5.1 of this chapter the model of Heijnen *et al.* [1979] and the model of Bajpai and Reuß [1980, 1981] are carefully analyzed and compared from a biochemical point of view. Although both models claim to be accurate descriptions of the penicillin G fed–batch fermentation process, feeding strategy optimization studies —described in Chapter 4— indicate that the realizable gain —i.e. the optimal product amount compared with the outcome of a constant feeding pattern in the same time with zero initial substrate amount— depends highly on the model used. Moreover, the Heijnen *et al.* model is very sensitive towards different feeding policies, while the Bajpai and Reuß model is not. In this chapter both the *conceptual* differences —found back in *structural* differences— between the two modeling approaches and the corresponding *parameter sets* used are shown to play in important role. The *parameter estimation problem* is illustrated with some examples. As a matter of fact, several different parameter sets can be determined which fit the experimental data resulting from simple constant feed rate fed–batch fermentations with low initial substrate amount. However, using a simple parametric optimization technique we have shown that some of these parameters may have a great influence upon feeding strategy optimization results. Furthermore, the simulations suggest that feeding strategy optimization studies can be a valuable tool in the design of real life experiments for parameter estimation purposes : *optimization for parameter estimation.* We give some further comments on this paradigm at the end of this section.

To complete this analysis, we have investigated in Section 5.2 how to determine the exact metabolism involved —i.e. the exact model structure— and the possible effects of different metabolic assumptions upon feeding strategy optimization results. Therefore, based on the new concept of *endogenous fractions* introduced in Chapter 1 we have constructed a *new unifying unstructured model* which adequately corrects the deficiencies in the models of Heijnen *et al.* and Bajpai and Reuß. At most two additional parameters —with a clear physical interpretation— are required to obtain a more complete model representation. In this model structural differences are completely due to different values of these additional parameters. Its most striking features are the guarantee for physically acceptable values of all variables under all conditions, and a smooth transition between maintenance and endogenous metabolism as a function of the substrate concentration. Using a similar parametric optimization technique as in Section 5.1 we have illus-

trated the *structure characterization problem.* The results indicate that an appropriate choice of the input feeding strategy can give indications about the metabolic nature of the mould also. In addition, we have shown that the model structure characterization problem is in some sense *decoupled* from the parameter estimation problem

Therefore, in Section 5.3 this model structure characterization problem is studied in more detail using optimal control theory. It is illustrated that the computational algorithm developed in Chapter 3 is independent of the exact nature of the metabolism (maintenance or endogenous). However, as shown by simulations, the nature of the metabolism may be a key factor in concluding whether or not altering the substrate feeding strategy has an important influence on the final amount of product. Apart from the large influence of the model structure upon optimization, the results suggest that the real metabolism can be determined when applying an optimal feed rate profile : *optimization for model structure characterization.* The general heuristic optimization methodology based on mathematical and microbial insight has been extended to this unifying model. We have presented some suboptimal heuristic controllers that proved to be a successful alternative for the optimal control, independent of the metabolic conditions. Since these controllers have a more realistic control objective, namely set–point control, they can serve as a basis for the development of more practical and reliable *optimal adaptive control schemes* (see Chapter 6).

At the end of this chapter we want to make some additional remarks, in particular on our new paradigm *optimization for model discrimination.*

1. It should be clear that the example of penicillin G fed–batch fermentation is chosen only as a vehicle for presenting the basic ideas, methodology and results. In fact this process is representative for the whole class of secondary metabolite fermentation processes. We believe that a similar unifying model can be very useful for other fermentation processes as well.

2. Clearly, both the parameter estimation problem and the structure characterization problem may be interpreted well within the theory of *persistence of excitation.* In contrast to the optimal strategy, a simple constant feed rate profile with low initial substrate amount does not seem to be sufficiently rich to allow for a complete model identification. Therefore, future research should concentrate in the first place on the

design of a sufficiently exciting feeding pattern. This is precisely what is meant by our new paradigm *optimization for model discrimination.*

3. The approach presented in this chapter allows for solving both the performance measure optimization problem and the model discrimination problem at the same time. The simulations indicate that we can determine the correct process model involved when feeding with an optimal strategy.

4. However, in order to do so the following paradox remains to be solved : determination of a (sufficiently exciting) optimal strategy by applying optimal control theory requires a complete knowledge of the process model *in advance.* The solution is then to determine a suboptimal (but also sufficiently exciting) feed rate strategy which makes only use of the general structure of the model, i.e. the general balance equations (5.1), while the specific rates (and possibly the model parameters) are treated as time varying parameters which can be estimated on–line using *software sensors.* In order to guarantee nearly optimal performance, we will incorporate as much as possible information obtained during preliminary optimal control studies into an adaptive control strategy : *optimal adaptive control.* We will illustrate that the *heuristic controllers* presented throughout this thesis can link together the *optimal control* approach and the *adaptive control* approach in a very natural way. A general methodology for fed–batch fermentation processes is presented in Chapter 6.

Chapter 6

Optimal adaptive control Case study : fed-batch fermentation processes

In this chapter we consider the design of a substrate feeding rate controller for a class of biotechnological processes in stirred tank reactors, characterized by a decoupling between biomass growth and product formation. More specifically, we consider the most common case of a process with monotonic specific growth rate and non–monotonic specific production rate as functions of substrate concentration. The main contribution is to illustrate how the insight, obtained by preliminary optimal control studies, leads to the design of easy to implement adaptive controllers. The controllers derived in this way combine a nearly optimal performance with good robustness properties against modeling uncertainties and process disturbances. Since they can be considered model–independent, they may be very helpful also in solving the model identification problem as discussed in Chapter 5. As an example, simulation results are given for the penicillin G fed–batch fermentation process using the new unifying model.

In Section 6.1 the concept of optimal adaptive control is motivated in detail. Starting from the optimal control solution, the heuristic substrate controllers presented at different places throughout this thesis are briefly reconsidered with respect to a real life implementation. We illustrate that a straightforward implementation is not robust at all. However, as these controllers are the translation of a realistic control objective —namely set–

point control—, they can serve as a basis for the development of more reliable, robust model–independent adaptive control schemes. To do so, they are interpreted within the framework of nonlinear linearizing control theory. By doing so, we incorporate a mechanism that makes them both stable and robust against disturbances.

The next step is then to cope with the monitoring problem, i.e. how to determine on–line the variables needed in the controller. In other words, how to make the nonlinear linearizing controller adaptive. Note that we prefer to apply nonlinear adaptive control theory. Since a fermentation process is known to be inherently nonlinear, it is reasonable to expect that better control would result by exploiting from the outset the nonlinearities in the model in the design of a nonlinear adaptive control algorithm. A detailed survey of the use of adaptive controllers in bioreactor control is given by Bastin and Dochain [1990].

We present in Sections 6.2, 6.3 and 6.4 three possible solutions depending on which variables are on–line available. The use of software sensors is clearly illustrated. Both a linear regression estimator and a state observer based estimator can be used for on–line tracking of the specific rates which we consider as time varying parameters (minimal modeling concept). Furthermore, we illustrate that it is possible to take a measurement delay into account.

A remarkable result is the following. If there are no state inequality constraints, we only specify a substrate reference level for the production phase. However, the controllers we propose can be implemented without difficulty from the start of the fermentation on. The first growth phase is then mainly used to obtain estimator convergence. Furthermore, the extension to a problem with constraints is straightforward.

The three solutions are compared with simulation results for the penicillin G fed–batch fermentation process.

Finally, in Section 6.5 we present some conclusions. The main contribution of this chapter is to illustrate that the design of an adaptive controller for this class of fermentation processes can be successfully based on a preliminary optimal control study. For instance, we are able to design a substrate concentration reference profile which guarantees suboptimal performance. As such, this chapter can be considered as an extension of the methods presented in Chapter 5 of [Bastin and Dochain 1990] where the reference substrate concentration is kept constant throughout the whole fermentation process.

6.1 Optimal adaptive control : motivation

6.1.1 Problem statement

In this chapter we consider the class of fed–batch fermentation processes described by an (unstructured) model of the form (3.1) or (5.1) :

$$\begin{aligned} \frac{dS}{dt} &= -\sigma X + C_{s,in}u \\ \frac{dX}{dt} &= \mu X \\ \frac{dP}{dt} &= \pi X - k_h P \\ \frac{dV}{dt} &= u \end{aligned} \tag{6.1}$$

or, using concentrations as state variables as in (3.2) :

$$\begin{aligned} \frac{dC_s}{dt} &= -\sigma C_x - C_s\frac{u}{V} + C_{s,in}\frac{u}{V} \\ \frac{dC_x}{dt} &= \mu C_x - C_x\frac{u}{V} \\ \frac{dC_p}{dt} &= \pi C_x - C_p\frac{u}{V} - k_h C_p \\ \frac{dV}{dt} &= u \end{aligned} \tag{6.2}$$

For an explanation of all symbols used, we refer to the Nomenclature (Appendix B).
As usual, dissolved oxygen is considered non–limiting, by maintaining a sufficiently high aeration level. The *shape* of the specific rates μ_{substr} and π as functions of substrate concentration C_s is as depicted in Figure 6.1 : μ_{substr} is a monotonically increasing function, while π is non–monotonic exhibiting a maximum. In other words, the enzyme catalyzed production is *not associated* to the microbial growth (see also Section 3.5.1). The specific rates σ, μ and π are interrelated by (1.11) :

$$\sigma = \mu/Y_{x/s} + m + \pi/Y_{p/s}$$

We consider exactly the same optimization problem as formulated in Sections 4.2.3, 4.3.3 and 5.3.1 for the Heijnen *et al.*, the Bajpai and Reuß, and the unifying model respectively. It can be summarized as follows :

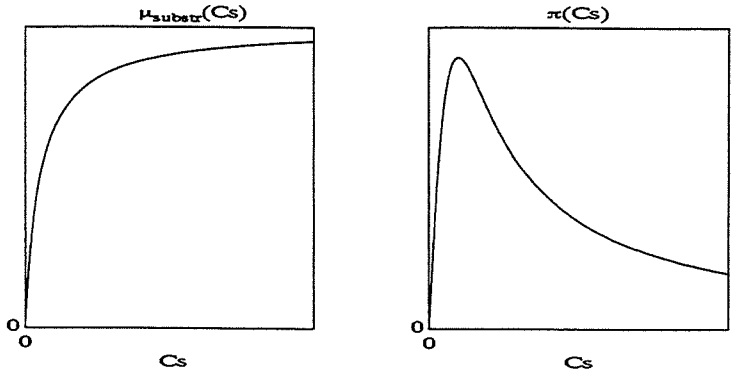

Figure 6.1: Process with monotonic μ_{substr} and non–monotonic π

Determine for the set of dynamic equations (6.1) the optimal volumetric substrate feed rate profile $u^*(t)$ which maximizes the final amount of product $P(t_f)$, subject to the following constraints :

1. $t_0 = 0$, t_f = *free*
2. $P(0) = P_0$ and $X(0) = X_0$ are given. $S(0) = S_0$ is *free*. $V(0) = V_0$ follows from (4.31) :

$$V_0 = V_* + S_0/C_{s,in}$$

with V_* the initial volume without substrate.

3. the total amount of substrate available for fermentation α is *fixed*. In other words, the final reactor volume is fixed $V(t_f) = V_f$.

6.1.2 Optimal control strategy

The solution to this problem using optimal control theory has been described in detail in Sections 3.5.2, 4.2.5, 4.3.5 and 5.3.1, for a general model, the Heijnen *et al.* model, the Bajpai and Reuß model and the new unifying model respectively. Due to the decoupling between growth and production, the fermentation behaves as a *biphasic* process. As in Chapter 5, we limit ourselves to a problem with unconstrained input u and state $\mathbf{x}$ and free initial substrate concentration $C_s(0)$. The extension to problems involving one or more constraints is straightforward, as illustrated for instance in Section

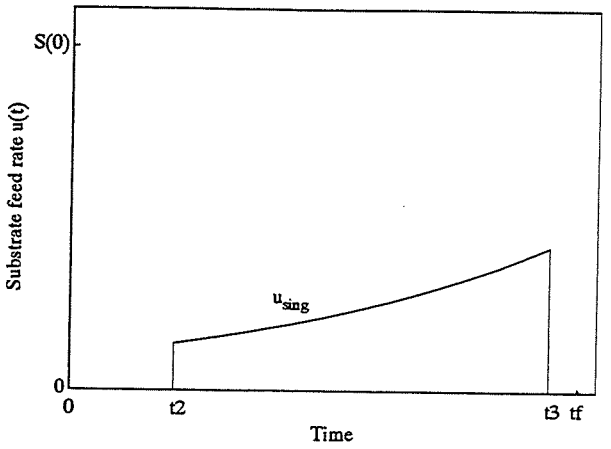

Figure 6.2: Optimal control sequence

3.5.3. The optimal profile can be summarized as follows (see also Figure 6.2) :

1. The *growth phase* is a *batch* phase. All substrate consumed during growth α_{growth} is added all at once at time $t = 0$, thus ensuring the highest possible specific growth rate μ for all $t \in [0, t_2]$.

2. During the *production phase*, a *singular control* of the form (3.16) forces the process to produce the product as fast as possible. At any time, there is a balance between glucose feeding and glucose demand for production and maintenance, thus ensuring the lowest possible growth rate. When $V(t_3) = V_f$, the fermentation continues in *batch* until the net product formation rate dP/dt equals zero at $t = t_f$.

In other words, the general two point boundary value problem has been reduced to the *two dimensional optimization of the initial substrate amount $S(0) = S_0$ and the time t_2 at which the switching from batch to singular control occurs.* In Section 3.3.2 we already pointed out that for the performance measure considered here *the singular control* (3.16) *is a nonlinear feedback law of the state variables S, X, P and V only.* In other words, the costate $\boldsymbol{\lambda}$ has been eliminated completely.

E	π_m	$S(0)$	t_2	t_f	$P(t_f)$
10^{-9}	$4.0000\ 10^{-3}$	528.	28.271	132.033	63.846
10^{+12}	$5.2861\ 10^{-3}$	1411.	42.106	122.493	89.709

Table 6.1: Numerical results for optimal control for two limiting cases

6.1.3 Case study : the penicillin G fed-batch fermentation process

As a test case for all methods presented in this chapter we consider again the penicillin G fed–batch fermentation process modeled by our new unifying model described in Chapter 5. Remember that this model reduces to the slightly modified Bajpai and Reuß model if μ_{substr} is modeled with Contois kinetics (4.20) within a maintenance metabolism viewpoint, i.e. $E \to 0$: the only difference is that C_s can not become negative. The numerical value of the model parameters for $E \to 0$ is given in Set 2 of Table 4.7. Note that the value of π_m depends on the value of E as shown in Figure 5.9 while the other parameters remain the same when changing E. The operational and initial conditions are summarized also in Table 4.7.

The optimal control results for two limiting cases are repeated in Table 6.1. Remember that $E = 10^{-9}$ g/L simulates a completely *maintenance* metabolism, while $E = 10^{+12}$ g/L represents a completely *endogenous* metabolism. The corresponding time profiles have been shown in Figure 5.13.

6.1.4 Heuristic control strategies

In Section 3.7 we already discussed some drawbacks of the optimal control solution. The most important ones with respect to real life implementation are reconsidered here.

1. Optimal control is a very *model sensitive* technique. It requires a complete knowledge of the process model. Since in biotechnology this assumption is in practice never fulfilled, the optimal profile is in general calculated using a highly simplified model describing the process more or less correctly only from a qualitative viewpoint. Therefore, the resulting optimal profiles can be used only to increase the insight in both the process and the quality of the model at hand. As an example, a careful optimal control study of both the Heijnen *et al.* model (Section 4.2) and the Bajpai and Reuß model (Section 4.3) has lead to the construction of the new unifying model presented in Section 5.2.

2. We already mentioned that for the performance measure at hand (i.e. maximization of final product amount) the optimal feed rate profile is obtained in complete state feedback form except for the switching time t_2 between the batch growth phase and the singular production phase (Figure 6.2). In general, t_2 must be determined numerically in advance using the computational algorithm proposed in Section 3.5.2. The results of Table 6.1 sufficiently illustrate the important influence of e.g. the metabolic conditions —and thus the model structure— on the value of t_2. In Section 3.6 we derived necessary and sufficient conditions for which t_2 also becomes function of state variables only. However, even if a perfect process model is available which satisfies all conditions to obtain the complete optimal solution in closed loop, real life implementation is still hampered by the lack of *reliable sensors* suited to real time monitoring of the process variables needed in the controller. Remember that, besides a perfect analytical knowledge of all specific rates and corresponding parameters, the control during the singular phase (3.16) requires on–line measurements of all state variables S, X, P and V.

Therefore, it is very useful to construct *suboptimal* strategies that do not suffer from the above difficulties, at the expense of an as small as possible decrease in performance. At different places in this thesis we have considered the design of suboptimal *heuristic* controllers for both the substrate concentration C_s (*heuristic C_s–control*) and the overall specific growth rate μ (*heuristic μ–control*). A general discussion can be found in Section 3.7. In Sections 4.2.7, 4.3.7 and 5.3.2 this methodology is applied to the penicillin G fed–batch fermentation process using the Heijnen *et al.* model, the Bajpai and Reuß model and the new unifying model respectively. We have illustrated the excellent performance of these heuristic controllers as compared with the corresponding optimal control solution. This performance proves independent of the model used and/or the metabolism involved. The results for the same limiting cases as in Table 6.1 are given in Table 6.2.

Note that we can even allow the specific rates μ_{substr} and π to be functions of other component concentrations as well (e.g. C_x), provided these specific rates as functions of substrate concentration C_s have the general shape shown in Figure 6.1. As an example, the results of Table 6.2 are obtained with μ_{substr} modeled by Contois kinetics (4.20).

E	π_m	$S(0)$	t_2	t_f	$P(t_f)$
10^{-9}	$4.0000\ 10^{-3}$	533.	28.355	131.323	63.597
10^{+12}	$5.2861\ 10^{-3}$	1404.	42.059	121.974	89.430

Table 6.2: Numerical results for heuristic C_s–control for two limiting cases – $C_s(t_2) = (K_p K_i)^{1/2}$

The main contribution of this chapter is to present a methodology for the *design of robust and easy to implement feed rate strategies with nearly optimal performance based on these heuristic controllers in presence of modeling uncertainties and monitoring difficulties.* In order to do so, we will combine concepts and techniques from both *optimal control* and *adaptive linearizing control* : *optimal adaptive control.*

6.1.5 Linearizing control

If we assume that μ_{substr} and π (and thus σ) are functions of substrate concentration C_s only, then the *optimal* feed rate during the production phase is given by [see equation (3.40)] :

$$u_{sing} = \frac{\sigma C_x V}{C_{s,in} - C_s} + k_h \, \mathcal{F}[C_s, C_x, C_p] \tag{6.3}$$

which is linear in the specific product decay rate k_h and a feedback law of state variables only. Observe that the factor $\mathcal{F}$ in the second term requires knowledge of an analytical expression of the derivatives of all specific rates up to second order. One of the results of Theorems 3.1 and 3.2 is that $k_h = 0$ is a necessary and sufficient condition for substrate concentration C_s to be constant along the singular arc.

If we *neglect* product decay when designing a suboptimal substrate feed rate controller, we obtain a much simpler control law :

$$u_{production} = \frac{\sigma C_x V}{C_{s,in} - C_s} \tag{6.4}$$

This *heuristic* substrate controller keeps substrate concentration C_s constant during production, say at $C_s = C_s^*$. A detailed motivation from both a microbiological and a mathematical point of view is given in Section 3.7.

Depending on whether or not the substrate concentration level C_s^* during production is an additional degree of freedom, we obtain a *one or two dimensional optimization problem.* From Section 3.7 we know that the substrate concentration which maximizes π is an appropriate (initial) value for the set–point C_s^*.

With respect to a real life implementation, the heuristic controller (6.4) has the following advantages over the optimal controller (6.3).

1. The switching time t_2 (Figure 6.2) —and thus the complete control— is known in closed loop as a function of the state : if substrate concentration C_s equals the predetermined set–point C_s^* the production phase starts using controller (6.4).

2. As for the modeling uncertainty problem, only the specific substrate consumption rate σ is required.

3. As for the on–line monitoring problem, the number of state variables to be measured on–line has been reduced by one : there is no need for a measurement of the product P. This is an important advantage in cases where the product remains (almost) completely in the liquid phase of the reactor.

However, we are still far away from a real life implementation. Two important problems remain to be solved.

1. Although the number of unknowns has been reduced, this controller still needs on–line measurements or at least reliable estimates of substrate, biomass, volume of the liquid phase and the specific substrate consumption rate.

2. The closed loop stability is not guaranteed a priori. For the general model (6.2), the closed loop dynamics for substrate C_s when using controller (6.4) are simply :

$$\frac{dC_s}{dt} = 0$$

Clearly, even a small disturbance can move substrate concentration irreversibly away from its set–point C_s^*, resulting in performance degradation.

At this point, we want to emphasize that the primary goal of a substrate feedback controller for a fed–batch fermentation process is *not to*

stabilize the process globally, but rather to *optimize* it while *keeping an inherent unstable behavior under control* (see also [Bastin and Dochain 1990]). As an example, consider the growth phase of a fed–batch fermentation process with a substrate inequality constraint. From the analysis of Section 3.5.3 we know that the optimal strategy consists of keeping C_s at its maximum value $C_{s,MAX}$ using a control of the form (6.4). The closed loop dynamics of biomass are then using (6.1) and (6.2) :

$$\frac{dX}{dt} = \mu(C_{s,MAX})X$$

or

$$\frac{dC_x}{dt} = [\mu(C_{s,MAX}) - \frac{\sigma(C_{s,MAX})}{C_{s,in} - C_{s,MAX}}C_x]C_x$$

During growth, in general the specific growth rate μ is much larger than the dilution rate $D = u/V$. As a result, both the absolute amount X and the concentration C_x of biomass increase in an exponential way. Clearly, the substrate controller (6.4) *does not stabilize* the growth phase. It *optimizes* growth by keeping substrate concentration at its optimal value.

In the following we illustrate how to design controllers based on the heuristic approach that do not suffer from the above drawbacks.

The stability problem

Let us start with the second problem. When replacing the optimal controller (6.3) by the heuristic controller (6.4) the control objective becomes more realistic, namely *set–point control* or more generally *tracking* of a reference profile. The heuristic controller (6.4) performs well if there are no disturbances, measurement errors, ..., and if the switch from growth to production occurs exactly when $C_s = C_s^*$. As in general these assumptions are not fulfilled, we must incorporate in control law (6.4) some mechanism which controls the *tracking error* in presence of disturbances, ... At this point we can make use of the principle of *linearizing control.* An excellent introduction and several applications can be found in [Bastin and Dochain 1990] and the references therein.

1. In the application considered here, the control variable is the volumetric feed rate u, while the controlled variable is the substrate concentration C_s. So an *input/output model* for this case is simply the first equation of (6.2) :

$$\frac{dC_s}{dt} = -\sigma C_x - C_s\frac{u}{V} + C_{s,in}\frac{u}{V} \tag{6.5}$$

This input/output model —which is linear in the control input u— is of *relative degree one.*

2. A *linear stable* ($\lambda > 0$) *reference model* for the tracking error is then :

$$\frac{d(C_s - C_s^*)}{dt} = -\lambda(C_s - C_s^*) \tag{6.6}$$

Note that the reference model is of the same degree as the input/output model. At this point, the reference signal C_s^* may be time varying.

3. A *nonlinear linearizing controller* is then obtained by eliminating dC_s/dt between (6.5) and (6.6) :

$$u_0 = \frac{\sigma C_x + \frac{dC_s^*}{dt} - \lambda(C_s - C_s^*)}{C_{s,in} - C_s}V$$

In the application considered here, we want a *constant* substrate concentration during the production phase, so :

$$u_0 = \frac{\sigma C_x - \lambda(C_s - C_s^*)}{C_{s,in} - C_s}V$$

In most practical situations the control action (i.e. the feeding pump capacity) is bounded. The resulting controller is then :

$$u_{production} = \begin{cases} u_0 & \text{if } 0 \le u_0 \le U_{MAX} \\ 0 & \text{if } u_0 \le 0 \\ U_{MAX} & \text{if } u_0 \ge U_{MAX} \end{cases} \tag{6.7}$$

REMARKS

1. Obviously, this controller reduces to heuristic controller (6.4) if the tracking error due to disturbances, measurement errors, ... equals zero.

2. An important advantage as compared with the heuristic controller (6.4) is the following.

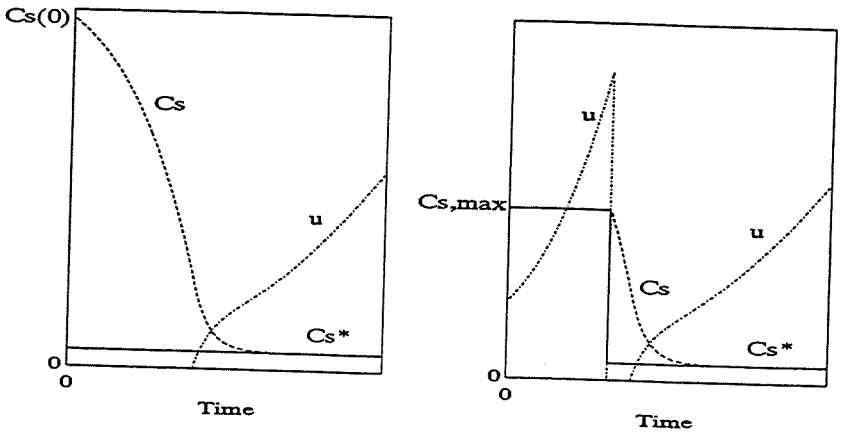

Figure 6.3: Nonlinear linearizing controller
Left plot: no constraints – Right plot: inequality constraint on C_s

If there are no inequality constraints on the state $\mathbf{x}$ and the initial substrate concentration is free, the control sequence is as shown in Figure 6.2 with u_{sing} replaced by the above nonlinear linearizing controller. The growth phase is a *batch* phase, as all substrate consumed during growth α_{growth} is added at time $t = 0$ in order to maximize the specific growth rate μ. In other words, there is no reference profile for substrate concentration during the growth phase. However, *controller* (6.7) *can be implemented from* $t = 0$ *on by considering* C_s^* *as the set-point from* $t = 0$ *on.* This idea can be motivated as follows. In general, the optimal initial substrate amount S_0 is sufficiently high so that during growth $C_s >> C_s^*$, with C_s^* the desired level during production. As a result the tracking error is a very large positive number, so the control calculated using (6.7) is set equal to $u = 0$, i.e. a *batch* phase as required. Furthermore, the feed rate switches *automatically* to positive values as soon as $C_s \to C_s^*$, so the switching time t_2 *needs not be specified a priori.* Clearly, this is a *two dimensional optimization problem with the initial substrate concentration* $C_s(0)$ *and the reference concentration during production* C_s^* *as degrees of freedom.*

The extension to the case of a substrate inequality constraint during growth is straightforward. The optimal initial substrate concentration is then (see also Section 3.5.3) $C_s(0) = C_{s,MAX}$. During growth, a controller of the form (6.7) tries to keep C_s at $C_{s,MAX}$ —which is then the reference value— until at time $t = t_1$ the amount of substrate reserved to growth α_{growth} is added. At $t = t_1$ the reference level switches to the level C_s^* which is optimal for production. Since at $t = t_1$ the actual substrate concentration $C_s >> C_s^*$, controller (6.7) switches to zero as required. If $C_s \to C_s^*$, controller (6.7) switches *automatically* to positive values to keep C_s around C_s^*. Again the switching time t_2 *needs not to be specified a priori.* The two degrees of freedom are now *the time* t_1 *—or equivalently the amount of substrate reserved to growth* α_{growth}*— and again the reference substrate concentration level during production* C_s^*.

Both cases are illustrated in a qualitative way in Figure 6.3 where we assume that the measurements are all perfect and that there are no disturbances. Observe that this nonlinear linearizing controller becomes positive *before* C_s reaches C_s^*. This guarantees a smooth transition in the substrate concentration profile while the control itself does not change abruptly (i.e. remains continuous) at the start of the production phase. This behavior can be obtained using a small value of λ in the reference model (6.6). On the other hand, a large value of λ increases stability margin, tracking behavior and disturbance rejection. This can be easily seen when calculating the closed loop response of substrate concentration to e.g. a constant disturbance Δ. We have using (6.2) and (6.7) :

$$\frac{dC_s}{dt} = -\lambda(C_s - C_s^*) + \Delta$$

Note that the closed loop behavior is *linear*, although the process itself is *nonlinear.* The solution is :

$$C_s(t) = C_s^* + (C_s(0) - C_s^*)\exp[-\lambda t] + \frac{\Delta}{\lambda}(1 - \exp[-\lambda t]) \to C_s^* + \frac{\Delta}{\lambda}$$

Since λ is at the disposal of the user, this parameter can be used to search for an optimal *trade off.* ■

The monitoring problem

In the following we consider the first problem, i.e. monitoring of all variables required in controller (6.7). We present three solutions depending on which measurements are available on–line. The remaining variables are then estimated on–line using *software sensors*. The three algorithms proposed are all based on the *minimal modeling concept* introduced in Section 1.1.5 (see also [Bastin and Dochain 1990]). In this approach no assumption is made concerning the exact analytical structure of the specific rates required in the control law, thus circumventing the modeling and corresponding parameter identification problem. Instead, they are treated as *time varying parameters* which are estimated on–line. By doing so, the nonlinear linearizing controller (6.7) is made *adaptive* and becomes even *model–independent.*

Simulation results for the penicillin G fed–batch fermentation process modeled by our new unifying unstructured model (Chapter 5) illustrate each of the variants proposed.

6.2 Optimal adaptive control using on-line measurements of C_s and C_x

6.2.1 Mathematical description

In this section, we make the following assumptions.

1. Both substrate concentration C_s and biomass concentration C_x are measured on–line.

2. The results of the on–line measurement devices become available to the controller only after a time delay ΔT, which we assume equal for both measurements. This delay represents the time required to analyze a sample from the reactor contents.

3. In agreement with the minimal modeling concept, no assumption has been made concerning the exact analytical structure of the specific rates σ and μ.

The dynamic equations for C_s, C_x and V are [see equations (6.2)] :

$$\begin{aligned}
\frac{dC_s}{dt} &= -\sigma C_x - C_s\frac{u}{V} + C_{s,in}\frac{u}{V} \\
\frac{dC_x}{dt} &= \mu C_x - C_x\frac{u}{V} \\
\frac{dV}{dt} &= u
\end{aligned}$$

In practice, a control algorithm will be implemented in discrete time. So we first discretize these equations. As an on–line measurement device can take a new sample from the reactor only after finishing the analysis of the previous one, we set the discretization interval equal to the sampling interval ΔT. A first order forward Euler discretization results in the following equations :

$$\begin{aligned}
C_{s,k+1} - C_{s,k} &= -\sigma_k C_{x,k}\Delta T - C_{s,k}\frac{u_k}{V_k}\Delta T + C_{s,in}\frac{u_k}{V_k}\Delta T \\
C_{x,k+1} - C_{x,k} &= \mu_k C_{x,k}\Delta T - C_{x,k}\frac{u_k}{V_k}\Delta T \\
V_{k+1} - V_k &= u_k\Delta T
\end{aligned} \tag{6.8}$$

As an alternative to minimizing the tracking error over an extended time horizon by using a reference model of the form (6.6), we can design a *one–step–ahead controller* which minimizes a performance index of the form :

$$J_{k+1}[u_k] = \frac{1}{2}(C_{s,k+1} - C_s^*)^2$$

However, excessive control effort u_k may be needed to bring $C_{s,k+1}$ to the set–point C_s^* in only one step. Therefore, we will minimize a slightly generalized version of this performance index :

$$J_{k+1}[u_k] = \frac{1}{2}[(C_{s,k+1} - C_s^*)^2 + \rho u_k^2] \tag{6.9}$$

which aims to achieve a compromise between bringing $C_{s,k+1}$ to the set–point C_s^* and the amount of effort u_k needed, by tuning the weighting factor ρ. Substituting the first equation of (6.8) in performance index (6.9) and minimizing the resulting expression with respect to the control u_k leads to the following *nonlinear* control law for the production phase :

$$u_k = \frac{\Delta T}{V_k}(C_{s,in} - C_{s,k})\frac{\sigma_k C_{x,k}\Delta T - (C_{s,k} - C_s^*)}{(C_{s,in} - C_{s,k})^2(\frac{\Delta T}{V_k})^2 + \rho}$$

As usual, the controller action is limited by :

$$u_{production} = \begin{cases} u_k & \text{if } 0 \le u_k \le U_{MAX} \\ 0 & \text{if } u_k \le 0 \\ U_{MAX} & \text{if } u_k \ge U_{MAX} \end{cases} \qquad (6.10)$$

As in the case of controller (6.7), it can be seen that depending on the relative magnitude of both terms in the numerator this controller can switch to positive values as soon as $C_s \to C_s^*$. To increase the sensitivity around C_s^* (see Figure 6.3), we can introduce an additional degree of freedom λ :

$$u_k = \frac{\Delta T}{V_k}(C_{s,in} - C_{s,k})\frac{\sigma_k C_{x,k}\Delta T - \lambda(C_{s,k} - C_s^*)}{(C_{s,in} - C_{s,k})^2(\frac{\Delta T}{V_k})^2 + \rho}$$

An appropriate value for the parameter λ is discussed later on. Note that if $C_s = C_s^*$, $\rho = 0$, and $\Delta T \to 0$, this control law reduces to the heuristic C_s–controller (6.4).

Since the discrete time model equations (6.8) are *linear* in the specific rates, they can be estimated using a *recursive least squares algorithm with forgetting factor* ζ fed with on–line data of C_s and C_x. A standard textbook formulation of RLS can be found e.g. in [Goodwin and Sin 1984].

However, due to the measurement delay, at time $t = k\Delta T$ only $C_{s,k-1}$ and $C_{x,k-1}$ are known. An adaptive version of controller (6.10) can then be obtained using the following algorithm (a hat "^" denotes an estimated value).

Algorithm

Step 1 : *Estimation of σ_{k-1} and μ_{k-1} using RLS*

Using equation (6.8) the *residuals* ε can be written as :

$$\begin{aligned} \varepsilon_{C_s,k-1} &\triangleq C_{s,k-1} - \hat{C}_{s,k-1} \\ &= C_{s,k-1} + \hat{\sigma}_{k-2}C_{x,k-2}\Delta T - (C_{s,in} - C_{s,k-2})\frac{u_{k-2}}{V_{k-2}}\Delta T - C_{s,k-2} \\ \varepsilon_{C_x,k-1} &\triangleq C_{x,k-1} - \hat{C}_{x,k-1} \\ &= C_{x,k-1} - \hat{\mu}_{k-2}C_{x,k-2}\Delta T + C_{x,k-2}\frac{u_{k-2}}{V_{k-2}}\Delta T - C_{x,k-2} \end{aligned}$$

The gain K is obtained via :

$$\begin{aligned} P_{k-1} &= P_{k-2}/(\zeta + C_{x,k-2}^2\Delta T^2 P_{k-2}) \\ K_{k-1} &= -C_{x,k-2}\Delta T P_{k-1} \end{aligned}$$

An estimation of σ_{k-1} and μ_{k-1} is then :

$$\begin{aligned} \hat{\sigma}_{k-1} &= \hat{\sigma}_{k-2} + K_{k-1}\varepsilon_{C_s,k-1} \\ \hat{\mu}_{k-1} &= \hat{\mu}_{k-2} - K_{k-1}\varepsilon_{C_x,k-1} \end{aligned}$$

Step 2 : *Prediction of $C_{s,k}$, $C_{x,k}$ and V_k*

These variables can be calculated by using the estimates $\hat{\sigma}_{k-1}$ and $\hat{\mu}_{k-1}$ from Step 1 in the discrete equations (6.8) rewritten at time k.

Step 3 : *Calculation of the controller action u_k*

As σ varies slowly as compared with the dynamics of the system, we take :

$$\hat{\sigma}_k = \hat{\sigma}_{k-1}$$

u_k is calculated by substituting the results of the previous steps in (6.10) :

$$u_k = \frac{\Delta T}{V_k}(C_{s,in} - \hat{C}_{s,k})\frac{\hat{\sigma}_k\hat{C}_{x,k}\Delta T - \lambda(\hat{C}_{s,k} - C_s^*)}{(C_{s,in} - \hat{C}_{s,k})^2(\frac{\Delta T}{V_k})^2 + \rho}$$

REMARKS

1. Following a same line of reasoning as presented in Section 6.1.5 we conclude that this controller can also be implemented from $k = 0$ on.

2. Instead of a *linear regression estimator* we could also use an *observer based estimator* for the estimation of the specific rates σ and μ. Observer based estimators will be used in the following sections.

3. Although the specific growth rate μ is not explicitly required in controller (6.10), an estimate is needed in order to predict the state at time $t = k\Delta T$ in Step 2 of the algorithm. Obviously, this complication is entirely due to the measurement delay ΔT.

4. If we set ρ equal to zero, then the one–step–ahead controller (6.10) can be interpreted as a discrete time version of the nonlinear linearizing controller (6.7) designed over an extended time horizon.

5. Let us consider now the influence of the additional degree of freedom λ. If we assume again that $\rho = 0$, then using equation (6.8) the closed loop response of substrate concentration $C_{s,k}$ to e.g. a constant disturbance Δ is given by :

$$C_{s,k+1} = (1 - \lambda)C_{s,k} + \lambda C_s^* + \Delta$$

To guarantee stability, we must have :

$$|\,1 - \lambda\,| < 1 \quad \text{or} \quad 0 < \lambda < 2$$

A similar *trade off* as described for the linearizing controller (6.7) between stability margin, tracking behavior, disturbance rejection and smoothness of the controller action can be made.

$\boxed{\lambda = 0}$

The one–step–ahead controller (6.10) reduces to the discrete time version of heuristic controller (6.4). The closed loop behavior reduces to :

$$C_{s,k+1} = C_{s,k} + \Delta$$

which is only stable in the absence of disturbances, modeling inaccuracies, ...

$\boxed{0 < \lambda < 2}$

In this case, the closed loop response tends asymptotically to :

$$C_{s,\infty} = C_s^* + \frac{\Delta}{\lambda}$$

Obviously, values of λ in the half open interval $]0, 1]$ result in a stable monotonic transient behavior, a smooth controller action but also disturbance amplification. On the other hand, values of λ in the half open interval $[1, 2[$ result in a stable oscillating transient behavior and disturbance rejection at the expense of a less smooth controller action. ■

6.2.2 Simulation results

Consider again the penicillin G fed–batch fermentation modeled by our new unifying model. All simulations are carried out using a *continuous time process model* and a *discrete time controller*. Between two samples the controller action is kept constant.

We have used the following values : $\Delta T = 0.1$ h, $\rho = 0$, $P_0 = 25$ and $\lambda = 1$.

$\boxed{E = 10^{-9}\ \text{g/L}}$

For the *maintenance* model, we obtain a final product amount $P(t_f) = 62.848$ g at $t_f = 115.02$ h when using the same initial substrate amount $S_0 = 533$ g as given in Table 6.2 for the heuristic controller. The forgetting factor ζ is equal to 0.6, while the control input is considered unbounded ($U_{MAX} = \infty$). The convergence of the estimation of the specific rates σ and μ is illustrated in Figure 6.4, using an initial estimate $\sigma_0 = \mu_0 = 0$. Figure 6.5 shows the convergence of the predicted substrate concentration towards its real value, and the corresponding adaptive control. From both figures we conclude that the algorithm has converged shortly after the beginning of the production phase.

$\boxed{E = 10^{+12}\ \text{g/L}}$

For the completely endogenous model we obtain a final penicillin amount $P_f = 87.978$ g at $t_f = 108.99$ h when using $S_0 = 1404$ g —i.e. the optimal initial substrate amount for the heuristic controller (Table 6.2)—, $\lambda = 0.7$ and $U_{MAX} = 10^{-2}$ L/h.

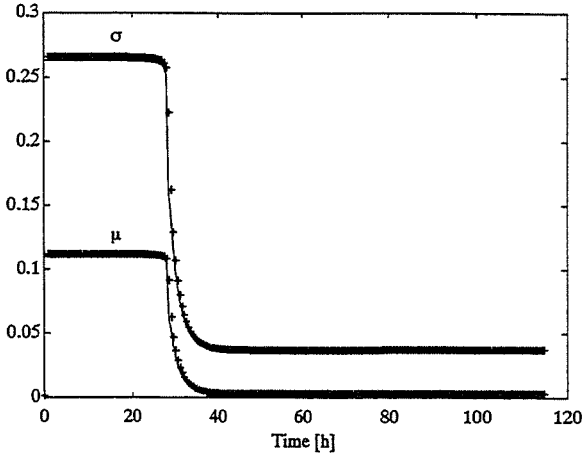

Figure 6.4: Estimation of σ and μ

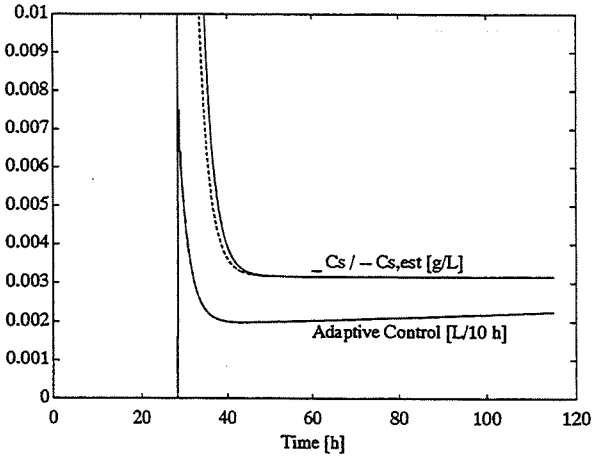

Figure 6.5: Prediction of C_s and adaptive controller

For $\Delta T = 1$ h the controller did *not* converge. Remember that ΔT represents both the sampling interval in discretizing the model equations and the measurement delay. As for Step 1 in the algorithm, it can be easily verified that there always exist an initial value P_0 and a forgetting factor ζ such that the estimations σ_{k-1} and μ_{k-1} and the corresponding gain K_{k-1} remain bounded if biomass concentration C_x is strictly positive for all t and if the control input u is bounded. As a result, the instability at too large values of ΔT is completely due to the increasing inaccuracy of the predictions made in Step 2. It can be expected —and this has been confirmed during simulations— that if the measurement delay ΔT becomes too large, especially the prediction of substrate concentration C_s around the transition from growth to production becomes worse.

6.3 Optimal adaptive control using on-line measurements of C_s

6.3.1 Mathematical description

In this section, we make the following assumptions.

1. Besides the volume V, substrate concentration C_s is the only available on–line measurement.
2. We neglect the measurement delay ΔT.
3. In agreement with the minimal modeling concept, no assumption is being made concerning the exact analytical structure of the specific rate σ.

An *adaptive* implementation of controller (6.7) can be obtained as follows. Since $C_{s,in}$ and λ are known constants, we only need an on–line estimate of both the specific substrate consumption rate σ and the biomass concentration C_x.

We define the specific rate β —considered as a time varying parameter— as follows :

$$\sigma C_x \triangleq \beta C_s$$

Since C_s is available on–line, the only unknown is exactly the specific rate β. In the following continuous time algorithm, β is estimated using a *state observer based parameter estimator.*

Algorithm

Step 1 : *Estimation of* β

$$\frac{d\hat{C}_s}{dt} = -\hat{\beta}C_s + (C_{s,in} - C_s)\frac{u}{V} + \omega_s(C_s - \hat{C}_s)$$
$$\frac{d\hat{\beta}}{dt} = -\gamma_s C_s(C_s - \hat{C}_s)$$

Step 2 : *Calculation of the controller action* u

$$u_0 = \frac{\hat{\beta}C_s - \lambda(C_s - C_s^*)}{C_{s,in} - C_s}V$$
$$u = \begin{cases} u_0 & \text{if } 0 \le u_0 \le U_{MAX} \\ 0 & \text{if } u_0 \le 0 \\ U_{MAX} & \text{if } u_0 \ge U_{MAX} \end{cases}$$

REMARKS

1. Tuning of the state observer based parameter used in Step 1 reduces to the calibration of the (positive) constants ω_s and γ_s.

2. Obviously, in practice both the estimator and the controller must be implemented in discrete time.

3. In the above algorithm, a measurement delay ΔT can be easily incorporated by adding a prediction step between Step 1 and Step 2 of the discrete time implementation. An example is given in Section 6.2.

4. The estimation of biomass concentration C_x has been avoided by defining the specific rate β. As an alternative, biomass concentration C_x can be estimated by extending the observer used in Step 1 as follows :

$$\frac{d\hat{C}_x}{dt} = \hat{\mu}\hat{C}_x - \hat{C}_x\frac{u}{V} + \omega_x(C_s - \hat{C}_s)$$
$$\frac{d\hat{\mu}}{dt} = \gamma_x\hat{C}_x(C_s - \hat{C}_s)$$

   Note that this involves also the estimation of the specific growth rate μ, which is not explicitly required.

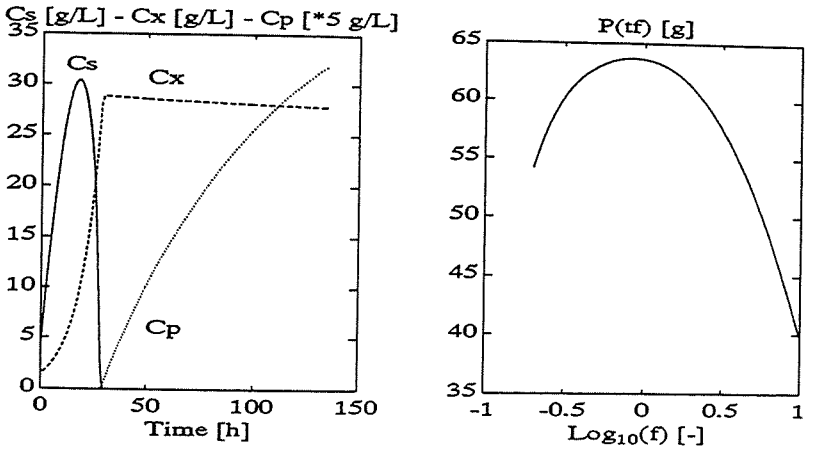

Figure 6.6: Adaptive control using C_s measurements for $E = 10^{-9}$ g/L
Left plot: concentration profiles for $C_s^* = \sqrt{K_p K_i}$
Right plot: optimization of $P(t_f)$ as function of f

5. Just like the controller proposed in Section 6.2, this controller does not need any a priori information either, such as e.g. yield coefficients, ... Moreover, treating β (and thus σ) as a time varying parameter makes it robust against modeling uncertainties. ■

6.3.2 Simulation results

Some simulation results for the unifying penicillin G model using $E = 10^{-9}$ g/L (i.e. maintenance metabolism) are shown in Figure 6.6. In order to sufficiently excite the system to guarantee estimator convergence, the amount of substrate consumed during growth α_{growth} is added as follows : 500 g is fed in feedforward using a constant strategy during 25 hrs, the rest is added at $t = 0$. Using $\omega_s = 10^5$, $\gamma_s = 10^9$, $\lambda = 3000$, an initial estimate of $\beta = 0.075$ (true value 0.084) and $\alpha_{growth} = 533$ g (see Table 6.2), we obtain a final penicillin amount $P(t_f) = 63.592$ g. The set–point C_s^* is set equal to $(K_p K_i)^{1/2}$ which maximizes π. The corresponding concentration profiles are shown in the left plot.

The right plot shows the optimization of $P(t_f)$ with respect to the choice of the set–point C_s^* during the production phase for a fixed initial substrate

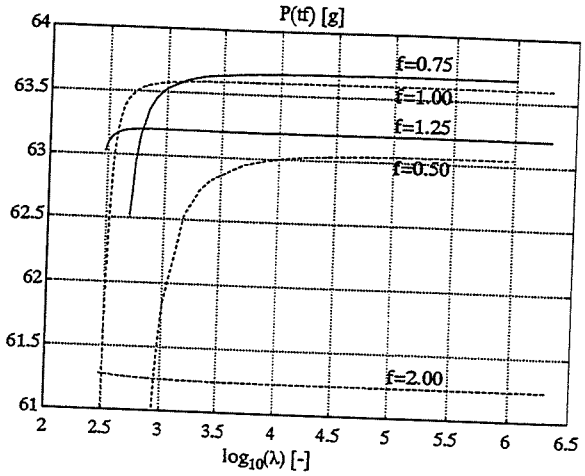

Figure 6.7: Influence of f and λ on $P(t_f)$

concentration. We define a factor f as :

$$f \triangleq \frac{C_s^*}{(K_p K_i)^{1/2}}$$

The optimum value is $P(t_f) = 63.680$ g for $f = 0.85$. Due to the shape of this plot, it is clear that in practice three experiments should suffice to optimize the process.

Figure 6.7 illustrates the influence of both the value of the set–point during production and the choice of λ in reference model (6.6) on the final product amount.

6.4 Optimal adaptive control using on-line measurements of *CER*

6.4.1 Mathematical description

In the algorithm of Section 6.3, the major bottle–neck is the *accuracy of the on–line substrate concentration measurements.* Kleman *et al.* [1991] reported a control algorithm maintaining C_s as tight as 0.49 ± 0.04 g/L during growth of *E. coli.* However, in the case of penicillin fed–batch fermentation

the situation becomes even more critical. Using the parameter values reported by Bajpai and Reuß (see Table 5.2), the substrate concentration C_s at which π is maximum is $(K_p K_i)^{1/2} = 3.16\ 10^{-3}$ g/L, which is two orders of magnitude smaller.

This problem can be circumvented as follows. If the specific growth rate μ is a monotonically increasing function of substrate concentration C_s (see Figure 6.1), then prespecifying a reference profile for C_s can be replaced by *prespecifying a reference profile for the specific growth rate.* In the case of μ function of C_s only this is even identical. An appropriate reference profile is then : during growth, we want μ as high as possible, while during production, we want $\mu = \mu^*$, μ^* constant.

Obviously, we now need an on–line estimation of the specific growth rate μ. This can be done e.g. using the easily accessible measurement of CO_2 in the effluent gas from the fermentor. In Section 1.1.1 we derived the dissolved carbon dioxide dynamics :

$$\frac{dC_c}{dt} = CER - DC_c - Q_{out}$$

with C_c the dissolved carbon dioxide concentration and Q_{out} the rate of outflow of carbon dioxide from the reactor in gaseous form. This model is valid only if the dissolved carbon dioxide concentration C_c is lower than the saturation concentration $C_{c,sat}$. In agreement with (1.11) and (1.12) the carbon dioxide evolution rate CER can be described with equation (1.13) :

$$CER = [Y_{c/x}\mu + m_c + Y_{c/p}\pi]C_x$$

under suitably controlled conditions for pH. At any time during the fermentation, carbon dioxide arises from (i) growth and associated energy production (yield coefficient $Y_{c/x}$), (ii) maintenance energy (specific rate m_c), and (iii) product biosynthesis and other possible specialized metabolism (yield coefficient $Y_{c/p}$).

In most applications $C_{c,sat}$ is very low, so using a *singular perturbation technique* (see Section 1.1.6) we obtain :

$$Q_{out} = CER$$

which means that an on–line CO_2 analysis of the effluent gas from the fermentor can be used to extract the variables needed.

Calam and Ismail [1980] reported the following slightly simplified relation in the case of penicillin G fermentation :

$$CER = Y_{c/x}\mu C_x + m_c C_x + k_p \tag{6.11}$$

Based on experimental results, a *constant* value k_p representing the contribution of product synthesis is proposed, instead of a term involving the penicillin production rate. This could be motivated as follows. First, during the main production period the rate of biosynthesis is remarkably steady. Second, it is known that penicillin production is accompanied by decomposition (see e.g. the hydrolysis constant k_h present in all penicillin models in this work). Therefore, it seems possible that as production later appears to slow down, biosynthesis itself may be continuing or may be diverted to non–antibiotic substances.

In the following algorithm the adaptive observer for C_x and μ is inspired by Di Massimo *et al.* [1989]. This is only a *partially* adaptive observer, as some model constants are required a priori.

Algorithm

Step 1 : *Estimation of μ and C_x*

$$\begin{aligned}
\frac{d\hat{C}_x}{dt} &= \hat{\delta} - \hat{C}_x u/V + \omega(CER - C\hat{E}R) \\
\frac{d\hat{\delta}}{dt} &= \gamma(CER - C\hat{E}R) \\
C\hat{E}R &= Y_{c/x}\hat{\delta} + m_c\hat{C}_x + k_p \\
\hat{\mu} &= \frac{\hat{\delta}}{\hat{C}_x} \\
\hat{\sigma} &= \hat{\mu}/Y_{x/s} + m
\end{aligned}$$

Step 2 : *Calculation of the controller action u*

$$\begin{aligned}
u_0 &= \frac{\hat{\sigma}\hat{C}_x - \lambda(\hat{\mu} - \mu^*)}{C_{s,in}}V \\
u &= \begin{cases} u_0 & \text{if } 0 \le u_0 \le U_{MAX} \\ 0 & \text{if } u_0 \le 0 \\ U_{MAX} & \text{if } u_0 \ge U_{MAX} \end{cases}
\end{aligned}$$

REMARKS

1. During estimation of σ in Step 1 we neglect the contribution of π. This approximation can be justified by e.g. the experimental results reported by Calam and Ismail [1980]. In the denominator of the controller action in Step 3 substrate concentration C_s is considered negligible as compared with $C_{s,in}$.

2. Note that this scheme requires the *a priori* knowledge of the parameters $Y_{c/x}$, m_c and k_p (which may be all time varying), $Y_{x/s}$ and m. Clearly, this is the price to pay for estimating state variables using only on–line measurements of easily accessible auxiliary variables.

3. However, this estimation procedure has an additional benefit over the algorithms presented in Sections 6.2 and 6.3 when scaling up the production from a pilot plant towards an industrial fermentor. If we want to determine substrate and/or biomass on–line, it becomes very important where to place the sampling devices on such a large reactor (e.g. actual penicillin production on an industrial scale takes place in fermentors of about 150000 m^3). Due to a non perfectly mixed reactor, the question is whether a locally determined concentration is representative for the whole reactor contents. On the other hand, an analysis of the effluent gas from the fermentor provides in some sense averaged values of the reactor state which can be used immediately in the feed rate controller.

4. Obviously, this algorithm can also be implemented from time $t = 0$ on by considering the set–point for production μ^* as the reference from $t = 0$ on. In case of a substrate inequality constraint during growth, the reference profile has the form shown in the right plot of Figure 6.3 with $C_{s,MAX}$ and C_s^* replaced by the corresponding values for μ.

5. In the discrete time version we have added *integral action* to compensate for the approximations made above. ■

6.4.2 Simulation results

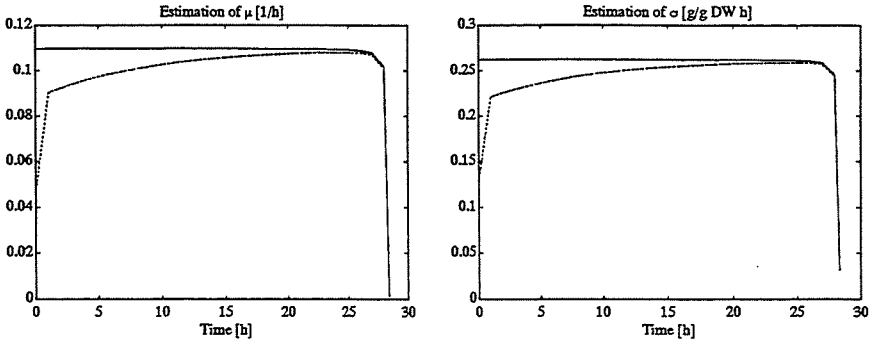

Figure 6.8: Estimation of μ and σ
Legend: —: true value, – –: estimated value

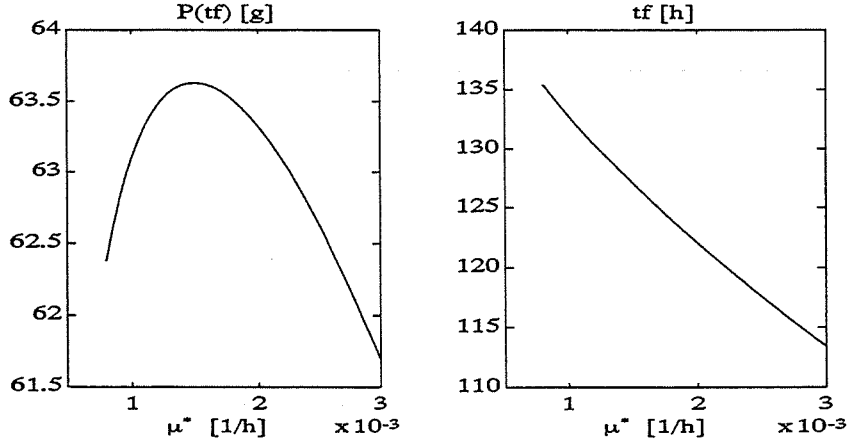

Figure 6.9: Adaptive control using *CER* measurements for $E = 10^{-9}$ g/L
Left plot: optimization of $P(t_f)$ as function of the set–point μ^*
Right plot: influence of the set–point μ^* on final time t_f

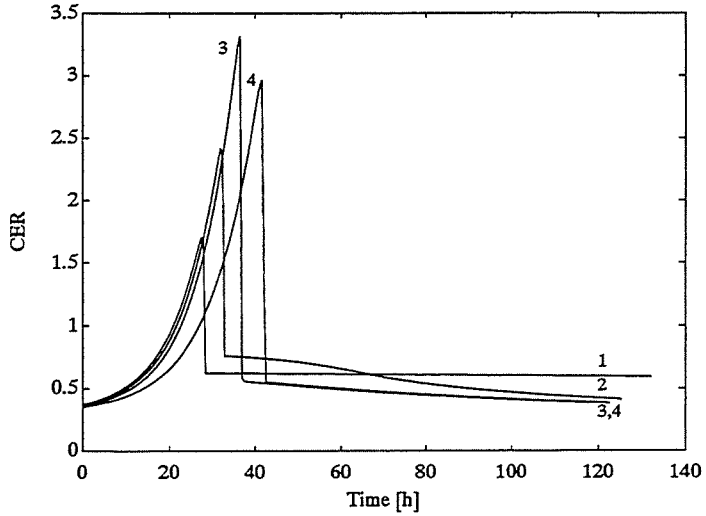

Figure 6.10: *CER* profile during optimal feed rate fermentation for the values of E of Table 5.8

We present now some simulation results for the penicillin fed–batch fermentation using $E = 10^{-9}$ g/L in the unifying model and $\alpha_{growth} = 533$ g (see Table 6.2). In the expression of *CER* we have used the values $Y_{c/x} = 0.4$, $m_c = 0.01$ and $k_p = 0.3$ [Nelligan and Calam, 1983]. The convergence of the estimations of σ and μ is illustrated in Figure 6.8. As for the algorithm of Section 6.2 the estimator has almost completely converged at the beginning of the production phase, i.e. at the moment the control action becomes different from zero.

The results of the optimization of final penicillin amount $P(t_f)$ with respect to the choice of the set–point μ^* for the production phase with a fixed initial substrate amount ($S_0 = 533$ g) are shown in the left plot of Figure 6.9. The optimal values are $P(t_f) = 63.630$ g for $\mu^* = 1.5\ 10^{-3}$ 1/h. In the right plot the corresponding total fermentation time t_f is shown. Obviously, a *trade off* can be made between $P(t_f)$ and t_f.

In Figure 6.10 the *CER* profiles during optimal feed rate fermentation for the values of E of Table 5.8 are shown. As compared with the growth phase, the value of *CER* during production does not change very much. As a result, an alternative suboptimal strategy could consist of selecting

an appropriate set–point for *CER* —which is an easily accessible variable— during production, and then tracking this set–point using a simple *PI* or even *P* controller. However, simulations indicate that the performance of this control strategy approximates the optimal performance only in the case of a maintenance metabolism (profile 1), and if we have a priori a good estimate of the switching time between growth and production. In the other cases (mixed and completely endogenous metabolism), the final product amount decreases significantly. This can be easily seen as follows. We already know that keeping substrate concentration C_s constant during production is an excellent suboptimal strategy, whatever the metabolic conditions. We also illustrated that this can be replaced by keeping the specific growth rate μ constant during the production phase. If μ is function of C_s only, this is even identical. From equation (6.11) it can be seen that keeping *CER* constant during production will result in a good performance only if biomass concentration C_x remains (almost) constant during production. Figure 5.13 illustrates that this is the case only for the maintenance model. For other metabolic conditions, the relative variation of *CER* during production can not be neglected. In other words, in contrast to the substrate concentration C_s, a constant value of *CER* during production seems not to be an intrinsic feature of this fermentation process.

6.5 Conclusions

In this chapter we presented the design of substrate feed rate controllers for a class of biotechnological processes, characterized by a decoupling between the biomass growth and the product formation. The major contribution was to show how the information obtained during optimal control studies leads to the design of *optimal adaptive controllers* which combine nearly optimal performance with excellent robustness properties and which are easy to implement. The design is essentially based on rewriting the heuristic controllers presented throughout this thesis within the framework of *nonlinear linearizing control.*

To illustrate this methodology we considered again the penicillin G fed–batch fermentation process modeled by our new unifying model presented in Chapter 5. We presented three possible implementations, depending on which variables are available by on–line measurements. The trade off between *on–line measurement requirements* (such as accessibility and accuracy) and *a priori information needs* (such as yield and maintenance coefficients) was clearly illustrated.

Chapter 7

Conclusions and open problems

In this thesis we have investigated whether the application of mathematical modeling techniques and modern model based control methods can contribute to the optimization of biotechnological processes, the dynamics of which are determined in the first place by a living microbial population. Until now this has been hampered by the following major problems :

1. The process kinetics are most often poorly understood nonlinear functions, while the corresponding parameters are time varying.

2. Until now there is a lack of reliable sensors suited to real time monitoring of process variables which are needed in advanced control algorithms.

As an illustrative case study of modeling the reaction kinetics, we presented a *new dynamic model describing microbial growth* in food products as a function of both time and temperature, over the whole range of growth and inactivation.
The main contributions of this thesis can be summarized in the following paradigms :

1. *Optimization for model discrimination*

2. *Optimal adaptive control*

Optimization for model discrimination

Modeling and parameter estimation have become prerequisites for the development of optimization and control methods. However, accurate mathematical modeling of a biotechnological process is still an extremely difficult and hazardous task. Very often a mathematical model turns out to be not practically identifiable. As an example, we have considered the modeling of the penicillin G fed–batch fermentation process. Two unstructured models reported in the literature have been analyzed in detail. A careful optimal control study has revealed some physical and biochemical shortcomings. Based on the recent advances in the biochemical knowledge concerning the penicillin fermentation, we were able to construct a *new unifying model* based on the new concept of *endogenous fraction.* We have illustrated that the application of an optimal feed rate profile instead of a commonly used constant feed rate profile contributes in solving both the *parameter estimation problem* and the *structure characterization problem.*

In other words, this approach allows for solving both the performance measure optimization problem and the model discrimination problem at the same time. Obviously, in order to determine in practice a sufficiently exciting optimal feed rate profile, application of optimal control theory requires a complete knowledge of the process model in advance. The solution is then to design a model–independent suboptimal feed rate strategy using optimal adaptive control.

Observe that the penicillin fermentation process has been used only as a vehicle for presenting the basic ideas, analysis and results. A similar analysis can be performed for any fermentation process.

Optimal adaptive control

This thesis contributes in bridging the gap between two actual trends for the design of monitoring and control algorithms for biotechnological processes.

In a first approach, classical techniques such as optimal control theory are applied under the assumption that the model is perfectly known. In practice, this assumption is never fulfilled.

In a second approach, monitoring and control algorithms are designed based on the minimal modeling concept, i.e. without the need for a complete knowledge of the process model, using concepts from adaptive linearizing control. However, there is a priori no guarantee for at least suboptimality of the results obtained.

Both approaches are linked together by the *heuristic optimization methodology*, based on biochemical knowledge of the process under consideration and on a careful mathematical analysis of the optimal control solution. We have illustrated with a case study (fed–batch fermentation processes) that an adaptive model–independent implementation of these controllers combines excellent robustness properties with nearly optimal performance : *optimal adaptive control.*

During the preparation of this work we came along some problems which still call for further research.

In the case study of optimal adaptive control, we only considered fed–batch fermentation processes with monotonic specific growth rate and non–monotonic specific production rate. Although less common, the other types of processes characterized by growth/production decoupling (see Chapter 3) deserve some attention too. For instance, if the specific growth rate is a non–monotonic function of substrate concentration, the substrate feed rate controller we propose to track a reference specific growth rate profile is not a priori stable.

It is an interesting question whether the results presented here can be applied to fermentation processes characterized by more than four mass balance equations. This is for instance the case when considering structured compartment models, or mixed culture fermentation processes, ... An explicit solution of the optimal control along a singular arc is until now unknown. In the literature many techniques have been proposed to convert a singular control problem into a nonsingular one. We need to investigate whether an optimal control solution obtained in this way can be interpreted also using the available biochemical knowledge, in order to design similar optimal adaptive controllers as presented in this thesis.

Appendix A

References

S. Aiba, A.E. Humphrey and N.F. Millis 1973. *Biochemical engineering*, 85–207, Academic Press, New York - London

E. Alvarez, J.M. Cantoral, J.L. Barredo, B. Diéz and J.F. Martin 1987. Purification to homogeneity and characterization of acyl coenzyme A:6–aminopenicillanic acid acyltransferase of *Penicillium chrysogenum*. *Antimicrob. Agents Chemother.*, 11, 1675–1682

J.F. Andrews 1968. A mathematical model for the continuous culture of microorganisms utilizing inhibiting substrates. *Biotechnol. Bioeng.*, 10, 707–723

H.R.V. Arnstein and D. Morris 1960. The structure of a dipeptide, containing α–aminoadipic acid, cysteine and valine, present in the mycelium of *Penicillium chrysogenum*. *Biochem. J.*, 76, 357–361

K.J. Åström and B. Wittenmark 1984. *Computer controlled systems - theory and design*. Prentice–Hall, Englewood Cliffs, New Jersey

M. Athans and P.L. Falb 1966. *Optimal control*. McGraw–Hill, New York

M. Aynsley, A.C. Ward and A.R. Wright 1990. A mathematical model for the growth of mycelial fungi in submerged culture. *Biotechnol. Bioeng.*, 35, 820–830

R.K. Bajpai and M. Reuß 1980. A mechanistic model for penicillin production. *J. Chem. Tech. Biotechnol.*, 30, 332–344

R.K. Bajpai and M. Reuß 1981. Evaluation of feeding strategies in carbon–regulated secondary metabolite production through mathematical modelling. *Biotechnol. Bioeng.*, 23, 717–738

A. Ballio, V. Divitorio and S. Russi 1964. The isolation of trehalose and polyols from the conidia of *Penicillium chrysogenum* Thom.. *Arch. Biochem. Biophys.*, 107, 177–183

G. Banko and A.L. Demain 1987. δ–(L–α–Aminoadipyl)–L–cysteinyl–D–valine synthetase (ACV synthetase) : a multifunctional enzyme with broad substrate specificity for the synthesis of penicillin and cephalosporin precursors. *J. Am. Chem. Soc.*, 109, 2858–2860

G. Bastin and D. Dochain 1990. *On–line estimation and adaptive control of bioreactors.* Elsevier Science Publishing Co.

G. Bastin 1991. Nonlinear and adaptive control in biotechnology : a tutorial. *Proceedings of the 1991 European Control Conference*, Grenoble (France), 2001–2012

H.H. Beeftink, R.T.J.M. Van der Heijden and J.J. Heijnen 1990. Maintenance requirements : energy supply from simultaneous endogenous respiration and substrate consumption. *FEMS Microbiology Ecology*, 73, 203–210

W.D. Bigelow 1921. The logarithmic nature of thermal death time curves. *J. Infec. Dis.*, 29, 528

F. Blackman 1905. Optima and limiting factors. *Ann. Bot.*, 19, 281–295

G. Bonte, J.F. Van Impe and J.A. Spriet 1989. Feeding strategy optimization of the penicillin fed–batch fermentation using a mathematical model. In : Mededelingen Fac. Landbouww. Rijksuniv. Gent : *Proceedings of the 1989 Forum for Applied Biotechnology*, Gent (Belgium), 54 (4a), 1215–1224

R.P. Brent 1973. *Algorithms for minimization without derivatives.* Prentice–Hall, Englewood Cliffs, New Jersey

S.P. Brundidge, F.C.A. Gaeta, D.J. Hook, C. Sapino Jr., R.P. Elander and R.B. Morin 1980. Association of 6–oxo–piperidine–2–carboxylic acid with penicillin V production in *Penicillium chrysogenum* fermentations. *J. Antibiot.*, 33, 1348–1351

R. Brunner and M. Röhr 1975. Phenacyl:coenzyme A ligase. *Methods of Enzymology*, 43, 476–481

A.E. Bryson, Jr. and Y.–C. Ho 1975. *Applied optimal control.* Hemisphere, Washington - New York - London

C.T. Calam and B.A.-K. Ismail 1980. Investigation of factors in the optimisation of penicillin production. *J. Chem. Tech. Biotechnol.*, 30, 249–262

L. Chen 1992. Identification and control of complex biotechnological systems. *PhD thesis*, Université Catholique de Louvain, Louvain–la–Neuve (Belgium)

A. Constantinides, J.L. Spencer and E.L. Gaden Jr. 1970a. Optimization of batch fermentation processes. I : Development of mathematical models for batch penicillin fermentations. *Biotechnol. Bioeng.*, 12, 803–830

A. Constantinides, J.L. Spencer and E.L. Gaden Jr. 1970b. Optimization of batch fermentation processes. II : Optimum temperature profiles for batch penicillin fermentations. *Biotechnol. Bioeng.*, 12, 1081–1098

D. Contois 1959. Kinetics of bacterial growth relationship between population density and specific growth rate of continuous cultures. *J. Gen. Microb.*, 21, 40–50

C.L. Cooney and F. Acevedo 1977. Theoretical conversion yields for penicillin synthesis. *Biotechnol. Bioeng.*, 19, 1449–146

J.N. Dabes, R.F. Finn and C.R. Wilke 1973. Equations of substrate–limited growth : the case for Blackman kinetics. *Biotechnol. Bioeng.*, 15, 1159–1177

F.H. Deindoerfer and E.L. Gaden 1953.
Appl. Microbiol., 3, 253

J.S. Delderfield, E. Mtetwa, R. Thomas and T.E. Tyobeka 1981. Partial elimination of valine–oxygen during penicillin biosynthesis. *J. Chem. Soc. Chem. Comm.*, 650–652

C. Di Massimo, A.C.G. Saunders, A.J. Morris and G.A. Montague 1989. Non–linear estimation and control of mycelial fermentations. *Proceedings of the 1989 American Control Conference*, Pittsburgh (USA), 1994–1999

E. Duvivier and Y. Sevely 1988. Simulation de la commande en temps minimal d'un procédé de fermentation en semi–continu : transformation de Kelley et programmation dynamique. *R.A.I.R.O*, 22, 363–380

V.M. Fishman and V.V. Biryukov 1974. Kinetic model of secondary metabolite production and its use in computation of optimal conditions. *Biotechnol. Bioeng. Symp.*, 4, 647–662

C.G. Friedrichs and A.L. Demain 1978. Uptake and metabolism of α–aminoadipic acid by *Penicillium chrysogenum* Wis 54–1255. *Arch. Microbiol.*, 119, 43–47

E.L. Gaden, Jr. 1959. Fermentation process kinetics. *J. Biochem. Microbiol. Technol. Eng.*, 1, 413–429

A.R. Giona, L. Marelli, L. Toro and R. De Santis 1976a. Kinetic analysis of penicillin production by semicontinuous fermentors. *Biotechnol. Bioeng.*, 18, 473–492

A.R. Giona, R. De Santis, L. Marelli and L. Toro 1976b. The influence of oxygen concentration and of specific rate of growth on the kinetics of penicillin production. *Biotechnol. Bioeng.*, 18, 493–512

B. Gompertz 1825. On the nature of the function expressive of the law of human mortality, and on a new mode determining the value of life contingencies. *Philos. Trans. R. Soc. London*, 115, 513–585

G.C. Goodwin and K.S. Sin 1984. *Adaptive filtering, prediction and control.* Prentice–Hall, Englewood Cliffs, New Jersey

R. Guthke and W.A. Knorre 1981. Optimal substrate profile for antibiotic fermentations. *Biotechnol. Bioeng.*, 23, 2771–2778

A. Halme and A. Holmberg 1979. Application of control engineering to fermentation processes. In : A. Niemi (Ed.), *A link between science and applications of automatic control*, 291, Pergamon Press, Oxford

E. Hegewald, B. Wolleschensky, R. Guthke, M. Neubert and W.A. Knorre 1981. Instabilities of product formation in a fed–batch culture of penicillium chrysogenum. *Biotechnol. Bioeng.*, 23, 1563–1572

J.J. Heijnen, J.A. Roels and A.H. Stouthamer 1979. Application of balancing methods in modeling the penicillin fermentation. *Biotechnol. Bioeng.*, 21, 2175–2201

D. Herbert 1958. Some principles of continuous culture. In G. Tunevall (Ed.) *Recent Progress in Microbiology*, 381–396, Almqvist and Wiksell, Stockholm

G.J.M. Hersbach, C.P. Van Der Beek and P.W.M. Van Dijck 1984. The penicillins : properties, biosynthesis and fermentation. In : E.J. Vandamme (Ed.), *Biotechnology of Industrial Antibiotics*, 45–139, Marcel Dekker AG verlag, Basel

A. Holmberg and J. Ranta 1982. Procedures for parameter and state estimation of microbial growth process models. *Automatica*, 18, 181–193

J. Hong 1986. Optimal substrate feeding policy for a fed batch fermentation with substrate and product inhibition kinetics. *Biotechnol. Bioeng.*, 28, 1421–1431

P. Hosler and M.J. Johnson 1953. Penicillin from chemically defined media. *I & EC*, 45, 871–874

A. Isidori 1989. *Nonlinear control systems : an introduction.* 2nd Edition, Springer Verlag, Berlin Heidelberg

V.K. Jain, I. Toran–Diaz and J. Baratti 1985. Preparation and characterization of immobilized growing cells of *Zymomonas mobilis* for ethanol production. *Biotechnol. Bioeng.*, 27, 273–279

F.G. Jarvis and M.J. Johnson 1947. The role of the constituents of synthetic media for penicillin production. *J. Am. Chem. Soc.*, 69, 3010–3017

A. Johnson 1987. The control of fed–batch fermentation processes : a survey. *Automatica*, 23, 691–705

H.J. Kelley, R.E. Kopp and A.G. Moyer 1966. Singular extremals. In : G. Leitmann (Ed.), *Topics in optimization*, Vol. II Chapter 3, Academic Press, New York

D.E. Kirk 1970. *Optimal control theory.* Prentice–Hall, Englewood Cliffs, New Jersey

M. Kishimoto, T. Yoshida and H. Taguchi 1981a. Simulation of fed–batch culture for glutamic acid production with ethanol feeding by use of regression analysis. *J. Ferment. Technol.*, 59, 43–48

M. Kishimoto, T. Yoshida and H. Taguchi 1981b. On–line optimal control of fed–batch culture of glutamic acid production. *J. Ferment. Technol.*, 59, 125–129

G.L. Kleman, J.C. Chalmers, G.W. Luli and W.R. Strohl 1991. A predictive and feedback control algorithm maintains a constant glucose concentration in fed–batch fermentations. *Appl. Environ. Microbiol.*, 57, 910–917

H.-P.E. Kohler, A. Heitzer, and G. Hamer 1991. Improved unstructured model describing temperature dependence of bacterial maximum specific growth rates. In : H. Verachtert and W. Verstraete (Eds.), *International Symposium on Environmental Biotechnology*, 511–514, Royal Flemish Society of Engineers, Ostend (Belgium)

Ž. Kurtanjek 1991. Optimal nonsingular control of fed–batch fermentation. *Biotechnol. Bioeng.*, 37, 814–823

S.S. Lee and H.Y. Wang 1982. Repeated fed–batch rapid fermentation using yeast cells and activated carbon extraction system. *Biotech. Bioeng. Symp.*, 12, 221–231

H.C. Lim, Y.J. Tayeb, J.M. Modak and P. Bonte 1986. Computational algorithms for optimal feed rates for a class of fed–batch fermentation : numerical results for penicillin and cell mass production. *Biotechnol. Bioeng.*, 28, 1408–1420

M.J. López–Nieto, F.R. Ramos, J.M. Luengo and J.F. Martin 1985. Characterization of the biosynthesis in vivo of α–aminoadipyl–cysteinyl–valine in *Penicillium chrysogenum. Appl. Microbiol. Biotechnol.*, 22, 343–351

R. Luedeking and E.L. Piret 1959. A kinetic study of the lactic acid fermentation batch process at controlled pH. *J. Biochem. Microbiol. Technol. Eng.*, 1, 393–412

J.F. Martin and P. Liras 1989. Enzymes involved in the penicillin, cephalosporin and cephamycin biosynthesis. *Advances in Biochemical Engineering/Biotechnology*, 39, 153–187

E.P. Mc Cann and C.T. Calam 1972. The metabolism of *Penicillium chrysogenum* and the production of penicillin using a high yielding strain, at different temperatures. *J. Appl. Chem. Biotechnol.*, 22, 1201–1208

J.M. Modak, H.C. Lim and Y.J. Tayeb 1986. General characteristics of optimal feed rate profiles for various fed–batch fermentation processes. *Biotechnol. Bioeng.*, 28, 1396–1407

J.M. Modak and H.C. Lim 1989. Simple nonsingular control approach to fed–batch fermentation optimization. *Biotechnol. Bioeng.*, 33, 11–15

J. Monod 1942. *Recherches sur la croissance des cultures bactériennes.* Hermann, Paris

G.A. Montague, A.J. Morris, A.R. Wright, M. Aynsley and A.C. Ward 1986. Online estimation and adaptive control of penicillin fermentation. *IEE Proc. D*, 5, 240–246

M.O. Moss 1987. Morphology and physiology of *Penicillium* and *Acremonium.* In J.F. Peberdy (Ed.), *Penicillium and Acremonium*, 37–65, Plenum Press, New York - London

D.G. Mou 1979. Towards an optimum penicillin fermentation by monitoring and controlling growth through computer aided mass balancing. *PhD thesis*, MIT, Cambridge

D. Mou and C.L. Cooney 1983a. Growth monitoring and control through computer–aided on–line mass balancing in a fed–batch penicillin fermentation. *Biotechnol. Bioeng.*, 25, 225–255

D. Mou and C.L. Cooney 1983b. Growth monitoring and control in complex medium : a case study employing fed–batch penicillin fermentation and computer–aided on–line mass balancing. *Biotechnol. Bioeng.*, 25, 257–269

M.M. Nadkarni and T.A. Hatton 1985. Optimal nutrient retention during the thermal processing of conduction–heated canned foods : application of the distributed minimum principle. *J. Food Sci.*, 50, 1312–1321

I. Nelligan and C.T. Calam 1983. Optimal control of penicillin production using a mini–computer. *Biotechnology Letters*, 5, 561–566

E. Nestaas and D.I.C. Wang 1983. Computer control of the penicillin fermentation using the filtration probe in conjunction with a structured process model. *Biotechnol. Bioeng.*, 25, 781–796

B.M. Nicolaï, J.F. Van Impe, P.A. Vanrolleghem and J. Vandewalle 1991. A modified unstructured mathematical model for the penicillin G fed–batch fermentation. *Biotechnology Letters*, 13 (7), 489–494

B.M. Nicolaï, J.F. Van Impe, P.A. Vanrolleghem and J. Vandewalle 1992. Evaluation of two unstructured mathematical models for the penicillin G fed–batch fermentation. *Antonie van Leeuwenhoek*, in press

M. Nihtilä and J. Virkkunen 1977. Practical identifiability of growth and substrate consumption models. *Biotechnol. Bioeng.*, 19, 1831–1850

H. Ohno, E. Nakanishi and T. Takamatsu 1976. Optimal control of a semi-batch fermentation. *Biotechnol. Bioeng.*, 18, 847–864

S.J. Parulekar and H.C. Lim 1985. Modeling, optimization and control of semi–batch bioreactors. *Adv. Biochemical Eng. Biotechnol.*, 32, 207–258

S.J. Pirt 1965. The maintenance energy of bacteria in growing cultures. *Proc. R. Soc.*, B 163, 24

S.J. Pirt and R.C. Rhigelato 1967. Effect of growth rate on the synthesis of penicillin by *Penicillium chrysogenum* in batch and chemostat cultures. *Applied Microbiology*, 15, 1284–1290

S.J. Pirt 1990. Penicillin hydrolysis rate : its effect on the kinetics of penicillin fermentation. *J. Ferment. Bioeng.*, 69, 259–260

L.S. Pontryagin, V.G. Boltyanskii, R.V. Gamkrelidze and E.F. Mishchenko 1962. *The mathematical theory of optimal processes.* Wiley Interscience, New York

D.L. Preuss and M.J. Johnson 1967. Penicillin acyltransferase in *Penicillium chrysogenum. J. Bacteriol.*, 94, 1502–1508

S. Queener and N. Neuss 1982. The biosynthesis of β–lactam antibiotics. In R.B. Morin and M. Morgan (Eds.), *The chemistry and biology of β–lactam antibiotics*, Academic Press, London - New York

F.R. Ramos, M.J. López–Nieto and J.F. Martin 1985. Isopenicillin N synthetase of *Penicillium chrysogenum*, an enzym that converts δ–(L–α–aminoadipyl)–L–cysteinyl–D–valine to isopenicillin N. *Antimicrob. Agents Chemother.*, 27, 380–387

D.A. Ratkowsky, R.K. Lowry, T.A. McMeekin, A.N. Stokes and R.E. Chandler 1983. Model for bacterial culture growth rate throughout the entire biokinetic temperature range. *J. Bacteriol.*, 154, 1222–1226

D.A. Ratkowsky, J. Olley, T.A. McMeekin and A. Ball 1982. Relationship between temperature and growth rate of bacterial cultures. *J. Bacteriol.*, 149, 1–5

G. Revilla, M.J. López–Nieto, J.M. Luengo and J.F. Martin 1984. Carbon catabolite repression of penicillin biosynthesis by *Penicillium chrysogenum. J. Antibiot.*, 37, 781–789

R.C. Rhigelato, A.P. Trinci, S.J. Pirt and A. Peat 1968. The influence of maintenance energy and growth rate on the metabolic activity, morphology and conidation of penicillium chrysogenum. *J. gen. Microbiol.*, 50, 399–412

H.M. Robbins 1966. A generalized Legendre–Clebsch condition for the singular case of optimal control. *IBM Federal Systems Division Report* #66 – –825 2043

J.A. Roels 1983. *Energetics and kinetics in biotechnology.* Elsevier Biomedical Press, Amsterdam - New York - Oxford

D.Y. Ryu and J. Hospodka 1980. Quantitative physiology of *Penicillium chrysogenum* in penicillin Fermentation. *Biotechnol. Bioeng.*, 22, 289–298

D.Y. Ryu and A.E. Humphrey 1985. The practice of biotechnology : penicillins. In M. Moo–Young (Ed.), *Comprehensive biotechnology*, Volume 3, Pergamon Press, Oxford

I. Saguy and M. Karel 1979. Optimal retort temperature profile in optimizing thiamin retention in conduction–type heating of canned foods. *J. Food Sci.*, 44, 1485–1490

K.Y. San and G. Stephanopoulos 1984. A note on the optimality criteria for maximum biomass production in a fed–batch fermentor. *Biotechnol. Bioeng.*, 26, 1261–1264

K.Y. San and G. Stephanopoulos 1989. Optimization of fed–batch penicillin fermentation : a case of singular optimal control with state constraints. *Biotechnol. Bioeng.*, 34, 72–78

J. Schnute 1981. A versatile growth model with statistically stable parameters. *Can. J. Fish. Aquat. Sci.*, 38, 1128–1140

R.M. Schoolfield, P.J.H. Sharpe and C.E. Magnuson 1981. Non–linear regression of biological temperature–dependent rate models based on absolute reaction–rate theory. *J. theor. Biol.*, 88, 719–731

J.A. Spriet 1982. Modelling the growth of micro–organisms : a critical appraisal. In S. Rinaldi (Ed.), *Environmental Systems Analysis and Management*, 451–465, North Holland Publ.

J.A. Spriet 1987. The control of fermentation processes. *Med. Fac. Landbouww. Rijksuniv. Gent*, 52 (4), 1371–1381

J. Staniškis and D. Levišauskas 1984. An adaptive control algorithm for fed–batch culture. *Biotechnol. Bioeng.*, 26, 419–425

C.R. Stumbo 1973. *Thermobacteriology in food processing.* Second Edition. Academic Press, New York

K. Tait 1965. Singular problems in optimal control. *PhD thesis*, Harvard University

A.A. Teixeira and C.F. Shoemaker 1989. *Computerized food processing operations.* Ed. Van Rostrand Reinhold, New York

G. Tessier 1942. Croissance des populations bactériennes et quantités d'aliments disponibles. *Rev. Sci.*, Paris, 80–209

J.M. Thevelin 1984. Regulation of trehalose mobilisation in fungi. *Microbiol. Rev.*, 48, 42–59

V. Van Breusegem and G. Bastin 1992. A singular perturbation approach to the reduced dynamical modelling of reaction systems. *CESAME Technical Report #92–14*, Université Catholique de Louvain

J.F. Van Impe 1989. OPTCON : an interactive program for optimal control of fermentation processes. *Internal Report*, Department of Agricultural Engineering, K.U. Leuven

J.F. Van Impe, B.M. Nicolaï, P.A. Vanrolleghem, J.A. Spriet, B. De Moor and J. Vandewalle 1990. Optimal control of the penicillin G fed–batch fermentation : An analysis of the model of Heijnen *et al.*, *ESAT–SISTA Report 1990–23*, Dept. of Electr. Eng., K.U. Leuven, accepted for publication in *Optimal Control Applications and Methods.*

J.F. Van Impe, B.M. Nicolaï, J.A. Spriet, B. De Moor and J. Vandewalle 1991a. Optimal control of the penicillin G fed–batch fermentation : an analysis of the model of Bajpai and Reuß. In : E. Mosekilde (Ed.), *Modelling and Simulation 1991*, 867–872, Society for Computer Simulation SCS, San Diego

J.F. Van Impe, B.M. Nicolaï, B. De Moor and J. Vandewalle 1991b. Evaluation of on–line conventional and adaptive controllers for the penicillin G fed–batch fermentation based on simulations using a new mathematical model. In : E. Mosekilde (Ed.), *Modelling and Simulation 1991*, 873–878, Society for Computer Simulation SCS, San Diego

J.F. Van Impe, B.M. Nicolaï, P.A. Vanrolleghem, J.A. Spriet, B. De Moor and J. Vandewalle 1991c. Optimal control of the penicillin G fed–batch fermentation : an analysis of a new unstructured model. *Proceedings of the 1991 European Control Conference*, Grenoble (France), 1624–1629

J.F. Van Impe, B. Nicolaï, T. Martens, J. De Baerdemaeker and J. Vandewalle 1991d. Prediction of microbial growth during storage and thermal treatment of foods : an overview. In : Mededelingen Fac. Landbouww. Rijksuniv. Gent : *Proceedings of the 1991 Forum for Applied Biotechnology*, Gent (Belgium), 56 (4b), 1687–1692

J.F. Van Impe, P. Vanrolleghem, B. De Moor and J. Vandewalle 1991e. Model–based control of the activated sludge wastewater treatment process. In : H. Verachtert and C. Billiet (Eds.), *1991 Environmental Platform Proceedings*, Leuven (Belgium)

J.F. Van Impe, P.A. Vanrolleghem, W. Verstraete, B. De Moor and J. Vandewalle 1991f. Model based monitoring and control of activated sludge wastewater treatment processes. Part II : nonlinear control of the biotransformation and sedimentation process. In : E. Kerckhoffs, H. Koppelaar, A. Van der Beken and G. Vansteenkiste (Eds.), *Modelling and Control of Water Resources Systems and Global Changes*, 221–226, Society for Computer Simulation SCS, San Diego

J.F. Van Impe, B. Nicolaï, T. Martens, J. De Baerdemaeker and J. Vandewalle 1992a. Dynamic mathematical model to predict microbial growth and inactivation during food processing. *Applied and Environmental Microbiology*, 58 (9), 2901–2909

J.F. Van Impe, B. De Moor and J. Vandewalle 1992b. Properties of the optimal singular control of fed–batch fermentation processes. *ESAT–SISTA Report 1992–46*, Dept. of Electr. Eng., K.U. Leuven, to be presented at the *1993 European Control Conference*, Groningen (The Netherlands)

J.F. Van Impe, G. Bastin, B. De Moor, V. Van Breusegem and J. Vandewalle 1992c. Optimal adaptive control of fed–batch fermentation processes with growth/production decoupling. *Proceedings of the 5th International Conference on Computer Applications in Fermentation Technology and 2nd IFAC Symposium on Modeling and Control of Biotechnical Processes*, Keystone (Colorado), in press

J.F. Van Impe, B. Nicolaï, P. Vanrolleghem, J. Spriet, B. De Moor and J. Vandewalle 1992d. Optimal control of the penicillin G fed–batch fermentation : an analysis of a modified unstructured model. *Chemical Engineering Communications*, in press

J.F. Van Impe, B. Nicolaï, B. De Moor and J. Vandewalle 1992e. Optimal substrate controller design for the penicillin G fed–batch fermentation process using simulations. *Chemical and Biochemical Engineering Quarterly*, in press

J.F. Van Impe, P.A. Vanrolleghem, W. Verstraete and J. Vandewalle 1992f. New trends in model–based monitoring and control of the activated sludge wastewater treatment process. *Journal A, Special Issue on Environmental Control*, 33 (3), 19–29

J.F. Van Impe, B. De Moor and J. Vandewalle 1992g. Singular optimal control of fed–batch fermentation processes with growth/production decoupling and state inequality constraints. *ESAT–SISTA Report 1992–47*, Dept. of Electr. Eng., K.U. Leuven, accepted for presentation at the *12th IFAC World Congress 1993*, Sydney (Australia)

P.A. Vanrolleghem, J.F. Van Impe, J. Vandewalle and W. Verstraete 1991. Model based monitoring and control of activated sludge wastewater treatment processes. Part I : on–line estimation of crucial biological variables with the RODTOX. In : E. Kerckhoffs, H. Koppelaar, A. Van der Beken and G. Vansteenkiste (Eds.), *Modelling and Control of Water Resources Systems and Global Changes*, 215–220, Society for Computer Simulation SCS, San Diego

W.A. Weigand, H.C. Lim, C.C. Gregan and R.D. Mohler 1979. Optimization of a repeated fed–batch reactor for maximum cell productivity. *Biotechnol. Bioeng. Symp.*, 9, 335–348

W.A. Weigand 1981. Maximum cell productivity by repeated fed–batch culture for constant yield case. *Biotechnol. Bioeng.*, 23, 249–266

R.L. White, E.M. John, J.E. Baldwin and E.P. Abraham 1982. Stoichiometry of oxygen consumption in the biosynthesis of isopenicillin from a tripeptide. *Biochem. J.*, 203, 791–793

T. Yamane, M. Kishimoto and F. Yoshida 1976. Semi–batch culture of methanol–assimilating bacteria with exponentially increased methanol feed. *J. Ferment. Technol.*, 54, 229–240

T. Yamane, T. Kume, E. Sada and T. Takamatsu 1977. A simple optimization technique for fed–batch culture. *J. Fermentation Technol.*, 55, 587–598

M.H. Zwietering, I. Jongenburger, F.M. Rombouts and K. van 't Riet 1990. Modeling of the bacterial growth curve. *Appl. Environ. Microbiol.*, 56, 1875–1881

M.H. Zwietering, J.T. de Koos, B.E. Hasenack, J.C. de Wit and K. van 't Riet 1991. Modeling bacterial growth as a function of temperature. *Appl. Environ. Microbiol.*, 57, 1094–1101

Appendix B

Nomenclature

Chapter 1

t	: time	[h]
S	: absolute amount of substrate in the reactor	[g]
X	: absolute amount of biomass in the reactor	[g DW (Dry Weight)]
P	: absolute amount of product in the reactor	[g]
V	: reactor volume	[L]
F_{in}	: influent volumetric flow rate	[L/h]
F_{out}	: effluent volumetric flow rate	[L/h]
Q_{in}	: rate of mass inflow per unit reactor volume of a component in gaseous form	[g/L h]
Q_{out}	: rate of mass outflow per unit reactor volume of a component in gaseous form	[g/L h]
D	: dilution rate	[1/h]
$C_{s,in}$	: substrate concentration in the influent	[g/L]
C_s	: substrate concentration in the reactor and the effluent	[g/L]
C_x	: biomass concentration in the reactor and the effluent	[g/L]
C_p	: product concentration in the reactor and the effluent	[g/L]
C_o	: dissolved oxygen concentration	[mol O_2/L]
$C_{o,sat}$	: dissolved oxygen saturation concentration	[mol O_2/L]
C_c	: dissolved carbon dioxide concentration	[L CO_2/L]
OTR	: oxygen transfer rate	[mol O_2/L h]
OUR	: oxygen uptake rate	[mol O_2/L h]
CER	: carbon dioxide evolution rate	[L CO_2/L h]
k_La	: mass transfer coefficient	[1/h]
m	: overall specific maintenance demand	[g/g DW h]
m_s	: specific maintenance demand of substrate by the cells	[g/g DW h]
m_x	: specific maintenance demand of cell mass by the cells	[1/h]
m_o	: specific oxygen consumption rate for maintenance	[mol O_2/g DW h]
m_c	: specific CO_2 production rate in maintenance processes	[L CO_2/g DW h]
k_d	: specific rate of cell death	[1/h]

$Y_{x/s}$	: biomass on substrate yield coefficient	[g DW/g]
$Y_{p/s}$	: product on substrate yield coefficient	[g/g]
$Y_{p/x}$	: product on biomass yield coefficient	[g/g DW]
$Y_{x/o}$	: biomass on oxygen yield coefficient	[g DW/mol O_2]
$Y_{p/o}$	: product on oxygen yield coefficient	[g/mol O_2]
$Y_{c/x}$	: carbon dioxide on biomass yield coefficient	[L CO_2/g DW]
$Y_{c/p}$	: carbon dioxide on product yield coefficient	[L CO_2/g]
σ	: specific substrate consumption rate	[g/g DW h]
μ	: overall specific growth rate	[1/h]
μ_{substr}	: specific substrate to biomass conversion rate	[1/h]
π	: specific production rate	[g/g DW h]
f_m	: endogenous fraction of the overall specific maintenance demand	[-]
f_p	: endogenous fraction of the energy supply for product synthesis	[-]
$\mathbf{x}$	: $n \times 1$ vector of state variables	
$\boldsymbol{\lambda}$	: $n \times 1$ vector of costate variables	
$\mathbf{u}$	: $m \times 1$ vector of control inputs	
J	: cost index to be minimized	
g	: terminal cost	
$\mathcal{L}$	: integrand of the cost index	
$\mathcal{H}$	: Hamiltonian	

Chapter 2

t	: time	[h]
N	: population size	[number of organisms]
N_0	: initial population size	[number of organisms]
y	: $= \ln(N/N_0)$	
A	: $= \ln(N_\infty/N_0)$ asymptotic value of the growth curve	
μ	: overall specific growth rate	[1/h]
μ_{max}	: maximum specific growth rate	[1/h]
μ_{25}	: specific growth rate at 25 °C	[1/h]
λ	: lag time	[h]
T	: temperature	[°C] or [K]
T_l	: temperature at which the enzyme is 50 % inactivated due to low temperature	[K]
T_h	: temperature at which the enzyme is 50 % inactivated due to high temperature	[K]
H	: enthalpy of activation	[J/mol]
R	: gas constant	[J/mol K]
k	: reaction rate constant of high temperature inactivation	[1/h]

Chapter 3

$\mathcal{Y}$	: yield index ratio of final product quantity to total substrate amount consumed	[g/g]
$\mathcal{P}$	: productivity index ratio of final product quantity to total fermentation time	[g/h]
γ_x	: unit price associated with cell mass	
γ_p	: unit price associated with metabolite product	
γ_t	: unit operating cost	
α	: total amount of substrate consumed during fermentation	[g]
α_{growth}	: total amount of substrate consumed during growth	[g]

Chapter 4

$\mathcal{G}$	: gain due to substrate feeding rate optimization	[%]

The model of Heijnen, Roels and Stouthamer

S	: amount of substrate in broth	[mol]
X	: amount of cell mass in broth	[mol DW]
P	: amount of product in broth	[mol]
G	: total broth weight	[kg]
u	: substrate feed rate	[mol/h]
$C_{s,in}$	: glucose concentration in feed stream	[mol/kg]
k_h	: penicillin hydrolysis constant	[1/h]
r_c	: net rate of CO_2 conversion	[mol/h]
r_n	: net rate of nitrogen source conversion	[mol/h]
r_o	: net rate of oxygen conversion	[mol/h]
r_{su}	: net rate of sulphate source conversion	[mol/h]
σ	: specific substrate consumption rate	[mol/mol DW h]
$Q_{s,max}$	: maximum specific sugar uptake rate	[mol/mol DW h]
K_s	: Monod constant for sugar uptake	[mol/kg]
μ	: overall specific growth rate	[1/h]
π	: specific production rate	[mol/mol DW h]
$Q_{p,max}$	: maximum specific production rate	[mol/mol DW h]
μ_{crit}	: critical specific growth rate	[1/h]
B	: Dabes constant	[1/h]
m	: overall specific maintenance demand	[mol/mol DW h]
$Y_{x/s}$	: biomass on substrate yield coefficient	[mol DW/mol]
$Y_{p/s}$	: product on substrate yield coefficient	[mol/mol]

The model of Bajpai and Reuß

μ_C	: maximum specific growth rate for Contois kinetics	[1/h]
K_x	: Contois saturation constant for substrate limitation of biomass production	[g/g DW]
μ_M	: maximum specific growth rate for Monod kinetics	[1/h]
K_s	: Monod saturation constant for substrate limitation of biomass production	[g/L]
π_m	: specific production constant	[g/g DW h]
K_p	: Monod saturation constant for substrate limitation of product formation	[g/L]
K_i	: substrate inhibition constant for product formation	[g/L]

Chapter 5

U	: unit step function	
E_m	: parameter related to the endogenous fraction of maintenance requirements of biomass	[g/L]
E_p	: parameter related to the endogenous fraction of product synthesis	[g/L]

Chapter 6

λ	: $-\lambda$ is the stable pole of the reference model	
Δ	: disturbance	
$\hat{x}$	: estimate of x	
ΔT	: measurement delay	[h]
ρ	: control action weighting factor in one–step–ahead controller	
ζ	: forgetting factor	
ω, γ	: tuning parameters	

Appendix C

Nederlandse samenvatting

Modelbouw en Optimale Adaptieve Controle van Biotechnologische Processen

Biotechnologie is heden ten dage ongetwijfeld een wetenschappelijke discipline in volle ontwikkeling en expansie. Het domein omvat onder meer biotechnologische produktieprocessen of fermentatieprocessen, waarin een enorme verscheidenheid aan produkten gemaakt worden, en biologische afvalwater zuiveringsprocessen, met als voornaamste vertegenwoordigers actief slib zuiveringsprocessen. De dynamica van al deze processen wordt in de eerste plaats bepaald door een populatie levende micro–organismen.

Het principe van microbiële groeiprocessen kan als volgt vereenvoudigd worden [Holmberg en Ranta 1982] : de micro–organismen (zoals bacteriën, schimmels, gisten, ...) groeien dankzij de opname van voedingsstoffen of substraten (koolstofderivaten (zoals glucose), stikstof, zuurstof, ...), op voorwaarde dat alle omgevingscondities (temperatuur, pH, beluchting, roersnelheid, ...) gunstig zijn.

Bij het zoeken naar een oplossing voor bepaalde sociale en technische produktieproblemen hebben micro–organismen enkele niet te verwaarlozen voordelen. Vooreerst vormen zij een levende grondstof, die zo goed als onuitputtelijk is. Ten tweede kunnen stoffen die tot dusver waardeloos bleken, zoals bijvoorbeeld bepaalde afvalstoffen, nuttig gebruikt worden als groeibodem voor deze micro–organismen. In die zin gaat de ontwikkeling van de biotechnologie niet gepaard met een verder aantasten van de wereldvoorraad ruwe grondstoffen. Dit betekent ook dat het milieu minder belast wordt. Op lange termijn biedt biotechnologie een perspectief op een oplossing voor enkele problemen van wereldschaal : onderdrukken van epidemieën; milieubescherming; het voedselprobleem, waarbij dan zowel produktietekorten als overschotten aangepakt worden.

Het doel van een biotechnologische cultuur kan zijn :

1. *Biomassa produktie, zoals bakkersgist.*

2. *Produktie van synthese produkten. We onderscheiden (i) intracellulaire (proteïnen, endotoxinen, ...) en (ii) extracellulaire produkten (antibiotica, alcohol, ...). Een andere indeling is : (i) processen waarbij de produktvorming strikt geassocieerd is met de groei, zoals ethanol, en (ii) processen waarin de vorming van het gewenste produkt niet noodzakelijk geassocieerd is met de groei (de zogenaamde metabolieten), zoals enzymes en antibiotica.*

3. *Biologische zuivering van afvalwater, i.e. consumptie door micro–organismen van bepaalde afvalstoffen.*

Daarentegen is in het domein van de behandeling van levensmiddelen (sterilisatie, cook–chill methoden, ...), de groei van micro–organismen een ongewenst proces, met doorgaans nefaste gevolgen voor de houdbaarheid van dergelijke produkten.

Biotechnologische processen kunnen ook worden ingedeeld naargelang de bedrijfsvoering van de bioreactor waarin ze plaatsgrijpen.

Tijdens een batch fermentatie wordt geen substraat toegevoerd of produkt afgevoerd tot het einde van het proces. Hoewel bepaalde farmaceutische produkten volgens deze methode aangemaakt worden, is over het algemeen een batch fermentatie niet aantrekkelijk vanuit commercieel oogpunt.

Tijdens een continue fermentatie wordt voortdurend substraat toegevoegd. Er wordt ook voortdurend produkt afgevoerd, zodat het totaal volume van de cultuur constant blijft. Voorbeelden zijn de fermentatie van melk bij de bereiding van margarine, en de biologische zuivering van afvalwater.

Tijdens een fed–batch fermentatie (ook dikwijls aangeduid als een Zulauf proces) wordt substraat intermitterend of continu toegevoegd. Er is echter geen afvoer van produkt tijdens het proces. Vanuit het standpunt van de controle–ingenieur betekent deze procesvoering de grootste uitdaging. Ze biedt de mogelijkheid om de nutriënttoevoer zó te regelen dat, bijvoorbeeld, een optimale produktiviteit wordt bekomen, en terzelfdertijd problemen ten gevolge van bovenmaatse en ondermaatse substraattoevoer worden vermeden. Bakkersgist en allerhande antibiotica (zoals penicillines) worden op commerciële schaal geproduceerd in fed–batch.

C.1 Algemeen overzicht

Eén van de hoofddoelstellingen van dit werk is te onderzoeken in welke mate de toepassing van technieken uit de wiskundige modelbouw en uit de moderne modelgebaseerde regeltechniek kan bijdragen tot een optimalisering van biotechnologische processen.

We motiveren dit als volgt voor elk van de vermelde type–processen.

1. *Fermentatieprocessen* verbruiken soms zeer dure grondstoffen en vereisen zeer grote kapitaalsintensieve produktieëenheden, terwijl de synthese produkten doorgaans slechts in zeer kleine concentraties aangemaakt worden. Een beperkte verbetering in eender welke van deze variabelen leidt reeds tot een merkbare daling van de produktiekosten.

2. In het domein van de *biologische afvalwater zuivering* laat de nood aan betrouwbare automatische regelingen zich steeds sterker voelen, zowel wegens de toenemende kostprijs van energie als de strengere normen van overheidswege betreffende het milieu.

3. Het optimaliseren van de *thermische behandeling van levensmiddelen* streeft naar een evenwicht (*trade off*) tussen het vertragen of verhinderen van bederf door groeiende micro–organismen enerzijds, en het behoud van nutritieve en sensoriële kwaliteitseigenschappen anderzijds.

De ontwikkeling van wiskundige modellen voor biotechnologische processen, en daarop gebaseerde algoritmen voor toestandsschatting en regeling in ware tijd, is een uitdagend werkterrein voor zowel biotechnologen als controle–ingenieurs. In dit werk is het optimaliseren van een specifiek biotechnologisch proces (veel aandacht gaat bijvoorbeeld naar de penicilline G fermentatie) veeleer een *middel* dan een *doel* : elk voorbeeld behandeld in de tekst dient slechts ter illustratie van de basisideeën, de methodologie, en de bekomen resultaten. Anders gezegd, er wordt vooral gepoogd beter inzicht te krijgen in zowel het potentieel nut als de beperkingen van technieken uit de wiskundige modelbouw en moderne regeltechniek, toegepast op processen waarvan de dynamica in de eerste plaats beheerst wordt door een levende populatie micro–organismen.

In vele praktische toepassingen wordt accurate modelbouw (en bijgevolg ook modelgebaseerde regeling) sterk bemoeilijkt door de volgende factoren.

1. Zeer vaak tast men nog in het duister omtrent de ware (niet–lineaire) aard van de *proceskinetica*. Daarenboven zijn de bijbehorende parameters vaak tijdsinvariant.

2. Tot op de dag van vandaag is er een zeer grote nood aan betrouwbare *sensoren* voor metingen van procesvariabelen in ware tijd. Nochtans vereisen geavanceerde regelalgoritmen een goede kennis van de procesvariabelen.

Dit verklaart waarom bij de eerste pogingen om een biotechnologisch proces te regelen helemaal geen model werd gebruikt. De trajectories van voorafgaande succesvolle fermentaties werden in de procescomputer opgeslagen. Via een regeling in open kring werden deze trajectories dan zo goed mogelijk gevolgd. Merk op dat zeer veel industriële fermentaties nog steeds op deze manier geregeld worden.

Meer geavanceerde ontwerpstrategieën van algoritmen voor toestandsschatting en regeling van biotechnologische processen kunnen ingedeeld worden in twee grote groepen [Bastin 1991].

> In een *eerste aanpak* gaat men ervan uit dat men over een perfect model van het proces beschikt. Een zeer groot aantal artikels uit de wetenschappelijke literatuur is gewijd aan de toepassing van min of meer klassieke methoden, zoals bijvoorbeeld Kalman filteren, en optimale controle. Gezien de reeds vermelde moeilijkheden bij het afleiden van een voldoend accuraat procesmodel, is het zeer twijfelachtig dat bij een implementatie van de bekomen regelaars in ware tijd (bovendien in de veronderstelling dat de vereiste sensoren beschikbaar zijn) het dynamisch gedrag in gesloten kring zou overeenstemmen met de voorspelde simulatieresultaten.
>
> In een *tweede aanpak* is het de bedoeling specifieke algoritmen voor toestandsschatting en regeling te ontwerpen, waarbij geen nood is aan een volledige kennis van het procesmodel. Hierbij worden technieken uit adaptieve controle en niet–lineaire lineariserende controle gebruikt. Een zeer uitgebreide analyse van deze aanpak is beschreven in [Bastin en Dochain 1990] en de daarin vermelde referenties.

In dit werk nemen we een eerder pragmatisch standpunt in : we proberen het beste van beide trends te combineren in één unificerende methodologie voor optimalisering van biotechnologische processen : *optimale adaptieve controle*. Dit kan als volgt gemotiveerd worden.

> Via modelgebaseerde *optimale controle* studies verwerft men inzicht in het theoretisch haalbare optimum. Bovendien wordt in dit werk geïllustreerd dat optimale controle nuttig kan zijn als een techniek om uit verschillende modelstructuren voor een bepaald proces de meest relevante te selecteren. Niettemin zal, zoals reeds aangehaald, een implementatie in ware tijd falen, voornamelijk door (te) grote onzekerheden op het gebruikte model.
>
> Anderzijds kunnen robuuste, model–onafhankelijke *adaptieve regelaars* ontworpen worden. Nadeel is hier dat men er geen idee van heeft hoever de resultaten afwijken van het theoretisch haalbare.

In dit werk wordt de kloof tussen beide methodes overbrugd door de ontwikkeling van *heuristische regelstrategieën* met een quasi optimale performantie onder alle omstandigheden. Deze suboptimale regelaars zijn gebaseerd op de beschikbare biochemische en microbiologische kennis van het proces, én op een diepgaande mathematische analyse van de oplossing bekomen via optimale controle. Implementatie van deze heuristische regelaars op een adaptieve model–onafhankelijke manier garandeert dan terzelfdertijd een suboptimale performantie en uitstekende robuustheidseigenschappen.

C.2 Overzicht hoofdstuk per hoofdstuk

Het aantal onderwerpen behandeld in dit werk is eerder groot. De tekst is voornamelijk bedoeld voor controle–ingenieurs. Zoals reeds vermeld is het de bedoeling om het (industrieel zeer belangrijke) probleem van wiskundige modelbouw, toestandsschatting, en regeling van biotechnologische processen, te analyseren binnen het algemeen gehanteerde raamwerk (en de bijbehorende terminologie) van de controle–ingenieur.

Niettemin is de tekst ook gericht tot bio–ingenieurs die reeds enige noties van regeltechniek hebben, en die beter willen begrijpen hoe wiskundige modelbouw en regeltechniek kunnen toegepast worden op biotechnologische processen.

Daarom hebben we gepoogd de tekst in een pedagogische stijl te schrijven. De klemtoon ligt niet op het afleiden van theoretische resultaten als dusdanig, maar veeleer op hun interpretatie vanuit het standpunt van de bio–ingenieur.

In wat volgt worden de voornaamste bijdragen hoofdstuk per hoofdstuk beknopt samengevat.

Hoofdstuk 1

Technieken uit de systeemtheorie en de regeltechniek

In het eerste hoofdstuk wordt de vereiste basiskennis bondig samengevat. In plaats van te streven naar volledigheid, beperken we ons tot het vastleggen van het algemeen raamwerk waarbinnen de algoritmen voor toestandsschatting en regeling in de volgende hoofdstukken zullen afgeleid worden. Niettemin worden ook reeds enkele nieuwe concepten en resultaten voorgesteld.

De eerste paragraaf is volledig gewijd aan het modelleren van biotechnologische processen. We maken een onderscheid tussen fysiologische, ongestructureerde, en gestructureerde modellen. In de volgende hoofdstukken beperken we ons tot ongestructureerde modellen.

Vervolgens voeren we het nieuwe concept *endogene fractie* in. Dit concept laat toe een unificerend raamwerk op te stellen, waarbinnen elk mogelijk metabolisme voor onderhoud van biomassa (en eventueel voor produkt synthese) kan beschreven worden. Hiermee leggen we reeds de grondslag voor de resultaten van Hoofdstuk 5.

Een belangrijk deelaspect van biotechnologische modelbouw betreft de selectie van een geschikt model voor de reactiekinetiek(en). We verwijzen naar Hoofdstuk 2 voor een uitgewerkt voorbeeld. In dat hoofdstuk ontwikkelen we een dynamisch model dat de groei van micro–organismen in levensmiddelen beschrijft als functie van de tijd en de temperatuur.

De band met het algemeen toestandsmodel voor een biotechnologisch proces, ingevoerd door Bastin en Dochain [1990], wordt geïllustreerd met een eenvoudig voorbeeld. We vermelden tevens twee technieken, die tot doel hebben de complexiteit van het bekomen toestandsmodel te reduceren : enerzijds het concept van *minimale modellering*, en anderzijds de *singuliere perturbatietechniek*.

Wat betreft gestructureerde modellen beperken we ons tot enkele algemeenheden, om de tekst niet te veel te overladen. Voor een beschrijving van ons recent werk omtrent de ontwikkeling van algoritmen voor toestandsschatting en regeling voor een actief slib afvalwater zuiveringsproces, op basis van een gestructureerd model, verwijzen we naar de desbetreffende referenties.

De tweede paragraaf geeft een beknopt overzicht van de voornaamste resultaten uit *optimale controle theorie*, vertrekkende vanaf parametrische optimaliseringsmethoden tot en met het Minimumprincipe van Pontryagin [1962]. Singuliere optimale controle problemen worden expliciet behandeld voor de klasse van systemen die in dit werk aan bod komen.

Daarenboven bewijzen we nodige voorwaarden indien bepaalde (of alle) begintoestanden kunnen beschouwd worden als additionele vrijheidsgraden van het optimaliseringsprobleem.

Tenslotte formuleren we een nieuw, eenvoudig, maar tegelijk algemeen theorema, dat toelaat om onder bepaalde voorwaarden optimale controleprofielen te berekenen voor een continu maar niet differentieerbaar toestandsmodel (zie Conjecture 1.1). We sluiten dit inleidend hoofdstuk af met een schets van het bewijs, en een beknopte discussie omtrent de praktische toepassingen van dit theorema.

Het nieuw concept endogene fractie, en het daarop gebaseerde unificerend raamwerk waarbinnen elk mogelijk metabolisme voor onderhoud van biomassa (en eventueel voor produkt synthese) kan behandeld worden, is beschreven in de referenties [Van Impe et al. 1991c, 1992d]. Het nieuw theorema uit de tweede paragraaf (Conjecture 1.1) komt uit [Van Impe et al. 1990].

Ons recent werk omtrent de ontwikkeling van algoritmen voor toestandsschatting en regeling voor een actief slib afvalwater zuiveringsproces, op basis van een gestructureerd model, is terug te vinden in de referenties [Vanrolleghem et al. 1991] en [Van Impe et al. 1991e, 1991f, 1992f].

Hoofdstuk 2

Een dynamisch wiskundig model voor microbiële groei en inactivatie tijdens de behandeling van levensmiddelen

In dit hoofdstuk behandelen we de modellering van de reactiekinetiek(en), één van de basisingrediënten in het algemeen toestandsmodel voor een biotechnologisch proces. Bij wijze van voorbeeld bestuderen we de modellering van (ongewenste) microbiële groei in levensmiddelen. Bij fermentatieprocessen zijn de substraten (en soms ook de gevormde produkten) doorgaans belangrijkere invloedsfactoren voor microbiële groei dan de omgevingscondities (ondermeer temperatuur, pH, ...). Bij de (thermische) behandeling van levensmiddelen is de situatie juist omgekeerd. We beperken ons hier tot die levensmiddelen waarvoor *temperatuur de enige belangrijke invloedsfactor is.*

De hoofddoelstelling van dit hoofdstuk is het toepassen van geavanceerde concepten uit de mathematische modelbouw in het domein van de predictieve microbiologie. De literatuur vermeldt reeds heel wat wiskundige modellen die bacteriële groei beschrijven als functie van tijd en temperatuur. Spijtig genoeg zijn dit allemaal statische, expliciete uitdrukkingen. Bijgevolg is hun predictief karakter beperkt tot constante temperaturen binnen het temperatuursgebied voor microbiële groei. In dit hoofdstuk ontwikkelen we een *nieuw dynamisch model* dat bacteriële groei beschrijft als functie van tijd en temperatuur, en dit over het gehele temperatuursgebied van groei én inactivatie. Dit model laat toe om op een consistente manier voorspellingen te maken onder tijdsvariante temperatuurscondities. Andere markante eigenschappen zijn : (i) de voorgeschiedenis van het beschouwde levensmiddel kan op een natuurlijke wijze in rekening gebracht worden, (ii) het model kan allerlei micro–organismen, gekenmerkt door een verschillend gedrag bij temperaturen in de transitiezone van groei naar inactivatie, op een eenvoudige manier beschrijven, (iii) in het geval van een constante temperatuur in het temperatuursgebied van groei, reduceert het model tot het experimenteel gevalideerde expliciet model van Zwietering *et al.* [1990,1991], en (iv) het hele model heeft de vereiste wiskundige eigenschappen om geavanceerde niet–lineaire parameter estimatieschema's en moderne optimaliseringstechnieken zonder meer toe te passen.

Het materiaal behandeld in dit hoofdstuk is gepubliceerd in [Van Impe et al. 1991d] en [Van Impe et al. 1992a].

Hoofdstuk 3

Optimale controle van fed-batch fermentatieprocessen

In dit hoofdstuk bestuderen we de optimalisering van fed–batch bioreactoren. De bekomen resultaten zijn in die zin zeer algemeen, dat ze geschreven zijn in termen van de specifieke reactiesnelheden. Anders gezegd, een precieze analytische uitdrukking voor elk van die reactiesnelheden is a priori niet vereist. Daarenboven worden geen veronderstellingen gemaakt aangaande het metabolisme voor onderhoud van biomassa (en eventueel voor produkt synthese). We besteden veel aandacht aan een zorgvuldige motivering vanuit microbiologisch standpunt van zowel de gebruikte methodologie, als de bekomen resultaten. Op die manier zijn ook nieuwe interpretaties mogelijk van reeds gedeeltelijk gepubliceerde resultaten.

Na een beschrijving van de belangrijkste voordelen van fed–batch bedrijfsvoering, en een overzicht van de literatuur omtrent de toepassing van (optimale) controle op fed–batch fermentatieprocessen, formuleren we een algemeen ongestructureerd model voor een fed–batch bioreactor met volume V, gekenmerkt door één limiterend substraat S, één micro–organisme X, en eventueel één produkt P :

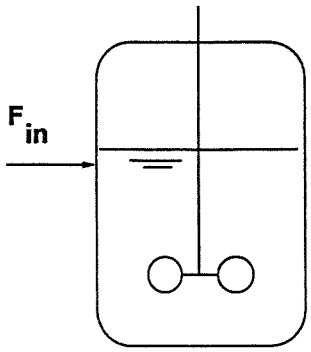

$$\begin{aligned}
\frac{dS}{dt} &= -\sigma X + C_{s,in}F_{in} \\
\frac{dX}{dt} &= \mu X \\
\frac{dP}{dt} &= \pi X - k_h P \\
\frac{dV}{dt} &= F_{in}
\end{aligned}$$

Hierin is σ de specifieke substraatconsumptiesnelheid, μ de (globale) specifieke groeisnelheid, en π de specifieke produktiesnelheid. Afbraak van produkt wordt gemodelleerd door een eerste orde model met afbraakconstante k_h. Het limiterend substraat S wordt gevoed met een (volumetrisch) debiet F_{in}. De concentratie in de voedingsstroom is $C_{s,in}$.

Vervolgens formuleren we een zeer algemeen optimaliseringsprobleem, met het volumetrisch voedingsdebiet van substraat, F_{in}, als de te manipuleren ingang. Daarbij beschouwen we kostfuncties zowel van het type *opbrengst*, als van het type *produktiviteit*. De optimalisering van de initiële substraatconcentratie wordt hierin opgenomen. Dit algemeen optimaliseringsprobleem wordt dan herschreven binnen het raamwerk van optimale controle theorie, hetgeen leidt tot een probleem met gescheiden randwaarden. We tonen aan dat het origineel probleem zich herleidt tot de bepaling van de *optimale controlesequentie*, en de bijbehorende *schakelogenblikken*.

Als inleidend voorbeeld behandelen we een eenvoudig microbieel groeiproces. Hoewel de oplossing reeds eerder gepubliceerd werd [Parulekar en Lim 1985], wordt dit probleem opnieuw volledig geanalyseerd in deze tekst, en wel om de volgende drie redenen. Ten eerste worden de afgeleide controlesequenties hier gejustifieerd op basis van microbiologisch inzicht in het proces. Ten tweede is de uitbreiding naar fermentatieprocessen met groei–geassocieerde produktvorming voor de hand liggend. Ten derde zullen we een analoge redenering aanhouden bij de studie van fed–batch fermentatieprocessen gekenmerkt door een ontkoppeling tussen microbiële groei en produktvorming.

In overeenstemming met het werk van Modak *et al.* [1986], worden fermentatieprocessen met een ontkoppeling tussen groei en produktvorming geclassificeerd op basis van het kwalitatief gedrag van de specifieke groei– en produktiesnelheid als functie van de substraatconcentratie. Bij wijze van voorbeeld bestuderen we in detail de optimale controlesequentie voor fermentatieprocessen met een monotone specifieke groeisnelheid μ, en een niet–monotone specifieke produktiesnelheid π. We kunnen aantonen dat de bekomen oplossing de kostindex globaal minimaliseert. Daarenboven presenteren we voor het eerst een complete oplossing in het (realistisch) geval van beperkingen van het type ongelijkheid op de substraat– en biomassaconcentraties. We bespreken ook de voordelen van het bijbehorend numeriek algoritme, in vergelijking met het algoritme voorgesteld door Lim *et al.* [1986].

Het singulier interval wordt zeer zorgvuldig geanalyseerd vanuit mathematisch oogpunt. De bekomen resultaten, samengevat in de Stellingen 3.1 en 3.2, vormen de basis voor een *heuristische optimaliseringsmethodologie* die als een rode draad doorheen dit werk loopt. Deze heuristische regelaars worden ook uitvoerig geïnterpreteerd vanuit een microbiologisch standpunt. In tegenstelling tot de oplossing bekomen via optimale controle theorie, voldoen deze regelaars aan een meer realistisch regelobjectief, namelijk instelwaarderegeling. In Hoofdstuk 6 wordt aangetoond hoe ze kunnen geïmplementeerd worden op een adaptieve, model–onafhankelijke manier.

De Stellingen 3.1 en 3.2 zijn te vinden in [Van Impe et al. 1992b]. De optimalisering van een fermentatieproces met beperkingen van het type ongelijkheid op de substraat– en biomassaconcentraties is beschreven in [Van Impe et al. 1992g].

Hoofdstuk 4

Analyse van twee ongestructureerde modellen voor de penicilline G fed-batch fermentatie

De technieken en resultaten, ontwikkeld en afgeleid in Hoofdstuk 3, worden in dit hoofdstuk toegepast op de optimalisering van de penicilline G fed–batch fermentatie.

In de eerste paragraaf geven we een bondig literatuuroverzicht omtrent de mathematische modelbouw van dit (industrieel zeer belangrijk) fermentatieproces.

De tweede paragraaf is volledig gewijd aan de analyse van het ongestructureerd model van Heijnen, Roels en Stouthamer [1979]. Dit model wordt gekenmerkt door een continue maar niet differentieerbare, groei–geassocieerde specifieke produktiesnelheid. Het metabolisme voor onderhoud van biomassa en produktvorming wordt volledig endogeen ondersteld. Gebruikmakend van theorema 1.1 uit Hoofdstuk 1, bepalen we voor de eerste maal het optimaal substraat voedingsprofiel dat een maximale hoeveelheid produkt voortbrengt voor een gegeven totale hoeveelheid beschikbaar substraat. De simulatieresultaten illustreren de efficiëntie van het numeriek algoritme ontwikkeld in Hoofdstuk 3, zelfs voor deze min of meer gedegenereerde kinetieken. Met behulp van hetzelfde theorema 1.1 bewijzen we een stelling die het singulier interval voor deze toepassing karakteriseert (Stelling 4.1). Deze stelling is de logische uitbreiding van de stellingen uit Hoofdstuk 3. De realiseerbare winst door optimalisering van het voedingsprofiel, vergeleken met het resultaat van een constant profiel gedurende dezelfde tijd en met initiële substraatconcentratie gelijk aan nul, bedraagt enkele honderden procenten. Bovendien blijkt de opbrengst, voorspeld met dit model, zeer gevoelig voor verschillende voedingsstrategieën. Deze resultaten, samen met het feit dat het (experimenteel vastgesteld) tweefasig gedrag in de penicilline fermentatie verdwijnt na optimalisering, doen enkele vragen rijzen omtrent de voorwaarden waarbinnen dit model geldig is.

In de derde paragraaf analyseren we het ongestructureerd model voorgesteld door Bajpai en Reuß [1980,1981]. Dit model wordt gekenmerkt door een monotone specifieke groeisnelheid, en een niet–monotone specifieke produktiesnelheid. Daarenboven wordt een onderhoudsmetabolisme gemodelleerd. Bij het oplossen van hetzelfde optimaliseringsprobleem als geformuleerd voor het model van Heijnen *et al.*, vergelijken we verschillende suboptimale voedingsstrategieën met het voedingsprofiel bekomen via het Minimumprincipe. Als een uitbreiding van de bevindingen van Bajpai en Reuß zelf (deze auteurs onderzochten enkel voedingsprofielen met vooraf gespecificeerde structuur), besluiten we dat alle beschouwde profielen een hoeveelheid produkt genereren die de optimale opbrengst zeer goed benadert, op voorwaarde dat de geassocieerde vrijheidsgraden hun optimale waarde aannemen. Bij gebruik van dit model varieert de realiseerbare winst van enkele procenten tot meerdere honderden procenten, afhankelijk van de gebruikte parameterset. We onderzoeken ook de optimalisering van de produktiviteit. Het conflict tussen opbrengst en produktiviteit in fed–batch bioreactoren wordt hiermee duidelijk geïllustreerd. Opnieuw blijkt het voorgestelde numeriek algoritme zeer betrouwbaar en efficiënt, onafhankelijk van het beschouwde performantiecriterium. Tenslotte wordt een vergelijking gemaakt met de numerieke resultaten bekomen door Lim *et al.* [1986].

Naast het afleiden van optimale controleprofielen voor beide modellen, zijn de belangrijkste bijdragen van dit hoofdstuk de volgende. Alhoewel beide modellen min of meer vergelijkbare voorspellingen maken van experimentele gegevens bij aanleggen van een constant voedingsprofiel, blijken zij een fundamenteel verschillend gedrag te hebben na optimalisering van het voedingsprofiel. Dit leidt tot een eerste vaststelling, namelijk dat een studie gebaseerd op optimale controle theorie zeer nuttig kan zijn bij de karakterisering van een procesmodel. Dit wordt verder uitgewerkt in Hoofdstuk 5 : *optimalisering voor modeldiscriminatie.* Ten tweede zijn de heuristische regelaars, ingevoerd in Hoofdstuk 3, onder alle omstandigheden een excellente benadering van de optimale strategieën, ondanks het feit dat deze laatste (en dus ook de realiseerbare winst) zeer sterk afhankelijk zijn van het gebruikte model. Op die manier kunnen zij inderdaad als vertrekpunt fungeren bij de ontwikkeling van suboptimale, model–onafhankelijke regelstrategieën. Dit vormt het onderwerp van Hoofdstuk 6 : *optimale adaptieve controle.*

Het model van Heijnen et al. wordt geanalyseerd in [Van Impe et al. 1990]. Een analyse van het model van Bajpai en Reuß is te vinden in [Van Impe et al. 1991a].

Hoofdstuk 5

Een unificerend ongestructureerd model voor de penicilline G fed-batch fermentatie

De tegenstrijdige resultaten afgeleid in Hoofdstuk 4 vormen de motivering voor een meer diepgaande vergelijking tussen het model van Heijnen, Roels en Stouthamer [1979] en het model van Bajpai en Reuß [1980,1981].

In de eerste paragraaf analyseren we de verschillen tussen beide modellen vanuit microbiologisch standpunt. De laatste resultaten omtrent de *pathway* van de penicillinesynthese worden schematisch samengevat. Binnen dit kader onderzoeken we de *structurele* verschillen tussen beide modellen, alsook de corresponderende *parameters*. Een zorgvuldige analyse laat toe de fysische en biochemische tekortkomingen in beide modellen te detecteren.

Daarenboven wordt het *parameter estimatieprobleem* duidelijk geïllustreerd : hoewel bepaalde modelparameters niet voldoende nauwkeurig kunnen geschat worden op basis van experimentele resultaten bekomen via een constant voedingsprofiel en lage initiële substraatconcentratie (anders gezegd, deze strategie exciteert het proces onvoldoende), kunnen zij toch een beslissende invloed hebben op het al dan niet gevoelig zijn van de uiteindelijke hoeveelheid produkt voor een verandering (optimalisering) van de voedingsstrategie. Het potentieel nut van voedingsstrategie optimaliseringsstudies bij het ontwerp van experimenten voor parameterestimatie wordt duidelijk aangegeven.

Om deze analyse te vervolledigen, onderzoeken we in de tweede paragraaf hoe het reële metabolisme (in andere woorden, de correcte *modelstructuur*) kan bepaald worden, alsook de mogelijke invloed op voedingsstrategie optimalisering. Dit vormt de motivering voor de constructie van een *nieuw unificerend ongestructureerd model.* In dit model worden tevens de fysische en biochemische tekortkomingen van beide besproken modellen gecorrigeerd. Het is in essentie gebaseerd op het unificerend concept van *endogene fractie* van de energietoevoer voor onderhoud van biomassa (en eventueel voor produkt synthese), ingevoerd in Hoofdstuk 1. De belangrijkste voordelen van dit model zijn de consistentie van de voorspellingen voor alle waarden van de variabelen, en de mogelijkheid om op een elegante manier verschillende metabolische condities te beschrijven. Dit nieuw model kan beschouwd worden als de vertaling van de meest recente vorderingen geboekt in het onderzoek naar de biochemie van de penicilline biosynthese.

Simulatieresultaten, bekomen via een zeer eenvoudige parametrische optimalisering, tonen aan dat er, naast het reeds vermelde parameter estimatieprobleem, ook een *modelstructuur karakteriseringsprobleem* bestaat. Door een geschikte keuze van de substraat voedingsstrategie kan interessante informatie bekomen worden omtrent het correcte metabolisme gedurende de fermentatie. Bovendien blijkt dit modelstructuur karakteriseringsprobleem in zekere zin *ontkoppeld* te zijn van het parameter estimatieprobleem.

In de derde paragraaf wordt het modelstructuur karakteriseringsprobleem in meer detail bestudeerd met de niet–parametrische optimale controle techniek. De bekomen resultaten wijzen erop dat er een maximaal realiseerbare winst bestaat als functie van de metabolische condities. Het numeriek algoritme van Hoofdstuk 3 kan echter zonder meer toegepast worden, onafhankelijk van het metabolisme. In dezelfde zin wordt ook de (uitstekende) performantie van de heuristische regelaars ten opzichte van de optimale oplossing niet beïnvloed door de metabolische condities. De simulatieresultaten illustreren dat dit nieuw unificerend model een belangrijk hulpmiddel kan zijn bij het discrimineren tussen verschillende mogelijke modelstructuren (i.e. bij het bepalen van het reële metabolisme), op voorwaarde dat een optimaal voedingsprofiel wordt aangelegd.

In de vierde paragraaf tenslotte formuleren we nog enkele aanvullende beschouwingen bij het nieuw paradigma : *optimalisering voor modeldiscriminatie.*

Een evaluatie van de modellen van Heijnen et al. en Bajpai en Reuß is gedeeltelijk terug te vinden in [Nicolaï et al. 1992]. Het nieuw unificerend ongestructureerd model wordt voorgesteld in [Nicolaï et al. 1991], en in detail geanalyseerd in [Van Impe et al. 1991c]. Het gedrag van dit model bij optimalisering van de hoeveelheid produkt, met betrekking tot de substraat voedingsstrategie, is gepubliceerd in [Van Impe et al. 1992d].

Hoofdstuk 6

Optimale adaptieve controle

Gevalstudie : fed-batch fermentatieprocessen

De belangrijkste bijdrage van dit laatste hoofdstuk bestaat erin te illustreren hoe het inzicht, verworven tijdens een voorafgaande optimale controle studie, kan gebruikt worden bij het ontwerp van eenvoudig te implementeren adaptieve regelaars. Dergelijke regelaars paren een bijna optimale performantie aan uitstekende robuustheidseigenschappen tegen modelonzekerheden en procesverstoringen. Juist omdat zij model–onafhankelijk zijn, kunnen deze regelaars zeer nuttig zijn bij het oplossen van het modeldiscriminatie probleem, zoals reeds besproken in Hoofdstuk 5.

Bij wijze van gevalstudie, beschouwen we het ontwerp van een regelaar voor het substraat voedingsdebiet, voor de klasse van fermentatieprocessen gekenmerkt door een ontkoppeling tussen groei van biomassa en produkt synthese. Meer specifiek analyseren we het meest voorkomend geval van een monotone specifieke groeisnelheid en een niet–monotone specifieke produktiesnelheid als functies van de substraatconcentratie.

In een eerste paragraaf wordt het concept van *optimale adaptieve controle* uitvoerig gemotiveerd. We vertrekken hierbij van de optimale controle oplossing. Vervolgens worden de hiervan afgeleide heuristische regelaars, die op tal van plaatsen in dit werk aan bod kwamen, geëvalueerd vanuit het standpunt van een implementatie in ware tijd. We tonen aan dat een rechtstreekse implementatie zeker niet voldoende robuustheidseigenschappen heeft. Anderzijds, in tegenstelling tot de optimale controle oplossing, voldoen deze regelaars aan een meer realistisch regelobjectief, namelijk instelwaarderegeling. Deze heuristische regelaars worden daarom als vertrekpunt gekozen voor het ontwerp van meer robuuste, model–onafhankelijke *adaptieve regelaars.* Daartoe worden ze geïnterpreteerd binnen het kader van *niet–lineaire lineariserende controle.* Op die manier kan een mechanisme ingebouwd worden dat de gesloten kring zowel stabiel als robuust maakt.

In een volgende stap wordt dan het meetprobleem aangepakt, i.e. hoe kunnen de niet meetbare variabelen, die nodig zijn voor het berekenen van de regelactie, in ware tijd bepaald worden. Anders gezegd, hoe kunnen de niet–lineaire lineariserende regelaars adaptief gemaakt worden. In de volgende paragrafen stellen we drie mogelijke oplossingen voor, afhankelijk van de metingen die in ware tijd beschikbaar zijn. Bij

wijze van voorbeeld worden simulatieresultaten gegeven voor de penicilline G fed–batch fermentatie, beschreven door het nieuw unificerend model uit Hoofdstuk 5. Het nut van *software sensoren* wordt duidelijk geïllustreerd. We wijzen ook op de *trade off* tussen de *vereisten aangaande metingen in ware tijd* (zoals aantal, nauwkeurighied,...), en de *vereisten aangaande a priori informatie* (zoals opbrengst– en onderhoudscoëfficiënten). Zowel een *lineaire regressie schatter* als een *schatter afgeleid van een toestandsschatter* kunnen gebruikt worden voor de bepaling in ware tijd van de specifieke reactiesnelheden, die we (in overeenstemming met het concept van *minimale modellering*) als tijdsvariante parameters beschouwen. Bovendien tonen we aan dat een vertraging op de metingen in rekening kan gebracht worden.

Een merkwaardig resultaat is het volgende. Indien er geen beperkingen zijn van het type ongelijkheid op de toestandsvariabelen, moet de wenswaarde voor de substraatconcentratie in de fermentor enkel gespecificeerd worden voor de produktiefase. Daarentegen kunnen de voorgestelde regelaars zonder meer geïmplementeerd worden vanaf de start van de fermentatie. De eerste fase, de groeifase, wordt gebruikt om convergentie van de schatter te bekomen. Bovendien is de uitbreiding naar problemen mét beperkingen voor de hand liggend. Samengevat, we zijn nu in staat om een wenswaardeprofiel voor de substraatconcentratie in de fermentor af te leiden dat een suboptimale performantie garandeert. In die zin kan dit hoofdstuk beschouwd worden als een uitbreiding van de methodologie voorgesteld in Hoofdstuk 5 uit het boek van Bastin en Dochain [1990], waar de referentiewaarde voor de substraatconcentratie constant gehouden is voor de gehele fermentatieduur.

De tekst van dit hoofdstuk is gebaseerd op de publikaties [Van Impe et al. 1991b] en [Van Impe et al. 1992c en 1992e].

Hoofdstuk 7

Conclusies

Naast het ontwikkelen van een nieuw dynamisch model voor microbiële groei als functie van tijd en temperatuur, kunnen de voornaamste bijdragen van dit werk samengevat worden in de volgende paradigma's :

1. *Optimalisering voor modeldiscriminatie*
2. *Optimale adaptieve controle*

Suggesties voor verder onderzoek staan vermeld achteraan in de tekst.